



Functional characterisation of microRNAs encoded by avian herpesviruses

James Popplestone

Wolfson College

University of Oxford

Nuffield Department of Clinical Laboratory Sciences

Medical Sciences Division

Submitted to University of Oxford for the degree of Doctor of Philosophy

2015

Abstract

MicroRNAs (miRNAs) have now been identified in a vast array of organisms and a great deal of research has been carried out to elucidate the role they play. The dysregulation of miRNA expression has been implicated in a number of disease states and their importance has been highlighted by the beginning of their utilisation as therapeutics.

The focus of this study was to identify the role played by miRNAs encoded by the Marek's disease vaccine viruses, Marek's disease virus serotype 2 (MDV-2) and Herpesvirus of turkeys (HVT). In order to better understand the functions of these miRNAs we wanted to identify their targets within the host cell. Using a combination of bioinformatic and biochemical approaches we were able to build up a library of potential targets. Three viral miRNA targets; *AKT3*, *RAP1A* and *DEK*, were further validated using dual-luciferase assays to highlight the exact site of miRNA targeting, and western blots to demonstrate an effect of miRNA targeting on protein abundance. An attempt at using label-free proteomics to observe the viral miRNA mediated changes in the host proteome is also described, however this proved to be unsuccessful.

Additionally the function of one particular MDV-2 miRNA, *mdv2-miR-M21*, was explored in more detail, describing its role as a potential ortholog of the host miRNA; *gga-miR-29b*. By using the observation that the viral miRNA contained an identical 'seed' region to the host miRNA, we were able to use the data collected from existing studies on *miR-29b* to search for targets of *mdv2-miR-M21*. We demonstrated that *mdv2-miR-M21* targeted *DNMT3B*, crucial for epigenetic modification of the genome.

The final part of this study aimed to understand the wider context the viral miRNAs played in the viral biology and protective ability of the vaccine viruses. The miRNAs were deleted from the viruses, and then the miRNA-deletion viruses were used to vaccinate birds before challenge with the oncogenic Marek's disease virus serotype 1 (MDV-1), survival rates to the 'wild-type' MDV-2 and HVT vaccine viruses were then compared.

Table of Contents

Abstract 2
Table of Contents 3
Table of Figures 8
Table of Tables 14
Abbreviations 16
Acknowledgements 21
Declaration 22
1 Introduction 23
1.1 Marek's Disease 23
1.1.1 Mardivirus encoded microRNAs 23
1.1.2 Vaccination against Marek's Disease 26
1.2 Introduction to miRNAs 27
1.2.1 History of discovery 27
1.3 Identification of novel miRNAs 28
1.3.1 Cataloguing of further miRNA discoveries 29
1.4 miRNA biogenesis and function 30
1.4.1 Canonical biogenesis pathway 30
1.4.2 Post-transcriptional regulation by miRNAs 32
1.5 Epigenetics and miRNAs 35
1.6 miRNA functional understanding through identifying miRNA targets 36
1.6.1 Bioinformatic Approaches 36
1.6.2 Biochemical Approaches 40
1.7 Viral miRNAs 45
1.7.1 Biogenesis 45
1.7.2 Virus regulation of viral miRNA expression 46
1.7.3 Targeting of viral miRNAs 47
1.7.4 Finding targets of viral miRNAs 50
1.7.5 Targetome studies in MDV-1 and EBV 51
1.8 Summary of hypothesis 53
2 Methods 54
2.1 Solutions and buffers 54
2.1.1 Tissue culture 54

2.1.2 Bacterial cell culture 55
2.1.3 Protein analysis 56
2.1.4 Nucleic acid analysis 57
2.1.5 Cell manipulation 58
2.2 Backbone vectors 59
2.3 General Methods 61
2.3.1 Glycerol stock production 61
2.3.2 Plasmid DNA extraction – miniprep scale (using Qiagen miniprep kits) 61
2.3.3 Plasmid DNA extraction – maxiprep scale (using Qiagen maxiprep kits) 61
2.3.4 BAC DNA STET miniprep 62
2.3.5 BAC DNA maxiprep – (using Qiagen maxiprep columns) 63
2.3.6 Polymerase chain reaction (PCR) 63
2.3.7 A-Tailing of PCR Products for TA Cloning 64
2.3.8 RNA Extraction – (Using Qiagen miRNEasy mini Kit) 64
2.3.9 RNA Extraction – Using Trizol reagent (Invitrogen) 65
2.3.10 Use of DNeasy kit for multiple extractions of total DNA from cells 65
2.3.11 Determining protein yield from sample 66
2.3.12 Preparation of Protein Samples for Mass Spectrometry (MS) 66
2.3.13 Generation of Electrocompetent EL250 *E. coli* 67
2.3.14 miRNA TaqMan 67
2.3.15 Gene Expression TaqMan 69
2.3.16 Detection of viral genome copy number by TaqMan 71
2.3.17 Generating inducible HVT miRNA expression construct 72
2.3.18 Creating DF-1 cell line stably transfected with pRTS-HVT miRNA construct 73
2.3.19 General Molecular Cloning 74
2.3.20 Creating reporter constructs for dual luciferase assay 74
2.3.21 Creating miRNA expression vectors 76
2.3.22 Transformation of chemically competent *E. coli* 76
2.3.23 Transformation of electro-competent *E. coli* 76
2.3.24 Nucleic acid electrophoresis 77
2.3.25 SDS protein electrophoresis 77
2.3.26 Western blot 77
2.3.27 Transfection of DF-1 cells 78
2.3.28 Transfection of Chicken embryo fibroblasts (CEF) cells 79

2.3.29 Fixing and staining CEF for detection of viral plaques 80
2.3.30 Production of viral stocks from BAC DNA 81
2.3.31 Determination of viral titre in CEF 81
2.3.32 Luciferase reporter assay 82
2.3.33 List of DNA oligos used in each chapter of the thesis 85
2.3.34 Construction of mutant HVT and MDV-2 BAC viruses 90
2.3.35 Antibodies used for immunofluorescent staining of viral plaque 94
2.3.36 Table of primers and probes used to determine levels of MDV-2 and HVT via qRT-PCR. 94
3 Using comparative studies and bioinformatic miRNA target prediction algorithms to highlight targets of HVT and MDV-2 encoded miRNAs 95
3.1 Does MDV-2 encode a functional ortholog of the host miRNA *gga-miR-29b*? 95
3.1.1 Evidence for other viral orthologs of host miRNAs 95
3.1.2 DNA Methyltransferase 3-Beta (*DNMT3B*) 98
3.1.3 Experimental outline 99
3.1.4 Results 100
3.2 Using TargetScan miRNA target prediction program to find targets of all MDV-2 and HVT miRNAs 108
3.2.1 Performing the searches 108
3.2.2 Results from TargetScan 110
3.2.3 Validation of predicted targets 121
3.2.4 Further validation of targets highlighted from dual-luciferase assay 128
3.3 Discussion 134
3.3.1 Viral miRNA *mdv2-miR-M21* is targeting *DNMT3B* 134
3.3.2 Identification of viral miRNA targets 136
4 Proteomics Approach to Identify HVT miRNA Targets 147
4.1 Introduction 147
4.1.1 Global Identification of viral miRNA targets 147
4.1.2 Ago2 Immunoprecipitation 147
4.1.3 Proteomics 149
4.2 Results 150
4.2.1 Generating inducible HVT miRNA expression construct 150
4.2.2 Testing miRNA expression from the pRTS construct 152
4.2.3 Initial analysis of miRNA expression from pRTS-HVT miRNA transfected DF-1 cells 156

4.2.4 Confirming expression of all HVT miRNAs from pRTS-HVT miRNA transfected DF-1 cells 158
4.2.5 Preparing samples for label-free proteomics 162
4.2.6 Label-Free Quantitative Proteomics 165
4.2.7 Further analysis of the Proteomics Data 172
4.3 Discussion 177
4.3.1 Creating cell line to examine proteome changes induced by viral miRNA expression 177
4.3.2 Changes in host-cell proteome as a result of viral miRNA targeting 179
4.3.3 Examining proteomics data for correlation with luciferase validation data of TargetScan custom data 180
4.3.4 Analysis of comparative gene ontology study 181
4.4 Conclusion 181
5 What effect does the deletion of miRNAs have on HVT and MDV-2? 183
5.1 Introduction 183
5.1.1 BAC mutagenesis 183
5.1.2 The effect of miRNA deletion on virus infection and replication 184
5.2 Results 187
5.2.1 Creating miRNA deletion HVT and MDV-2 BAC clones 187
5.2.2 Further analysis of miRNA-single and –double copy miRNA deletion BAC clones 193
5.2.3 Generation of single-copy miRNA revertant BAC clones 195
5.2.4 Creating viral stocks of miRNA-deletion BAC viral genomes 203
5.2.5 Analysis of viral miRNA levels from CEF cells infected with virus stock 203
5.2.6 Animal experiment to observe *in vivo* effects of miRNA deletion from viral genomes 206
5.3 Discussion 220
5.3.1 Creation of the miRNA deletion BACs 220
5.3.2 Testing of viral stocks generated from BAC clones 221
5.3.3 Outcome of animal trial 222
6 Summary of results, general discussion, further work, and conclusions 225
6.1 Future work 229
6.1.1 Chapter 3 229
6.1.2 Chapter 4 229
6.1.3 Chapter 5 229
6.2 Concluding remarks 231

7 References 232

8 Appendices 242

8.1 Appendix 1 – Methodology of power calculations to determine chicken group sizes, provided by Sue Baigent 242

8.2 Appendix 2 – Evidence for the presence of internal promoter in 4.6kb HVT miRNA 'cassette', following detection of *hvt-miR-H15* in cells transfected with the HVT-miR-H1-H18 cassette in a promoter-less vector – (page 151) 243

8.3 Appendix 3 – Full dataset of TargetScan predicted targets of MDV-2 and HVT encoded miRNAs 244

8.4 Appendix 4 - Full dataset from proteomic analysis of DF-1 cells following stable transfection with either pRTS-HVT-miR-H1-H18 or pRTS-empty 245

8.5 Appendix 5 – Statistical Analysis of dual-luciferase assay analysis of predicted viral miRNA targeting of host genes 246

8.6 Appendix 6 – List of the different subheadings found under main headings identified in the PantherDB pie chart figures 248

8.7 Appendix 7 – Workflow diagram to describe how stably transfected DF-1 cells were prepared for proteomics work in chapter 249

8.8 Appendix 8 – Analysis of challenge virus levels in individual unvaccinated birds from KV86 trail 250

8.9 Appendix 9 – Analysis of vaccine virus levels in individual unvaccinated birds from KV86 trail 251

Table of Figures

Figure 1 - Map showing the location of MDV-1, MDV-2 and HVT encoded miRNAs within the viral genomes. IR_L = Inverted repeat region long, IR_s = Inverted repeat region short, TR_L = Terminal repeat region long, TR_S = Terminal repeat region short. 25
Figure 2 – Canonical miRNA biogenesis pathway leading to miRNA-induced gene expression regulation. Adapted from (Filipowicz et al. 2008). 31
Figure 3 - Schematic representation of the different mechanisms of miRNA mediation gene expression regulation. Adapted from Pasquinelli, 2012 (Pasquinelli 2012) 34
Figure 4 - Overview of different experimental strategies for identifying miRNA targets. Taken from (Thomas et al. 2010). 44
Figure 5 - An overview of the mechanisms of function of virally encoded miRNAs**.** A and B show viral miRNAs regulating the expression of viral genes through either complete pairing of miRNA and target leading to degradation (A) or incomplete miRNA pairing to target resulting target repression (B). C shows viral miRNAs targeting host cell encoded mRNAs. Taken from (Gottwein and Cullen 2008). 49
Figure 6 - Overview of the steps involved in miRNA luciferase assay to see if selected miRNA is targeting a gene 3'UTR. (A) Construction of reporter construct by annealing oligos containing predicted target site of miRNA in 3'UTR. (B) Generation of miRNA expression vector by cloning mature miRNA sequence (plus additional flanking sequence) into pEF6-V5/His TOPO expression vector. (C) Actual process of dual-luciferase assay, whereby the two previously constructed vectors are co-transfected into a cell line, and the effects of predicted miRNA targeting of cloned 3'UTR are detected by changes in light expression by luminometer machine. 83
Figure 7 - Equation used to calculate the down-regulation of Renilla luciferase by miRNA mediated gene regulation. Renilla luciferase readings 1-4 (RL1-4), Firefly luciferase readings 1-4 (FF1-4). 84
Figure 8 - Sequence similarities between viral miRNAs and their host encoded orthologs, identical residues highlighted in red. A - Alignment of *hsa-miR-155* and *kshv-miR-K12-11*. B - Alignment of *gga-miR-155* and *mdv1-miR-M4*. C - Alignment of *gga-miR-29b* with *mdv2-miR-M21* and *blv-miR-B4-3p*, also shown *hsa-miR-29b* which has identical sequence to *gga-miR-29b*. 97
Figure 9 – (A) Highlighted in yellow is the predicted match for the *miR-29b* seed sequence within the chicken *DNMT3B* gene (NCBI Gene ID: 419287). Prediction made by TargetScan custom program.(B)Predicted interaction between miRNA and *DNMT3B* 3'UTR calculated by RNA hybrid (Rehmsmeier et al. 2004) 101
Figure 10 – Bar graph showing the relative decrease of renilla luciferase expression caused by miRNA mediated targeting of *DNMT3B* 3'UTR following dual-luciferase assay in DF-1 cells. The labels show whether the full-length 3'UTR (DNMT3B (wt/mut) F) or 'short' 3'UTR (DNMT3B (wt/mut) S) reporter construct was co-transfected with either *gga-miR-29b*, *mdv2-miR-M21* or pEF6-empty vector and the degree of down-regulation of gene expression observed. Any significant down-regulation between miRNA wild-type 3'UTR reporter construct co-transfected with corresponding miRNA expression vector and all other controls, was determined by a P-value under 0.05, calculated by a 2-way ANOVA statistical test with multiple comparisons, using the Tukey method to correct for multiple comparisons. 104

Figure 11 – (**A**) *DNMT3B* transcript levels determined via TaqMan gene expression assay following transfection of DF-1 cells with either host *gga-miR-29b* or *mdv2-miR-M21* miRNA expression vector. Levels of gene expression following miRNA transfection were compared to relative gene expression from pEF6 empty vectortransfected DF-1 cells and normalised to levels of *gga-miR-let7a*. ** denotes significant down-regulation calculated by a P-value under 0.01, calculated by a paired 2-tailed T-test. (**B**) TaqMan miRNA expression assay on above transfected DF-1 cells to confirm expression of miRNAs compared to DF-1 cells transfected with pEF-6 empty vector transfected cells. Empty vector transfected cells were tested for expression of both *gga-miR-29b* and *mdv2-miR-M21* (only expression of *gga-miR-29b* plotted), miRNA expression levels are normalised relative to *gga-miR-let7a.* 107
Figure 12 - TargetScan custom program webpage. Example showing how to search for predicted targets of any miRNA in a selection of species. (A) TargetScan custom welcome page, the species 'chicken' has been selected and the seed region of *MDV2-miR-M14-5p* has been entered (nucleotides 2-8 of full mature miRNA sequence, UGUGGUACGGUGCACCCUGAGA). (B) List of predicted targets of *mdv2-miR-M14-5p* generated by TargetScan. List order based upon the 'type' and frequency of seed-target matches. 109
Figure 13 - Outline of TargetScan custom results. (A) Summary of the TargetScan custom output for both the HVT and MDV-2 encoded miRNAs. (B and C) Top 20 highest ranked predicted targets for all MDV-2 and HVT encoded miRNAs, respectively. The ranking is based solely on the number of conserved predicted target sites in the 3'UTR of the genes. 111
Figure 14 – Biological process gene ontology analysis of predicted targets of all HVT encoded miRNAs, analysis was performed by Panther Classification System (www.pantherdb.org). The number of unique mapped ids found in classification system was 881, 323 IDs were not mapped by Pantherdb. 114
Figure 15 – Bar chart to show the results of the statistical overrepresentation analysis performed by Pantherdb on biological processes of predicted HVT miRNA targets, to determine if the frequency of predicted targets involved in certain biological processes, is significantly above background levels. 115
Figure 16 - Biological process gene ontology analysis of predicted targets of all MDV-2 encoded miRNAs, analysis was performed by Panther Classification System (www.pantherdb.org). The number of unique mapped ids found in classification system was 999, 308 IDs were not mapped by Pantherdb. 116
Figure 17 - Bar chart to show the results of the statistical overrepresentation analysis performed by Pantherdb on biological processes of predicted MDV-2 miRNA targets, to determine if the frequency of predicted targets involved in certain biological processes is significantly above background levels. 117
Figure 18 – Fluorescent microscope image of DF-1 cells, 48-hours following transfection with pMAX-GFP vector using lipofectamine 2000 transfection reagent (Invitrogen). The high transfection percentage indicates that the transfection conditions are suitable..... 124
Figure 19 – miRNA TaqMan analysis to determine expression levels of various HVT and MDV-2 encoded miRNAs, following transfection of the corresponding miRNA expression vector into DF-1 cells. Relative quantification levels were normalised to detection levels (background) from DF-1 cells transfected with the pEF6-V5/His vector. Error bars show maximum and minimum relative quantification (RQ) values as calculated by 7500 Fast software (Applied Biosystems) from Ct values, normalised to *gga-miR-let7a*. 125

Figure 20 - Bar graph showing the relative decrease of renilla luciferase expression caused by miRNA mediated targeting of target gene 3'UTR following dual-luciferase assay in DF-1 cells. The predicted target gene 3'UTRs cloned downstream of the renilla luciferase gene in psiCHECK-2 are labelled along with the corresponding targeting miRNA. * denotes significant down-regulation between miRNA wild-type 3'UTR reporter construct co-transfected with corresponding miRNA expression vector and all other controls (results highlighted by red box in appendix 5). Determined by a P-value under 0.05, calculated by a 2-way ANOVA statistical test with multiple comparisons, using the Tukey method to correct for multiple comparisons. 127
Figure 21 – Western blot analysis to determine protein abundance of four targets of virally encoded miRNAs, following transfection of the corresponding miRNA expression vector in DF-1 cells. Underneath each blot are the loading control blot for α-tubulin and the calculated band intensity for each target protein normalised to the abundance of the α-tubulin loading control. Band intensity analysis was performed using ImageJ software (http://rsb.info.nih.gov/ij/index.html) (Schneider et al. 2012). 130
Figure 22 – TaqMan gene expression analysis of transcript levels of viral miRNA targets. Transcript abundance following transfection of targeting miRNA expression vector into DF-1 cells is shown relative to transcript abundance following transfection with empty miRNA expression vector. Error bars show maximum and minimum relative quantification (RQ) values as calculated by 7500 Fast software (Applied Biosystems) from Ct values, normalised to *RPL7* levels. 133
Figure 23 –Simplified vector map of pRTS-HVT miRNA H1-H18 construct. Generated to scale using vector NTI software (Invitrogen). Abbreviations in figure: pA = PolyA tail (multiple adenosine monophosphates), tdTomato = Tomato fluorescent protein gene, oriP = origin of plasmid replication. Blue lines indicate the locations of each HVT miRNA as amplified from BAC DNA, with a few miRNA labelled for reference. 151
Figure 24 - Fluorescent microscope images of puromycin selected, stably transfected DF-1 cells, containing either: pRTS-empty vector (A), pRTS-HVT miRNA vector clone 6 (B) or clone 7 (C). Two pictures in each set show bright field and UV fluorescence microscopy. Title above pairs of pictures describes if expression from the pRTS bi-directional promoter has been induced by the addition of 1µg/ml doxycycline or not. 153
Figure 25 – Initial TaqMan analysis of *hvt-miR-H15* expression from both; doxycycline induced and uninduced DF-1 cells stably transfected with different clones of the pRTS-HVT miRNA vector compared to empty vector. Error bars show the 95% confidence intervals and *** denotes significant increase in *hvt-miR-H15* expression in samples, relative to control, as calculated by a P-value under 0.001, calculated by a paired 2-tailed T-test. 155
Figure 26 – PCR amplification of the tdTomato fluorescent protein gene and chicken *β-actin* from DF-1 cells stably transfected with pRTS-empty and pRTS-HVT miRNA constructs. The red box highlights the expected size PCR product generated from the *tdTomato* PCR, the green box highlights the expected size PCR product generated from the *β-actin* control PCR and the purple box highlights the larger size fragment produced by the *β-actin* PCR if genomic DNA is present (suggesting genomic DNA contamination in the RNA used for producing cDNA). 157

Figure 27 – Mean number of counts of all of the HVT miRNAs detected by miRNA microarray analysis performed by LC Sciences. The left-hand column shows the number of miRNA counts in doxycycline-induced, pRTS-empty vector stably transfected DF-1 cells. The right-hand column shows the number of miRNA counts in doxycycline-induced, pRTS-HVT miRNA vector stably transfected DF-1 cells. Standard deviation of different runs and p-values are also shown. The signal values are derived by background subtraction and normalisation. A transcript to be listed as detectable must meets at least two conditions: signal intensity higher than 3×(background standard deviation) and spot CV < 0.5. CV is calculated by (standard deviation)/(signal intensity). 160
Figure 28 – Heat-map (Provided by LC Sciences) showing detection of the 18 most highly detected viral miRNAs in the pRTS-HVT miRNA transfected DF-1 cells. The detection from the six repeats for each sample are shown, where dark red demonstrates high relative levels of miRNA, bright green demonstrates low levels. 161
Figure 29 – Log_{10} relative expression levels of three different HVT miRNAs (H1, H15 and H18) from DF-1 cells stably transfected with either pRTS-empty vector pRTS-HVT miRNA vector, clone 7. Cells were harvested at different time points after doxycycline induction of pRTS bi-directional promoter, 0 hours (uninduced), 24 hours and 48 hours. Expression levels are relative to expression of the miRNAs detected in pRTS-empty uninduced (background). Error bars show maximum and minimum relative quantification (RQ) values as calculated by 7500 Fast software (Applied Biosystems) from Ct values, normalised to gga-miR-let7a..... 164
Figure 30 - Heat map generated using GENE-E software (Broad Institute), showing the fold change of 362 chicken proteins as detected by more than 2 peptides label-free proteomics experiment. Fold change was calculated by dividing average normalised protein abundance from pRTS-HVT miRNA transfected cells by average normalised protein abundance from pRTS-empty transfected cells. Uniprot accession numbers and specific fold changes are given for the 5 greatest fold increases, and 10 greatest fold decreases in protein abundance. 167
Figure 31 - Heat map generated using GENE-E software (Broad Institute), showing the fold change of 108 chicken proteins whose CV value between duplicate run was >0.2. Fold change was calculated by dividing average normalised protein abundance from pRTS-HVT miRNA transfected cells by average normalised protein abundance from pRTS-empty transfected cells. Uniprot accession numbers are displayed next to the colour representing the amount fold-change of that protein in the presence of HVT miRNAs. 169
Figure 32 - Power analysis performed on the label-free proteomics experimental data, using Progenesis LC-MS software (Nonlinear Dynamics). Image provided by Dr Dong Xia. 171
Figure 33 - Biological process gene ontology analysis of proteins with a greater than 10% knock-down in the proteomic analysis following overexpression of HVT encoded miRNAs. Analysis was performed by Panther Classification System (www.pantherdb.org). 175
Figure 34– Bar chart to show the results of the statistical overrepresentation analysis performed by Pantherdb on biological processes of HVT miRNA targets from proteomic analysis, to determine if the frequency of predicted targets involved in certain biological processes, is significantly above background levels. 176
Figure 35 - Overview of the BAC mutagenesis strategy. Note the different colours representing the different regions of homology utilised for each homologous recombination event. 186
Figure 36 - Restriction digests of both pSB-1 BAC3 (*EcoRI*) *and* pHVT3 (*BamHI*) single-copy miRNA deletion BAC DNA extracted from bacterial clones (1-6). 188

Figure 37 – Restriction digests of both pSB-1 BAC3 (*EcoRI*) and pHVT3 (*BamHI*) double-copy miRNA deletion BAC DNA extracted from clones (1-3) analysed alongside parental (described a 'wild-type') BAC DNA. 192
Figure 38 – Fluorescent images of CEF transfected with DNA of different miRNA deletion BAC clones after fixing with ice-cold acetone:methanol and staining with either serum from HVT vaccinated birds (HVT BAC transfected CEF) or anti-MDV-2 Y5.9 monoclonal antibody (SB-1 BAC transfected CEF) followed by an Alexa Fluor® 488 secondary antibody. 194
Figure 39 – Fluorescent microscope images of CEF transfected with either parental or single-copy miRNA revertant pHVT3 or SB-1 BAC3 clones after fixing with ice-cold acetone:methanol and staining with either serum from HVT vaccinated birds (HVT BAC transfected CEF) or anti-MDV-2 Y5.9 monoclonal antibody (SB-1 BAC transfected CEF) followed by an Alexa Fluor® 488 secondary antibody.. Negative control image of mock transfected CEF is visible in the left-hand panes. 197
Figure 40 – TaqMan analysis of miRNA expression from CEF transfected with different miRNA deletion clones of either pSB-1 BAC3 (A) or pHVT3 (B). All expression levels are relative to CEF transfection control and normalised to the host endogenous miRNA *gga-miR-let7a*. Error bars show maximum and minimum relative quantification (RQ) values as calculated by 7500 Fast software (Applied Biosystems) from Ct values, normalised to gga-miR-let7a. 200
Figure 41 – PCR analysis on BAC DNA of the pHVT3 and pSB-1 miRNA manipulation constructs. DNA was analysed by gel electrophoresis on a 1% agarose gel with NEB 2-log ladder run in the left hand lane for reference. Blue boxes highlight the band of expected size for viral miRNA clusters, green boxes highlight the band of expected size for KanSacB cassette and red boxes highlight the band of expected size for spectinomycin resistance cassette. 202
Figure 42 – Relative levels of viral miRNAs detected in infected CEF cells four days after infection with the BAC derived virus. miRNA expression levels are normalised to the viral genes described in each graph title. Error bars show the upper limits of relative quantification, calculated to 95% confidence by 7500 FAST software (Applied Biosystems). 204
Figure 43 - Distribution of birds for KV86 trial. Location of each group is shown by its number and name. The birds in group 7 (unvaccinated) are shown in red and their distribution amongst vaccinated birds can be seen. 209
Figure 44 – Survival graphs of Birds in KV86 experiment. (A) Shows groups 1, 2, and 3 that were vaccinated with different miRNA deletion clones of the pHVT3 BAC and group 7 – unvaccinated. (B) Shows groups 4, 5, and 6 that were vaccinated with different miRNA deletion clones of the pSB-1 BAC and group 7 – unvaccinated. The percentage survival of the birds is displayed relative to the days post challenge (dpc) with 1,000pfu of RB-1B challenge virus. 213
Figure 45 – Mean RB-1B levels in the different groups that were vaccinated with the different pHVT3 BAC clones throughout the KV86 animal trial, as calculated by the mean number of RB-1B genomes per 10^4 Peripheral Blood Lymphocytes (PBLs) extracted from each bird. Error bars display upper and lower limits of the 95% confidence intervals. 215
Figure 46 – Mean RB-1B levels in the different groups that were vaccinated with the different pSB-1 BAC3 clones throughout the KV86 animal trial, as calculated by the mean number of RB-1B genomes per 10^4 Peripheral Blood Lymphocytes (PBLs) extracted from each bird. Error bars display upper and lower limits of the 95% confidence intervals. 216

Figure 47 – Mean pHVT3 BAC vaccine virus levels in the different groups that were vaccinated with the different pHVT3 BAC clones throughout the KV86 animal trial, as calculated by the mean number of BAC genomes per 10^4 Peripheral Blood Lymphocytes (PBLs) extracted from each bird. Error bars display upper and lower limits of the 95% confidence intervals. 218
Figure 48 – Mean pSB-1 BAC3 vaccine virus levels in the different groups that were vaccinated with the different pSB-1 BAC3 clones throughout the KV86 animal trial, as calculated by the mean number of BAC genomes per 10^4 Peripheral Blood Lymphocytes (PBLs) extracted from each bird. Error bars display upper and lower limits of the 95% confidence intervals. 219
Figure 49 - TaqMan analysis of *hvt-miR-H15* expression from DF-1 cells transfected with different clones of the promoter-less TOPO-XL-HVT-H1-H18 vector. Quantification levels are relative to *hvt-miR-H15* expression from DF-1 cells transfected with empty TOPO-XL vector. Error bars show maximum and minimum relative quantification (RQ) values as calculated by 7500 Fast software (Applied Biosystems) from Ct values, normalised to gga-miR-let7a. 243

Table of Tables

Table 1 – Adapted from (Shirdel et al. 2011) which lists commonly used miRNA target prediction programs and highlights the different characteristics that miRNA:transcript interactions looks for when scoring the likelihood of an interaction 39
Table 2 - Table listing TaqMan microRNA assays used throughout this study, with corresponding assay IDs and catalogue numbers. Sequences of probes and primers in the assays are intellectual property of Life Technologies (www.lifetechnologies.com). 69
Table 3 - Table listing TaqMan gene expression assays used throughout this study, with corresponding assay IDs and catalogue numbers. Sequences of probes and primers in the assays are intellectual property of Life Technologies (www.lifetechnologies.com). 70
Table 4 – Details of primary and secondary antibodies used throughout this study. 78
Table 5 - Amounts of Lipofectamine 2000 and DNA required for transfection of different tissue culture vessels 79
Table 6 - Table of oligos used to generate dual-luciferase reporter constructs and miRNA expression constructs. 85
Table 7 - Table listing oligos used to amplify the pre-miRNA sequence from BAC DNA from the corresponding miRNAs. 85
Table 8 - Table listing oligos that were annealed together, and subsequently ligated into *Xho*I and *Not*I digested psiCHECK2 vectors. Naming structure is gene name_ (MUT if there are changes in 3'UTR sequence) _miRNA predicted to target_TOP or BOT(bottom) to distinguish oligos in the pair.... 86
Table 9 - Table listing oligos that were annealed together,and subsequently ligated into *Xho*I and *Not*I digested psiCHECK2 vectors. Naming structure is gene name_ (MUT if there are changes in 3'UTR sequence) _miRNA predicted to target_TOP or BOT (bottom) to distinguish oligos in the pair... 87
Table 10 - Table listing all the oligonucleotide primers used to create and sequence the HVT miRNA expression construct 88
Table 11 - Table listing primers used to generate miRNA deletion BAC clones of HVT and MDV2 viral genomes. Primers were ordered from Eurofins MWG Operon at either 0.1µM (<60 bp) or 0.5µM scale. MDV2 miRH1-H18 89
Table 12 - Information about antibodies used for fluorescent staining of pHVT3 and pSB-1 BAC3 plaques in chapter 5. 94
Table 13 - Details of different qRT-PCR primers and probes used to determine levels of MDV-2 and HVT virus in different experiments, also included is the primer and probe sequence for qRT-PCR detection of the *ovo* reference gene. Further detail can be found in the references provided. 94
Table 14 - Table listing the predicted targets of various HVT and MDV-2 encoded miRNAs, as predicted by TargetScan. Information includes; the miRNA predicted to be targeting, a gene ID, and Pantherdb gene ontology classifications. 119
Table 15 - Table listing the predicted targets of various HVT and MDV-2 encoded miRNAs, as predicted by TargetScan. Information includes; the miRNA predicted to be targeting, a gene ID, and Pantherdb gene ontology classifications. 120
Table 16 - Results from band intensity analysis performed using ImageJ software (Schneider et al. 2012). 131

Table 17 - List of all proteins that were both; predicted to be targeted by HVT miRNAs by TargetScan custom (chapter 3) and identified by at least 2 peptides in the label-free proteomics experiment (chapter 4). The fold change in normalised protein abundance in cells transfected with pRTS-HVT miRNA construct compared with pRTS-empty construct is shown. Also shown are the HVT miRNAs that were predicted to be targeting the specific protein genes. * represents the proteins that has a CV value<0.2 between duplicate runs (see section 4.2.6.1)..... 173
Table 18 - Table showing the number of colonies present on each plate following overnight incubation of pHVT miRNA single-copy deletion (pHVT3 ΔmiR-1) and pSB-1 BAC3 miRNA single-copy deletion (pSB-1 BAC3 ΔmiR-1) clones. Lawn indicates that colonies were greater than 500 and too close together to accurately count. 190
Table 19 - List of sub-headings found under the initial 'biological processes' in Panther Gene Classification 248

Abbreviations

aa	Amino acid
AEC	3-amino-9-ethylcarbazole
Ago	Argonaute protein
Akt	v-akt murine thymoma viral oncogene homolog
ATP	Adenosine-5'-triphosphate
BAC	Bacterial artificial chromosome
BACH1	BTB and CNC Homology 1
BAD	Bcl-2-associated death promoter
BCL11A	B-cell CLL/lymphoma 11A (zinc finger protein)
BGH	Bovine Growth Hormone
Bis-Tris	2-[Bisamino]-2--1,3-propanediol
BLV	Bovine leukaemia virus
bp	base pairs
C. elegans	*Caenorhabditis elegans*
C_{25}	25µg/ml Chloramphenicol
cDNA	Complementary DNA
CEBPβ	CCAAT/enhancer binding protein
CEF	Chicken embryo fibroblasts
CLASH	Crosslinking, ligation, and sequencing of hybrids
Ct	Threshold-cycle
CtBP1	C-terminal binding protein 1
DAVID	Database for Annotation, Visualization and Integrated Discovery
del Rev	Single-copy miRNA revertant BAC clone
DGCR8	DiGeorge syndrome critical region gene 8
DMSO	Dimethyl sulfoxide
DNA	Deoxyribose nucleic acid

DNMT	DNA Methyltransferase
dox	Doxycycline
dpc	Days-post challenge
dpv	Days-post vaccination
dsDNA	Double stranded DNA
E. coli	Escherichia coli
EBF-1	Early B-Cell Factor 1
EBV	Epstein Barr-virus
EDTA	Ethylenediaminetetraacetic acid
EF1α	Eukaryotic translation elongation factor 1 alpha
ERBB4	Erythroblastic Leukaemia Viral Oncogene Homolog-4
FAM	6-carboxyfluorescein
FC126	Strain of HVT
FLuc/FF	Firefly luciferase
H. pylori	Helicobacter pylori
HIV	Human immunodeficiency virus
HMGB	High-mobility group protein
HMGB1	High-mobility group protein 1
HSV	Herpes Simplex virus
HVT	Herpesvirus of turkeys
K_{50}	50µg/ml Kanamycin
kb	Kilo bases
KRAS	v-Ki-ras2 Kirsten rat sarcoma viral oncogene homolog
KSHV	Kaposi's sarcoma virus
LB	Lysogeny broth
LNA	Locked nucleic acid
MCL1	Myeloid leukaemia cell differentiation protein 1

MD	Marek's Disease
MDV-1	Marek's disease virus serotype 1
MDV-2	Marek's disease virus serotype 2
meq	Marek's disease virus *Eco*RI-Q fragment
MES	2-(N-morpholino)ethanesulfonic acid
miRISC	MicroRNA-induced silencing complexes
miRNA/miR	MicroRNA
MRE	microRNA response elements
mRNA	Messenger RNA
MS	Mass spectrometry
muPyV	Murine polyomavirus
MUT/mut	Mutant
MYBL1	V-Myb Myeloblastosis Viral Oncogene Homolog (Avian)-Like 1
NCBI	National Center for Biotechnology Information
NEB	New England Biolabs
Ovo	Chicken ovotransferrin gene
PBL	Peripheral blood lymphocytes
PBS	Phosphate buffered saline
PCR	Polymerase chain reaction
Pfu	Plaque forming units
PITA	Probability of Interaction by Target Accessibility
PNK	Polynucleotide Kinase
Pol II	RNA polymerase II
qPCR	Quantitative PCR
qRT-PCR	Quantitative reverse transcription polymerase chain reaction
RAS	Rat sarcoma viral oncogene
RB-1B	Strain of MDV-1

RIPA	Radioimmunoprecipitation assay
RIR	Rhode Island red
RLuc/RL	Renilla luciferase
RNA	Ribonucleic acid
rRNA	Ribosomal ribonucleic acid
S_{50}	50µg/ml Spectinomycin
SB-1	Strain of MDV-2
SDS	Sodium dodecyl sulphate
SDS	Sodium dodecyl sulphate
SILAC	Stable isotope labelling by/with amino acids in cell culture
siRNA	Small interfering ribonucleic acid
SOC	Super Optimal Broth with Catabolite repression
SPF	Specific pathogen free
STET	Saline/Tris/EDTA/Triton™ X-100
SV40	Simian vacuolating virus 40
TAMRA	Tetramethylrhodamine
TBE	Tris-borate-EDTA
TE	Tris-EDTA
TIAM1	T-Cell Lymphoma Invasion And Metastasis 1
TK	Thymidine kinase
TP53	Tumour protein 53
TRBP	TAR RNA binding protein
UCSC	University of California, Santa Cruz
UTR	Untranslated region
UV	Ultraviolet
v/v	Volume to volume
w/v	Weight to volume

Wt	Wild type
X-α-Gal	X-alpha galactosidase
ΔmiR	Double-copy miRNA deletion BAC mutant

Acknowledgements

I would like to thank my supervisors; Venugopal Nair and Yongxiu Yao at the Pirbright Institute, Compton and Charles Lawrie and Francesco Pezzella at the NDCLS, University of Oxford for their patience, support and guidance throughout this project.

In particular I would like to thank Lorraine Smith for her help with the sampling throughout the animal experiment, Sue Baigent for her endless guidance with TaqMan data analysis and Dr. Dong Xia at the University of Liverpool for performing the label-free proteomics and spending the time explaining the procedures to me.

Finally the support from the entire Viral Oncogenesis laboratory at Compton has been fantastic and I really can't thank you guys enough for the endless support and help you have provided me throughout my time in the lab.

This work was funded by the Biotechnology and Biological Science Research Council and the without their financial support it would not have been possible.

Declaration

The research presented in this thesis is my own work except where indicated otherwise. The study was carried out at the Pirbright Institute and registered at University of Oxford under the supervision of Professor Venugopal Nair and Dr Charles Lawrie.

James Popplestone

1 Introduction

1.1 Marek's Disease

Marek's disease (MD) was first described at the beginning of the 20th century, following the discovery of mononuclear cells that had infiltrated the spinal fluid of four paralysed male cockerels (Marek 1907). Although MD was recognised early on as contagious, it was not until 1967 that the causative agent, Marek's Disease Virus (MDV) was identified (Churchill and Biggs 1967). Nowadays MD is known to be a virulent, T-cell lymphoma of chickens with rapid onset and the disease has a sizeable economic impact on the poultry industry. The causative virus (MDV-1) is now classified in the subfamily *Alphaherpesviridae* and in the genus *Mardivirus* with two other serotypes of the virus: Marek's disease virus serotype 2 (MDV-2) and the antigenically related Herpes Virus of Turkey (HVT). These two serotypes, MDV-2 and HVT, are shown to be non-oncogenic (Bulow et al. 1975) and are therefore widely used as live vaccine strains to defend against the oncogenic MDV-1.

The oncogenic determinants within MDV-1 and the molecular pathways leading to tumour formation are not fully understood. Certain proteins encoded by the virus (including a basic leucine zipper protein, Marek's disease virus EcoRI-Q fragment (*meq*)) are known to be implicated, following studies where deletion of the *meq* gene has led to elimination of MDV-1 oncogenicity (Lupiani et al. 2004).

1.1.1 Mardivirus encoded microRNAs

Following the discovery of microRNAs (miRNAs) in other herpesviruses, it was not long before miRNAs were discovered to be encoded by MDV-1 (Burnside et al. 2006; Yao et al. 2008), then subsequently MDV-2 (Yao et al. 2007) and HVT (Yao et al. 2009, (Waidner et al. 2009)) (all shown in figure 1).

The microRNAs discovered in both MDV-2 and HVT were found to contain no sequence similarities to those identified in MDV-1, however they were found as clusters in the repeat regions of the viral genome, as in MDV-1 (Yao et al. 2007; Yao et al. 2009). The MDV-2 and HVT miRNAs were originally identified by creating a library of small RNAs (19-24 nucleotides in length) from total RNA and screening this library for potential miRNAs through sequence analysis. Expression of putative miRNAs

was then confirmed through Northern blot analysis (Yao et al. 2007; Yao et al. 2009). The original tally of 11 HVT miRNAs identified by Yao et al was later added to by Waidner et al. Total RNA from HVT infected cells was extracted from cells and analysed by deep sequencing followed by sequence analysis, this methodology identified 6 additional miRNAs taking the number to 17 (Waidner et al. 2009).

Work has been carried out to identify the functional roles of the miRNAs encoded by MDV-1 to determine their role in MDV oncogenicity. In a study by Zhao et al, a cluster of miRNAs encoded within the repeat region of the viral genome was either deleted, or non-functional mutations were made, within the pRB-1B bacterial artificial chromosome (BAC) clone of the virus. These BAC clone-derived viruses were then injected into chickens and the mortality of the miRNA minus viruses was compared to that of the wild type virus (Y. Zhao et al. 2011).

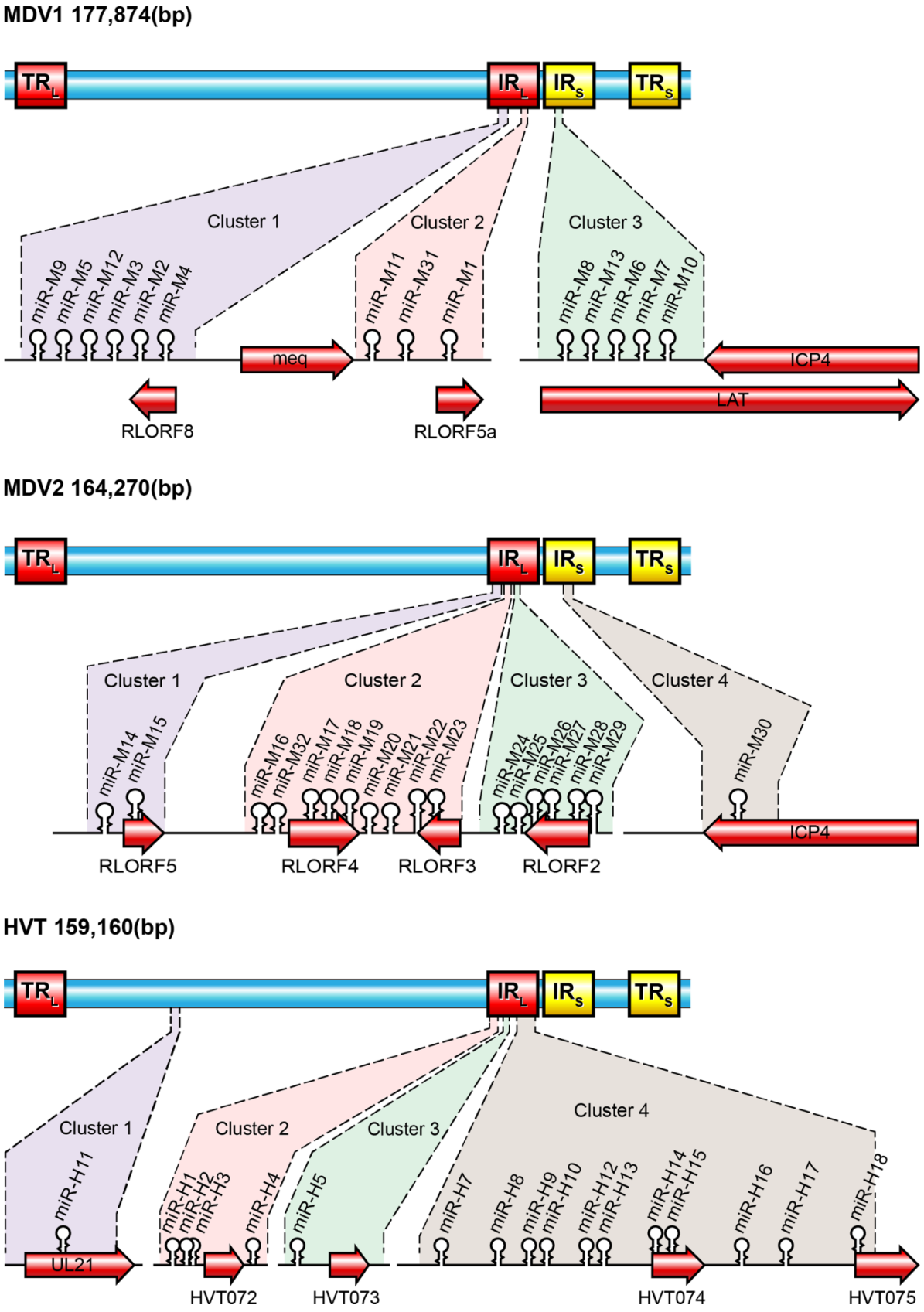


Figure 1 - Map showing the location of MDV-1, MDV-2 and HVT encoded miRNAs within the viral genomes. IR_L = Inverted repeat region long, IR_S = Inverted repeat region short, TR_L = Terminal repeat region long, TR_S = Terminal repeat region short.

One hundred percent survival was seen in the birds infected with the miRNA-deleted virus whereas in birds infected with the parent pRB-1B5 virus there was a 100 percent incidence of MD, through mortality or the presence of tumours. This study highlighted a crucial role played by miRNAs in viral infection, and in part led to the work of this project to examine the roles of the MDV-2 and HVT encoded miRNAs. Further understanding of the exact roles of miRNAs in virus biology is still needed, which could potentially contribute to possible future intervention strategies and vaccinations.

1.1.2 Vaccination against Marek's Disease

Over time there have been a number of different vaccines developed against MDV-1. Vaccination against MDV-1 was in fact the first example of a vaccine being used as a preventative measure against a cancer. The first vaccine to be produced against MDV-1 was generated through attenuation (through serial passage in chicken kidney cells) of the oncogenic MDV-1 strain, HPRS-16 (Churchill et al. 1969). This vaccine was superseded by the two naturally occurring, non-oncogenic, *Mardivirus* serotypes MDV-2 (SB-1) and HVT, both of which have been used either individually or in unison as vaccines against MDV-1 ((Calnek et al. 1983; Schat and Calnek 1978; Witter et al. 1970) respectively). In addition, a naturally attenuated MDV-1 strain, called CVI 988 or Rispens vaccine (Rispens et al. 1972), is now also in use in Europe and parts of Asia.

It is thought that the administration of the vaccine viruses into birds causes a persistent latent infection of the avirulent vaccine virus, which stimulates the immune response. Upon challenge with virulent MDV-1, this immune stimulation can reduce the initial spread of virus in the blood, protecting against the development of tumours and eventual mortality (Baigent et al. 2013). Despite success in reducing losses from Marek's disease lesions by up to 99% (Witter 2001) these vaccines are described as 'imperfect' as they do not prevent replication and shedding of pathogenic virus in infected birds (Islam and Walkden-Brown 2007; Singh et al. 2010). This shed virus is then able to infect and cause mortality in non-vaccinated birds.

There has been continuous evolution of more virulent field strains of MDV-1 (Witter 1997), thought to be caused by the inability of MDV-1 vaccines to induce sterilising immunity in chickens, thereby establishing an environment in which virulent strains are selected to escape immune responses. There has been a continued drive for the production of new vaccines, with some strategies now focused on insertion and deletion of certain genes within the virus genome, to produce ever more efficacious vaccines (Gao et al. 2011; L. F. Lee et al. 2008).

While there are a large number of similarities between the oncogenic MDV-1 and the non-oncogenic MDV-2 and HVT viruses there are also significant differences. The genomes of these *Mardiviruses* are all similar in their gene arrangement, however there are transcripts uniquely expressed; including the oncogene *meq* in MDV-1 (Jones et al. 1992), a Bcl-2 homologue in the HVT genome (Afonso et al. 2001) and all of the virally encoded miRNAs, additionally vaccination with a combination of MDV-2 and HVT viruses provides a protective synergy compared to vaccination with either HVT or MDV-2 alone (Witter and Lee 1984). In MDV-1, *meq* has traditionally been thought as the key player in tumourigenesis (Lupiani et al. 2004), however recent research has highlighted an important, if not critical role of the miRNAs in tumour formation (Y. Zhao et al. 2011; Yu et al. 2014). Zhao et al highlighted the importance of miRNAs in viral infection, and this project hopes to use similar techniques to develop an understanding of the roles played by the miRNAs encoded by HVT and MDV-2 in virus biology.

1.2 Introduction to miRNAs

1.2.1 History of discovery

miRNAs are a class of small non-coding RNAs approximately 22 nucleotides in length and have been identified within a vast array of multicellular organisms and viruses. The term 'miRNAs' was first adopted in 2001 (Ambros 2001); however, the first identification of a miRNA was in 1993 with the description of *lin-4* in *Caenorhabditis elegans (C. elegans)* (R. C. Lee et al. 1993). Lee et al discovered that the *lin-4* transcript in *C. elegans* didn't encode a protein, but instead generated two short RNA

transcripts that repressed the developmental nuclear protein *lin-14*, through complementarity with the 3'UTR of *lin-14* (R. C. Lee et al. 1993).

The importance of this finding was not established until the discovery of a second miRNA encoding gene *let-7* in 2000 (Reinhart et al. 2000). *Let-7* was later found to be conserved in a wide range of organisms (Pasquinelli et al. 2000) suggesting further the importance of these small regulatory miRNAs.

1.3 Identification of novel miRNAs

Once the importance of miRNAs was recognised, it was initially estimated that the human genome could code for just a few hundred miRNAs (Lim et al. 2003), however these initial estimates proved to be a long way off and it took many years for the scale of their expression in a multitude of different species to be understood (Berezikov et al. 2006). The difficulty in identifying the number of miRNAs initially was due to a lack of understanding of exactly what a miRNA was. In 2003 Ambros et al set out criteria for what defines a miRNA, and this has continued to be the benchmark for deciding which small RNAs are miRNAs or not (Ambros et al. 2003). Broadly speaking three criteria should be met; a mature miRNA should be a 'distinct transcript' under 22nt long that is experimentally detectable, it should have been processed from a longer precursor with a hairpin in its secondary structure and finally the mature miRNA should be processed from the precursor by Dicer (Ambros et al. 2003), summarised in (Berezikov et al. 2006). In practise however, not all miRNAs have been found to satisfy all these (and other additional) criteria, however being produced from a hairpin precursor (pre-miRNA) is essential to be considered as a mature miRNA (Ambros et al. 2003).

Forward genetics (identifying a genotype from a phenotype) was responsible for the discovery of the first two miRNAs *lin-14* and *let-7* as described previously, however only a few additional miRNAs have been identified in such a manner during subsequent years. Therefore other methods of identification have been devised. Initial experimental approaches required cloning of small RNA sequences into plasmids followed by Sanger sequencing and further analysis (Aravin and Tuschl 2005). This was a time

intensive procedure as each clone had to be individually amplified and prepared for sequencing, additionally this method had the disadvantage the detection of highly expressed miRNAs was greatly favoured (He and Hannon 2004).

An improvement on the original experimental approach includes the isolation of small RNA species followed by next generation sequencing (NGS) This approach eliminates the need for time-intensive cloning techniques, required in the Sanger sequencing method and additionally allows the sequencing of large numbers of small RNAs in a single run (Aldridge and Hadfield 2012). New miRNAs are discovered through direct observation of their mature sequences, following sequencing, and subsequent validation of correct folding of flanking genomic DNA, using computer modelling (Berezikov et al. 2006).

In the absence of experimental validation (or in addition to), *in silico* predictive algorithms have also been widely utilised (Jha and Shankar 2013). As costs of NGS methods continue to decrease, they are now routinely used to profile miRNA expression in different samples, where previously methods such as microarray and qRT-PCR had been used.

1.3.1 Cataloguing of further miRNA discoveries

In the past decade the number of miRNAs that have been discovered has grown exponentially although now tailing off as a result of the proliferation of whole genome sequencing studies. The sequences of miRNAs are catalogued in miRBase the *de facto* miRNA database, hosted and maintained by the Faculty of Life Sciences at the University of Manchester (www.mirbase.org) (Griffiths-Jones 2004; Griffiths-Jones et al. 2006; Griffiths-Jones et al. 2008; Kozomara and Griffiths-Jones 2011). The most current release (v. 21) contains over 35,000 mature miRNAs, spanning 223 different animals, plants and viruses. Within this ever-expanding database of miRNAs there have been 502 mature miRNAs identified in viruses, of which 474 are within the family *Herpesviridae,* including 90 within the genus *Mardivirus* (MDV-1, MDV-2 and HVT).

1.4 miRNA biogenesis and function

1.4.1 Canonical biogenesis pathway

The synthesis of miRNAs can be broadly grouped into five stages (Kim 2005). The first stage requires the transcription of a large 5'-capped polyadenylated transcript that is transcribed by an RNA Polymerase-II (Cai et al. 2004; Y. Lee et al. 2004a). This primary miRNA transcript (pri-miRNA) frequently contains more than one miRNA sequence with clusters of up to eight miRNAs being identified in some pri-miRNA transcripts (Altuvia et al. 2005). The second step involves the cleavage of the large pri-miRNA sequence into hairpin precursors of miRNAs; pre-miRNAs. These smaller (~60-80nt) pre-miRNAs each encode a single mature miRNA, which are excised from the pri-miRNA by the Microprocessor complex, consisting of the nuclear RNAseIII *Drosha* and its cofactor *DGCR8* (DiGeorge syndrome critical region gene 8), or Pasha in *C. elegans* and *Drosophila* (figure 2) (Y. Lee et al. 2003; Yeom et al. 2006).

The third stage requires the transport of the pre-miRNA from the nucleus to the cytoplasm to allow further processing. Exportation of the pre-miRNA is a Ran-GTP dependent process involving the nuclear export receptor Exportin-5 (Lund et al. 2004; Yi et al. 2003). Following nuclear export the pre-miRNAs are further processed by the cytoplasmic RNaseIII Dicer (Y. S. Lee et al. 2004b) in complex with cofactors (e.g. TRBP in humans (Chendrimada et al. 2005)) to ~22nt long mature miRNAs (figure 2). The removal of the stem-loop from pre-miRNA leads to the formation of a short-lived asymmetric duplex intermediate; (miRNA*: miRNA duplex) (Cai et al. 2004). The strand within the duplex that becomes the active mature miRNA is largely dependent upon which strand has the lowest free energy 5' end (Khvorova et al. 2003) (i.e. the strand with 5' unstable base pairing). The final step in creating a miRNA silencing complex involves the loading of the mature miRNA, along with the Argonaute protein (Ago 1-4) and other co-factors, creating miRNA induced silencing complex (miRISC) where the miRNA targets the miRISC to silence gene expression of its target (Gregory et al. 2005).

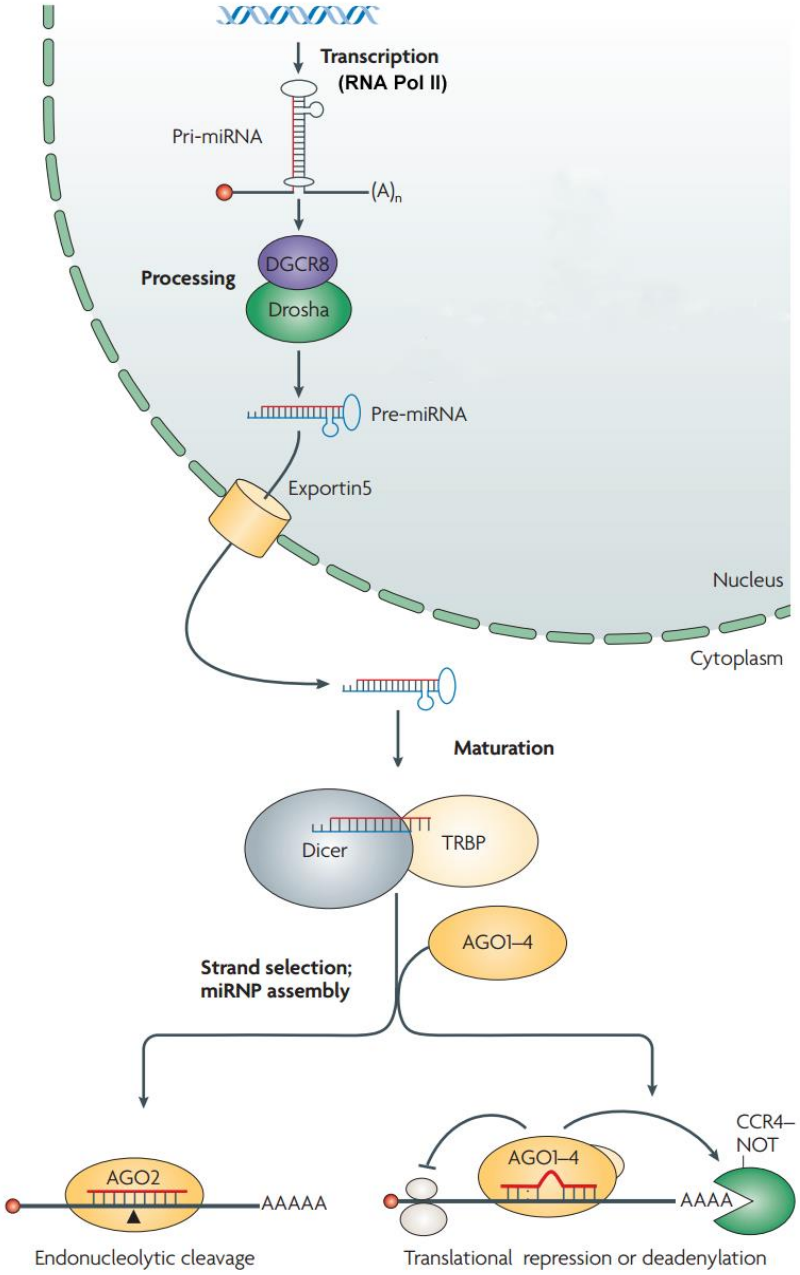


Figure 2 – Canonical miRNA biogenesis pathway leading to miRNA-induced gene expression regulation. Adapted from (Filipowicz et al. 2008).

1.4.2 Post-transcriptional regulation by miRNAs

Earliest discoveries of miRNA function came about following studies where key components of the miRNA biogenesis pathway were mutated and the effects were observed. In one study, mutants of the endoribonuclease Dicer showed a variety of developmental defects (Hatfield et al. 2005; Knight and Bass 2001). Similar developmental defects were also observed following disruption of the Argonaute protein, another component of the miRNA biogenesis pathway (Grishok et al. 2001). It is now known that miRNAs function through base-pairing to their target mRNAs which regulates protein synthesis.

The majority of studies agree that an overwhelming percentage of miRNAs bind 'imperfectly' within the 3'-untranslated region (UTR) of their target sequence (Gottwein and Cullen 2008). An exception to this non-canonical binding occurs within the 'seed' region of the miRNA (positions 2-8) where perfect or near perfect homology with the target is usually seen (Brennecke et al. 2005; Brodersen and Voinnet 2009; Doench and Sharp 2004). In addition to binding in the 3'UTR, binding can also occur in the coding sequence or the 5' UTR of the target gene (Forman et al. 2008; Zhou et al. 2009). Broadly speaking miRNAs inhibit protein synthesis through translational repression or deadenylation that brings about degradation of the mRNA target (reviewed (Chekulaeva and Filipowicz 2009; Eulalio et al. 2008; Filipowicz et al. 2008) and sumarised in figure 3).

Initial work carried out by the pioneers in the field of miRNAs, suggested that the levels of miRNA-targeted mRNAs remained unchanged despite a decrease in the protein levels. However as work continued in this field, more studies have observed a decrease in the levels of target transcript. Data from transcriptome studies where miRNA levels have either been decreased (by inhibition) or increased (by artificial expression) have seen corresponding changes in transcript levels (Krutzfeldt et al. 2005; Lim et al. 2005; Schmitter et al. 2006). Since the vast majority of miRNAs do not bind with complete homology to their target, degradation is not a result of endonucleolytic cleavage. Many plant miRNAs have perfect homology to their target mRNAs, where the actions of miRNAs are tantamount to that of siRNAs, leading to mRNA degradation (Ossowski et al. 2008), however there are examples of

non-perfect matches have been described (Brousse et al. 2014). Perfect homology in animals is rare and only a few examples exist such as *miR-196* (Gottwein and Cullen 2008; Yekta et al. 2004).

Instead animal miRNAs have been shown to direct their targets to the mRNA decay pathway, where upon removal of the poly-A tail the transcript is decapped and digested 5'-to-3' via endonucleases (Eulalio et al. 2009; Giraldez et al. 2006; Huntzinger and Izaurralde 2011; Piao et al. 2010).

Mechanisms of translational repression are less well understood. Evidence suggesting mechanisms of translational repression at both the initiation and post-initiation stages of translation have been proposed. The miRNA directed recruitment of the RISC to the target transcript has been shown to 'block' the binding of crucial components of translation, thus inhibiting protein synthesis at the initiation stage (Mathonnet et al. 2007; Thermann and Hentze 2007). More evidence for translational repression at the post-initiation stage of translation includes early studies describing miRNA-targeted transcripts that showed no sign of decreased abundance, and were still recruited to polysomes (i.e. translation has been initiated) (Olsen and Ambros 1999; Seggerson et al. 2002). A model to explain the findings of these studies (and other supporting studies) was proposed by Petersen et al. This model suggested that miRNAs caused the ribosome to dissociate before completing translation of the transcript. This was supported by their findings of miRNAs being found on actively translated mRNAs and the fact that miRNAs can target transcripts that are translated independently of cap-proteins (Petersen et al. 2006).

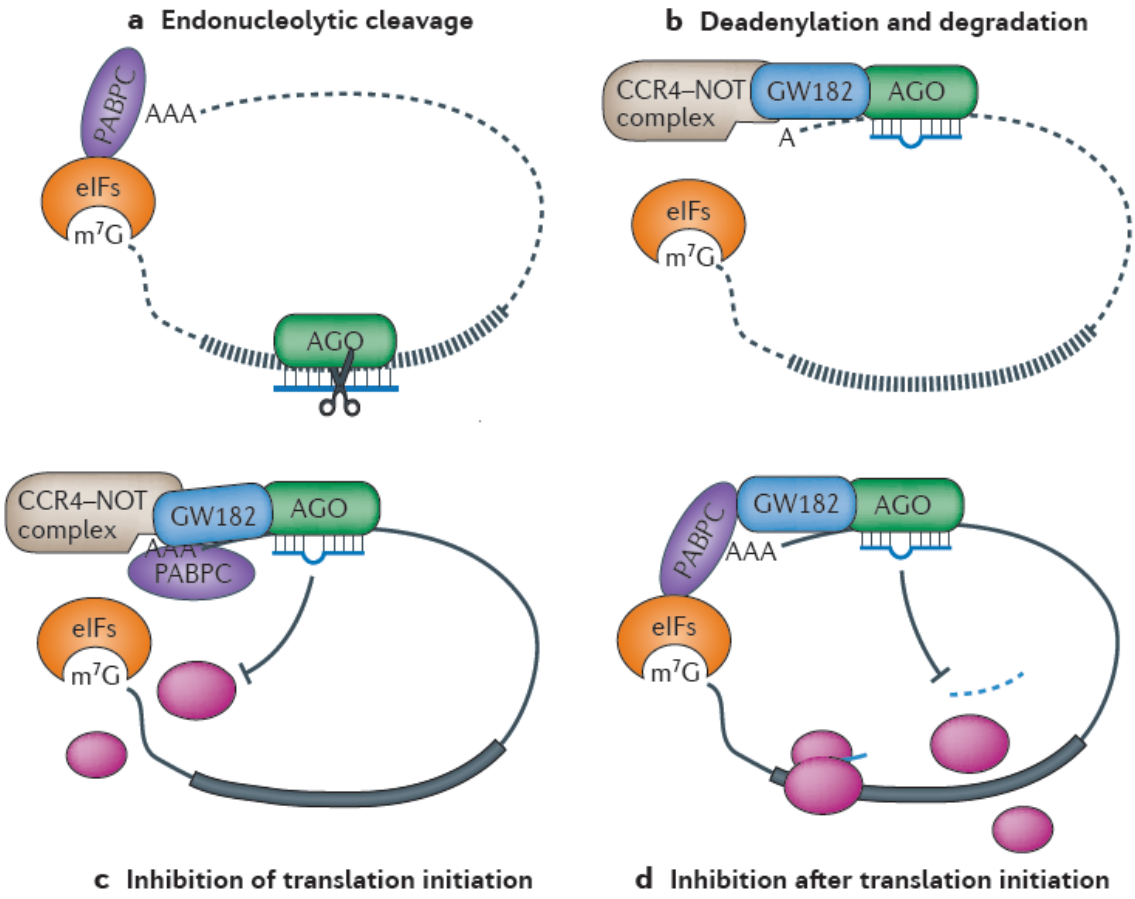


Figure 3 - Schematic representation of the different mechanisms of miRNA mediation gene expression regulation. Adapted from Pasquinelli, 2012 (Pasquinelli 2012)

Support for a model of target mRNA destabilisation and degradation model was provided by Guo et al (H. L. Guo et al. 2010) wherein their large scale study found that 84% of miRNA-mediated protein repression can be accounted for by a decrease in mRNA levels. Additionally a review by Huntzinger and Izaurralde gives their support to target degradation being the main contributor to repression (Huntzinger and Izaurralde 2011) making it arguably the best model for miRNA regulation at present.

1.5 Epigenetics and miRNAs

The term epigenetics broadly describes the mechanisms within a cell that can cause changes in gene expression, which do not involve altering the underlying DNA sequence. Research in this field has expanded in recent years, since the involvement of epigenetics was identified in numerous physiological events including embryogenesis and cancer (Taby and Issa 2010). The involvement of epigenetics in cancer challenged the original view that genetic alterations were solely responsible.

The most widely studied epigenetic mechanisms are: DNA methylation, histone modifications and noncoding RNAs. In DNA methylation and histone modification, gene expression is repressed by the presence of repressor proteins that attach to a certain region of the DNA, and these changes to gene expression are preserved for multiple cell divisions (Bird 2007).

The mechanisms of epigenetics do not only regulate the expression of protein coding genes, DNA methylation and histone modification has been implicated in the expression levels of a number of mammalian miRNAs; including *miR-9*, *miR-34* and *miR-148* (Sato et al. 2011). Equally miRNAs have been previously identified to regulate various regulators of epigenetics, including the expression of certain DNA Methyltransferases (DNMTs) (Fabbri et al. 2007) and histone deacetylases (Noonan et al. 2009). It is therefore appropriate to consider epigenetics and miRNAs as a complicated "epigenetics–miRNA regulatory circuit" which can work together to organise the gene expression profile of the cell (Sato et al. 2011).

1.6 miRNA functional understanding through identifying miRNA targets

Since the first study linking the dysregulation of miRNA expression with disease (Calin et al. 2002) abberant expression of miRNAs has been associated with many types of disease ranging from diabetes (Zhu et al. 2011) to heart disease (van Rooij et al. 2006). In particular, it has been suggested that dysregulation of miRNAs are probably involved in all human cancers (Croce 2009).

While a great deal of research has been carried out to identify which miRNAs are dysregulated in which diseases, much less is known about the biological mechanisms by which they act. In particular, identifying the *true* target genes that are regulated by specific miRNAs (the targetome) is currently a hotly debated topic in miRNA research.

The major problem of identifying miRNA target genes is that animal miRNAs show only limited sequence homology to their target mRNA making their identification difficult to predict. Both biological and bioinformatic approaches to targetome identification are currently employed by miRNA researchers and their relative strengths and weaknesses are discussed.

1.6.1 Bioinformatic Approaches

There are multiple different bioinformatic target prediction algorithms available, each one focusing on slightly different criteria to determine a predicted target. Target prediction programs such as TargetScan and picTar, look for their predictions upon the fulfilment of criteria, including some degree of base pairing (especially within the seed region), stability of the miRNA:mRNA duplex, conservation of target region across species and the presence of multiple target sites within transcript. Not all of these criteria have to be fulfilled and different algorithms place an emphasis on different criteria. Table 1 lists some of the most frequently used algorithms, summarising the different search criteria utilised by each algorithm (Shirdel et al. 2011). A number of the different considerations taken by different prediction algorithms, and the implications of each, are discussed briefly below.

The importance of base pairing between the seed sequence and its target transcript is now well established; therefore all miRNA target prediction algorithms require a seed sequence match within the predicted mRNA target, allowing for some mismatches and a G:U 'wobble' match (Shirdel et al. 2011). The conservation of the predicted miRNA targeting site within the transcript is taken into consideration by many of the prediction algorithms as it is thought to increase the reliability of predictions (Shirdel et al. 2011). Unlike a seed sequence match, this is not taken into consideration by all algorithms.

The free-energy of the miRNA:target mRNA interaction is taken into account by a number of algorithms. This is a measure of the energy required to form a duplex between the miRNA and target mRNA transcript (Shirdel et al. 2011). Often a threshold in set to determine favourable miRNA:mRNA interactions, increasing the liklihood of a genuine interaction being predicted (Rehmsmeier et al. 2004).

Accessibility of the target site of the miRNA is taken into consideration with the Probability of Interaction by Target Accessibility (PITA) algorithm, the energy required for the target mRNA to fold so that miRNA can get to the target site is calculated as a ΔΔG value where a more negative ΔΔG suggests a more favourable folding energy for a miRNA:mRNA interaction to occur (Shirdel et al. 2011). The results from PITA do suggest that by considering the accessibility of the target site the conservation of the target site is inadvertantly considered, because accessible regions of the 3'UTR frequently fall within conserved regions (Kertesz et al. 2007).

As new experimentally validated targets of miRNAs are elucidated they are collated into specialised databases. A commonly used example is miRecords (Xiao et al. 2009) which not only lists validated targets, but also can be used to show which algorithms predicted these targets. Information gained from the interactions between miRNAs and validated targets has been used to tweak existing programs and develop new ones, increasing prediction accuracy. Despite the advancement of biochemical techniques to identify candidate target genes of the miRNAs, prediction algorithms

continue to be maintained, updated and remain the major mechanism used to assign function to specific miRNA in many areas of miRNA research (Hunter et al. 2013; Meijer et al. 2013).

	Targetscan Conserved	Targetscan Non-Conserved	micro-RNA.org	microCosm (formerly mirBase)	PITA Top Hits	PITA All Hits	picTar 4-way	picTar 5-way	DIANA microT
Conservation	X*		X	X	§	§	X	X	X
Site Accessibility					X	X			
Local AU content	X	X							
Multiple Binding Sites (1 microRNA)	X	X	X	X	X	X	X	X	X
Multiple Binding Sites (>1 microRNA)							X¥	X¥	
Uses miRanda			X	X					
Free Energy of Duplex			X	X	X	X	X	X	X
Examines surrounding Sequence	X	X			X	X			
Weighted 5′ end or considers seed type	X	X	X	X					X

*Targetscan Conserved uses conservation, but it is not integrated into the context score.
§PITA does not explicitly use conservation in scoring targets. However, accessible microRNA binding sites tend to show high conservation.
¥picTar does have predictions for multiple microRNAs binding to a single 3′ UTR; however, that data was not used in this study.
doi:10.1371/journal.pone.0017429.t002

Table 1 – Adapted from (Shirdel et al. 2011) which lists commonly used miRNA target prediction programs and highlights the different characteristics that miRNA:transcript interactions looks for when scoring the likelihood of an interaction.

When using miRNA target prediction programs to find candidate miRNA targets, many studies use multiple algorithms and look for consensus between the different programs to identify higher confidence targets (Zhang and Verbeek 2010). Proper integration of multiple prediction programs has been shown to increase accuracy of the predictions. However targets predicted by the combination of programs are still not guaranteed to be genuine and therefore experimental validation within the system being studied remains essential. This is especially true as the same miRNA can target different genes under different circumstances. For example, *miR-222* is over-expressed in hepatocarcinoma where it targets tumour suppressor PTEN (Garofalo et al. 2009), but is down-regulated in erythroblastic leukaemias where it targets the KIT oncogene (Felli et al. 2005).

The problem faced in this study, and others, is that the vast majority of algorithms are designed to find mammalian targets of mammalian encoded miRNAs (particularly human, mouse and rat) and do not allow custom database integration such as is required in viral studies. With this limitation in mind we were restricted to the use of a single algorithm for our research (TargetScan). The TargetScan custom algorithm allows the user to input the seed region of their miRNA of interest (nucleotides 2-8) and then asks the user to select, from a list of species, within which one to find predicted targets. The results generated by TargetScan custom contain only targets that are conserved across species, this adds another level of confidence, but could also miss some species specific targets.

1.6.2 Biochemical Approaches

Although bioinformatic approaches to miRNA target discovery have progressed over the last decade they are still far from perfect, and frequently predict a high number of false positive results (Didiano and Hobert 2006; Lewis et al. 2005). Subsequently a number of biochemical approaches to miRNA target identification have been developed, some of which are discussed in this section and summarised in figure 4.

The initial biochemical approaches to identifying miRNA target genes relied on the immunoprecipitation (IP) of the miRISC (frequently using antibodies directed toward the Ago-2 protein

of the complex) coupled with the targeted transcript. These transcripts immunoprecipitated in complex with the miRISC were then analysed by microarray (RIP-ChIP) (Beitzinger et al. 2007; Dölken et al. 2010b; Hendrickson et al. 2008; Landthaler et al. 2008). An early example of using this RIP-CHIP methodology to identify targets of viral miRNAs was performed by Dölken et al on Epstein–Barr virus (EBV) and Kaposi's sarcoma-associated herpesvirus (KSHV) encoded miRNAs (Dölken et al. 2010b). In this study, cells expressing the viral miRNAs, through either lentiviral expression or latent infection were used for immunoprecipitation, following lysis. A monoclonal antibody to human Ago2 was used for the immunoprecipitation of the miRISC complex, which was loaded onto Protein G Sepharose beads in a column. The efficiency of the IPs was determined by measuring the enrichment of miRNAs in the Ago2 IP sample compared to a negative control, by miRNA TaqMan. Microarray analyses were performed to identify which transcripts were in complex with the miRISC. Thresholds of enrichment were set by the group to try and determine transcripts that were genuinely in complex as a result of miRNA-directed targeting. Transcripts found significantly enriched in IPs were screened for potential target sites for the corresponding miRNAs. Luciferase reporter assays were then performed to determine if that transcript was in fact being targeted by that viral miRNA.

Some concerns were raised against these initial methods, suggesting that post cell lysis association of mRNA transcripts to the immunoprecipitated RISC was possible (Mili and Steitz 2004). In response improved methods have been developed with an initial ultraviolet (UV)-crosslinking of the transcripts to the RISC. Cells or tissues are subjected to UV radiation prior to any lysis which cross-links, and thus stabilises the targeted mRNA transcripts to the RISC. Cells are then lysed, followed by RNase treatment, degrading all RNA fragments that are not offered 'protection' within the RISC (Pasquinelli 2012). These RNA RISC protected fragments are then analysed with high-throughput sequencing (HITS-CLIP) (Chi et al. 2009). The large datasets of RNA fragments then undergo complex bioinformatic analysis to identify the genes the RNA fragments belong to, and thus a library of genes found associated with miRISCs is produced. A variation of this technique called Photoactivatable-Ribonucleoside-Enhanced Crosslinking Immunoprecipitation (PAR-CLIP) is currently being used to great

effect to identify targets of miRNAs (Hafner et al. 2010). In this technique cells are cultured with photoreactive ribonucleoside analogues, such as 4-thiouridine (4-SU) and 6-thioguanosine (6SG), then prior to lysis, are subjected to irradiation by 365nm UV light to induce cross-linking of RNAs (containing 4-SU or 6SG) to the miRISC. Immunoprecipitation of the miRISC is preceded by the isolation of the cross-linked and co-immunoprecipitated target transcripts. These RNAs are then converted in a cDNA library which undergoes deep sequencing using high-throughput sequencing technology (Hafner et al. 2010).

Recently an additional method for identifying miRNA targets has been developed, cross-linking ligation and sequencing of hybrids (CLASH) (Helwak et al. 2013). Compared to the cross-linking methodologies described above, CLASH identifies the specific site of miRNA targeting within the target mRNA transcript. This is done by ligating together the miRNA-target duplexes that are linked to the previously isolated AGO protein. As in other methods a cDNA library is generated, but when the sequence is analysed, CLASH will identify which miRNA is targeting which mRNA transcript and the specific site of targeting within that transcript. This removes the need for any bioinformatic prediction of miRNA targeting, and has already produced interesting data which challenges previously established ideas of miRNA targeting, such as to which regions of target mRNAs are targeted by miRNAs. Most notably the fact that the largest proportion of miRNA targeting in their study appeared within the coding region of mRNA transcripts not the 3'UTR as commonly thought (Helwak et al. 2013). These approaches do still have their drawbacks as it should be noted that if a transcript is found associated with a miRISC this offers no guarantee that it is under miRNA regulation. Furthermore in endogenous conditions further predictions and validation is required to identify the miRNA that is responsible for the targeting of the RISC (Pasquinelli 2012).

When the targets of individual, or small clusters of, miRNAs are of interest, their levels can be artificially increased or decreased and the subsequent effects analysed. There are a range of different methods to change miRNAs levels, from locked nucleic acid (LNA) (Elmen et al. 2008) and miRNA

'sponges' (Ebert et al. 2007) (down-regulation), to miRNA mimics (commercially available from a number of suppliers) and miRNA expression vectors (Y. Zhao et al. 2009) (up-regulation). The effect of changes in levels of miRNAs can be observed through both RNA-expression analysis and protein-expression analysis. Genome-wide RNA expression analyses include the methods described previously (microarray and deep-sequencing), and changes in levels of specific transcripts (brought about through mRNA destabilisation) can be observed by Northern blotting and quantitative PCR (qPCR) (Pasquinelli 2012).

Protein-expression analyses are also used in conjunction with miRNA inhibition or over-expression studies to give a picture of the outcome of miRNA-mediated gene regulation (Pasquinelli 2012). As with RNA studies, specific targets can be analysed with western blotting (Y. Zhao et al. 2009), or whole proteome changes can be studied using various methods of mass spectrometry (Jovanovic et al. 2010; Selbach et al. 2008). Often, protein-expression assays are not sensitive enough to show small changes in protein level or changes in the levels of low-abundance proteins (Pasquinelli 2012). However, if a change can be confidently seen in the protein level of a miRNA target then it could be argued that the miRNA is likely having a physiological effect on that gene (Ebert et al. 2007).

As more data is being published identifying targets of host encoded miRNAs, databases now exist where one can search for miRNA targets that have both been predicted through bioinformatics and targets that have been experimentally validated (Hsu et al. 2011).

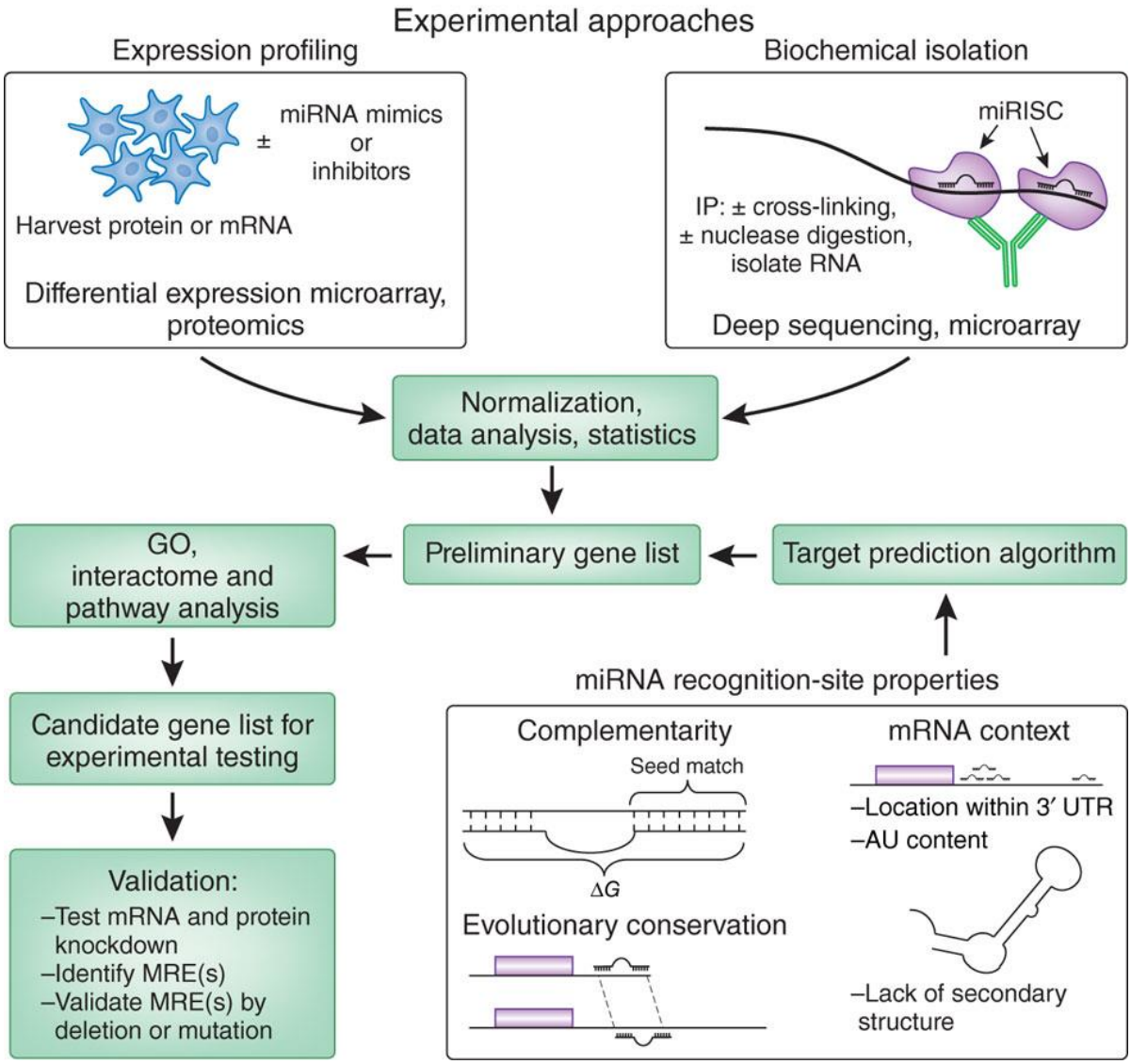


Figure 4 - Overview of different experimental strategies for identifying miRNA targets. Taken from (Thomas et al. 2010).

1.7 Viral miRNAs

The lack of immunogenicity, functional flexibility and small size are potentially advantageous characteristics of miRNAs in their role as virally encoded regulators of both viral and host cell gene expression. MiRNA expression in viruses is almost exclusively restricted to DNA viruses and in particular herpesviruses (Griffiths-Jones 2004; Griffiths-Jones et al. 2006; Griffiths-Jones et al. 2008; Kozomara and Griffiths-Jones 2011). Why this should be the case is the subject of much debate. Viral miRNAs are also detectable in other DNA virus families (i.e. polyomavirus and adenovirus) but the validity of miRNAs reported in RNA viruses, such as HIV remain contentious. Although there are four reported mature miRNAs (*hiv1-miR-H1, hiv1-miR-N367, hiv1-miR-TAR-5p, hiv1-miR-TAR-3p*) encoded by the HIV-1 genome, the failure to detect these miRNAs by other researchers, as well as questions raised about the proposed mechanisms of miRNA processing in RNA viruses initially resulted in scepticism (Cullen 2011). However later detection and validation of miRNAs encoded by another retrovirus bovine leukaemia virus (BLV), in the persistently infected B-cell line BL3, plus the description of a processing pathway by which the BLV pre-miRNAs are only processed from RNA polymerase III transcripts has once again reopened the debate (Kincaid et al. 2012). The finding of this study prompted Klase et al, to once again propose new criteria for what constitutes a viral miRNA (Klase et al. 2013)

1.7.1 Biogenesis

Nearly all viral miRNAs are processed via the canonical pathway (described in section 1.4.1). However in the case of adenovirus and murine γ-herpesvirus different initial processing pathways are also utilised to produce functional miRNAs (Cullen 2011). In adenoviruses, RNA polymerase III produces a highly-structured RNA species of ~160nt , *VA1*. This RNA is then directly exported from the nucleus via exportin 5 where it interacts with Dicer to produce miRNAs via the miRNA canonical pathway (S. H. Lu and Cullen 2004). In the case of murine γ-herpesvirus MHV68 a tRNA/pre-miRNA hybrid is produced by RNA polymerase III, this is processed in the nucleus by tRNase Z (as opposed to Drosha) to produce

two pre-miRNA stem-loops which are then exported and processed further via the canonical pathway (Bogerd et al. 2010).

1.7.2 Virus regulation of viral miRNA expression

Viral miRNA expression by the virus has been shown to be regulated both during transcription and post-transcription (Cullen 2011). Transcriptional regulation is clearly implicated in the expression of Epstein-Barr Virus (EBV) miRNAs. EBV miRNAs are expressed in two distinct pri-miRNA clusters, the *miR-BHRF1* miRNA cluster and the *miR-BART* miRNA cluster, and the levels of expression of the mature miRNAs are quite different (Cai et al. 2006). It has been observed in other viruses, that the expression of some miRNAs appears to be driven by certain promoters driving gene expression in the different stages of viral infection, from acute replication to latency (Grey et al. 2005; Jurak et al. 2010; Sullivan et al. 2005), all suggesting that the virus is capable of controlling miRNA expression to help control the environment within the infected cell. Evidence for post-transcriptional regulation of viral miRNAs comes from work on the expression of certain KSHV miRNAs. It has been reported that two KSHV miRNAs, *miR-K4* and *miR-K7*, have very different levels of expression despite being encoded by the same pri-miRNA transcript. A similar phenomenon has also been observed with miRNAs from EBV (Pratt et al. 2009) and Herpes Simplex virus serotype 1 (HSV-1) (Umbach et al. 2009). This differential expression of distinct miRNAs arising from the same pri-miRNA transcript appears to be the result of post-transcriptional regulation by different components of the miRNA biogenesis pathway as well as differential rates of miRNA degradation (Davis and Hata 2009).

Additionally some studies have shown an 'artificial' inhibition of virus replication by cellular miRNAs, by mutating viruses to contain target sites for some tissue-specific miRNAs, creating attenuated strains of the virus (Barnes et al. 2008; Kelly et al. 2008). However, natural targeting of host miRNAs to viral genomes remains unlikely, as it has been suggested that it would be too easy for the virus to select for mutations in the target site of cellular miRNAs that would have a deleterious effect on the virus replication (Cullen 2011).

It has been demonstrated also that co-infection of viruses can affect the miRNA expression profiles of viruses. The expression levels of a number of HVT and MDV-1 miRNAs was shown to be altered upon co-infection with both viruses, with *mdv1-miR-M2-3p, hvt-miR-H17-3p, hvt-miR-H7-5p and hvt-miR-H13* all showing significant up-regulation at both 7dpi and 42dpi (Goher et al. 2013). This particular observation suggests there is interplay between the viruses that regulates the expression of viral miRNAs over the course of an infection.

1.7.3 Targeting of viral miRNAs

In recent years a great deal of work has been performed to identify the probable cellular targets of miRNAs encoded by different viruses. Once processed, viral miRNA are thought to target transcripts in a similar manner as host miRNAs (Gottwein and Cullen 2008) (summarised in figure 5). Recent reviews highlight a number of host transcripts which are targeted by virally encoded miRNAs (Grundhoff and Sullivan 2011; Skalsky and Cullen 2010; Kincaid and Sullivan 2012) (and references therein). From the studies reviewed in these articles (and summarised below) it has become clear that viruses have utilised miRNAs as a tool to control the environment they are in and to defend themselves against the host immune response.

1.7.3.1 Regulation of cell death in virally infected cells

If a virus wishes to persist in an infected cell it must disrupt the apoptotic pathways that lead to cell death. EBV encoded miRNAs have been shown to target, the pro-apoptotic genes; p53 upregulated modulator of apoptosis (*PUMA*) (Choy et al. 2008), Bcl-2-like protein 11 (*BIM*) (Marquitz et al. 2011) and BCL2-associated transcription factor 1 (*BCLAF1*) (Riley et al. 2012). Additionally both Human cytomegalovirus (HCMV) and KSHV miRNAs have both been shown to target *BCLAF1* (Lee et al. 2012; Ziegelbauer et al. 2009), while MDV1-encoded miRNA *miR-M3* has been shown to target the host Mothers against decapentaplegic homolog 2 (*SMAD2*) gene, leading to a reduction in induced apoptosis *in vitro* (Xu et al. 2011).

1.7.3.2 Roles in the induction of tumours

It has been suggested that the promotion of tumourigenesis by virally encoded miRNAs is a consequence of the virus utilising miRNAs in immune evasion, prevention of cell death and cell cycle regulation, and actually provides no advantage for the virus (Moore and Chang 2010). Nonetheless, expression of miRNAs encoded by EBV, KSHV and MDV-1 has been implicated in the induction of tumours (Kincaid and Sullivan 2012). KSHV and MDV-1 have both been shown to encode a functional ortholog of the host encoded miRNA *miR-155* (Skalsky et al. 2007; Zhao et al. 2009); a well-established oncomiR (Jiang et al. 2010). The importance of the MDV-1 miRNA *miR-M4* in inducing tumours was proven *in vivo* by the decreased ability of a *miR-M4* knockout virus to induce tumours in infected chickens (Zhao et al. 2011). However a recent publication has shown slightly different results in very virulent MDV-1 infected birds, demonstrating *mdv1-miR-M4* is not essential to oncogenicity but does still play an important role (Yu et al. 2014).

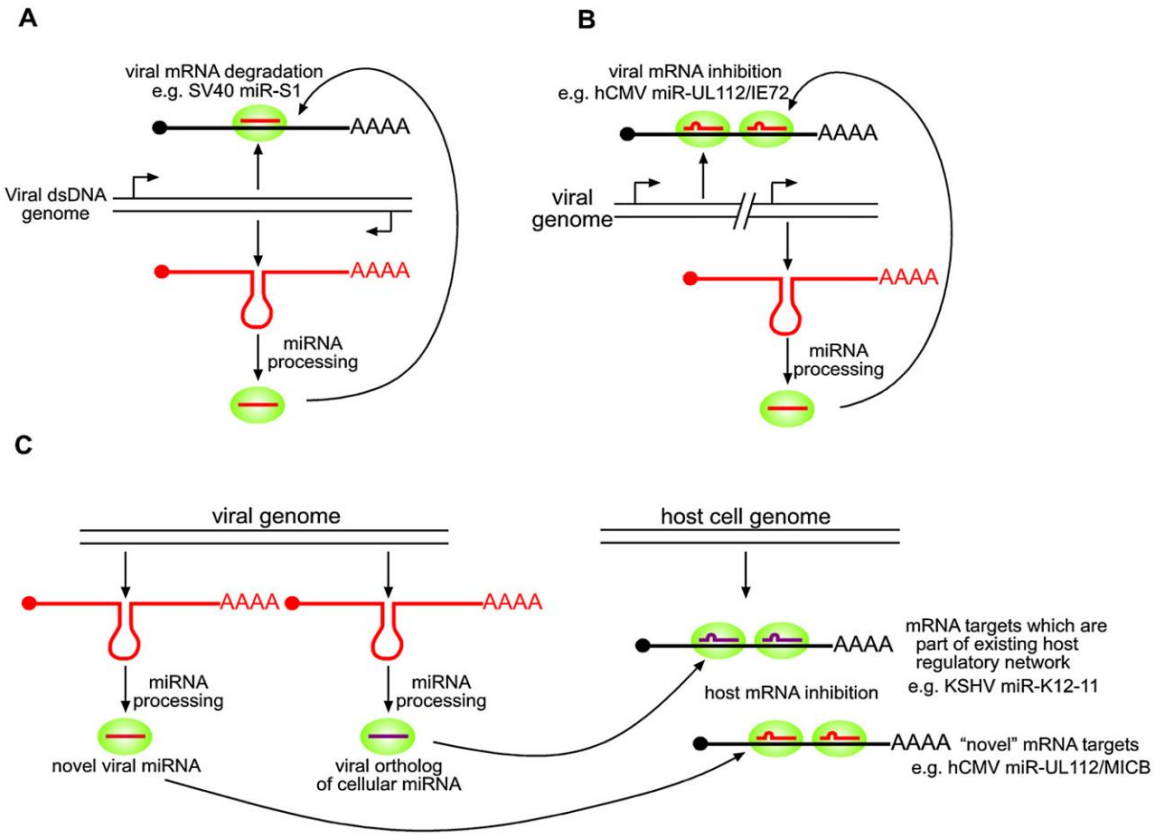


Figure 5 - An overview of the mechanisms of function of virally encoded miRNAs**.** A and B show viral miRNAs regulating the expression of viral genes through either complete pairing of miRNA and target leading to degradation (A) or incomplete miRNA pairing to target resulting target repression (B). C shows viral miRNAs targeting host cell encoded mRNAs. Taken from (Gottwein and Cullen 2008).

1.7.3.3 Roles in evading the host immune response

Studies on Simian vacuolating virus 40 (SV40) -encoded miRNAs showed they target early viral transcripts, thus resulting in decreased early gene expression during lytic replication (Sullivan 2008). The implications of SV40 miRNAs being utilised in the evasion of immune response came from a study in which there was increased cytotoxic T-cell lysis of cells infected with a miRNA mutant virus, compared to miRNA positive virus (Sullivan et al. 2005). A miRNA encoded by murine polyomavirus (muPyV) has also been shown to negatively regulate viral early gene expression in this manner, suggesting that it too, could be involved in evading the immune response (Nachmani et al. 2009).

Strong evidence for miRNA involvement in viral evasion of the immune response had been demonstrated through *in vivo* miRNA deletion study in murine cytomegalovirus (MCMV). Deletion of *miR-M23-2* and *miR-M21-1* from MCMV resulted in reduced viral titres in some mice. The link between these miRNAs immune evasion was further demonstrated in this study, when the phenotype was reverted in mice lacking key elements of the adaptive and innate immune response (Dölken et al. 2010a).

1.7.3.4 Controlling virus lytic cycle

By restricting the lytic phase of virus replication, miRNAs can help maintain persistent infection in the host. A number of virally encoded miRNAs have been shown to regulate latent to lytic infection balance by targeting regulators of these cycles, including in HSV-1, KSHV and HCMV (Kincaid and Sullivan 2012). One such example is the targeting of the KSHV miRNAs *miR-K12-7-5p* and *K12-9-5p* of the master lytic switch protein (*RTA*) transcript that leads to maintenance of latent infection (Bellare and Ganem 2009; Lin et al. 2011).

1.7.4 Finding targets of viral miRNAs

There are two broad approaches to look for targets of viral miRNAs. The first approach follows the over-expression of viral miRNAs in cells (through either infection or artificial delivery) and identifies potential targets utilising methods described previously and deducing which are likely to have a

relevant effect on virus replication. The second is a 'top-down' approach, following mutation or deletion of the viral miRNAs (Grundhoff and Sullivan 2011). Ideally both approaches should be used to increase confidence in miRNA target identification, as is commonly done in the study of other gene regulation mechanisms, such as transcription factors (Atkins and Jain 2007).

1.7.5 Targetome studies in MDV-1 and EBV

Recently a large study of the global targets of the EBV miRNAs has been completed (Skalsky et al. 2012). This study uses an adaptation of a miRISC immunoprecipitation method described in section 1.6.2, PAR-CLIP (Hafner et al. 2010) which, in addition to UV-crosslinking the miRISC to target transcripts, combines a photo-reactive ribonucleoside analogue mapping of the precise site of miRNA–mRNA interaction. Combining PAR-CLIP with deep sequencing has produced a comprehensive collection of all targets of miRNA-mediated regulation in the EBV strain B95-8-infected lymphoblastoid cell line. This data set has undergone further bioinformatic analysis to identify which of these miRISC associated transcripts are mediated by viral miRNAs. The results of which, have highlighted a number of validated mRNA transcripts that are targeted for regulation by EBV miRNAs that are considered relevant to viral infection, and thus could highlight new targets for EBV therapeutics (Skalsky et al. 2012).

More recently, similar studies have been reported for the identification of MDV-1 and MDV-2 miRNA targetome (Parnas et al. 2014). This study performed PAR-CLIP analysis on the MSB-1 cell line, which is derived from a chicken T-cell lymphoma that is infected with both MDV-1 and MDV-2 virus. Aspects of MDV-1 and MDV-2 viral miRNA expression that had been previously identified were confirmed by this study, as well as the targeting of viral miRNAs to certain regions of the viral genome and chicken mRNA transcripts. In particular the targeting of multiple MDV-1 and MDV-2 miRNAs to the 3'UTR of interleukin-18 was explored further, demonstrating an impact of viral miRNA targeting on the growth of MSB-1 cells. However the study concludes by confirming that only limited validation and phenotypic analysis of PAR-CLIP identified targets had been performed.

Both the MDV-1 and EBV targetome study mentioned above highlight the global effect that miRNAs can have on gene regulation and biological processes. The biological processes that are implicated in these studies include immunomodulation, cell signalling and apoptosis, all of which could affect immune responses to infection and vaccination.

1.8 Summary of hypothesis

miRNAs are increasingly shown to play major role in the regulation of gene expression in a number of areas of biology, including modulation of immune responses. Additionally virus-encoded miRNAs are significant in virus replication and virus-host interactions, including miRNAs encoded by pathogenic herpesviruses such as MDV, which have been shown to be directly associated with the pathogenesis.

Using either an RNA or proteomics based approach this study hopes to perform a targetome study and identify targets of the MDV-2 and HVT encoded miRNAs to better understand the role that they play in the biology of these viruses.

This hypothesis was tested through a number of approaches by the examination of the putative targets of the virus-encoded miRNAs using established biochemical/proteomic approaches, as well as through functional approaches using modified viruses using the BAC technology.

2 Methods

2.1 Solutions and buffers

2.1.1 Tissue culture

DF-1 cell growth medium

Dulbecco's Modified Eagle Medium	89ml
Fetal Bovine Serum	10ml
Sodium Pyruvate (0.5M)	1ml
100U/ml penicillin & 100µg/ml streptomycin	0.1ml
Fungizone (solubilised Amphotericin B)	0.1ml

Chicken Embryo Fibroblast growth medium

Trypstose Phosphate Broth	50ml
199 medium (10X)	50ml
New born calf Serum	10ml
Na Bicarb (7.5%)	43.5ml
L-Glutamine	5ml
100U/ml penicillin & 100µg/ml streptomycin	0.1ml
Fungizone (solubilised Amphotericin B)	0.1ml
dH_20	380ml

Chicken Embryo Fibroblast maintenance medium

199 medium (10X)	10ml
Fetal Bovine Serum	5ml
L-Glutamine	1ml
100U/ml penicillin & 100µg/ml streptomycin	0.1ml
Fungizone (solubilised Amphotericin B)	0.1ml
dH_20	76ml

2.1.2 Bacterial cell culture

Liquid Lysogeny Broth (LB)

Tryptone	10g
Yeast extract	5g
NaCl	10g
dH_2O	to 1L

Solid Lysogeny Broth

Lysogeny Broth (above)	
Agar	1%(w/v)

Super optimal recovery broth

Bacto-tryptone	20g
Bacto-yeast extract	5g
NaCl (8.65mM)	0.5g
KCl (2.5mM)	0.186g
dH_20	to 1L

Terrific Broth

Tryptone	12g
Yeast Extract	24g
KH_2PO_4 monobasic	2.31g
K_2HPO_4 dibasic	12.54g
Glycerol	4ml
dH_20	to 1L

X-α-Gal

X-α-Gal	0.04g
DMSO	10ml

Antibiotics (Stock concentrations)

Ampicillin	100µg/ml
Kanamycin	50µg/ml
Spectinomycin	100µg/ml
Chloramphenicol	50µg/ml
Puromycin	1µg/ml

2.1.3 Protein analysis

2X SDS loading buffer

Tris-HCl (pH 6.8)	100mM
Glycerol	20%(v/v)
SDS	1%(v/v)
Bromophenol Blue	0.05%(v/v)
β-mercaptoethanol	1%(v/v)

RIPA buffer

Tris-HCl	50mM
NaCl	150mM
SDS	0.1%(v/v)
Triton X-100	1%(v/v)
Proteinase inhibitor cocktail (Roche)	1X
Diluted in dH_2O	

Western Blot Running buffer

NuPAGE MES SDS running buffer	20ml
dH_20	480ml

Western Blot Wash buffer

Tween-20	0.05%(v/v)
PBSa	to 1L

Western Blot Blocking buffer

Dried milk powder (Marvel)	5%(w/v)
Tween-20	0.05%(v/v)
PBSa	to 1L

2.1.4 Nucleic acid analysis

TBE (10X)

Tris	890mM
Boris Acid	890mM
EDTA (pH 8.0)	40mM
Diluted in dH_2O	

STET

Sucrose	4g
Triton X-100	2.5ml
EDTA (0.25M)	0.2ml
Tris HCl (1M)	2.5ml
Sodium Azide (20%)	0.05ml
dH_2O	to 20ml

TE

Tris-HCl (pH 7.5)	100mM
EDTA (pH 8.0)	500mM

2.1.5 Cell manipulation

PBSa

NaCl	8g
KCl	0.2g
Na_2HPO_4	1.44g
KH_2PO_4	0.24g
dH_2O	to 1L

Versene (pH 7.4)

NaCl	8g
KCl	0.2g
Na_2HPO_4	1.44g
KH_2PO_4	0.24g
EDTA	0.2g
dH_2O	to 1L

Acetone Methanol tissue fixing solution

Acetone	50%(v/v)
Methanol	50%(v/v)

2.2 Backbone vectors

pGEMT-Easy

pGEMT-Easy is produced by Promega and used as a sub cloning vector with T residue overhangs to allow TA cloning of PCR products. It also contains X-Gal blue/white reporter for blue/white screening of colonies.

pRTS-1-tomato

pRTS-1-tomato was obtained from A. Brown, Imperial College London, UK. It contains a doxycycline inducible bi-directional promoter and a puromycin resistance cassette driven by another promoter.

psiCHECK-2

psiCHECK-2is produced by Promega and contains a renilla luciferase gene as the primary reporter gene with a multiple cloning site downstream of the renilla stop codon. There is also a second reporter gene within the psiCHECK-2 vector, firefly luciferase. Expression levels of firefly luciferase should remain unchanged within different reporter constructs; and therefore allows normalisation of renilla luciferase expression.

pHVT3

Bacterial artificial chromosome (BAC) clone of HVT strain FC126 generated by Lawrence Petherbridge (Baigent et al. 2006) allowing manipulation and modification of the HVT genome.

pSB-1

BAC clone of SB-1 strain of MDV-2 generated by Lawrence Petherbridge (Petherbridge et al. 2009) allowing manipulation and modification of the MDV-2 genome.

pEF6-V5/His TOPO

Commercial vector available as part of a kit from Invitrogen, it contains the powerful human EF-1α promoter for high expression levels. Vector allows rapid TOPO cloning and additionally contains Blasticidin resistance gene and C-terminal V5 and 6xHis epitopes.

pCR-TOPO-XL

Commercially available TOPO Cloning vector optimised for cloning and bacterial expression of long (3-10kb) PCR products. Derived from pCR vector (Invitrogen) and contains a kanamycin resistance cassette. Provided as part of a kit from Invitrogen.

2.3 General Methods

2.3.1 Glycerol stock production

Prior to plasmid DNA isolation 500µl of overnight bacterial culture was removed and added to 500µl 50% glycerol in a fresh freezing tube. Glycerol stocks were stored at -80°C and recorded on communal database.

2.3.2 Plasmid DNA extraction – miniprep scale (using Qiagen miniprep kits)

A single colony was picked from selective agar plate using a sterile pipette tip and used to inoculate 5ml of selective liquid medium. The culture was incubated at 37°C, shaking at 2.5xg overnight. A glycerol stock was prepared from the culture (500µl) and the remaining culture centrifuged at 4,000xg for 20 minutes at 4°C. DNA was prepared using the Qiagen miniprep kit following the manufacturer's instructions. Briefly, supernatant was removed and the bacterial pellet resuspended in 250µl P1 buffer in a 1.5ml tube, following a brief vortex 250µl P2 buffer was added. The tube was then inverted 4-6 times before adding 350µl neutralizing reagent (N3 buffer) and inverted a further 4-6 times. Tubes were then spun at 13,000xg in a microfuge for 10 minutes at room temperature and supernatant transferred to a disposable miniprep column in a collection tube. Supernatant was then drawn through the columns via the application of a vacuum manifold (Qiagen). Once the supernatant had been completely drawn through the column 500µl PB buffer was added and drawn through the column as above. 750µl PE buffer was added to the columns to wash samples before elution, and was drawn through the columns first by vacuum, and then a 1 minute spin at 13,000xg to ensure all ethanol is removed. 50µl elution buffer (EB) was added directly to the column membrane before incubation at room temperature for 1 minute, the column was centrifuged at 13,000xg to elute the DNA, which was collected in a fresh 1.5ml tube.

2.3.3 Plasmid DNA extraction – maxiprep scale (using Qiagen maxiprep kits)

A single colony of high-copy number plasmid transformed bacteria was picked from selective agar plate using a sterile pipette tip, and used to inoculate 400ml of selective liquid medium. The culture

was incubated at 37°C, shaking at 2.5xg overnight. A glycerol stock was prepared from the culture (500µl) and the remaining culture centrifuged at 4,000xg for 20 minutes at 4°C. DNA was prepared using the Qiagen maxiprep kit and columns, following the manufacturer's instructions. Briefly, supernatant was removed and the bacterial pellet resuspended in 10ml P1 buffer in a 50ml tube, following a brief vortex, 10ml P2 buffer was added. The tube was then inverted 4-6 times and incubated at room temperature for 5 minutes, before adding 10ml neutralizing reagent (N3 buffer), inversion a further 4-6 times, followed by 20 minutes incubation on ice. Tubes were then spun at 4000xg for 30 minutes at room temperature to clear lysate before being transferred to a disposable maxiprep column (Qiagen). Supernatant was then drawn through the columns via gravity and flow-through collected in waste tray. Once the supernatant had been completely drawn through, the column was washed twice with 30ml QC buffer, each time drained by gravity. DNA was eluted with 10ml buffer QF into a fresh 50ml collection tube, 7ml of ice-cold isopropanol was added to precipitate the DNA, and the tube was centrifuged at 4000xg, 4°C for 1hour. Following centrifugation the supernatant was removed, and the DNA pellet washed with 10ml 70% ethanol then centrifuged at 4000xg for 30 minutes at 4°C. The DNA pellet was then air-dried until ethanol had evaporated then resuspended in an appropriate volume of TE buffer.

2.3.4 BAC DNA STET miniprep

1.5ml of culture was pelleted in an Eppendorf by centrifugation at 2500xg, 4°C for 10 minutes, and the supernatant discarded. The cell pellet was resuspended in 70µl of STET with vortexing, after which 200µl of alkaline SDS was added and mixed by inversion. Finally 150µl of 7.5M Ammonium Acetate was added and mixed by inversion before the sample was incubated on ice for 5 minutes. Samples were then centrifuged in a pre-cooled centrifuge at 4°C, 13000xg for 20 minutes. The supernatant was then transferred to a fresh 1.5ml collection tube and 240µl isopropanol was added and mixed by inversion. Samples were centrifuged at 13000xg, room temperature for 5 minutes to pellet DNA. Supernatant was then discarded and the DNA pellet washed in 200µl 70% ethanol and centrifuged at 13000xg, room temperature for 3 minutes. Supernatant was again removed and discarded and the

DNA pellet air-dried at room temperature for 10 minutes (or until no ethanol remained). DNA was resuspended in 60µl TE buffer containing 5µg/ml RNase A and stored at 4°C.

2.3.5 BAC DNA maxiprep – (using Qiagen maxiprep columns)

BAC DNA maxipreps were performed using Plasmid Maxi kit, QIAGEN-tip 500 (Qiagen) following the protocol for "very low-copy Plasmid/Cosmid" purification in the product handbook.

2.3.6 Polymerase chain reaction (PCR)

PCR was performed using a thermocycler protocol as per the polymerase manufacturer's protocol. Either GoTaq 2X master mix (Promega) or Platinum Pfx (Invitrogen) DNA polymerase was used depending on the application. The recipes for both polymerases are detailed below:

GoTaq Master Mix 2X	25µl
DNA (10-100ng)	1µl
Forward primer (10 p/mol)	2.5µl
Reverse primer (10 p/mol)	2.5µl
dH_20	19µl

10X Pfx Amplification Buffer	5µl
PCR Enhancer Solution	2.5µl
dNTP mixture (10mM)	1.5µl
$MgSO_4$ (50mM)	1µl
Platinum Pfx DNA polymerase	1µl
Forward primer (10 p/mol)	1.5µl
Reverse primer (10 p/mol)	1.5µl
Template DNA (10-100ng)	1µl
dH_20	35µl

2.3.7 A-Tailing of PCR Products for TA Cloning

Many sub-cloning vectors rely on adenine residue overhangs for ligation, these overhangs are removed by proof-reading DNA polymerases. An adenine residue can be added using GoTaq DNA polymerase (Promega):

Purified blunt-ended DNA fragment	4.4µl
5X GoTaq Reaction Buffer	2µl
1mM dATP	2µl
GoTaq Flexi DNA polymerase (5u/µl)	1µl
25mM MgCl2	0.6µl

The reaction was incubated at 70°C for 30 minutes. After the tailing reaction was completed, 2µl of the reaction was used, without further clean-up, for ligation into TA cloning vector systems.

2.3.8 RNA Extraction – (Using Qiagen miRNEasy mini Kit)

Qiagen miRNEasy RNA extraction kit was used for its ability to extract total RNA including small RNAs (<200nt). RNA extractions were performed following manufacturers protocol, briefly, cells were harvested directly from 6-well tissue culture plate by the addition of 700µl QIAzol Lysis Reagent and scraping. Samples were transferred to a 1.5ml tube and homogenised by vortexing for one minute and incubation at room temperature for 5 minutes. 140µl chloroform was added to the tube and mixed by vigorous shaking for 15 seconds. Samples were then centrifuged for 15 minutes at 12,000 x g at 4°C. The upper aqueous phase was transferred to a new 1.5ml tube and 525µl of 100% ethanol was added and mixed thoroughly by pipetting up and down several times. Sample was added (700µl at a time) to an RNeasy Mini spin column in a 2ml collection tube and centrifuged at 8000 x g for 15 seconds at room temperature, until the entire sample had passed through the column. 700µl Buffer RWT was added to the miRNeasy Mini spin column and centrifuged as before to pull-through the column. Two washes with 500µl Buffer RPE were performed, clearing via centrifugation, and any residual ethanol was removed by a 2 minute spin at 8000 x g. RNA was eluted in 50µl RNase-free water and stored at -

80°C if not being used immediately. If on-column DNase digestion was required, it was performed at the stage of Buffer RWT treatment as per Appendix B in the manufacturer's protocol.

2.3.9 RNA Extraction – Using Trizol reagent (Invitrogen)

For larger yields of RNA, extraction was performed using Trizol reagent. Homogenisation was performed by the direct addition of an appropriate volume of Trizol reagent directly to cell monolayer in the tissue culture vessel. Remaining steps in RNA extraction were performed following manufacturers protocol, with volumes scaled up if more than 1ml of Trizol was used in original homogenisation.

2.3.10 Use of DNeasy kit for multiple extractions of total DNA from cells

Total DNA was extracted from lymphocytes isolated from chicken blood using the Qiagen DNeasy 96 kit, enabling large numbers of samples to be processed at one time. Cells were collected in an appropriate manner and stored at -20°C prior to the DNA extraction in the provided 96-rack of collection tubes. Proteinase K (provided in the kit) was diluted 1 in 11 in PBS, then 220µl of the proteinase K in PBS solution was added to each sample in the collection tube rack and mixed thoroughly by vortexing. 200µl of buffer AL/E was added to each tube and mixed by shaking for 15 minutes; samples were then collected in the bottom of the tubes by brief centrifugation before incubation at 56°C for 10 minutes. Following incubation, 200µl of absolute ethanol was added to each sample then vortexed, and collected again by centrifugation at 3000xg. DNeasy 96 plate was placed upon an S-block and the mixture was transferred from the collection tubes to the DNeasy plate. The plate was sealed with an AirPore tape sheet, and then the plate and block were centrifuged together in the Sigma 4-15°C centrifuge at 5200xg for 4 minutes. The tape sheet was removed, and 500µL of wash buffer AW1 (with ethanol) was added to each well. The plate was sealed again with a tape sheet, and then the plate and block were centrifuged together in the Sigma 4-15°C centrifuge at 5200xg for 2 minutes. The tape sheet was removed, and 500µL of wash buffer AW2 (with ethanol) was added to each well, plate and block were centrifuged together at 5200xg for 15 minutes (no AirPore tape sheet

used). DNeasy 96 plate was placed on top of an appropriately labelled rack of elution microtubes and 200µl dH_2O was added to each filter and incubated for 1 minute at room temperature. DNA was eluted by centrifugation of plate and microtubes at 5200xg for 4 minutes, eluted DNA stored at -20°C until ready for processing.

2.3.11 Determining protein yield from sample

Cells were harvested following removal of culture medium by gentle cell scraping in ice-cold PBS on ice. Cells were transferred to a sterile 20ml tube and pelleted by centrifugation at 1700xg, 4°C for 20 minutes. Cell pellet was then resuspended in an equal volume of 0.1% RapiGest SF Surfactant (Waters) in 50mM ammonium bicarbonate. The sample was solubilised with a combination of heating at 80°C, freeze-thaw cycles with 5 minutes vortex after each cycle and 15 minutes of sonication. Protein samples were then transferred to a fresh microcentrifuge tube and protein concentration was determined with dilutions of the sample using DC Protein Assay (Bio-Rad), following manufacturers protocol.

2.3.12 Preparation of Protein Samples for Mass Spectrometry (MS)

This was performed in the Institute of Integrative Biology at the University of Liverpool. Samples were prepared and protein concentrations determined as described below. Dichlorodiphenyltrichloroethane (DDT) was then added to samples to a final concentration of 3mM and samples were incubated at 60°C for 10 minutes. The samples were then cooled back to room temperature before Indole-3-acetic acid (IAA) was added to a final concentration of 9mM, samples were then incubated in the dark at room temperature for 30 minutes. Trypsin was then added at a 50:1 protein:trypsin ratio and incubated overnight at 37°C with shaking. Trifluoroacetic acid (TFA) was added to a final concentration of 0.5% and samples were then incubated at 37°C for 1 hour. The samples were then centrifuged at 14,000xg, 4°C for 30 minutes. The supernatant was transferred to fresh collection tube and stored ready for MS analysis.

2.3.13 Generation of Electrocompetent EL250 *E. coli*

EL250 *E. coli* containing the appropriate BAC DNA was inoculated in a 2ml culture of LB medium containing 25µg/ml Chloramphenicol and any other appropriate antibiotics, and incubated overnight at 32°C, 2.5xg. 1ml of the overnight culture was inoculated the following morning into 20ml LB medium (no antibiotic) and incubated at 32°C, shaking at 2.5xg for 2.5 hours. The culture was then transferred to 42°C for 20 minutes (to induce expression of the genes required for recombination). The induced culture was then cooled on wet-ice for 5 minutes before centrifugation, to pellet the culture, at 4,000xg, 4°C for 20 minutes. Following centrifugation, the cell pellet was washed with 30ml ice-cold PBS and pelleted by centrifugation, in desktop centrifuge. The cell pellet was then washed by resuspension in 2ml ice-cold water then pelleted by centrifugation at 13000xg, 4°C for 30 seconds, this was then repeated twice more. The cell pellet was washed once more with 2ml 10% glycerol and pelleted by centrifugation as previously before being finally resuspended in 150µl of 10% glycerol, to produce three 50µl aliquots of electrocompetent cells. Aliquots were snap frozen in an ethanol and dry-ice bath and then stored at -80°C until needed.

2.3.14 miRNA TaqMan

Relative miRNA expression levels were determined from various samples by TaqMan qRT-PCR using miRNA specific RT primers and probes (listed in table 2). RNA was extracted from the samples and then diluted to a concentration of 2ng/µl. The first step was to perform a miRNA specific RT-PCR reaction using TaqMan miRNA Reverse Transcription Kit (Applied Biosystems), per reaction:

dNTP mix w/dTTp (100M total)	0.15µl
MultiScribe RT enzyme	1µl
10X RT buffer	1.5µl
RNase inhibitor (20U/µl)	0.19µl
RNase-free H_2O	4.16µl
Diluted RNA (2ng/µl)	5µl
5X miRNA RT Primer	3µl

Reverse transcription was performed following thermocycler protocol as described in the manufacturer's protocol:

1. 16°C > 30mins 2.42°C > 30mins 3.85°C > 5mins 4. 4°C > Hold

RT samples generated above (15µl volume) were diluted by the addition of 150µl RNase-free H_2O prior to qPCR, per reaction:

2X PCR master mix (Thermo Scientific)	10µl
20X miRNA probe and primer	1µl
Diluted RT reaction	9µl

qPCR was performed using 7500 Fast Instrument (Applied Biosystems) using standard 7500 protocol with a 15 minute enzyme activation step:

1. 50°C > 2mins 2.95°C > 15mins $\underbrace{\text{3.95°C > 15secs} \quad \text{4. 60°C > 1 min}}_{\text{40 cycles}}$

All runs were performed in triplicate and relative miRNA levels were determined after 40 cycles of qRT-PCR using the relative quantification template (comparing mean Ct values of samples, normalised to an endogenous control) within the 7500 Fast System SDS Software (Applied Biosystems).

Assay Name	Life Technologies Assay ID	Life Technologies Catalog Number
hvt-miR-H17	244247_mat	4440886
hvt-miR-H7-5p	244635_mat	4440886
hvt-miR-H12-5p	242611_mat	4440886
hvt-miR-H14	244267_mat	4440886
hvt-miR-H16-3p	243151_mat	4440886
hvt-miR-H15	242756_mat	4440886
hvt-miR-H18-5p	242396_mat	4440886
mdv2-miR-M16	243682_mat	4440886
mdv2-miR-M21	006915_mat	4440886
mdv2-miR-M22	242599_mat	4440886
mdv2-miR-M17	006733_mat	4440886
mdv2-miR-M30	008351_mat	4440886
hsa-miR-29b	000413	4427975
hsa-let-7a	000377	4427975

Table 2 - Table listing TaqMan microRNA assays used throughout this study, with corresponding assay IDs and catalogue numbers. Sequences of probes and primers in the assays are intellectual property of Life Technologies (www.lifetechnologies.com).

2.3.15 Gene Expression TaqMan

Relative gene expressions between two samples were determined in a similar manner to miRNAs above using TaqMan gene expression assays purchased from Applied Biosystems. Probes were labelled with the florescent reporter dye 4-carboxyfluorescein (FAM) at the 5' end, and the quencher N,N,N,N'-tetramethyl-6-carboxyrhodamine (TAMRA) at the 3' end (listed in table 3). In the qRT-PCR run the probe anneals to the mRNA then as DNA polymerase performs its 5' exo-nuclease function the FAM reporter becomes cleaved from the TAMRA quencher, inducing a fluorescent signal. The fluorescent signal increases throughout the qRT-PCR run and is detected and recorded following each cycle. Levels of mRNA were normalised to the amounts of ribosomal protein L7 (RPL7) transcript in the samples, a constituent of the eukaryote ribosome and thus present in every cell making it a useful 'house-keeping' gene.

One-step RT-PCR was performed using different reagents from Applied Biosystems, per reaction:

1:100 diluted of DNAse treated extracted RNA	2.5µl
2X FAST Master Mix (Applied Biosystems)	5µl
20X gene specific probe and primers	0.5µl
40X MultiScribe and RNase Inhibitor Mix	0.25µl
RNase-free H_2O	1.75µl

qRT-PCR performed using 7500 Fast Instrument (Applied Biosystems) under the following conditions:

1. 48°C > 30mins 2.95°C > 20 secs (3.95°C > 3 secs 4. 60°C > 30 secs) × 40 cycles

All runs were performed in triplicate and relative gene transcript levels were determined after 40 cycles of qRT-PCR using the relative quantification template (comparing mean Ct values of samples, normalised to an endogenous control) within the 7500 Fast System SDS Software (Applied Biosystems).

Gene Symbol	Life Technologies Assay ID	Life Technologies Catalog Number
RPL7	Gg03336533_m1	4351372
DNMT3B	Gg03344074_m1	4351372
AKT3	Gg03328405_m1	4351372
RAP1A	Hs01092205_g1	4331182
DEK	Gg03341257_m1	4351372
RALA	Hs00800233_s1	4331182

Table 3 - Table listing TaqMan gene expression assays used throughout this study, with corresponding assay IDs and catalogue numbers. Sequences of probes and primers in the assays are intellectual property of Life Technologies (www.lifetechnologies.com).

2.3.16 Detection of viral genome copy number by TaqMan

This qPCR differs from the other two methods as it is performed directly on DNA, therefore no RT step is required. DNA was extracted from samples using the Qiagen DNeasy 96 kit, and viral copy number of BAC or challenge (MDV-1) virus can be determined depending on the probe and primer set used, a list of all qRT-PCR primers and probes used to detect virus levels can be found in table 13, section 2.3.36. The reference gene used was *ovotransferin*. Per reaction:

2x Thermo-Start PCR Master Mix (Thermo Scientific)	12.5µl
100µM Virus gene - Forward Primer	0.1µl
100µM Virus gene - Reverse Primer	0.1µl
100µM Reference gene - Forward Primer	0.1µl
100µM Reference gene - Reverse Primer	0.1µl
100µM Virus gene probe	0.05µl
100µM Reference gene probe	0.05µl
H_2O	8µl

qPCR performed using 7500 Fast Instrument (Applied Biosystems) using standard 7500 protocol with a 15 minute enzyme activation step:

1. 50°C > 2mins 2.95°C > 15mins 3.95°C > 15 secs 4. 60°C > 1 min

40 cycles

On every plate a standard curve for both the reference gene and virus gene was prepared with serial dilutions of known viral copy numbers. Ct values were determined on the Fast 7500 Software (Applied Biosystems) and further analysis to determine actual virus copy numbers was performed in Microsoft Excel.

2.3.17 Generating inducible HVT miRNA expression construct

The region of DNA containing the HVT miRNAs, *hvt-miR-H1* to *hvt-miR-H18*, was PCR amplified from pHVT3 BAC DNA (20ng) using Platinum Pfx DNA polymerase (Invitrogen) following the protocol described in the methods section 2.3.6. The primers used for amplification (table 10) were designed to add *Bgl*II and *Sal*I restriction enzyme cut sites that were utilised for later downstream cloning. Following amplification, the PCR products were analysed by gel electrophoresis and the correct DNA products extracted and purified using QIAquick Gel Extraction Kit (Qiagen) following manufacturers protocol. The purified PCR products were then A-tailed using GoTaq DNA polymerase (Promega), and cloned into the pCR-XL-TOPO sub-cloning vector using TOPO XL PCR Cloning Kit (Invitrogen) following manufacturers protocol. Sub-cloning the PCR product, allowed for sequencing and easy digestion of the PCR product, prior to cloning into the final expression vector.

Following ligation, transformation and screening of colonies containing the correct constructs, cultures were grown and plasmid DNA extracted by QIAprep Spin Miniprep Kit (Qiagen). The plasmid DNA was then sent for Sanger sequencing at Source BioScience Oxford, to check for any mutations within the miRNA sequence. Clones were sequenced with M13F and M13R primers along with other sequencing primers (H1-H18_Seq_1-14) detailed in table 10. The correctly sequenced construct was then used to create the pRTS-SVP-Tom inducible miRNA expression construct.

The 4.6kb HVT miRNA cassette was digested from the sequenced pCR-XL-TOPO construct by digestion with *Bgl*II and *Sal*I restriction enzymes and ligated into pRTS-SVP-Tom vector which had previously been digested with *Bgl*II and *Xho*I restriction enzymes. The compatibility of the *Sal*I and *Xho*I overhangs was utilised in ligation due to the pRTS vector only containing *Bgl*II and *Xho*I restriction sites for cloning, but the HVT miRNA cassette containing an internal *Xho*I restriction site.

Ligation was performed using Rapid DNA Ligation Kit (Roche), following manufacturer's protocol. Following ligation the reaction was transformed into ElectroMax DH10B electrocompetent cells (Invitrogen) and general molecular cloning protocols were performed (section 2.3.19). Positive clones

were screened by digestion with different restriction enzymes, following overnight incubation and miniprep plasmid purification.

2.3.18 Creating DF-1 cell line stably transfected with pRTS-HVT miRNA construct

Plasmid DNA purified by QIAprep Spin Miniprep Kit (Qiagen) was transfected into DF-1 cells using Lipofectamine 2000 (Invitrogen), as detailed in the methods section 2.3.27. The DF-1 cells were seeded in a six well plate with the appropriate number of cells (table 5), 24 hours prior to transfection. Two different sequenced pRTS-HVT miRNA constructs (clones 6 and 7) along with empty pRTS-SVP-Tom vector were transfected in duplicate into wells of the six-well tissue culture plate. Following transfection and 24 hours incubation, the duplicate wells of transfected cells were transferred from the six-well plate into a T25 tissue culture vessel containing 6.5ml DF-1 medium with 1µg/ml puromycin. Puromycin resistance is inferred upon transfection with the pRTS construct, therefore successfully transfected DF-1 cells could be selected for and continued to be cultured. DF-1 selection medium was refreshed every 3 days, until T25 flask was confluent.

2.3.19 General Molecular Cloning

Target DNA sequence was amplified via PCR and digested by appropriate restriction enzymes (following restriction enzyme manufacturer's protocol) to leave overhangs. Compatible overhangs were produced in the target vector by restriction enzyme digestion. DNA insert was ligated into vector by T4 DNA ligase using Roche Rapid DNA Ligation Kit, following manufacturer's protocol. Ligation mix was then transformed into *E. coli* and incubated overnight at 37°C on antibiotic selection media. Colonies present the following day were screened by colony PCR, restriction digest and/or sequencing to ensure the correct clone was generated. Plasmid DNA was generated from an appropriate volume of liquid culture of a positive clone, using plasmid purification kit (mini or maxi-prep) from Qiagen.

2.3.20 Creating reporter constructs for dual luciferase assay

110bp oligos (sequences in tables 8 and 9) were ordered at 0.05µM scale from Eurofins MWG Operon, desalt purification and shipped lyophilised. Oligos were resuspended in dH_2O to a concentration of 100µM in preparation for phosphorylation, prepared as detailed below.

Oligo Phosphorylation

100µM oligo stock	2µl
10x PNK Buffer (NEB)	2µl
10mM ATP	2µl
T4 PNK (NEB)	0.5µl
dH_2O	13.5µl

The phosphorylation reaction was incubated at 37°C for 1 hour. 10µl of the phosphorylation reaction from complementary oligos was mixed and annealed together by heating at 95°C for 2 minutes then gradually cooled to room temperature. The annealed oligo mix (20µl) was then diluted by the addition of 230µl dH_2O.

psiCHECK2 vector was digested with *Xho*I and *Not*I restriction enzymes (NEB) following manufacturers protocol and digested vector extracted following electrophoresis using Qiagen Gel Extraction mini kit, following manufacturer's protocol. Digested psiCHECK2 vector was then dephosphorylated using Roche Rapid DNA Dephos & Ligation Kit.

Vector Dephosphorylation

*Not*I + *Xho*I digested psiCHECK2 vector	16µl
rAPid Alkaline Phosphatase Buffer (10x)	2µl

Dephosphorylation reactions were incubated at 37°C for 30 minutes, then heat inactivated for 2 minutes at 75°C.

Phosphorylated, annealed oligos and dephosphorylated vector were ligated together using Roche Rapid DNA Dephos & Ligation Kit following manufacturers protocol, with the reaction mix detailed below.

Ligation Reaction

Digested, dephosphorylated psiCHECK2 vector (50ng)	1µl
Diluted, phosphorylated, annealed oligos	2µl
DNA dilution buffer (10x)	2µl
dH_2O	5µl
T4 DNA ligase buffer (2x)	10µl
T4 DNA ligase	1µl

Ligation mix was incubated at room temperature for 15 minutes, and then 2µl was transformed into Subcloning Efficiency™ DH5α™ *E. coli* (Invitrogen) as described in section 2.3.22.

2.3.21 Creating miRNA expression vectors

The complete pre-miRNA sequence of the miRNA of interest, along with 100bp flanking sequence up- and down-stream, was amplified from a suitable source (e.g. chicken spleen cDNA library (1:10 dilution),pSB-1 or pHVT3 BAC DNA (1:100 dilution)) using primers in table 7 following general molecular cloning techniques (section 2.3.19) . The additional flanking sequence was added to ensure correct processing of the pre-miRNA to mature miRNA, following expression. The PCR products were then TA cloned into pEF6-V5/His TOPO vector (Invitrogen) following manufacturers protocol.

2.3.22 Transformation of chemically competent *E. coli*

A 50µl aliquot of Subcloning Efficiency™ DH5α™ *E. coli* (Invitrogen) was thawed on ice. 2µl of ligation reaction was added to the cells and mixed by stirring with pipette tip. Cell and ligation reaction mix was incubated on ice for a further 30 minutes, cells were then heat-shocked via transfer to 42°C water bath for 20 seconds before returning to ice for a further 2 minutes. Following heat-shock cells were recovered in 950µl pre-warmed SOC and incubated at 37 °C for 1 hour and 2.5xg. After recovery the transformation mix was plated on selective LB agar and incubated overnight at 37°C, and any resulting colonies screened the following day.

2.3.23 Transformation of electro-competent *E. coli*

An aliquot of *E. coli* was thawed on ice. 2µl of ligation reaction was added to the cells and mixed by stirring with pipette tip. Cell and ligation reaction mix was incubated on ice for a further 20 minutes before transferred into a chilled 0.1 cm cuvette. Electroporation was performed using BioRad GenePulser electroporator under the following conditions: 2.0 kV, 200 Ω, 25 µF. Following electroporation cells were recovered in 950µl pre-warmed SOC and incubated at 37 °C for 1 hour and 2.5xg. After recovery the transformation mix was plated on selective LB agar and incubated overnight at 37°C, and any resulting colonies screened the following day.

2.3.24 Nucleic acid electrophoresis

A 0.8-1% Agarose gel was prepared in TBE buffer with 0.005% Ethidium Bromide, and cast in gel tray with comb containing a suitable number of wells. Once set, the gel was submersed in TBE buffer and the comb removed prior to sample loading. 6X DNA loading buffer was added to samples to be run on Agarose gel, then samples were loaded into gel, with a ladder (generally 2-Log DNA Ladder (New England Biolabs)) flanking the samples. Samples were run at around 150 volts (around 100mAmps) for 30-40 minutes before visualisation under ultraviolet light.

2.3.25 SDS protein electrophoresis

A 4-12% NuPage BIS-TRIS pre-cast gel (Invitrogen) was submersed in NuPAGE MES SDS running buffer in gel cassette. The comb was removed from gel and the wells washed by pipetting up and down. Prepared protein samples were incubated at 95°C in 2X SDS loading buffer prior to loading into gels and run alongside a molecular weight marker (generally broad range molecular weight marker (Bio-Rad)). Samples were run at 150 volts for 45 minutes before removal from gel case for downstream applications.

2.3.26 Western blot

Prepared protein samples were first run on 4-12% NuPage BIS-TRIS pre-cast gels (Invitrogen) as described in section2.3.26. Following protein electrophoresis protein was transferred onto a nitrocellulose membrane using the iBlot system (Invitrogen) following manufacturers protocol (transfer time 6 minutes) and blocked in PBS-Tween (0.05%) containing 5% skimmed milk powder for 1 hour at room temperature with gentle agitation. The membrane was then incubated with primary antibody diluted in blocking solution (as above) at the concentrations detailed in table 4; incubation was at room temperature for 1 hour with gentle agitation (or sometimes overnight at 4°C). The membrane was then washed 3 times (5 minutes per wash, with agitation) in PBS-Tween before the addition of the secondary antibody diluted in blocking solution (as above) at the concentrations detailed in table 4; incubation was at room temperature for 1 hour with gentle agitation. The

membrane was then washed 3 times (5 minutes per wash, with agitation) in PBS-Tween and finally incubated with ECL developing solution for 1 min. Membrane was covered with plastic film, then an Amersham® Hyperfilm® ECL™ Film (GE Healthcare) was exposed to the membrane in an Autoradiography Cassette for varying times and developed using the Xograph system.

Antibody	Clonality	Manufacturer	Raised in	Catalogue #	Western Blot Concentration
Anti-RALA	Polyclonal	Bioss	Rabbit	bs-5953R	1:250
Anti-DEK	Polyclonal	Biorbyt	Rabbit	orb10529	1:250
Anti-RAP1A	Monoclonal	BD Bioscience	Mouse	610195	1:500
Anti-AKT3	Polyclonal	Bioss	Rabbit	bs-5146R	1:250
Anti-DNMT3B	Polyclonal	AVIVA SYSBIO	Mouse	ARP-49124-P050	1:250
Anti-α-Tubulin	Monoclonal	Sigma	Mouse	T6199	1:1000
HRP conjugated Anti-Mouse Immunoglobulins	Polyclonal	Dako	Rabbit	P 0260	1:1000
HRP conjugated Anti-Rabbit Immunoglobulins	Polyclonal	Dako	Goat	P 0448	1:1000

Table 4 – Details of primary and secondary antibodies used throughout this study.

2.3.27 Transfection of DF-1 cells

Cells were seeded the previous day to produce 90-95% confluency of cells on tissue culture vessel prior to transfection. Lipofectamine 2000 transfection reagent (Invitrogen) diluted in Opti-MEM (Invitrogen) was used to transfect DNA into cells. The volumes of Lipofectamine 2000 and Opti-MEM, and amount of plasmid DNA varied depending on the size of tissue culture vessel (detailed in table 5). Diluted Lipofectamine 2000 and diluted DNA were mixed and incubated at room temperature for 30 minutes, before being added directly to cells. Cells then continued to be incubated at 38.5˚C with 5% CO_2 until they were ready for harvesting.

Culture Vessel	Surface Area per Well (cm^2)	Relative Surface Area (vs. 24-well)	Volume of Plating Medium	DNA (µg) and Dilution Volume (µl)	Lipofectamine 2000 (µl) and Dilution Volume (µl)
96-well	0.3	0.2	100µl	0.2µg in 25µl	0.5µl in 25µl
24-well	2	1	500µl	0.8µg in 50µl	2.0µl in 50µl
12-well	4	2	1ml	1.6µg in 100µl	4.0µl in 100µl
6-well	10	5	2ml	4µg in 250µl	10µl in 250µl
T25	25	12.5	5ml	10µg in 625µl	25µl in 625µl
T75	75	37.5	10ml	30µg in 1875µl	75µl in 1875µl

Table 5 - Amounts of Lipofectamine 2000 and DNA required for transfection of different tissue culture vessels

2.3.28 Transfection of Chicken embryo fibroblasts (CEF) cells

CEF cells were seeded the previous day in CEF growth medium to produce 80-90% confluency prior to transfection. For a 6-well plate transfection (per well), 10µl of Lipofectamine transfection reagent (Invitrogen) was added to 90µl of Opti-MEM, while 1µg of DNA was diluted in 100µl of Opti-MEM. Lipofectamine and DNA was combined (total volume 200µl) and incubated at room temperature for 45 minutes. Medium was removed from the CEF cells and they were washed once with Opti-MEM. 800µl Opti-MEM was added to the incubated Lipofectamine and DNA mix (total volume 1ml) before being added to the CEF and incubated for 6 hours at 38.5˚C with 5% CO_2. Following incubation 2ml CEF growth medium was added to cells (transfection mix not removed) and cells incubated overnight at 38.5˚C with 5% CO_2. The following day CEF growth medium was removed and replaced with 3ml of CEF maintenance medium and cells were incubated at 38.5˚C with 5% CO_2 until they were ready for harvesting.

2.3.29 Fixing and staining CEF for detection of viral plaques

Cell culture medium was removed from the tissue culture plate and the cell layer was washed twice gently and briefly with PBS. The cells were then fixed by the addition of ice-cold acetone:methanol for two minutes at room temperature. Acetone:methanol was removed and the cell layer washed twice more in PBS. PBS was then removed and non-specific binding was blocked by the addition of blocking buffer (PBS with 5% new-born calf serum) and incubation at room temperature for 1 hour with gentle rocking. Blocking buffer was removed following incubation and primary antibody, diluted as appropriate in blocking buffer, was added to the cell layer and incubated at room temperature for 1 hour with gentle rocking. Following incubation primary antibody was removed and the cell layer was washed three times with wash buffer (PBS with 0.05% Tween 20) for 5 minutes per wash. Secondary antibody was diluted as appropriate in blocking buffer and added to the cell layer following the third wash; the cells were then incubated at room temperature for 1 hour with gentle rocking. After incubation with secondary antibody the cell layer was washed three times as above. If a fluorescently labelled secondary antibody was used the cells were then visualised using a fluorescent microscope and images recorded. If an HRP-conjugated secondary antibody was used plaques must be developed. Developing solution was prepared fresh (per well of six well plate: 513µl 0.1M sodium acetate pH 4.8, 27µl 3-Amino-9-ethylcarbazole (AEC) and 9µl H_2O_2) and added to the cell layer following washes and incubated at 38.5°C until dark red/brown colour was visible. Developing solution was removed and the cell sheet washed 3 times in dH_2O then stored in dH_2O at 4°C.

2.3.30 Production of viral stocks from BAC DNA

BAC DNA was transfected into CEF seeded in a six-well plate using lipofectamine transfection reagent, as described in section 2.3.28. Once plaques became visible transfected CEF were transferred to T25 culture vessel containing 6ml CEF maintenance medium and incubated at 38.5°C, 5% CO_2 until confluent. Infected CEF were then harvested from T25 flask and distributed evenly over two T75 flasks containing $8x10^6$ fresh CEF. T75 flasks were cultured at 38.5°C, 5% CO_2 as appropriate until plaques became visible, cells were then harvested and pelleted by gentle centrifugation. The cell pellet from both T75 flasks was resuspended in 10ml freezing medium (CEF growth medium containing 10% foetal calf serum and 10% Dimethyl sulfoxide (DMSO)) and 1ml aliquots were taken stored in 2ml cryovials. Cryovials were frozen in Nalgene Mr. Frosty Freezing Container (Thermo Scientific) containing isopropanol at -80°C. Virus stock ampules were then transferred from Nalgene Mr. Frosty Freezing Container at -80°C to liquid nitrogen storage the following day.

2.3.31 Determination of viral titre in CEF

CEF were seeded 24-hours previously and incubated overnight in 3ml CEF growth medium at 38.5°C. 100µl of viral stock, recovered from liquid nitrogen, was diluted in 900µl of CEF growth medium. 10-fold serial dilutions were made, down to 10^{-4}, and 200µl of various dilutions was added to duplicate well of CEF. CEF were incubated at 38.5°C, 5% CO_2 as appropriate until plaques became visible. Cells were fixed and stained as described in section 2.3.29 and plaques counted under an inverted microscope at the dilution that gave the easiest distinction between plaques (roughly 10-60 plaques). Viral titre was calculated using the following equation:

$$\text{Count} \times 5 \times \text{dilution factor} = \text{titre (pfu per ml)}$$

2.3.32 Luciferase reporter assay

DF-1 cells were seeded at $3.3x10^4$ cells per well in a 96 well flat bottomed cell culture plate with 100µl DF-1 medium and incubated at 38.5°C overnight. psiCHECK-2 reporter constructs were diluted to a concentration of 20ng/µl and miRNA expression constructs to 100ng/µl. Co-transfection of plasmids was performed using Lipofectamine 2000 transfection reagent (Invitrogen) following manufacturers protocol for 96-well plate format. Per well the transfection mix was 0.5µl Lipofectamine 2000, 1µl psiCHECK-2 reporter construct, 1µl miRNA expression construct and 47.5µl opti-MEM, the co-transfections were performed in quadruplicate. Once transfection mix was added, the cells were incubated at 38.5˚C with 5% CO_2 until they were ready for harvesting.

Medium was removed from cells, and cells were washed once with PBSa prior to harvesting. Cells were harvested in 30µl of 1x Passive Lysis Buffer which is provided as part of the Dual-Glo Luciferase Assay System (Promega) with gentle agitation at room temperature for 30 minutes. 25µl of lysates were transferred directly from tissue culture plate to an Omniplate-96 white opaque 96-well microplate (PerkinElmer). The plate was loaded into gloMax Multi+ Luminometer (Promega) and the dual-luciferase assay program was run as detailed in manufacturers protocol. The readings of firefly luciferase (normalising amount of vector in cells) and renilla luciferase expression (expression of which was down regulated upon targeting of miRNA to inserted 3'UTR sequence) were obtained. Results were exported from the luminometer to Microsoft Excel where they were analysed. Figure 6 provides a summary of the dual-luciferase process, while figure 7 shows the equation used to determine relative knock-down of luciferase expression.

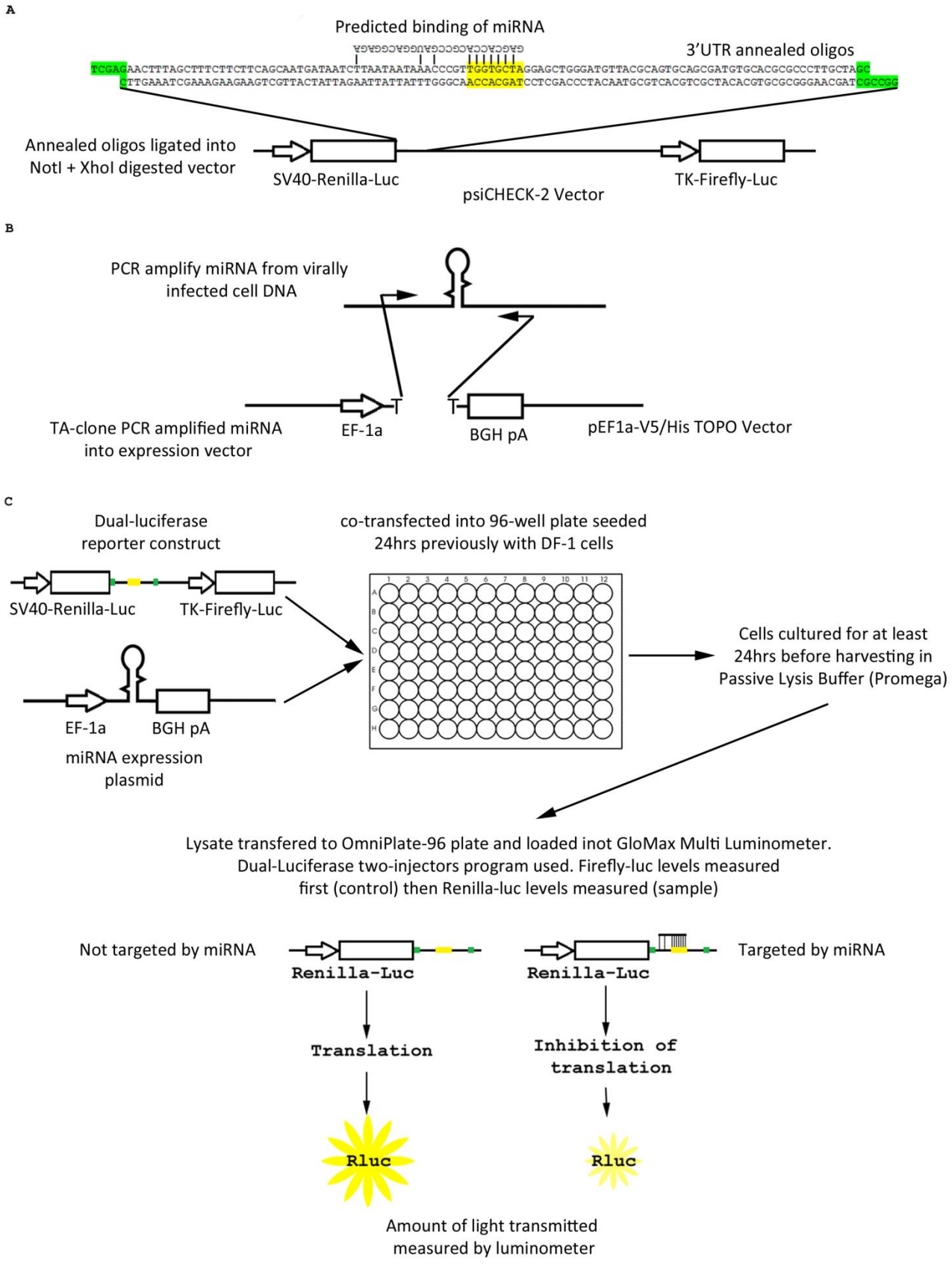


Figure 6 - Overview of the steps involved in miRNA luciferase assay to see if selected miRNA is targeting a gene 3'UTR. (**A**) Construction of reporter construct by annealing oligos containing predicted target site of miRNA in 3'UTR. (**B**) Generation of miRNA expression vector by cloning mature miRNA sequence (plus additional flanking sequence) into pEF6-V5/His TOPO expression vector. (**C**) Actual process of dual-luciferase assay, whereby the two previously constructed vectors are co-transfected into a cell line, and the effects of predicted miRNA targeting of cloned 3'UTR are detected by changes in light expression by luminometer machine.

$$\left(\left(\bar{x}\left(\frac{RL1}{FF1}+\frac{RL2}{FF2}+\frac{RL3}{FF3}+\frac{RL4}{FF4}\right)\right)_{\text{wild-type}} \div \left(\bar{x}\left(\frac{RL1}{FF1}+\frac{RL2}{FF2}+\frac{RL3}{FF3}+\frac{RL4}{FF4}\right)\right)_{\text{mutant}}\right)\times 100$$

Figure 7 - Equation used to calculate the down-regulation of Renilla luciferase by miRNA mediated gene regulation. Renilla luciferase readings 1-4 (RL1-4), Firefly luciferase readings 1-4 (FF1-4).

2.3.33 List of DNA oligos used in each chapter of the thesis

2.3.33.1 Chapter 3

Oligo Name	Sequence (5' to 3')
DNMT3b_Full_XhoI_F	ATAATACTCGAGCCCACGCTGCATCCCTCGTC
DNMT3b_Short_XhoI_F	ATAATACTCGAGCTCGGGGAAAGCAAACAAAG
DNMT3b_WT_NotI_R	ATAATAGCGGCCGCCCCACAAAACTTTGGACATC
DNMT3b_Mut_NotI_R	ATAATAGCGGCCGCCCCACAAAACTTTGGACATCAA AAATCCTTTAACTAAAAAAATGGTAACAGG
gga_miR_29b_F	CAGGGTAGTAGTGCTGTGAGCAG
gga_miR_29b_R	GGTCACAGCCTACTTAGGGAGTC
MDV2-miR-M21_F	TCTGCTCCGTCCTTAGCGTG
MDV2-miR-M21_R	CCCAGCCGACAACCCATTCT

Table 6 - Table of oligos used to generate dual-luciferase reporter constructs and miRNA expression constructs.

Oligo Name	Sequence (5' to 3')
HVT-miR-H5_F	CGAGGCCGGATATGATGAG
HVT-miR-H5_R	TAATGTGGACACCGGCATAG
HVT-miR-H7_F	GATGGTCGTCTCGGCAAG
HVT-miR-H7_R	CCACCTGGTTTTCAAATTCC
HVT-miR-H12_F	CTCGCGGATAGCGTAGATGT
HVT-miR-H12_R	CTAGAATCCCGCGGACAAC
HVT-miR-H14_F	GCCACCTGGCAATGATTC
HVT-miR-H14_R	AATACACTGGGCACACGAAAG
HVT-miR-H16_F	CGTTGTACGGGAAGAGTGC
HVT-miR-H16_R	ATAACTGCATGCCCACTTAATAC
HVT-miR-H17_F	GGTACGAACCCTTCATGTCG
HVT-miR-H17_R	CCGACTGGAAAAAGTCCATC
MDV2-miR-M16_F	GATCGGCTCTGAATTCTTCG
MDV2-miR-M16_R	CCCAACCGAGAAACCTATCC
MDV2-miR-M21_F	TCTGCTCCGTCCTTAGCGTG
MDV2-miR-M21_R	CCCAGCCGACAACCCATTCT
MDV2-miR-M22_F	GTTCACTGAATCGCAACGAG
MDV2-miR-M22_R	GCAGCCTAAAAGTCGCTCTG
MDV2-miR-M30_F	AGAGAGTCCTCCCCGGTTC
MDV2-miR-M30_R	AACTCCGATTGCTGGCTATG

Table 7 - Table listing oligos used to amplify the pre-miRNA sequence from BAC DNA from the corresponding miRNAs.

Oligo Name	Sequence (5' to 3')
JUN_H12-5p_TOP	TCGAGTAATGTTTCTGTTTCTGGAAAAAAAATCTAGAAGGTTCTATTATATTTAAGAAAAATAAAATACTTAAAATGCATTTCCTCCTCACACTTTTTTTTTTATTTTGC
JUN_H12-5p_BOT	GGCCGCAAAATAAAAAAAAAAGTGTGAGGAGGAAATGCATTTTAAGTATTTTATTTTTCTTAAATATAATAGAACCTTCTAGATTTTTTTTCCAGAAACAGAAACATTAC
JUN_MUT_H12-5p_TOP	TCGAGTAATGTTTCTGTTTCTGGAAAAAAAATCTAGAAGGTTCTATTATATTTGATACAAATAAAATACTTAAAATGCATTTCCTCCTCACACTTTTTTTTTTATTTTGC
JUN_MUT_H12-5p_BOT	GGCCGCAAAATAAAAAAAAAAGTGTGAGGAGGAAATGCATTTTAAGTATTTTATTTGTATCAAATATAATAGAACCTTCTAGATTTTTTTTCCAGAAACAGAAACATTAC
EBF1_H5_TOP	TCGAGGCCTTAACAATGCAAATCATATTCATTTCACCTGTACATTGTACTGTGCACCAGAACTGTCAATCATCACTAACATTCTAAGAAAAAAAAAAAAAAAAAGGAATGC
EBF1_H5_BOT	GGCCGCATTCCTTTTTTTTTTTTTTTTCTTAGAATGTTAGTGATGATTGACAGTTCTGGTGCACAGTACAATGTACAGGTGAAATGAATATGATTTGCATTGTTAAGGCC
EBF1_MUT_H5_TOP	TCGAGGCCTTAACAATGCAAATCATATTCATTTCACCTGTACATTGTACTGTGCGCTAAAACTGTCAATCATCACTAACATTCTAAGAAAAAAAAAAAAAAAAAGGAATGC
EBF1_MUT_H5_BOT	GGCCGCATTCCTTTTTTTTTTTTTTTTCTTAGAATGTTAGTGATGATTGACAGTTTTAGCGCACAGTACAATGTACAGGTGAAATGAATATGATTTGCATTGTTAAGGCC
CTBP1_H7-5p_TOP	TCGAGTGAATTCCCTTGTTTCAAAATGAAGACAACCTTGCAAAGAGATTTTGAGGAAAAAAAAAAAAAAAGGTTTTGTATAAATGAGCATTGTGCTTTTTGTCACCAGTGC
CTBP1_H7-5p_BOT	GGCCGCACTGGTGACAAAAAGCACAATGCTCATTTATACAAAACCTTTTTTTTTTTTTTCCTCAAAATCTCTTTGCAAGGTTGTCTTCATTTTGAAACAAGGGAATTCAC
CTBP1_MUT_H7-5p_TOP	TCGAGTGAATTCCCTTGTTTCAAAATGAAGACAACCTTGCAAAGAGATTTTGAGTACAGAAAAAAAAAAGGTTTTGTATAAATGAGCATTGTGCTTTTTGTCACCAGTGC
CTBP1_MUT_H7-5p_BOT	GGCCGCACTGGTGACAAAAAGCACAATGCTCATTTATACAAAACCTTTTTTTTTTTCTGTACTCAAAATCTCTTTGCAAGGTTGTCTTCATTTTGAAACAAGGGAATTCAC
ERBB4_H14_TOP	TCGAGTAGTTTGCACTTAAGCTCTGATTTTATTTGAACTGTTTTCTGGATTTTGAATGAAGCAATATGGAAGTGACCAGCAAAATACAAAATAATAATTTTAAATTTGC
ERBB4_H14_BOT	GGCCGCAAATTTAAAATTATTATTTTGTATTTTGCTGGTCACTTCCATATTGCTTCATTCAAAATCCAGAAAACAGTTCAAATAAAATCAGAGCTTAAGTGCAAACTAC
ERBB4_MUT_H14_TOP	TCGAGTAGTTTGCACTTAAGCTCTGATTTTATTTGAACTGTTTTCTGGATTTTTACTTAAGCAATATGGAAGTGACCAGCAAAATACAAAATAATAATTTTAAATTTGC
ERBB4_MUT_H14_BOT	GGCCGCAAATTTAAAATTATTATTTTGTATTTTGCTGGTCACTTCCATATTGCTTAAGTAAAAATCCAGAAAACAGTTCAAATAAAATCAGAGCTTAAGTGCAAACTAC
BCL11A_H17_TOP	TCGAGATGGCTATTTTTTAAATTGTCCCTGATTAGTTGCTGAGCAAACATGTTGCTGTTTCCAGTTCCATTTGGGAAAAAAAAAAAAAAAAAAAAAAAAAAGAAAGGC
BCL11A_H17_BOT	GGCCGCCTTTCTTTTTTTTTTTTTTTTTTTTTTTTTTTCCCAAATGGAACTGGAAACAGCAACATGTTTGCTCAGCAACTAATCAGGGACAATTTAAAAAATAGCCATC
BCL11A_MUT_H17_TOP	TCGAGATGGCTATTTTTTAAATTGTCCCTGATTAGTTGCTGAGCAAACATGTTGCGGCTGCCAGTTCCATTTGGGAAAAAAAAAAAAAAAAAAAAAAAAAAGAAAGGC
BCL11A_MUT_H17_BOT	GGCCGCCTTTCTTTTTTTTTTTTTTTTTTTTTTTTTTTCCCAAATGGAACTGGCAGCCGCAACATGTTTGCTCAGCAACTAATCAGGGACAATTTAAAAAATAGCCATC
RAN_H17_TOP	TCGAGAAACAAAAAAACACAACAAAACTTCATAATTTTGGACCTGCATATTTAGCTGTTTTTTGGACTGCAATTACTTCCCCTTTGAGTTTCAAATATAAGACTGCTGGC
RAN_H17_BOT	GGCCGCCAGCAGTCTTATATTTGAAACTCAAAGGGGAAGTAATTGCAGTCCAAAAAACAGCTAAATATGCAGGTCCAAAATTATGAAGTTTTGTTGTGTTTTTTTGTTTC
RAN_MUT_H17_TOP	TCGAGAAACAAAAAAACACAACAAAACTTCATAATTTTGGACCTGCATATTTAGCGGCTGTTTGGACTGCAATTACTTCCCCTTTGAGTTTCAAATATAAGACTGCTGGC
RAN_MUT_H17_BOT	GGCCGCCAGCAGTCTTATATTTGAAACTCAAAGGGGAAGTAATTGCAGTCCAAACAGCCGCTAAATATGCAGGTCCAAAATTATGAAGTTTTGTTGTGTTTTTTTGTTTC
RAP1A_H7-5p_TOP	TCGAGATTATATTCTAATTAAAAATGTTTGTGCATAAAGCTTTGGAAAAATGGGTCTTTTATAGGAAAAAAAAAACTGGGATAACTGATTTCTATGGCTTTAAAAGCAGC
RAP1A_H7-5p_BOT	GGCCGCTGCTTTTAAAGCCATAGAAATCAGTTATCCCAGTTTTTTTTTTCCTATAAAAGACCCATTTTTCCAAAGCTTTATGCACAAACATTTTTAATTAGAATATAATC
RAP1A_MUT1+2_H7-5p_TOP	TCGAGATTATATTCTAATTAAAAATGTTTGTGCATAAAGCTTTGTACAGATGGGTCTTTTATAGTACAGAAAAAACTGGGATAACTGATTTCTATGGCTTTAAAAGCAGC
RAP1A_MUT1+2_H7-5p_BOT	GGCCGCTGCTTTTAAAGCCATAGAAATCAGTTATCCCAGTTTTTTCTGTACTATAAAAGACCCATCTGTACAAAGCTTTATGCACAAACATTTTTAATTAGAATATAATC
MYBL1_M30_TOP	TCGAGTTGCACTACTAATTTTTTGGTATGCTGCAAAACAGTGAAATTAACTACAGTGTTAAATATATTTATTTGCAAATGGTACTAGAAGTAGGCAGAGAGGGGTGAAGC
MYBL1_M30_BOT	GGCCGCTTCACCCCTCTCTGCCTACTTCTAGTACCATTTGCAAATAAATATATTTAACACTGTAGTTAATTTCACTGTTTTGCAGCATACCAAAAAATTAGTAGTGCAAC

Table 8 - Table listing oligos that were annealed together, and subsequently ligated into *Xho*I and *Not*I digested psiCHECK2 vectors. Naming structure is gene name_ (MUT if there are changes in 3'UTR sequence) _miRNA predicted to target_TOP or BOT(bottom) to distinguish oligos in the pair

Oligo Name	Sequence (5' to 3')
MYBL1_MUT_M30_TOP	TCGAGTTGCACTACTAATTTTTTGGTATGCTGCAAAACAGTGAAATTAACTACAATATGAAATATATTTATTTGCAAATGGTACTAGAAGTAGGCAGAGAGGGGTGAAGC
MYBL1_MUT_M30_BOT	GGCCGCTTCACCCCTCTCTGCCTACTTCTAGTACCATTTGCAAATAAATATATTTCATATTGTAGTTAATTTCACTGTTTTGCAGCATACCAAAAAATTAGTAGTGCAAC
TIAM1_M30_TOP	TCGAGTTTGTATTTTACCTGAGATGCAGGGGCACAAAGGGATAAGAATTTTACAGTGTTAGCTTAGCTCCATGTCTAGGATACGAGGCTAGCTTTTTGCAGAGGGTTAGC
TIAM1_M30_BOT	GGCCGCTAACCCTCTGCAAAAAGCTAGCCTCGTATCCTAGACATGGAGCTAAGCTAACACTGTAAAATTCTTATCCCTTTGTGCCCCTGCATCTCAGGTAAAATACAAAC
TIAM1_MUT_M30_TOP	TCGAGTTTGTATTTTACCTGAGATGCAGGGGCACAAAGGGATAAGAATTTTACAATATGAGCTTAGCTCCATGTCTAGGATACGAGGCTAGCTTTTTGCAGAGGGTTAGC
TIAM1_MUT_M30_BOT	GGCCGCTAACCCTCTGCAAAAAGCTAGCCTCGTATCCTAGACATGGAGCTAAGCTCATATTGTAAAATTCTTATCCCTTTGTGCCCCTGCATCTCAGGTAAAATACAAAC
RALA_M22_TOP	TCGAGGTAGCTTGGTGAACTATGTGGTATCTTATAGCTAAAAGGTCAGAATATGTGTAAGATGGAAGTCAAAAGCCTATGGCACATCCGAGCCTGGAGTGGTTGCTTAGC
RALA_M22_BOT	GGCCGCTAAGCAACCACTCCAGGCTCGGATGTGCCATAGGCTTTTGACTTCCATCTTACACATATTCTGACCTTTTAGCTATAAGATACCACATAGTTCACCAAGCTACC
RALA_MUT_M22_TOP	TCGAGGTAGCTTGGTGAACTATGTGGTATCTTATAGCTAAAAGGTCAGAATATGTATGATATGGAAGTCAAAAGCCTATGGCACATCCGAGCCTGGAGTGGTTGCTTAGC
RALA_MUT_M22_BOT	GGCCGCTAAGCAACCACTCCAGGCTCGGATGTGCCATAGGCTTTTGACTTCCATATCATACATATTCTGACCTTTTAGCTATAAGATACCACATAGTTCACCAAGCTACC
TIAM1_M16_TOP	TCGAGTTTAGCTGTCCTATGCTGTACCCAGTGGAATACAGTCAGTTCTGGAATACTGGAAGGCTGGTACTGGGAAGGTACCGTTGTTCTTGTACATAATGTCATGACAGC
TIAM1_M16_BOT	GGCCGCTGTCATGACATTATGTACAAGAACAACGGTACCTTCCCAGTACCAGCCTTCCAGTATTCCAGAACTGACTGTATTCCACTGGGTACAGCATAGGACAGCTAAAC
TIAM1_MUT_M16_TOP	TCGAGTTTAGCTGTCCTATGCTGTACCCAGTGGAATACAGTCAGTTCTGGAATATTAGGAGGCTGGTACTGGGAAGGTACCGTTGTTCTTGTACATAATGTCATGACAGC
TIAM1_MUT_M16_BOT	GGCCGCTGTCATGACATTATGTACAAGAACAACGGTACCTTCCCAGTACCAGCCTCCTAATATTCCAGAACTGACTGTATTCCACTGGGTACAGCATAGGACAGCTAAAC
ERBB4_M16_TOP	TCGAGGGAGTCAGCCCAGCTCTCTGTGGGGTGCTGGTGGGAAGGGTCCTTGAAACTGGAAGAAAGAAACACTGGACTGGAGAAAACGCACATAGAGGTTCACTGGAAAGC
ERBB4_M16_BOT	GGCCGCTTTCCAGTGAACCTCTATGTGCGTTTTCTCCAGTCCAGTGTTTCTTTCTTCCAGTTTCAAGGACCCTTCCCACCAGCACCCCACAGAGAGCTGGGCTGACTCCC
ERBB4_MUT_M16_TOP	TCGAGGGAGTCAGCCCAGCTCTCTGTGGGGTGCTGGTGGGAAGGGTCCTTGAAATTAGGAGAAAGAAACACTGGACTGGAGAAAACGCACATAGAGGTTCACTGGAAAGC
ERBB4_MUT_M16_BOT	GGCCGCTTTCCAGTGAACCTCTATGTGCGTTTTCTCCAGTCCAGTGTTTCTTTCTCCTAATTTCAAGGACCCTTCCCACCAGCACCCCACAGAGAGCTGGGCTGACTCCC
DEK_M30_TOP	TCGAGGGAGTCAGCCCAGCTCTCTGTGGGGTGCTGGTGGGAAGGGTCCTTGAAACTGGAAGAAAGAAACACTGGACTGGAGAAAACGCACATAGAGGTTCACTGGAAAGC
DEK_M30_BOT	GGCCGCTTTCCAGTGAACCTCTATGTGCGTTTTCTCCAGTCCAGTGTTTCTTTCTTCCAGTTTCAAGGACCCTTCCCACCAGCACCCCACAGAGAGCTGGGCTGACTCCC
DEK_MUT_M30_TOP	TCGAGGGAGTCAGCCCAGCTCTCTGTGGGGTGCTGGTGGGAAGGGTCCTTGAAATTAGGAGAAAGAAACACTGGACTGGAGAAAACGCACATAGAGGTTCACTGGAAAGC
DEK_MUT_M30_BOT	GGCCGCTTTCCAGTGAACCTCTATGTGCGTTTTCTCCAGTCCAGTGTTTCTTTCTCCTAATTTCAAGGACCCTTCCCACCAGCACCCCACAGAGAGCTGGGCTGACTCCC
AKT3_M21_TOP	TCGAGAACTTTAGCTTTCTTCTTCAGCAATGATAATCTTAATAATAAACCCGTTGGTGCTAGGAGCTGGGATGTTACGCAGTGCAGCGATGTGCACGCGCCCTTGCTAGC
AKT3_M21_BOT	GGCCGCTAGCAAGGGCGCGTGCACATCGCTGCACTGCGTAACATCCCAGCTCCTAGCACCAACGGGTTTATTATTAAGATTATCATTGCTGAAGAAGAAAGCTAAAGTTC
AKT3_MUT_M21_TOP	TCGAGAACTTTAGCTTTCTTCTTCAGCAATGATAATCTTAATAATAAACCCGTTGATTCGAGGAGCTGGGATGTTACGCAGTGCAGCGATGTGCACGCGCCCTTGCTAGC
AKT3_MUT_M21_BOT	GGCCGCTAGCAAGGGCGCGTGCACATCGCTGCACTGCGTAACATCCCAGCTCCTCGAATCAACGGGTTTATTATTAAGATTATCATTGCTGAAGAAGAAAGCTAAAGTTC
DNMT3B_H16_TOP	TCGAGGAAATGCCTTTTTTTAATGCTTTGTAAAGGTTTCTAACTCTCCCTGGTGCTATTTTTTTAGTTAAAGGATTTTTGATGTCCAAAGTTTTGTGGGTTTTTATACGC
DNMT3B_H16_BOT	GGCCGCGTATAAAAACCCACAAAACTTTGGACATCAAAAATCCTTTAACTAAAAAAATAGCACCAGGGAGAGTTAGAAACCTTTACAAAGCATTAAAAAAAGGCATTTCC
DNMT3B_MUT_H16_TOP	TCGAGGAAATGCCTTTTTTTAATGCTTTGTAAAGGTTTCTAACTCTCCCTGGTGCGACTGTTTTAGTTAAAGGATTTTTGATGTCCAAAGTTTTGTGGGTTTTTATACGC
DNMT3B_MUT_H16_BOT	GGCCGCGTATAAAAACCCACAAAACTTTGGACATCAAAAATCCTTTAACTAAAACAGTCGCACCAGGGAGAGTTAGAAACCTTTACAAAGCATTAAAAAAAGGCATTTCC

Table 9 - Table listing oligos that were annealed together, and subsequently ligated into *Xho*I and *Not*I digested psiCHECK2 vectors. Naming structure is gene name_ (MUT if there are changes in 3'UTR sequence) _miRNA predicted to target_TOP or BOT (bottom) to distinguish oligos in the pair

2.3.33.2 Chapter 4

Oligo Name	Sequence (5' to 3')
H1-H18_BglII_F	ATATATAGATCTTTATACTATTGGCTTTAGGTG
H1-H18_SalI_R	ATAATAGTCGACAACCTCCAGTGACCTGTTTT
M13_F	GTAAAACGACGGCCAGT
M13_R	CAGGAAACAGCTATGAC
H1-H18_Seq_1	CAGGTCACTGGAGGTTGTCGAC
H1-H18_Seq_2	GTCAATGTGGCGGTTCCCGACG
H1-H18_Seq_3	TGTGATATGGTGTGATATGAATGCC
H1-H18_Seq_4	CGCCTTTATAGGCATCTACGTGC
H1-H18_Seq_5	CCATTGCGCGAATGTAATACAGTG
H1-H18_Seq_6	AATTCACGGGTCGTCTACGGGG
H1-H18_Seq_7	GGCCTTTGAGAGATTATATGAGCAA
H1-H18_Seq_8	CATGTCCCGAGATGGTCGTCTC
H1-H18_Seq_9	ACCAGGTGGACTTTATACAATCGTG
H1-H18_Seq_10	AGGGATGGGTAGTGTATTGCGAC
H1-H18_Seq_11	AGCTACGTTGTCCGCGGGATTC
H1-H18_Seq_12	GTGTATTGGGGGCGTGCTATGG
H1-H18_Seq_13	TAAACAGCCCCGATTTGACAGG
H1-H18_Seq_14	ACTTGTCCGGTGCCAGCAAAGC

Table 10 - Table listing all the oligonucleotide primers used to create and sequence the HVT miRNA expression construct

2.3.33.3 Chapter 5

Primer Name	Sequence 5' to 3'
HVT_miR Del KanSacB F	GGAAAGGCTATTATGTGTTAGGGGAGAGACCACGTGATCGGCATGCAAATGAGCAAGGCGAACGCGTCAGCGTTCTGTAAAACGACGGCCAGT
HVT_miR Del KanSacB R	AATCTCGGTCGCTTCATCCCGAAACCTCCAGTGACCTGTTTTCCCTCGGCCAGTGTCAGGCTCCGCGAAATCTTCCAGGAAACAGCTATGACC
HVT_miR Del Spec F	CGTCCGGCTAGTCCAATAGCGGGGTCGCGTTTCGTACCACGTGTTATAGACCGCCCTAAACTCGCACTCGGGGGTGGCCTGGTGATGATGGCGGGATCG
HVT_miR Del Spec R	TTCACACACGCCCTGTATTTCGGCTTTGCTGGCACCGGACAAGTCCTTCGTATTGCAACAAACAACAAGGGGGTATATTATGTACCTGACTGATG
HVT_miR PCR F	CGGTGTCTCTTTCAGTGGAG
HVT_miR PCR R	CAAAAACATTGCGACCAGAG
MDV2_miR Del KanSacB F	CTGGTGTTGGTTCGTCCGCCACGGAAGCTGGAACCCCATCGGACGTCTCGGCGCCCTGTTTGCAAAATGTCAGGTTGTAAAACGACGGCCAGT
MDV2_miR Del KanSacB R	TGACCTTAAAGGCCTAACCCTGACCATGACCCTAAGGGCCCGACCCTAACCCTAACCTAGTACCCTCCTTCCACACAGGAAACAGCTATGACC
MDV2_miR Del Spec F	TGAGGGGAGGGGGGGCTGAGTTTTTCTGTTATGGGTATCCTGAGGGGTCTACGTGAAAGTGACTGGCCTTCCGTTATCGATAAGCTTGATATC
MDV2_miR Del Spec R	CAACAATGAACTCGGCCGGTTTAAAGATTTATTTCGATGCGATGCGCGGTCACGCCCACCACAAAAATAGACCCT TATTATGTACCTGACTGATG
MDV2_miR PCR F	CTGAGACCTATCGCCTTTGG
MDV2_miR PCR R	CTAACCACGACCCCGAGAC

Table 11 - Table listing primers used to generate miRNA deletion BAC clones of HVT and MDV2 viral genomes. Primers were ordered from Eurofins MWG Operon at either 0.1µM (<60 bp) or 0.5µM scale. MDV2 miRH1-H18

2.3.34 Construction of mutant HVT and MDV-2 BAC viruses

A diagrammatic representation of this process can be found in figure 35 in section 5.1.2.

2.3.34.1 Single-copy miRNA knockouts

2.3.34.1.1 Preparing DNA for removal of miRNAs via homologous recombination

The KanSacB cassette was PCR amplified from the pGEM11Z-KanSacB vector using goTaq DNA polymerase as described in the methods (section 2.3.6). Amplification was carried out using the KanSacB primers listed in table 11. The primers were designed with a 75 base pair overhang, from the template DNA. This overhang matches a region adjacent either side of the miRNAs (in this virus genome) allowing recombination to occur. The KanSacB cassette was successfully amplified from the pGEM11Z-KanSacB vector containing the overhangs, matching regions in either the HVT or MDV2 genome. PCR products were purified by gel extraction following DNA electrophoresis, using Qiagen gel extraction kit, following the manufacturer's protocol. PCR products were confirmed further by Sanger sequencing at Source Bioscience, Oxford, using the same amplification primers for sequencing. Once confirmed visually by electrophoresis and sequence confirmed the purified KanSacB PCR products, with overhangs, were ready for transformation.

2.3.34.1.2 Creating electrocompetent *E. coli* containing parental BAC DNA

In order for a recombination event to occur, bacteria containing the parental (no alterations to BAC DNA) BAC clones were required. EL250 *E. coli* bacteria were used. EL250 are derived from DH10B that carry a bacteriophage lambda prophage with the genes *exo*, *bet* and *gam* under the control of a temperature-sensitive cI-repressor. These genes are switched off at 32°C and switched on at 42°C. *Gam* inhibits RecBCD nuclease from degrading linear DNA, and *Exo* and *Beta* provide double stranded break repair recombinase activity.

Electrocompetent EL250 containing pHVT3 and pSB-1 BAC3 DNA were generated, as described in methods (section 2.3.13), from previously established glycerol stocks of EL250.

2.3.34.1.3 Transforming KanSacB cassette for homologous recombination

Following the preparation of DNA for transformation and electrocompetent cells containing the pHVT3 and pSB-1 BAC3 DNA (separately), transformation was performed to induce homologous recombination. Purified KanSacB cassette PCR product (2µl) from above was added into one aliquot of electrocompetent EL250 cells that had been thawed on ice and mixed by stirring with pipette tip. Transformation was performed as described in the section 2.3.23. Total transformation mixture was then plated (250µl) over four LB Agar plates containing 25µg/ml Chloramphenicol (C_{25}) and 50µg/ml Kanamycin (K_{50}) and incubated overnight at 32°C.

2.3.34.1.4 Analysis of transformation

Following overnight incubation there were roughly 100 colonies present per plate, for both pHVT-3 and pSB-1 BAC3 miRNA first copy deletion. 6 colonies of both pHVT3 and pSB-1 single-copy miRNA deletion were picked from the plates and inoculated in 2ml Terrific Broth containing 25µg/ml Chloramphenicol (C_{25}) and 50µg/ml Kanamycin (K_{50}) and incubated overnight at 32°C, 2.5xg. The following morning, 500µl of culture was taken to create a glycerol stock, the remaining 1.5ml culture was used to perform a STET miniprep for quick analysis of the BAC DNA.

2.3.34.1.5 Testing sucrose sensitivity of clones

Cultures grown from the glycerol stocks of the 6 clones for both pHVT3 and pSB-1 BAC3 miRNA single-copy deletion were diluted 1 in 100 and plated on LB agar plates C_{25} with 10% sucrose, plates were then incubated overnight at 32°C. After overnight incubation, plates that contained a lawn of bacteria demonstrated that in those clones, the *SacB* section of the inserted KanSacB cassette was not working properly.

2.3.34.2 Double-copy miRNA knockouts

The spectinomycin cassette was amplified from the pR6K-photo-rpsL-amp-Ter vector (from Andrew Brown) with goTaq DNA polymerase (Promega) using the spectinomycin primers listed in table 11. Once again these forward and reverse primers contained a 5' 75bp region of homology (set 'inside' of the previous deletion) to the BAC viral genome. Spectinomycin resistance cassette PCRs were generated, containing homology to both the pHVT3 and pSB-1, these PCR products were analysed, gel purified and sequenced as described for the first copy miRNA deletion in section 2.3.34.1.

Transformation of the PCR products was the same as described in section 2.3.34.1, however this time the electro-competent EL250 *E. coli* contained either the pSB-1 BAC3 ΔmiR-1 or pHVT3 ΔmiR-1 constructs. Recombination was under the positive selection pressure of spectinomycin resistance, therefore the transformation cell mixture was plated on LB agar C_{25} K_{50} Spectinomycin 50µg/ml (S_{50}) plates, and positive recombinants were observed the following day after overnight incubation at 32°C. Fewer colonies were present on each plate than with the previous miRNA copy deletion, on the pHVT3-second copy miRNA deletion transformation there were approximately six colonies per plate (four plates) and in the pSB-1-second copy miRNA deletion transformation there were approximately 20 colonies per plate (four plates). Three colonies were inoculated from both pHVT3-second copy miRNA deletion and pSB-1 BAC3-second copy miRNA deletion in 2ml Terrific Broth C_{25} K_{50} S_{50}, incubated overnight at 32°C, 2.5xg.

2.3.34.3 Single-copy miRNA revertants

2.3.34.3.1 Transformation and initial screening of colonies

The original region of the BAC viral genomes, containing the miRNAs, was amplified from unmodified pHVT3 and pSB-1 BAC3 DNA. PCR amplification was performed using the primers listed in table 11, with Platinum Pfx DNA polymerase as described in the methods (section 2.3.6). Following amplification the PCR products were analysed by DNA gel electrophoresis and the correct PCR products purified by gel extraction using QIAquick Gel Extraction Kit (Qiagen) following manufacturer's protocol. As before the purified PCR products were transformed into electro-competent *E. coli* this time containing either pSB-1 BAC3- or pHVT3-miRNA double-copy deletion BAC DNA. Following transformation (methods section 2.3.23), the transformed *E. coli* cells were diluted 1:100 in LB broth then plated on LB agar plates C_{25} S_{50} containing 10% sucrose, then incubated overnight at 32°C.

The PCR products generated by both sets of primers contain all the miRNAs that were removed plus approximately 200bp of flanking sequence 5' and 3'. This flanking sequence allowed for efficient recombination to occur. Recombination was driven by the negative selection pressure of sucrose sensitivity within the KanSacB cassette, meaning in clones where the KanSacB cassette was not replaced with the miRNA sequence the sucrose in the plate will become toxic and the colony will not expand.

Following overnight incubation there were roughly 100 colonies per plate, before BAC STET minipreps were performed, the colonies were screened for loss of kanamycin resistance, as the KanSacB cassette should have been replaced by the miRNA sequence. Colonies were picked from the original overnight incubation plate then spotted using a sterile pipette tip on both an LB agar C_{25} S_{50} K_{50} plate and an LB agar C_{25} S_{50} 10% sucrose plate using a 6x8 grid for reference.

2.3.35 Antibodies used for immunofluorescent staining of viral plaque

Antibody	Clonality	Manufacturer	Raised in	Catalogue #	Dilution in OptiMEM
Serum from HVT vaccinated birds	Polyclonal	Viral Oncogeneis Group, IAH	Chicken	N/A	1:250
Anti-MDV-2 Y5.9	Monoclonal	L.F. Lee et al. 1983	Mouse	N/A	1:500
Alexa Fluor® 488 Anti-Chicken IgG (H+L)	Monoclonal	Life Technologies	Goat	A-11039	1:1000
Alexa Fluor® 488 Anti-Mouse IgG (H+L)	Monoclonal	Life Technologies	Goat	A-11001	1:1000

Table 12 - Information about antibodies used for fluorescent staining of pHVT3 and pSB-1 BAC3 plaques in chapter 5.

2.3.36 Table of primers and probes used to determine levels of MDV-2 and HVT via qRT-PCR

Target sequence	Primer /probe	Primer sequence (5'-3')	Reference
MDV-1 US2 gene	F Primer R Primer Probe	CATCCTGCCATTCTGTGGAA GCCGGAACTAGGGATTCGTT (*FAM*)-ATCCTGCAACATCTTCAAATAGCCGCAC-(*BHQ1*)	(Baigent et al. 2011)
DNA-Pol (MDV2)	F Primer R Primer Probe	AGCATGCGGGAAGAAAAGAG GAAAGGTTTTCCGCTCCCATA (*ROX*)-CGCCCGTAATGCACCCGTGACT-(*BHQ-2*)	(Islam et al. 2004)
SORF1 (HVT)	F Primer R Primer Probe	GGCAGACACCGCGTTGTAT TGTCCACGCTCGAGACTATCC (*CY5*) –AACCCGGGCTTGTGGACGTCTTC-(*BHQ-3*)	(Islam et al. 2004)
BAC constructs (pDS pHA1plasmid)	F Primer R Primer Probe	CCAGGTCCACTTCGCATATTAAG TGACGATGTATTTTTCGCTCATG (*FAM*)-TGACACGCGCGGCCTCGA-(*BHQ1*)	(Baigent et al. 2011)
Chicken ovotransferrin gene (*ovo*)	F Primer R Primer Probe	CACTGCCACTGGGCTCTGT GCAATGGCAATAAACCTCCAA (*VIC*)-AGTCTGGAGAAGTCTGTGCAGCCTCCA-(*TAMRA*)	(Baigent et al. 2005)

Table 13 - Details of different qRT-PCR primers and probes used to determine levels of MDV-2 and HVT virus in different experiments, also included is the primer and probe sequence for qRT-PCR detection of the *ovo* reference gene. Further detail can be found in the references provided.

3 Using comparative studies and bioinformatic miRNA target prediction algorithms to highlight targets of HVT and MDV-2 encoded miRNAs

3.1 Does MDV-2 encode a functional ortholog of the host miRNA *gga-miR-29b*?

3.1.1 Evidence for other viral orthologs of host miRNAs

It has been proposed, in herpesviruses at least, that the small size and lack of immunogenic nature of miRNAs makes them perfect candidates to manipulate host gene expression during the latent stage of infection to suit the requirements of the virus (Kincaid and Sullivan 2012).

While the location and expression levels of miRNAs from closely related herpesviruses appears to show similarity, the actual sequence of these miRNAs is not conserved (Ramalingam et al. 2012; Yao et al. 2007). In a small number of herpesviruses a functional ortholog of a host-encoded miRNA has been identified. The first example of a virally encoded miRNA that can act as an ortholog of a host miRNA was the KSHV miRNA miR-K12-11 (figure 8A), the second example was MDV-1 miRNA *mdv1-mir-M4*, both orthologous in function to host miRNA *miR-155* (figure 8B) (Skalsky et al. 2007; Y. Zhao et al. 2011). The functional similarities of the virally encoded miRNAs to the host *miR-155* was demonstrated in both studies by a number of experiments and assays demonstrating miRNA mediated targeting of a similar gene set, such as *PU.1* and *BACH-1*. Since those initial studies, the degree to which the viral miRNAs can act as orthologs of the host miRNA has been explored further. In a study by Zhao et al, host *gga-miR-155* was used to rescue the oncogenic phenotype in MDV1 miRNA *miR-M4* deleted virus, showing that both the host *miR-155* and virus *miR-M4* share oncogenic functions (Y. Zhao et al. 2011). *miR-155* is a well-characterised miRNA that is implicated in oncogenic transformation across a number of species (Croce 2009), including in mice where an over-expression of *miR-155* causes them to develop B-cell lymphomas (Costinean et al. 2006). As MDV infection can also cause lymphoma and the MDV viral ortholog targets the same genes as the host *miR-155*, it is tempting to suggest that viral

miRNAs are responsible for the oncogenicity of this virus. Therefore we were intrigued by the possibility of MDV-2 containing similar host miRNAs orthologs.

The KSHV and MDV1 viral miRNAs mentioned above were identified as potential orthologs on the basis of partial sequence homology between the host and viral miRNAs, notably within the seed regions (figure 8). It is widely accepted that the seed region, nucleotides 2-8, play an extremely important role in targeting transcripts (Friedman et al. 2009). Other viral miRNAs have been predicted to be functional orthologs of host encoded miRNAs based on seed sequence matches between DNA virus-encoded miRNAs and host miRNAs (Skalsky et al. 2007). Therefore it is a fair assumption that other viral miRNAs sharing identical seed sequences with host miRNAs may similarly share an orthologous function.

In addition to *miR-155*, a functional ortholog of *miR-29b* (*blv-miR-B4*) has been described in bovine leukemia virus (BLV) (Kincaid et al. 2012). *miR-29b* is a member of the *miR-29* family consisting of two additional mature miRNAs, *miR-29a* and *miR-29c*. Members of the *miR-29* family have been found to be up and down-regulated in different studies of cancers, as tumour-suppressors (Fabbri et al. 2007; J. J. Zhao et al. 2010), but also as oncogenes (Gebeshuber et al. 2009; Han et al. 2010). It has therefore been suggested that the function of the *miR-29* family miRNA is determined by the cellular context within which it is expressed (Pekarsky and Croce 2010). Additionally *miR-29b* is known to be an important regulator of immune response against infection (Ma et al. 2011). Intriguingly we have identified, and it has since been published (Morgan and Burnside 2011) that a similar sequence is present in the genome of MDV-2 (*mdv2-miR-M21-3p* (figure 8c)) and so the aim of this work is to ascertain whether this sequence is also a functional ortholog of *gga-miR-29b.*

All *miR-29* family members share the same seed sequence, and thus are also potential orthologs of *mdv2-miR-M21*.

	miRNA Name	miRNA Sequence
A	*hsa-miR-155-5p*	UUAAUGCUAAUCGUGAUAGGGGU
	kshv-miR-K12-11-3p	UUAAUGCUUAGCCUGUGUCCGA
B	*gga-miR-155*	UUAAUGCUAAUCGUGAUAGGGG
	mdv1-miR-M4-5p	UUAAUGCUGUAUCGGAACCCUUC
C	*hsa-miR-29b-3p*	UAGCACCAUUUGAAAUCAGUGUU
	gga-miR-29b-3p	UAGCACCAUUUGAAAUCAGUGUU
	mdv2-miR-M21-3p	GAGCACCACGCCGAUGGACGGAGA
	blv-miR-B4-3p	UAGCACCACAGUCUCUGCGCCUUU

Figure 8 - Sequence similarities between viral miRNAs and their host encoded orthologs, identical residues highlighted in red. **A -** Alignment of *hsa-miR-155* and *kshv-miR-K12-11*. **B** - Alignment of *gga-miR-155* and *mdv1-miR-M4*. **C -** Alignment of *gga-miR-29b* with *mdv2-miR-M21* and *blv-miR-B4-3p*, also shown *hsa-miR-29b* which has identical sequence to *gga-miR-29b*.

Determining if the virally encoded *mdv2-miR-M21* was indeed a functional ortholog of the host *miR-29* family miRNAs, is of interest because a great deal of work has been previously been performed to validate targets of the *miR-29* family miRNA (Kriegel et al. 2012). Using these studies we have generated a list of some potential targets of this virally encoded miRNA. *miR-29* family miRNAs have been shown to target a diverse range of proteins ranging from transcription factors, collagens and methyltransferases (Schmitt et al. 2012). It is the miRNA mediated targeting by viral *mdv2-miR-M21* of these genes, within the host, this part of the project aims to validate.

3.1.2 DNA Methyltransferase 3-Beta (*DNMT3B*)

In addition to a number of other targets validated for the human *miR-29* miRNA family (which are identical in sequence to the chicken miRNAs), *DNMT3B* is the only one that has been experimentally validated as a target for the chicken miRNA, *gga-miR-29b* (Rengaraj et al. 2011). *DNMT3B* is part of the DNMT3 family consisting also of *DNMT3A*, these methyltransferases are responsible for *de novo* methylation, as opposed to the maintenance of methylation performed by *DNMT1* (Okano et al. 1999). Methylation occurs through the addition of a methyl group to the DNA to cytosine adjacent to a guanine residue (CpG), this methylation leads to the silencing of gene expression.

New aberrant methylation (hypermethylation) of tumour suppressor genes has been identified and in a number of cancers the levels of the DNMT genes have been found to be increased (Fabbri et al. 2007). The restoration of normal DNA methylation patterns has been used as a treatment to overcome the inappropriate methylation of certain genes in various cancers (Lubbert 2000). The targeting of the *miR-29* family miRNAs of *DNMT3A* and *DNMT3B* therefore could potentially have clinically useful applications in the down-regulation of DNMTs and restoring normal methylation patterns of genes (Garzon et al. 2009).

3.1.3 Experimental outline

In order to determine if *mdv2-miR-M21* is acting as an ortholog of the host encoded miRNA *miR-29b,* the ability of *mdv2-miR-29b* to target *DNMT3B* (a previously identified target of *gga-miR-29b*) was explored. Initially bioinformatic tools were used to identify any potential target site for the viral miRNA within the *DNMT3B* 3'UTR. If target sites were found, reporter assays were generated along with miRNA expression assays so that any knockdown of gene expression could be observed. Any knockdown of gene expression was then quantified using qRT-PCR.

When miRNA mediated targeting of the *DNMT3B* gene was observed, western blots were performed to see if there is a resultant decrease in protein levels.

3.1.4 Results

3.1.4.1 Predicted Targeting of *DNMT3B* gene by viral miRNA *mdv2-miR-M21*

TargetScan custom miRNA target prediction program (http://www.targetscan.org/vert_50/seedmatch.html) (Lewis et al. 2005) was used to see, if like the host miRNA *gga-miR-29b*, *mdv2-miR-M21* is predicted to target the *DNMT3B* gene. As required by the TargetScan custom program, the seed region of *mdv2-miR-M21* (nucleotides 2-8) was entered into the program and the species selected as chicken (described in more detail in section 3.2). Unsurprisingly the TargetScan custom program recognised the miRNA as a member of the *miR-29* family as the program only performs searches based on the miRNA seed sequence, which is identical between *mdv2-miR-M21* and the *miR-29* family (figure 8). Therefore the program provided a list of the predicted targets of the *miR-29* family miRNAs, which included *DNMT3B*. The predicted target site was classified as an '8mer' (An exact match to positions 2-8 of the mature miRNA (the seed + position 8) followed by an A) and found conserved across numerous species. In addition to this information the precise predicted target site was identified within the 3'UTR (figure 9). This information was used to create the reporter constructs used for validation of predicted targets via dual-luciferase assay.

A **Predicted target site of gga-miR-29b in chicken DNMT3B 3'UTR**

```
   1 CCCACGCTGC ATCCCTCGTC TCTCCGTCCC AACGCAGCTC TGCTGCCCGG GGAGGGCTCA
  61 GCCCTGTGCC CACCATTCCC AGCACTGTGC CCCCGCTGCC GCAGGGCTCG GGAAGCGCCT
 121 TCAACCAAAG AACCTGGCCG GGTGCCTTCC TGACAGGGAC TACAGCCAGC GCTGCCTGGG
 181 AAATGATGGA CAAAACGAGC TTTAATCACC CAGCACAAAG CTGCGTGCAT CACTGATGAG
 241 GCGAGAAGTC TCCTCCAGAG CATTAAACAT TCCACTTGAG CCCAGAGCTG GGAAGCAGTG
 301 AGTGGTGGAG GCAGCTGCTG GCGTGCTGCA AATGTGGACT GCAGAGCTGC TCACCTCCTA
 361 AACAAGCATA AACCTCTCTT GAAACGACTG CCAAAAACCC TCAAGCTGCA GCAGCAGGTG
 421 TGAGGGCCCC AGGTCAGGTT ATGTACACTG AACGTGCAGA ACACACAAAC CAAATCTTTT
 481 TTTTTGTTTT TGATTTTTAA GACCTTTTTG TAAAACTTTT ACATTTTGTT GTTTAACGTC
 541 TATTGCTGCT TTAAGGCATT ACATACGAAT GTGGAGACTC CTAGACCTGA ATGTAGCTGA
 601 GACTGAACTG TGAGCTGATA GAATTACTTT TCTAGTTAGG GAGATACTGT TTTATGTGTT
 661 CAGCTGTAGT TTACGGATAT TCACTACGTC CTTTTCCAGG CATTTCCCTT TTTTCTCCTG
 721 ACGTTTCAAA ATGCTGCTGA GGGGGTTGGA TGGTTACACT GGGGCAGGGA AATGGGGCTG
 781 TTCTGAGAAT GAGTGCATGG GGTGGGCAGG GGTGGGCCGC TGTTGTCCCC CCCCwCCCCC
 841 CCCGTGCTCT CACCCAGCAG CAGCCCAGGA CTGTGGGTGC CACCGGGCTG CCCACCCCTC
 901 TGCCACCCCA TTCTATGAGT TTTGTTCCTT GGAGCCACGT GGGCTCCCCT CAGTCGCATC
 961 CTCTGTTTCA TGTGCTGGAT CTCACCTCCC TTCAGTCTGA TCAAAAGGAA AAGAGAGAAA
1021 GAAAGGACTC GGGGAAAGCA AACAAAGGAT AAAAGGGGAm CAAGAACGGT CCTbGCGTTA
1081 AGCTGACTTG ATGAGAATCG CAGTAGGACA AGTCTTTCCT TGGAACGCTG CCTTTCATGG
1141 TGTGCTCATC AACmCATTGC AAGGAGAGGT ACAGCTCAGA AATGCCTTTT TTTAATGCTT
1201 TGTAAAGGTT TCTAACTCTC CCTGGTGCTA TTTTTTTAGT TAAAGGATTT TTGATGTCCA
1261 AAGTTTTGTG GGTTTTTATA CAATCTTTTA AAATAAGAGr AAAAAAAAAA AGCCAAAAAA
1321 AAAAAAAAAA AAAAACCGAG GGGGGTCA
```

B

```
dataset: 1
TARGET : Chicken_DNMT3b_3'UTR
length: 1348
MIRNA  : mdv2-miR-M21
length: 24

mfe: -22.5 kcal/mol
p-value: undefined

position  1197
target 5' G  UU  AAA     UUCUAACUCUCCC       A 3'
           CU  GU     GGU              UGGUGCU
           GA  CA     CCG              ACCACGA
miRNA  3' A  GG  GGUAG   C                    G 5'
```

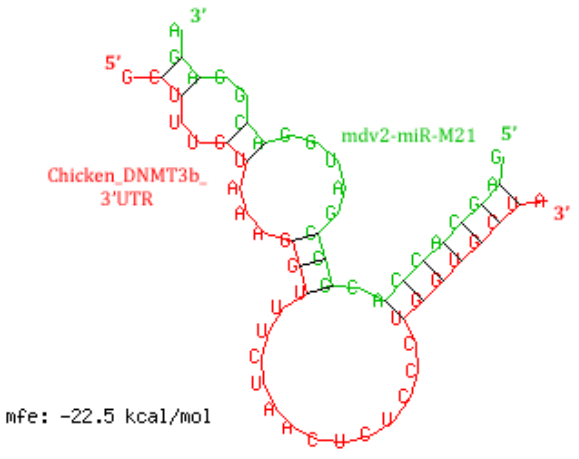


Figure 9 – (A) Highlighted in yellow is the predicted match for the *miR-29b* seed sequence within the chicken *DNMT3B* gene (NCBI Gene ID: 419287). Prediction made by TargetScan custom program.(B)Predicted interaction between miRNA and *DNMT3B* 3'UTR calculated by RNA hybrid (Rehmsmeier et al. 2004)

3.1.4.2 Validating predicted targeting on *DNMT3B* gene by viral miRNA *mdv2-miR-M21*

3.1.4.2.1 Creating luciferase reporter constructs

Reporter constructs were generated through amplification of regions of the *DNMT3B* 3'UTR, using PCR protocol described in section 2.3.6. Briefly, the 3'UTR (or portion of 3'UTR) was cloned downstream of the renilla luciferase gene in the psiCHECK-2 vector (Promega). A mutated version of the 3'UTR was cloned downstream of renilla luciferase in a separate vector (where nucleotides 2, 4 and 6 of the predicted target site are changed at random) reporter constructs were co-transfected into cells with a miRNA expression vector. The mutated 3'UTR construct acted as a control, whereby any miRNA-mediated down regulation of renilla expression in the wild-type construct was analysed relative to the mutated construct (where no miRNA targeting is predicted).

The reporter constructs were named either DNMT3B wt F (full-length 3'UTR) or DNMT3B wt S (predicted miRNA target site plus around 100bp of flanking region). The mutant constructs were made using a long reverse primer in the PCR reaction (that would result in positions 2, 4 and 6 of the seed target region being changed) in the manner described above; these were labelled DNMT3B mut F and DNMT3B mut S. The oligos used to generate these constructs are listed in table 6.

3.1.4.2.2 Creating miRNA expression constructs

miRNA expression vector were created for both the *mdv2-miR-M21* and host *gga-miR-29b* miRNAs. These were created as detailed in section 2.3.21 to be co-transfected with the luciferase reporter constructs to determine if the miRNAs were indeed targeting those regions of gene 3'UTR.

Both constructs underwent Sanger sequencing performed by Source BioScience Oxford prior to transfection to confirm that no mutations had occurred in important regions of the DNA.

3.1.4.2.3 Dual-luciferase Assay

Luciferase assays were performed as described in section 2.3.32. Two repeats were performed with four replicate transfections in each, an average and standard error of the mean was then calculated from the 8 results.

It is assumed that there is no down-regulation of renilla luciferase caused by the miRNA in the mutant construct, therefore the level of normalised luciferase is assumed to be 100%. The knockdown of luciferase expression when the 'wild-type' 3'UTR of the target gene is inserted in the psiCHECK2 vector is plotted. In addition to co-transfection with a miRNA expression vector all 'wild-type' and 'mutant' constructs were co-transfected with empty pEF6-V5/His TOPO vector and any knock-down of luciferase expression was calculated.

The results obtained are shown in figure 10.

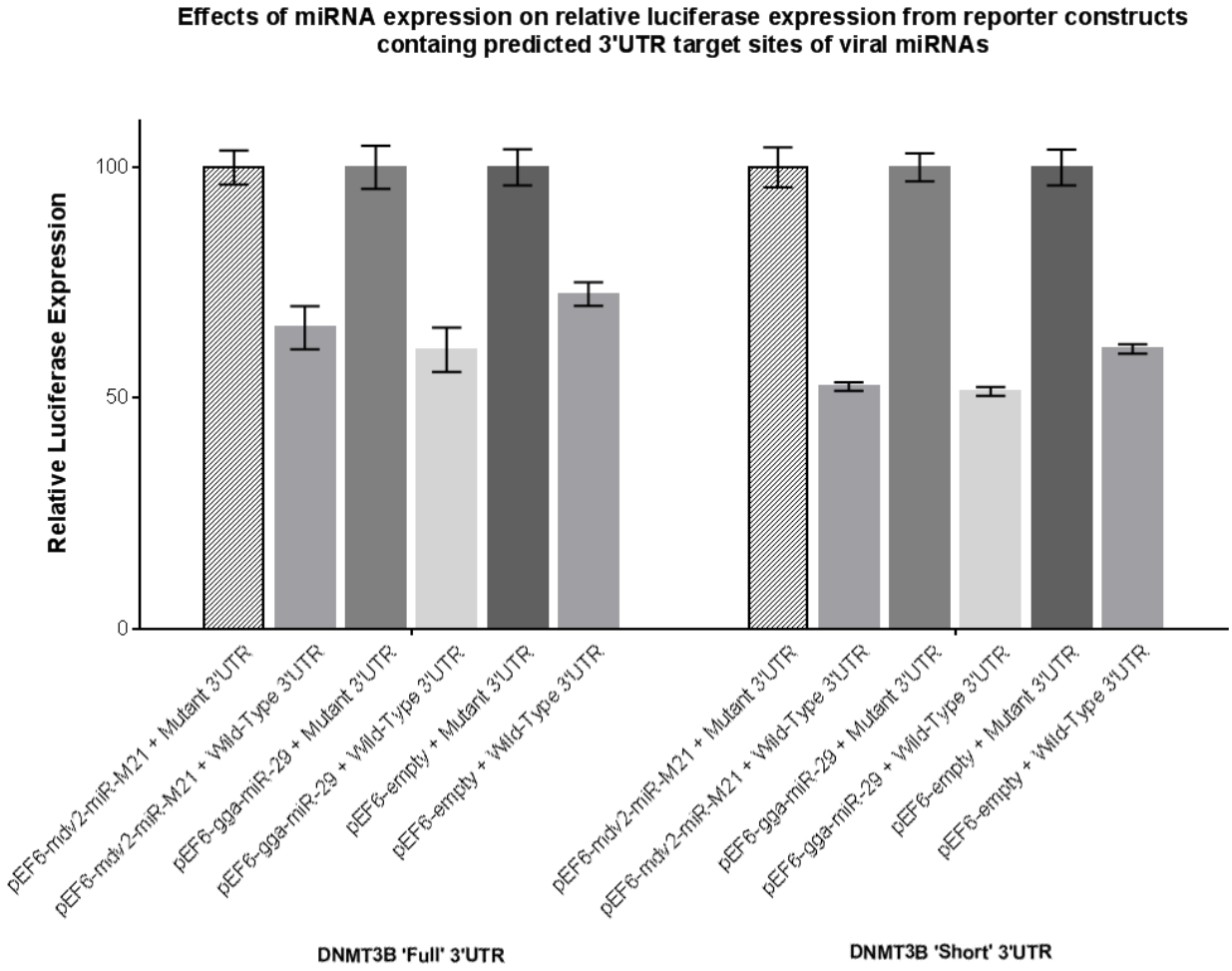


Figure 10 – Bar graph showing the relative decrease of renilla luciferase expression caused by miRNA mediated targeting of *DNMT3B* 3'UTR following dual-luciferase assay in DF-1 cells. The labels show whether the full-length 3'UTR (DNMT3B (wt/mut) F) or 'short' 3'UTR (DNMT3B (wt/mut) S) reporter construct was co-transfected with either *gga-miR-29b*, *mdv2-miR-M21* or pEF6-empty vector and the degree of down-regulation of gene expression observed. Any significant down-regulation between miRNA wild-type 3'UTR reporter construct co-transfected with corresponding miRNA expression vector and all other controls, was determined by a P-value under 0.05, calculated by a 2-way ANOVA statistical test with multiple comparisons, using the Tukey method to correct for multiple comparisons.

3.1.4.3 Effect of miRNA targeting on *DNMT3B* gene expression

The first noticeable observation is that when co-transfected with both the *mdv2-miR-M21* and *gga-miR-29b* expression vectors there is a knockdown of luciferase expression from the reporter constructs containing the wild-type (wt short and long) 3'UTR, relative to the mutant 3'UTR containing constructs. However when an empty pEF6-V5/His vector (containing no miRNA sequence) is co-transfected, similar levels of knockdown in luciferase expression from the wild-type reporter constructs is observed. The decrease in luciferase expression is slightly greater when either the *mdv2-miR-M21* or *gga-miR-29b* miRNA expression vector is co-transfected, compared to the empty miRNA expression vector; however this decrease is not statistically significant (as calculated by a 2-way ANOVA statistical test with multiple comparisons, using the Tukey method to correct for multiple comparisons). Another observation from this experiment is that the amount of knockdown of luciferase expression is quite similar (although slightly less) between the full-length and short 3'UTR. This result has implications when it comes to planning future reporter assays.

While there is knock-down of renilla luciferase expression when the wild-type *DNMT3B* 3'UTR is present in the reporter construct, compared to the mutated 3'UTR, there is no significant difference when co-transfected with a miRNA expression vector or empty vector control. This statement is true for both *mdv2-miR-M21* and *gga-miR-29b*, however figure 10 does appear to show a slight reduction in renilla luciferase expression when the miRNA expression vectors were co-transfected, and it is possible that with more repeats of the experiment this reduction may have become statistically significant. Therefore validation of this targeting was sought to determine if *mdv2-miR-M21* could reduce levels of *DNMT3B* in cells.

Initially a western-blot for DNMT3B following over-expression of *gga-miR-29b* or *mdv2-miR-M21* in cells was performed, however there are no commercially available antibodies to the chicken DNMT3B, and there was no cross-reactivity from the human DNMT3B antibodies (from Aviva Systems Biology) that were tried despite predicted cross-reactivity on the datasheet.

The remaining option was therefore to determine if the miRNAs were having an effect on the transcript levels of *DNMT3B* gene. Both the viral and host miRNA expression constructs were therefore transfected into DF-1 cells to over-express the miRNAs, while a control group of cells was transfected with empty pEF6-V5/His vector. Expression of *DNMT3B* mRNA levels were quantified using *DNMT3B* TaqMan qRT-PCR gene expression assay (Applied Biosystems Cat #4448892), as described in section 2.3.15.

As identified in figure 11A, the levels of *DNMT3B* transcript do appear to be statistically significantly down-regulated (as calculated by two-tailed student T-Test) 48 hours after the transfection of miRNA expression construct. Both *gga-miR-29b* and *mdv2-miR-M21* appear to decrease *DNMT3B* gene expression by around 50%. The expression of *gga-miR-29b* and *mdv2-miR-M21* from the pEF6-V5/His expression vectors was confirmed by miRNA TaqMan (section 2.3.14) as shown in figure 11B.

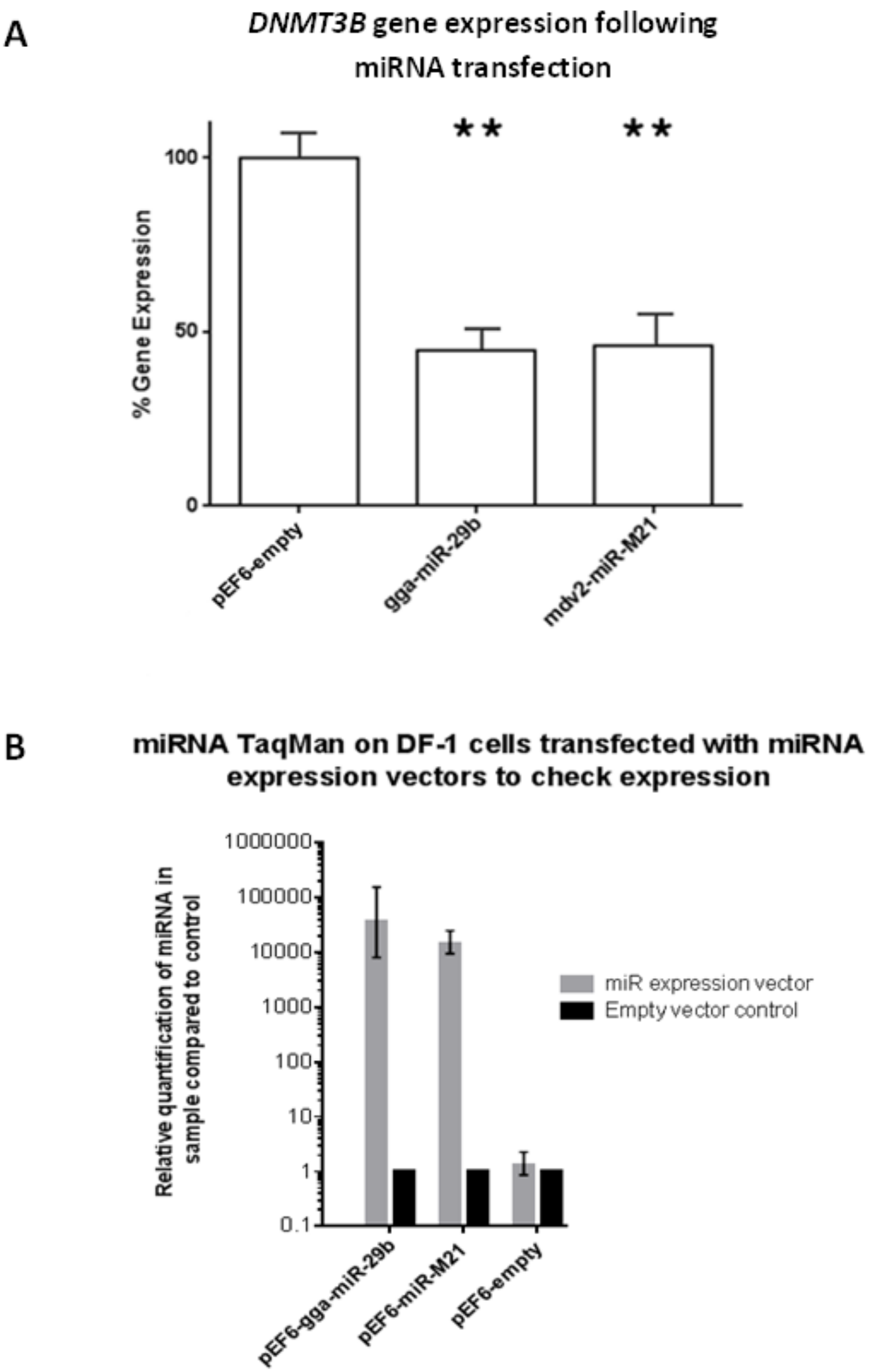


Figure 11 – (**A**) *DNMT3B* transcript levels determined via TaqMan gene expression assay following transfection of DF-1 cells with either host *gga-miR-29b* or *mdv2-miR-M21* miRNA expression vector. Levels of gene expression following miRNA transfection were compared to relative gene expression from pEF6 empty vectortransfected DF-1 cells and normalised to levels of *gga-miR-let7a*. ** denotes significant down-regulation calculated by a P-value under 0.01, calculated by a paired 2-tailed T-test. (**B**) TaqMan miRNA expression assay on above transfected DF-1 cells to confirm expression of miRNAs compared to DF-1 cells transfected with pEF-6 empty vector transfected cells. Empty vector transfected cells were tested for expression of both *gga-miR-29b* and *mdv2-miR-M21* (only expression of *gga-miR-29b* plotted), miRNA expression levels are normalised relative to *gga-miR-let7a.*

3.2 Using TargetScan miRNA target prediction program to find targets of all MDV-2 and HVT miRNAs

A broader approach to identifying targets of both the MDV-2 and HVT miRNAs was taken in order to identify a larger number of targets so that functions of miRNAs in virus biology could be explored. The different methods involved and results obtained are described below.

3.2.1 Performing the searches

As described in section 1.6.1 TargetScan custom looks for base pairing between the seed region of the miRNA of interest and the 3'UTR of a target gene. It then groups these base pairings into one of three categories; '8mer', '7mer-m8' and '7mer-1A'. A '8mer' is a match between all 7 of the nucleotides 2-8, followed by an A nucleotide in the target gene. A '7mer-m8' is a match between all nucleotides 2-8, not preceded by an A, and a '7mer-1A' is a match between transcript and nucleotides 2-7 of miRNA (the traditional 'seed' sequence) followed by an A nucleotide (Lewis et al. 2005).

The list generated by TargetScan (an example of which is shown in figure 12) ranks the favourability of base-pairing matches in the following hierarchy; '8mer' > '7mer-m8' > '7mer-1A'. However if there is two or more of a 'less favourable' pairing in the 3'UTR, that target would rank higher than one match of the 'more favourable' base pair match, see example.

The seed region from each individual MDV-2 and HVT miRNA (nucleotides 2-8) was entered into the TargetScan custom program and the species selected was chicken. A list of predicted targets for each miRNA was then generated by TargetScan and these were then collated into a spread-sheet for further analysis.

A



B



Human ortholog of target gene	Gene name	Conserved sites				Links to sites in UTRs
		total	8mer	7mer-m8	7mer-1A	
ADIPOR2	adiponectin receptor 2	1	1	0	0	Sites in UTR
AMD1	adenosylmethionine decarboxylase 1	1	1	0	0	Sites in UTR
ARID2	AT rich interactive domain 2 (ARID, RFX-like)	1	1	0	0	Sites in UTR
BAT2D1	BAT2 domain containing 1	1	1	0	0	Sites in UTR
CHSY3	chondroitin sulfate synthase 3	1	1	0	0	Sites in UTR
FAM19A1	family with sequence similarity 19 (chemokine (C-C motif)-like), member A1	1	1	0	0	Sites in UTR
HDAC4	histone deacetylase 4	1	1	0	0	Sites in UTR
PSD3	pleckstrin and Sec7 domain containing 3	1	1	0	0	Sites in UTR
RBBP4	retinoblastoma binding protein 4	1	1	0	0	Sites in UTR
RBM8A	RNA binding motif protein 8A	1	1	0	0	Sites in UTR
RUNX1	runt-related transcription factor 1 (acute myeloid leukemia 1; aml1 oncogene)	1	1	0	0	Sites in UTR
SCN1A	sodium channel, voltage-gated, type I, alpha subunit	1	1	0	0	Sites in UTR
SCN2A	sodium channel, voltage-gated, type II, alpha subunit	1	1	0	0	Sites in UTR
SCN3A	sodium channel, voltage-gated, type III, alpha subunit	1	1	0	0	Sites in UTR
SPRED2	sprouty-related, EVH1 domain containing 2	1	1	0	0	Sites in UTR
STRN3	striatin, calmodulin binding protein 3	1	1	0	0	Sites in UTR
ZNF608	zinc finger protein 608	1	1	0	0	Sites in UTR
MIER3	mesoderm induction early response 1, family member 3	1	0	1	0	Sites in UTR
SNX18	sorting nexin 18	1	0	1	0	Sites in UTR
ACVR2B	activin A receptor, type IIB	1	0	0	1	Sites in UTR

Figure 12 - TargetScan custom program webpage. Example showing how to search for predicted targets of any miRNA in a selection of species. (A) TargetScan custom welcome page, the species 'chicken' has been selected and the seed region of *MDV2-miR-M14-5p* has been entered (nucleotides 2-8 of full mature miRNA sequence, UGUGGUACGGUGCACCCUGAGA). (B) List of predicted targets of *mdv2-miR-M14-5p* generated by TargetScan. List order based upon the 'type' and frequency of seed-target matches.

3.2.2 Results from TargetScan

The mature miRNA sequences were submitted into TargetScan custom from HVT (23 miRNAs) and MDV-2 (24 miRNAs). The number of predicted potential targets sites was 1719 for the HVT encoded miRNAs and 1866 for MDV-2 encoded miRNAs (summarised in figure 13A, complete list uploaded as a file detailed in appendix 3). This was the total number of predicted gene targets, not unique targets, as some genes were predicted to be targeted by more than one viral miRNA.

The predicted targets for each virally encoded miRNA were ranked by the number of predicted targets sites, then in order of '8mer' > '7mer-m8' > '7mer-1A' sites, as discussed previously. Initially all of the predicted targets of each viral miRNA were pooled together and ranked in the manner above, the top 20 targets for both the MDV-2 and HVT miRNAs are shown in figures 13B and 13C.

When searching for targets within a particular species the TargetScan custom program only displays target sites within the 3'UTR that are broadly conserved, following alignment of 23 different species whole genomes, obtained from UCSC Genome Bioinformatics. We were looking for targets of the viral miRNAs within the chicken genome (build WUGSC 1.0/galGal2) aligned to the human genome.

A

Summary of Target Scan Predicted miRNA Targets

miRNAs Encoded by	Number of miRNAs searched	Total Number of Predicted Targets in Conserved Chicken 3'UTRs	Mean Number of Predicted Targets per miRNA
HVT	23	1719	74.74
MDV-2	24	1866	77.75

B

Ranked Predicted Targets of MDV-2 Encoded miRNAs

Human ortholog of target gene	Gene name	Conserved sites				Predicted targeting miRNA
		total	8mer	7mer-m8	7mer-1A	
SULF1	sulfatase 1	3	1	1	1	mdv2-miR-M16
STAG2	stromal antigen 2	3	1	2	0	mdv2-miR-M17
COL11A1	collagen, type XI, alpha 1	3	1	2	0	mdv2-miR-M21
ZBTB34	zinc finger and BTB domain containing 34	3	1	2	0	mdv2-miR-M21
IKZF2	IKAROS family zinc finger 2 (Helios)	3	0	0	3	mdv2-miR-M16
SRGAP2	SLIT-ROBO Rho GTPase activating protein 2	3	0	0	3	mdv2-miR-M16
TRIB2	tribbles homolog 2 (Drosophila)	3	0	2	1	mdv2-miR-M21
RNF148	ring finger protein 148	3	0	0	3	mdv2-miR-M23
KLF12	Kruppel-like factor 12	3	0	0	3	mdv2-miR-M30
FBXW7	F-box and WD repeat domain containing 7	2	2	0	0	mdv2-miR-M15
PBX3	pre-B-cell leukemia homeobox 3	2	2	0	0	mdv2-miR-M15
TMEM1	transmembrane protein 1	2	2	0	0	mdv2-miR-M16
ATAD2B	ATPase family, AAA domain containing 2B	2	2	0	0	mdv2-miR-M21
COL4A5	collagen, type IV, alpha 5 (Alport syndrome)	2	2	0	0	mdv2-miR-M21
COL1A2	collagen, type I, alpha 2	2	2	0	0	mdv2-miR-M21
COL3A1	collagen, type III, alpha 1	2	2	0	0	mdv2-miR-M21
DLG2	discs, large homolog 2, chapsyn-110 (Drosophila)	2	2	0	0	mdv2-miR-M21
ADAMTS6	ADAM metallopeptidase with thrombospondin type 1 motif, 6	2	2	0	0	mdv2-miR-M21
DCX	doublecortex; lissencephaly, X-linked (doublecortin)	2	1	1	0	mdv2-miR-M15
KLF4	Kruppel-like factor 4 (gut)	2	1	1	0	mdv2-miR-M16

C

Ranked Predicted Targets of HVT Encoded miRNAs

Human ortholog of target gene	Gene name	Conserved sites				Predicted targeting miRNA
		total	8mer	7mer-m8	7mer-1A	
DLGAP2	discs, large (Drosophila) homolog-associated protein 2	4	1	1	2	hvt-miR-H12-5p
TEAD1	TEA domain family member 1 (SV40 transcriptional enhancer factor)	3	1	1	1	hvt-miR-H15
CPEB2	cytoplasmic polyadenylation element binding protein 2	3	0	3	0	hvt-miR-H16-3p
FRMD4A	FERM domain containing 4A	2	2	0	0	hvt-miR-H7-5p
HIC2	hypermethylated in cancer 2	2	2	0	0	hvt-miR-H7-5p
TFAP2B	transcription factor AP-2 beta (activating enhancer binding protein 2 beta)	2	2	0	0	hvt-miR-H7-5p
HIC2	hypermethylated in cancer 2	2	2	0	0	hvt-miR-H9-5p
TNS1	tensin 1	2	2	0	0	hvt-miR-H10
MKL2	MKL/myocardin-like 2	2	2	0	0	hvt-miR-H12-5p
TMSB4X	thymosin beta 4, X-linked	2	2	0	0	hvt-miR-H17
ZNF781	zinc finger protein 781	2	1	1	0	hvt-miR-H5
CUX1	cut-like homeobox 1	2	1	1	0	hvt-miR-H7-5p
MAFK	v-maf musculoaponeurotic fibrosarcoma oncogene homolog K (avian)	2	1	1	0	hvt-miR-H7-5p
MARCKS	myristoylated alanine-rich protein kinase C substrate	2	1	1	0	hvt-miR-H7-5p
TNRC6A	trinucleotide repeat containing 6A	2	1	1	0	hvt-miR-H7-5p
GRIA2	glutamate receptor, ionotropic, AMPA 2	2	1	1	0	hvt-miR-H12-5p
AFF4	AF4/FMR2 family, member 4	2	1	1	0	hvt-miR-H13
CAMTA1	calmodulin binding transcription activator 1	2	1	1	0	hvt-miR-H14
CASK	calcium/calmodulin-dependent serine protein kinase (MAGUK family)	2	1	1	0	hvt-miR-H15
CTDSPL2	CTD (carboxy-terminal domain, RNA polymerase II, polypeptide A) small phosphatase like 2	2	1	1	0	hvt-miR-H15

Figure 13 - Outline of TargetScan custom results. (A) Summary of the TargetScan custom output for both the HVT and MDV-2 encoded miRNAs. (B and C) Top 20 highest ranked predicted targets for all MDV-2 and HVT encoded miRNAs, respectively. The ranking is based solely on the number of conserved predicted target sites in the 3'UTR of the genes.

3.2.2.1 Making sense of candidate target list generated for all viral miRNAs

The TargetScan custom algorithm generated too many potential targets for the viral miRNAs to validate each prediction individually. Therefore we needed a strategy to pick the most 'interesting' target genes for validation. Selecting just the highest ranked genes, based on the number of predicted target sites, seemed to be obvious approach to start with. However, a look at both the MDV-2 and HVT predicted targets shows that just one or two miRNAs appear responsible for the vast majority of high ranked targets, and therefore validating only these targets would limit the investigation into all of the other viral miRNAs.

Therefore we decided to use gene ontology to see whether any particular gene pathways were enriched within the predicted target list.

3.2.2.2 Gene Ontology of predicted targets

All of the predicted targets of both the MDV-2 and HVT encoded miRNAs underwent functional analysis to group the list of targets into certain gene ontology groups, the program used to do this was Panther Classification System (http://www.pantherdb.org/) (Mi et al. 2013). The gene ontology results for both the HVT and MDV-2 miRNA predicted targets are shown in figures 14-17. The first subheadings for each biological process terms are shown in table 19 in appendix 6, further sub-headings for each biological process can be found at http://www.pantherdb.org/.

The bar charts in figures 15 and 17 only include the results whose P value <0.05 as calculated using the binomial statistic by Pantherdb.

In the graphs below the Pantherdb analysis of both MDV-2 and HVT predicted targets; similar gene ontology terms were highlighted. Of particular interest was the targeting of the viral miRNAs to pathways involved in the regulation of transcription, which could play a role in the maintenance of latency by repressing the expression of certain host genes to favour conditions for the virus. Further exploration of the terms under the heading of biological processes, shows that 46 of the predicted targets of MDV-2 encoded miRNAs and 36 of the HVT-encoded miRNAs are involved in apoptotic

processes. This is higher than expected by the statistical over-representation analysis, but not significant (P value >0.05). Repression of the genes involved in the apoptotic pathways would ally to the findings of other groups who have shown other herpesviruses to inhibit apoptosis by various pathways (Yee et al. 2011).

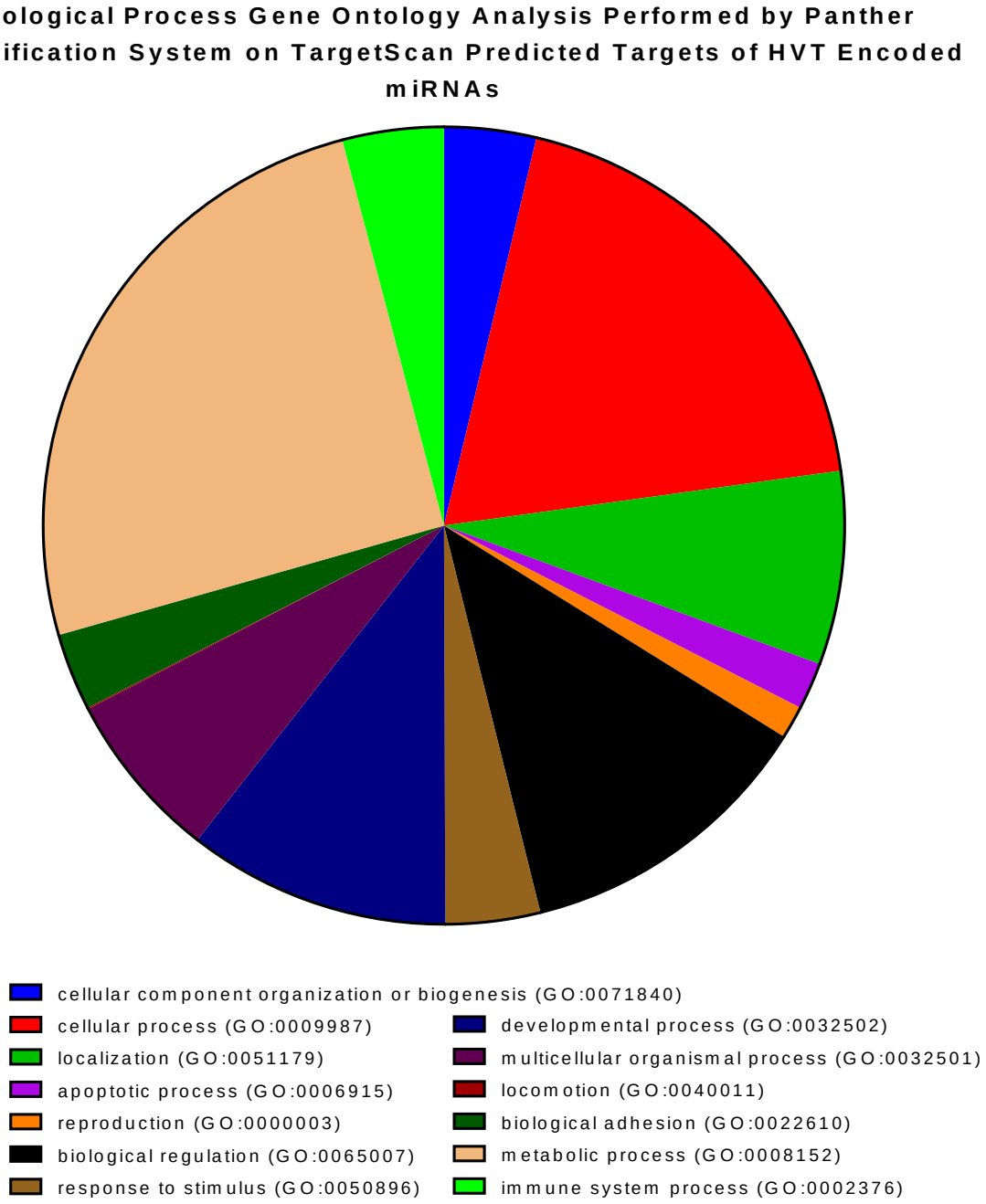


Figure 14 – Biological process gene ontology analysis of predicted targets of all HVT encoded miRNAs, analysis was performed by Panther Classification System (www.pantherdb.org). The number of unique mapped ids found in classification system was 881, 323 IDs were not mapped by Pantherdb.

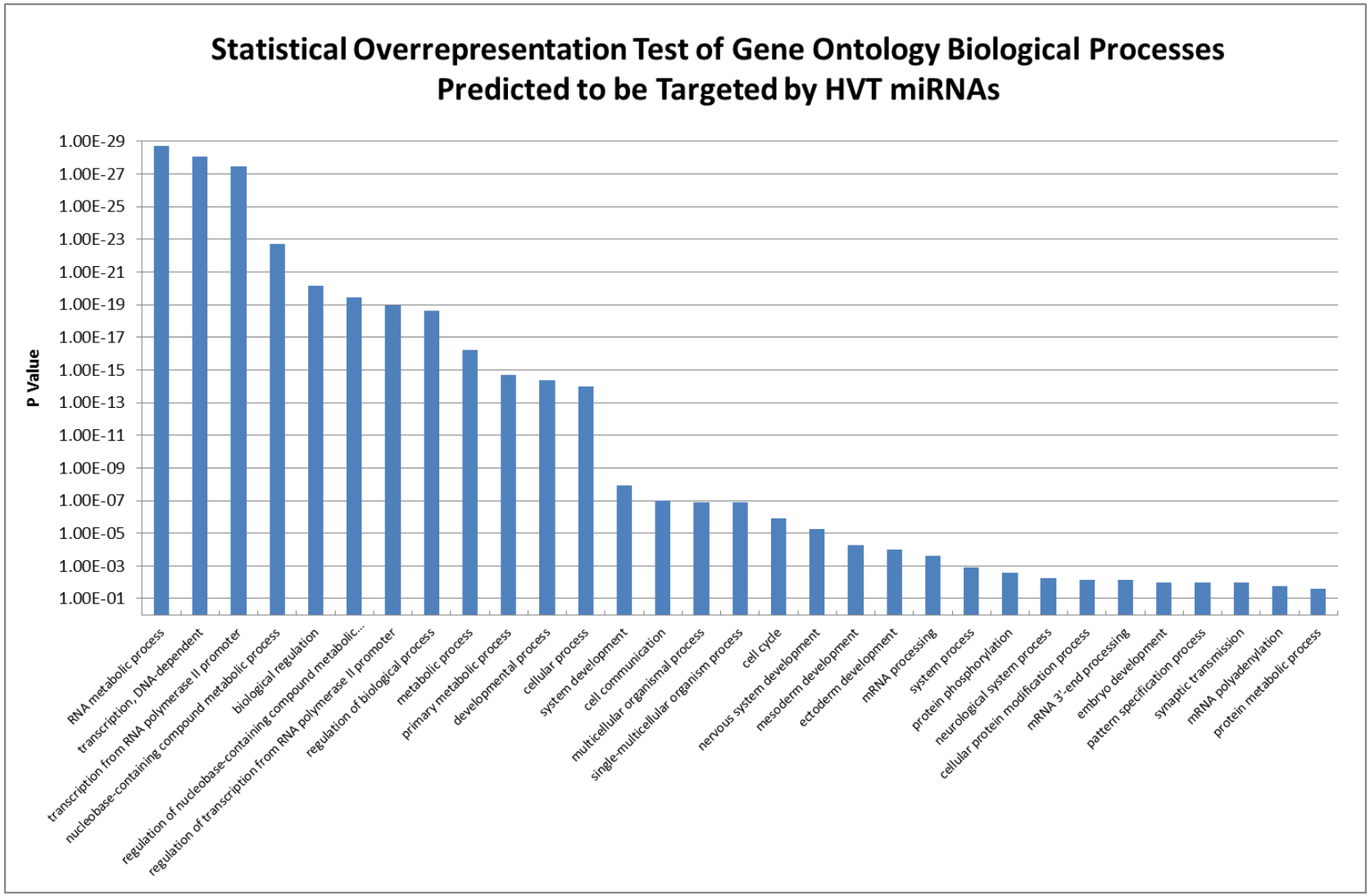


Figure 15 – Bar chart to show the results of the statistical overrepresentation analysis performed by Pantherdb on biological processes of predicted HVT miRNA targets, to determine if the frequency of predicted targets involved in certain biological processes, is significantly above background levels.

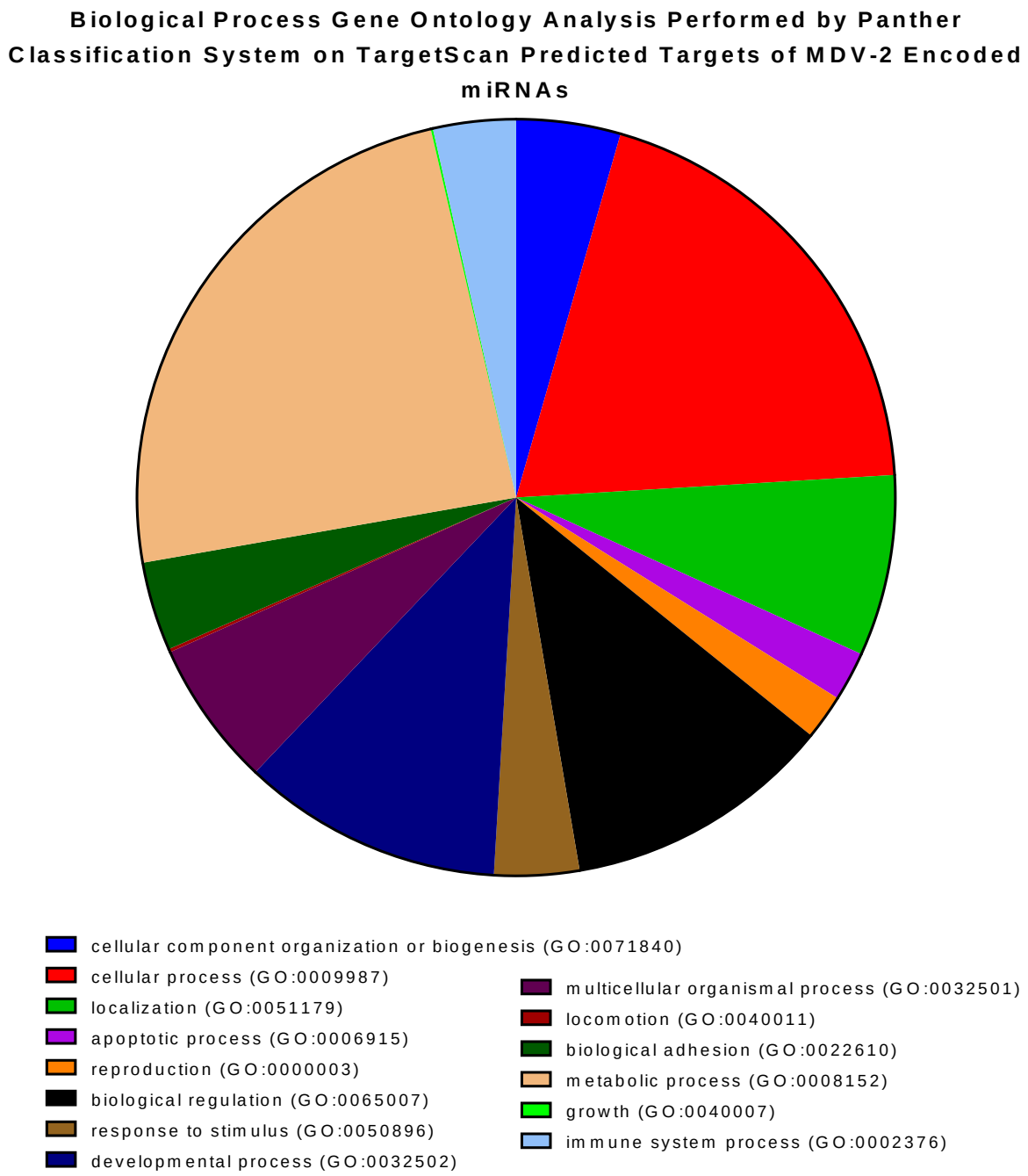


Figure 16 - Biological process gene ontology analysis of predicted targets of all MDV-2 encoded miRNAs, analysis was performed by Panther Classification System (www.pantherdb.org). The number of unique mapped ids found in classification system was 999, 308 IDs were not mapped by Pantherdb.

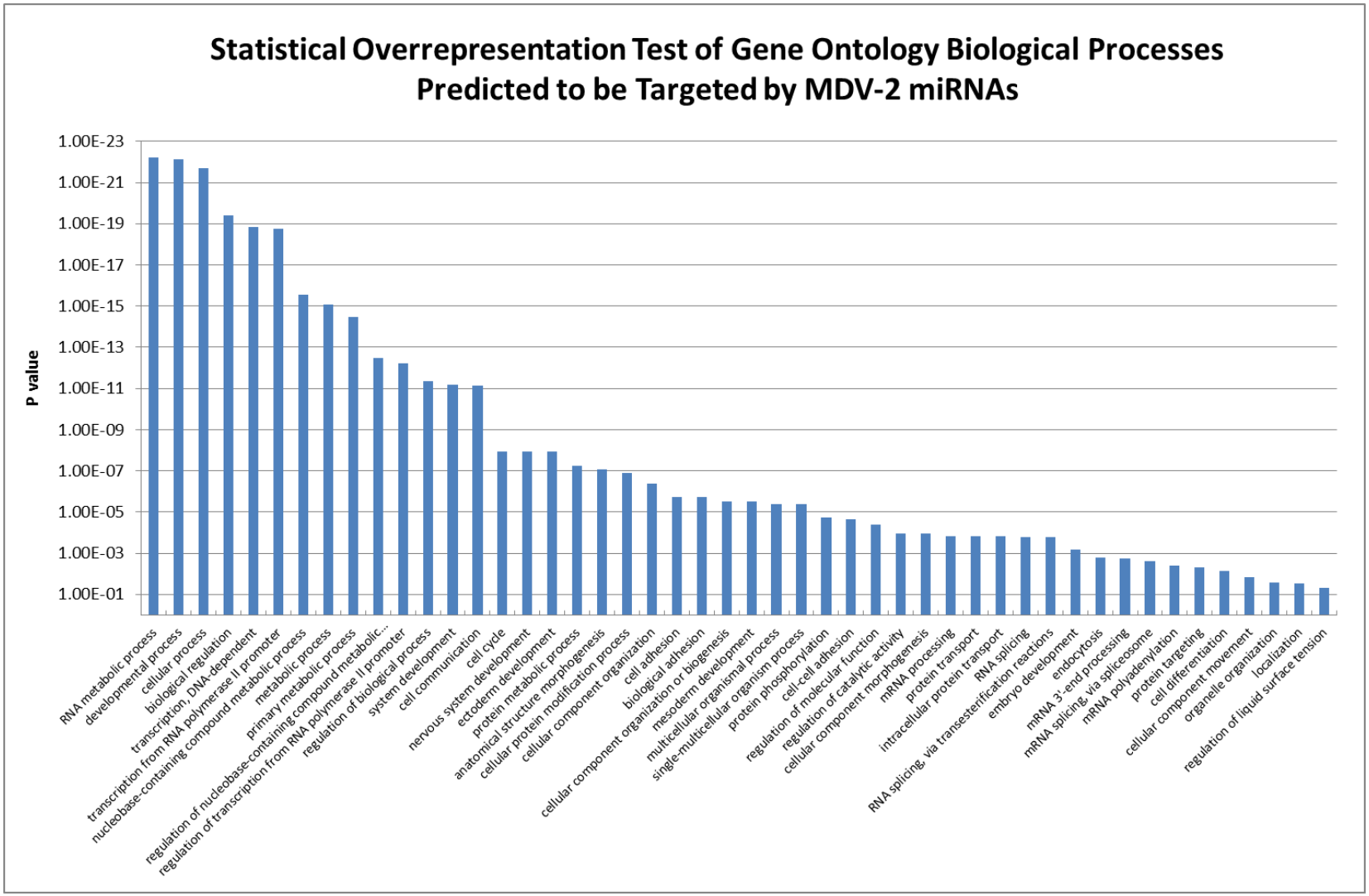


Figure 17 - Bar chart to show the results of the statistical overrepresentation analysis performed by Pantherdb on biological processes of predicted MDV-2 miRNA targets, to determine if the frequency of predicted targets involved in certain biological processes is significantly above background levels.

By using this analysis an overall idea of the processes targeted by the virally encoded miRNAs was developed. Targets enriched in processes with the highest confidence of being genuinely enriched, compared to background, were then chosen for further validation.

Targets chosen for further validation by luciferase are listed in tables 14 and 15. These predicted targets were chosen for further validation based on their association with biological processes that appear to be targeted by MDV-2 and HVT miRNAs, based on the Panther analysis above.

miRNA	Mapped ID	GO Molecular Function	GO Biological Process	Panther Protein Class
hvt-miR-H7	CTBP1	transcription cofactor activity, sequence-specific DNA binding transcription factor activity, oxidoreductase activity, sequence-specific DNA binding transcription factor activity, protein binding	carbohydrate metabolic process, cellular amino acid biosynthetic process	transcription cofactor, dehydrogenase
hvt-miR-H12	JUN	sequence-specific DNA binding transcription factor activity, sequence-specific DNA binding transcription factor activity	transcription from RNA polymerase II promoter, cell cycle, cell communication, regulation of transcription from RNA polymerase II promoter	transcription factor, nucleic acid binding
mdv2-miR-M21	AKT3	protein kinase activity, calcium ion binding, calmodulin binding, calcium-dependent phospholipid binding	gamete generation, apoptotic process, nitric oxide biosynthetic process, protein phosphorylation, cell cycle, cell communication, cellular component morphogenesis, apoptotic process, negative regulation of apoptotic process, cellular component organization	non-receptor serine/threonine protein kinase, transfer/carrier protein, non-receptor serine/threonine protein kinase, annexin, calmodulin
mdv2-miR-M22	RALA	GTPase activity, protein binding	metabolic process, cellular component movement, synaptic transmission, cell adhesion, neurological system process, embryo development, intracellular protein transport, receptor-mediated endocytosis	small GTPase
hvt-miR-H7	RAP1A	GTPase activity, protein binding	metabolic process, synaptic transmission, cell adhesion, neurological system process, intracellular protein transport, receptor-mediated endocytosis	small GTPase
mdv2-miR-M30	TIAM1	catalytic activity, receptor binding, small GTPase regulator activity, guanyl-nucleotide exchange factor activity	B cell mediated immunity, metabolic process, cell communication, neurological system process, cellular defense response, regulation of catalytic activity	signaling molecule, guanyl-nucleotide exchange factor
mdv2-miR-M30	DEK	DNA binding, histone binding	regulation of double-strand break repair	

Table 14 - Table listing the predicted targets of various HVT and MDV-2 encoded miRNAs, as predicted by TargetScan. Information includes; the miRNA predicted to be targeting, a gene ID, and Pantherdb gene ontology classifications.

miRNA	Mapped ID	GO Molecular Function	GO Biological Process	Panther Protein Class
mdv2-miR-M30	MYBL1	sequence-specific DNA binding transcription factor activity, sequence-specific DNA binding transcription factor activity	apoptotic process, purine nucleobase metabolic process, transcription from RNA polymerase II promoter, rRNA metabolic process, cellular amino acid biosynthetic process, cell cycle, apoptotic process, regulation of transcription from RNA polymerase II promoter, negative regulation of apoptotic process	transcription factor, DNA binding protein
hvt-miR-H14	ERBB4	ATP binding, epidermal growth factor receptor binding, protein homodimerization activity, receptor signaling protein tyrosine kinase activity, transcription regulatory region DNA binding	apoptotic process, cell proliferation, cell-cell adhesion, apoptotic process, nervous system development	
hvt-miR-H17	RAN	GTPase activity, protein binding	nucleobase-containing compound metabolic process, cell cycle, cell communication, RNA localization, intracellular protein transport, nuclear transport	small GTPase
hvt-miR-H17	BCL11A	sequence-specific DNA binding transcription factor activity, sequence-specific DNA binding transcription factor activity	transcription from RNA polymerase II promoter, regulation of transcription from RNA polymerase II promoter	zinc finger transcription factor, nucleic acid binding
hvt-miR-M16	ERBB4	ATP binding, epidermal growth factor receptor binding, protein homodimerization activity, receptor signaling protein tyrosine kinase activity, transcription regulatory region DNA binding	apoptotic process, cell proliferation, cell-cell adhesion, apoptotic process, nervous system development	
hvt-miR-M16	TIAM1	catalytic activity, receptor binding, small GTPase regulator activity, guanyl-nucleotide exchange factor activity	B cell mediated immunity, metabolic process, cell communication, neurological system process, cellular defense response, regulation of catalytic activity	signaling molecule, guanyl-nucleotide exchange factor
hvt-miR-H16	DNMT3B	DNA (cytosine-5-)-methyltransferase activity, DNA-methyltransferase activity, protein binding, transcription corepressor activity	DNA methylation, methylation-dependent chromatin silencing, negative regulation of transcription from RNA polymerase II promoter, positive regulation of gene expression	

Table 15 - Table listing the predicted targets of various HVT and MDV-2 encoded miRNAs, as predicted by TargetScan. Information includes; the miRNA predicted to be targeting, a gene ID, and Pantherdb gene ontology classifications.

By validating just a limited number of the predicted targets of the virally encoded miRNAs, we can evaluate the efficiency of the TargetScan custom program at predicting true host gene targets of virally encoded miRNAs, compared to false positives.

3.2.3 Validation of predicted targets

Once the predicted targets of the virally encoded miRNAs that warranted further validation had been selected, the biochemical analysis was carried out. A number of different methods exist to validate if a miRNA is having an effect on a target gene, some involve observing a change in the RNA or protein level of a gene, others use assay based systems. In this study a dual-luciferase reporter assay was used, which is a rapid method for determining whether or not a particular transcript (or portion of a transcript, i.e. 3'UTR) is being targeted by an individual miRNA.

3.2.3.1 Generating reporter constructs

In addition to highlighting the potential target genes of miRNAs, TargetScan custom also identifies where within the 3'UTR the transcript are being targeted. Using this information reporter constructs containing either a 'wild-type' or 'mutant' section of target gene 3'UTR were generated. Various different luciferase reporter assays have been previously proven to be a valid functional method for the validation of several miRNA targets (Skalsky et al. 2007; Y. Zhao et al. 2009), in this study the psiCHECK-2 Vector (Promega) developed for target knockdown experiments was used.

Complementary 110bp oligos were designed to include the predicted target site, or miRNA response element (MRE), of the miRNA 'seed region' in the 3'UTR of the target gene (8 nucleotides) and approximately 45bp of flanking region either side of the MRE (Tables 8 and 9). Reporter constructs were created following the protocol described in section 2.3.20.

In total 30 different constructs were made from the 60 oligos, as discussed two constructs were made for each gene to be analysed, a 'wild-type' and 'mutant'. *RAP1A*, targeted *by hvt-miR-H7*, had two

predicted target sites for *hvt-miR-H7* in the 3'UTR of this gene, therefore within the mutant construct both mutated sites were mutated (MUT 1+2).

3.2.3.2 Generating miRNA expression constructs

In the dual-luciferase miRNA reporter assay the miRNA predicted to be targeting the gene of interest needed to be co-expressed with the reporter construct. Following the protocol outlined by Zhao et al, the pEF6-V5/His TOPO vector (Invitrogen) was used as the expression construct backbone (Y. Zhao et al. 2009). Firstly the full-length pre-miRNA of the miRNA of interest was amplified, as described in section 2.3.6, from either the MDV-2 or HVT BAC DNA along with around 100bp flanking seqeunce either side, to ensure correct processing (oligo sequence shown in table 7).

The amplification was performed with goTaq DNA polymerase (Promega), following manufacturers protcol. Amplification with goTaq polymerase resulted in an amplification product containing an adenine (A) overhang at either end. This overhang was utilised to clone the pre-miRNAs into pEF6-V5/His TOPO vector via TOPO cloning, using the kit provided with the vector from Invitrogen, following manufacturers protocol.

Expression from the pEF6-V5/His TOPO vector was driven by the EF1α promoter, generating high levels of miRNA in transfected cells.

3.2.3.3 Sequencing

Prior to performing the dual-luciferase assay, all constructs (reporter and miRNA expression) were sequenced by sending 600ng of plasmid DNA to Source Bioscience (Oxford), to perform overnight service Sanger sequencing. No mutations were detected in the 3'UTR or pre-miRNA sequence in the vectors, which was important as any changes could well affect miRNA targeting or expression and skew the results.

3.2.3.4 Confirming expression of miRNAs from miRNA expression constructs

Despite the sequencing data confirming the presence of the miRNAs in the pEF6-V5/His TOPO vectors, this was not a guarantee that mature miRNA was being expressed and processed correctly. To confirm that miRNAs were being properly expressed in transfected cells, duplicate transfections of each miRNA expression vector were performed in DF-1 cells using lipofectamine 2000 (section 2.3.27). RNA extracted from transfected cells was analysed by miRNA TaqMan (section 2.3.14) in triplicate (figure 19).

Additionally a control transfection was performed using the pMAX-GFP vector (Lonza Group Ltd) to confirm that a suitabe rate of transfection was occuring in the DF-1 cells (figure 18).

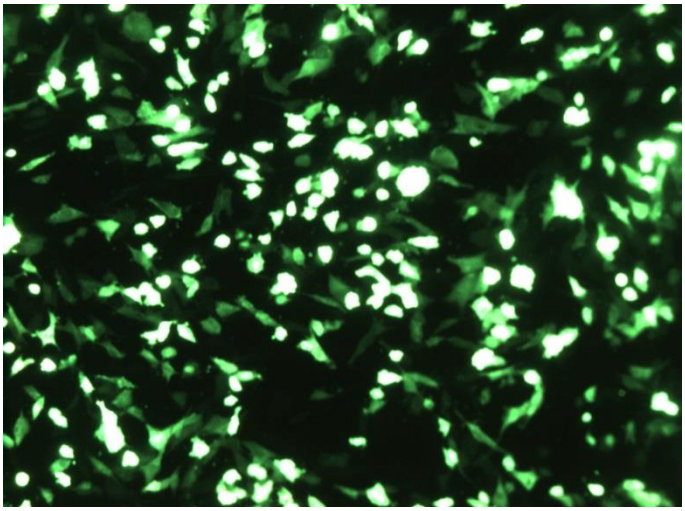


Figure 18 – Fluorescent microscope image of DF-1 cells, 48-hours following transfection with pMAX-GFP vector using lipofectamine 2000 transfection reagent (Invitrogen). The high transfection percentage indicates that the transfection conditions are suitable

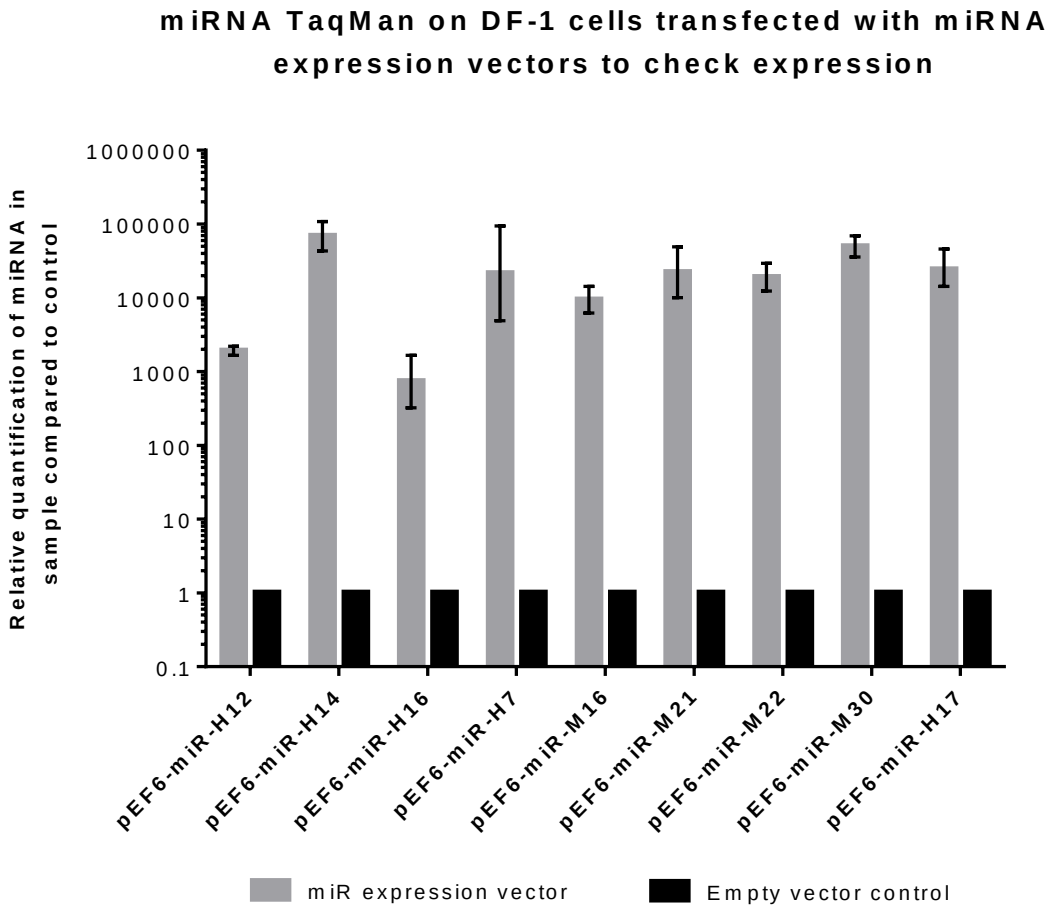


Figure 19 – miRNA TaqMan analysis to determine expression levels of various HVT and MDV-2 encoded miRNAs, following transfection of the corresponding miRNA expression vector into DF-1 cells. Relative quantification levels were normalised to detection levels (background) from DF-1 cells transfected with the pEF6-V5/His vector. Error bars show maximum and minimum relative quantification (RQ) values as calculated by 7500 Fast software (Applied Biosystems) from Ct values, normalised to *gga-miR-let7a*.

3.2.3.5 Dual-luciferase reporter assay

Luciferase assays were performed as described in section 2.3.32. Four replicate transfections were performed, on two separate occasions and then an average calculated from the 8 results.

It is assumed that there is no down-regulation of renilla luciferase caused by the miRNA in the mutant construct, therefore the level of normalised luciferase is given is assumed to be 100%. The knockdown of luciferase expression when the fragment of 'wild-type' 3'UTR of the target gene is inserted in the psiCHECK2 vector is plotted in figure 20. In addition to co-transfection with a miRNA expression vector all 'wild-type' and 'mutant' constructs were co-transfected with empty pEF6-V5/His TOPO vector and any knock-down of luciferase expression was calculated.

Significant (P value <0.05) knock-down of luciferase expression was determined using a two-way ANOVA multiple comparisons statistical test, correcting for multiple comparisons using the Tukey method. All analysis was performed using the Graph Pad Prism software (version 6.02), and full details of the statistical analysis can be seen in appendix 5. In order to be confident that it was the expression of miRNAs that were responsible for the knock-down it was determined that there must be a statistically significant difference (p-value<0.05) between the 'wild-type' luciferase construct co-transfected with the miRNA expression vector and all other co-transfections. Additionally there should be no statistically significant difference between any of the other three co-transfections (mut+miRNA, wt+empty and mut+empty).

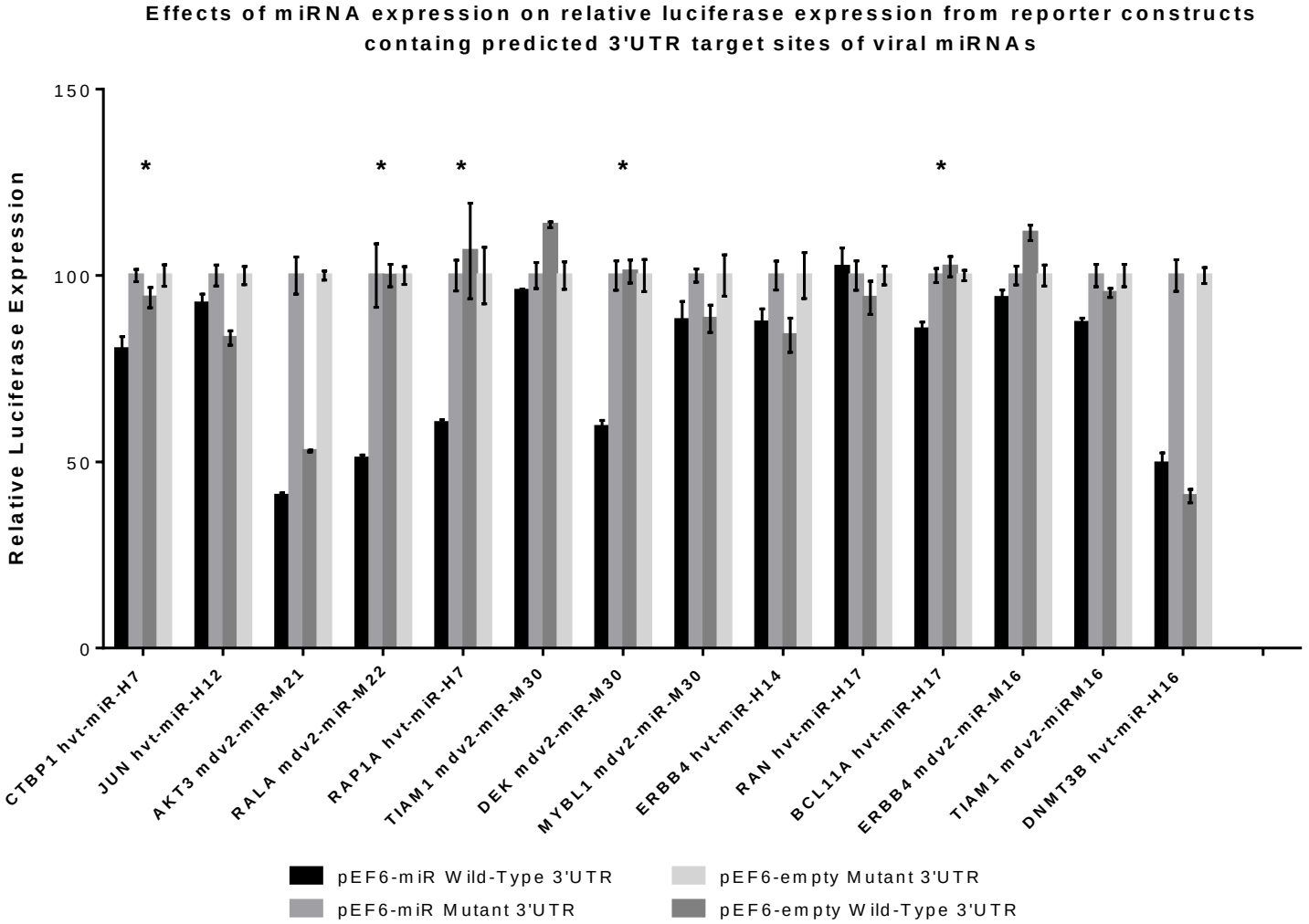


Figure 20 - Bar graph showing the relative decrease of renilla luciferase expression caused by miRNA mediated targeting of target gene 3'UTR following dual-luciferase assay in DF-1 cells. The predicted target gene 3'UTRs cloned downstream of the renilla luciferase gene in psiCHECK-2 are labelled along with the corresponding targeting miRNA. * denotes significant down-regulation between miRNA wild-type 3'UTR reporter construct co-transfected with corresponding miRNA expression vector and all other controls (results highlighted by red box in appendix 5). Determined by a P-value under 0.05, calculated by a 2-way ANOVA statistical test with multiple comparisons, using the Tukey method to correct for multiple comparisons.

Using the above criteria it was determined which miRNAs were genuinely targeting the 3'UTR region within the reporter constructs. In figure 20 CTBP1-miR-H7, RALA-miR-M22, RAP1A-miR-H7, DEK-miR-M30 and BCL11A-miR-H17 all showed a knock-down of luciferase expression when co-transfected with the corresponding miRNA (denoted by a * in figure 20). Although statistically significant, the amount of knock-down of both the CTBP1-miR-H7 and BCL11A-miR-H17 reporter constructs was relatively small. Additionally there was a significant knock-down in luciferase expression between wild-type and mutant constructs for both the AKT3-miR-M21 and DNMT3B-miR-H16 reporter constructs, however this difference in luciferase expression was seen regardless of the presence of the viral miRNA. The knock-down of the AKT3-miR-M21 reporter construct was slightly increased when co-transfected with the *mdv2-miR-M21* expression vector, however the DNMT3B-miR-H16 reporter construct showed increased luciferase knock-down when co-transfected with the pEF6-empty vector.

Based on the observations above the following targets were chosen for further validation; RALA-miR-M22, RAP1A-miR-H7, DEK-miR-M30 and AKT3-miR-M21. AKT3-miR-M21 was chosen despite the fact it did not originally meet the criteria for genuine knock-down, outlined above. Based on the observations in section 3.1 that the viral miRNA *mdv2-miR-M21* is acting as an ortholog of the host *gga-miR-29b*, it is feasible that the host miRNA could be responsible for luciferase knock-down observed in the wild-type reporter-pEF6 empty co-transfection. Therefore the targeting of *mdv2-miR-M21* to AKT3 could be genuine, and warranted further analysis.

3.2.4 Further validation of targets highlighted from dual-luciferase assay

3.2.4.1 Western blot analysis of target protein abundance

The next logical step to determine if the miRNAs were genuinely targeting the genes highlighted above was to see if overexpression of the viral miRNA had an effect on the protein level of the target. miRNA expression vectors were transfected into DF-1 cells in a 6-well plate as described previously. Forty-eight hours after transfection cells were harvested and western blot analysis performed as described

in section 2.3.26. Table 4 in section 2.3.26 provides information about the concentrations of antibodies used in this study.

Once western blots were performed, band intensity analysis was performed on both the protein of interest blots and the α-tubulin control blots. This analysis was performed using ImageJ software (http://rsb.info.nih.gov/ij/index.html) (Schneider et al. 2012) to calculate the density of the bands produced. The intensity of the protein band was normalised to the intensity of the α-tubulin band, to account for any loading differences. The abundance of target protein, following transfection of the corresponding miRNA expression vector, was then calculated relative to the abundance following transfection with an empty miRNA expression construct. The results from the western blot can be seen in figure 21 (expected size protein bands highlighted in red box) and full abundance analysis is shown in table 16.

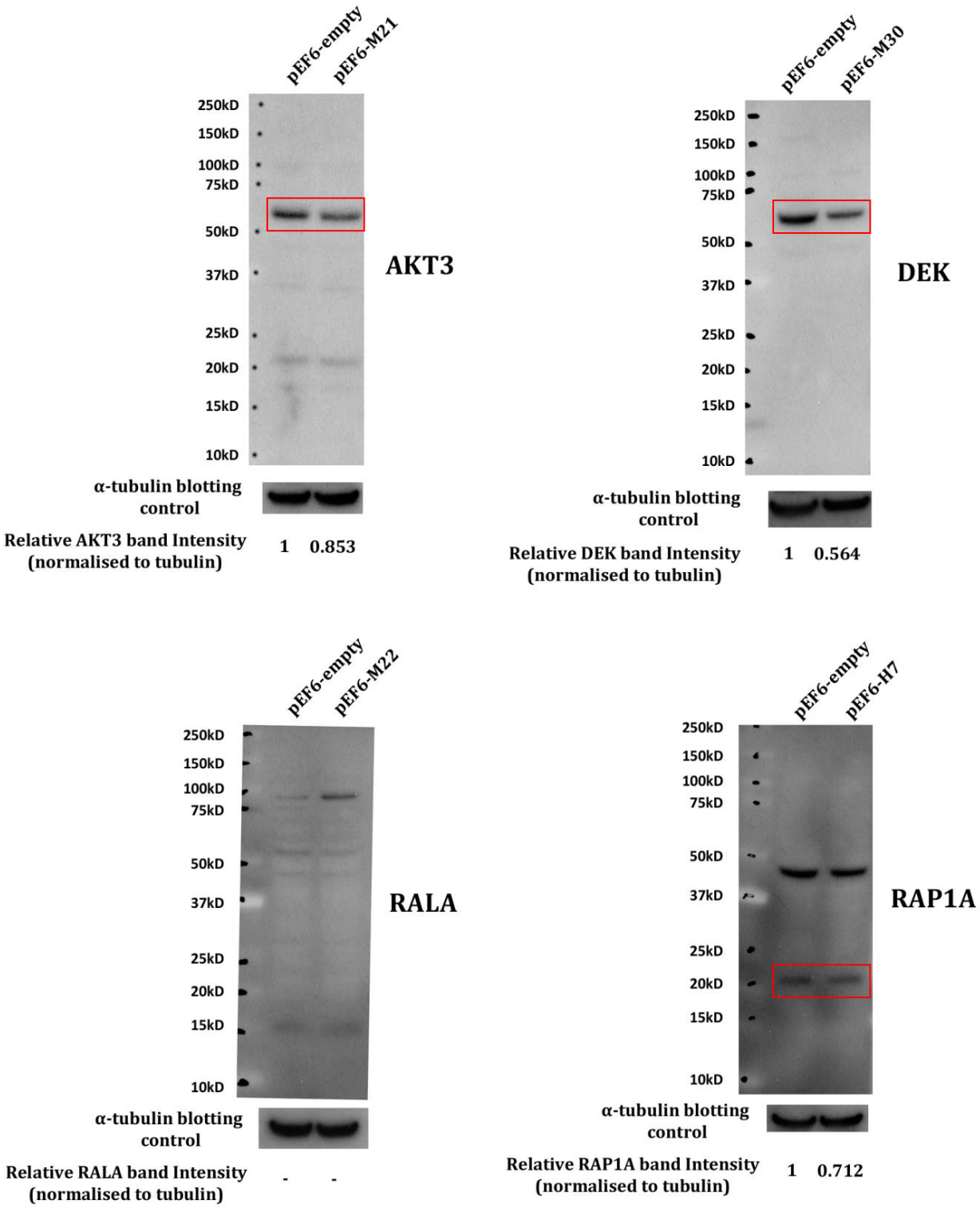


Figure 21 – Western blot analysis to determine protein abundance of four targets of virally encoded miRNAs, following transfection of the corresponding miRNA expression vector in DF-1 cells. Underneath each blot are the loading control blot for α-tubulin and the calculated band intensity for each target protein normalised to the abundance of the α-tubulin loading control. Band intensity analysis was performed using ImageJ software (http://rsb.info.nih.gov/ij/index.html) (Schneider et al. 2012).

	AKT3-empty	AKT3-M21		DEK-empty	DEK-M30		RAP1A-empty	RAP1A-H7
Target Protein Band Intensity	15828.619	13766.447		30160.359	17528.681		5019.154	4200.598
Tubulin Band Intensity	31500.108	32121.451		18597.418	19171.539		13094.912	15393.497
Target Protein/Tubulin	0.502494118	0.42857488		1.621749804	0.914307453		0.383290396	0.272881334
Relative band intensity	1	0.852895316		1	0.563778365		1	0.711944096

Table 16 - Results from band intensity analysis performed using ImageJ software (Schneider et al. 2012) on western blots shown in figure 21.

The results of the western blot analysis are promising, in three of the four blots some knock-down of protein levels is evident when co-transfected with the targeting miRNA-expression vector. The blot for RALA did not produce a band at the predicted size of ~25kD as described in the manufacturers' datasheet, so abundance analysis was not performed on this blot. The decrease in relative protein abundance for AKT3, DEK and RAP1A are shown beneath the blots in figure 21, DEK showed the greatest decrease in protein abundance, 43.6% relative to the empty miRNA expression vector transfected cells. RAP1A and AKT3 showed smaller decreases in protein abundance, 28.8% and 14.7% respectively, relative to the empty miRNA expression vector transfected cells.

3.2.4.2 Analysis of target transcript abundance

The final analysis to perform on the highlighted viral miRNA targets was to determine if the miRNA targeting resulted in a decrease in transcript abundance. As discussed in the introduction a large proportion of miRNA-mediated targeting leads to a decrease in target transcript levels. DF-1 cells were once again transfected with either miRNA expression construct or empty pEF6-V5/His constructs and cultured for forty-eight hours. Gene expression TaqMan was performed in triplicate for each viral miRNA target as described in section 2.3.15 on RNA extracted from transfected cells, transcript abundance was normalised from each sample using the *RPL7*. This was repeated twice and figure 22 shows the analysis of combined results of these two repeats.

From the results in figure 22 it is clear to see that none of the four target transcripts show any significant knock-down at transcript levels.

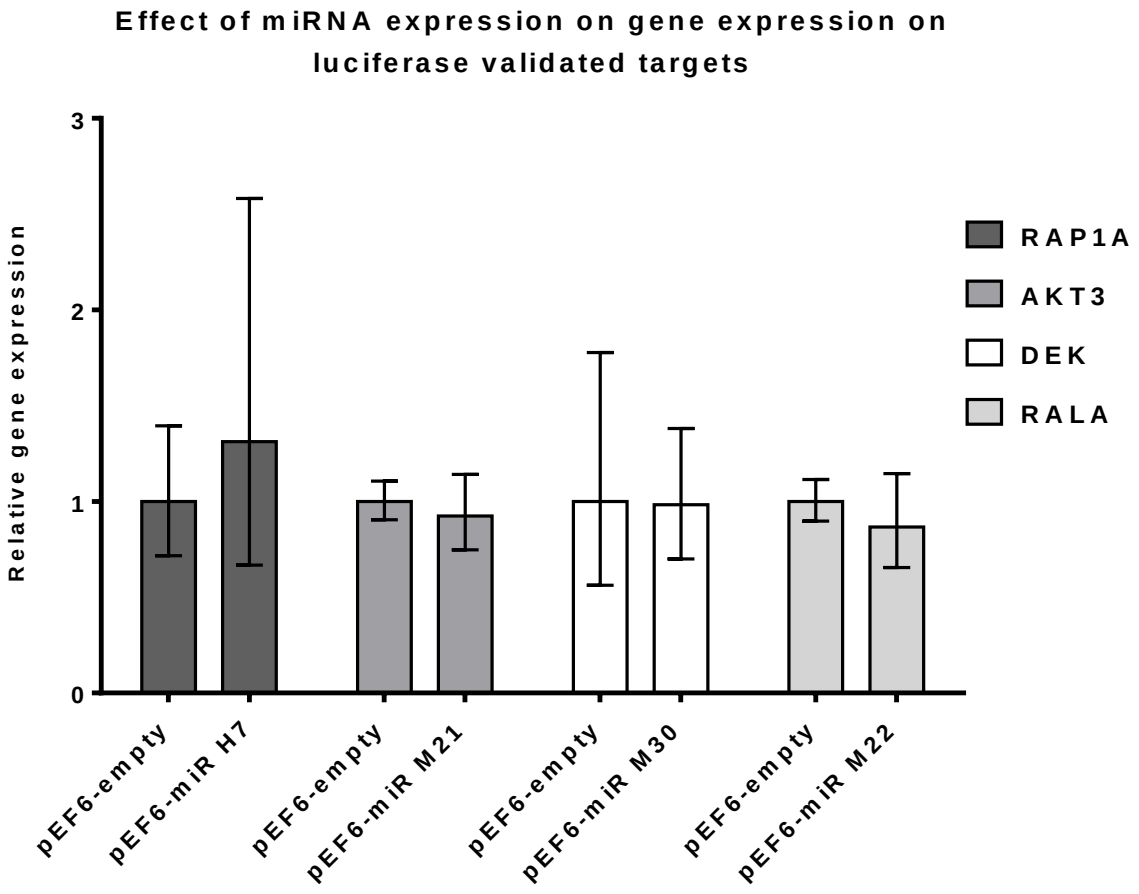


Figure 22– TaqMan gene expression analysis of transcript levels of viral miRNA targets. Transcript abundance following transfection of targeting miRNA expression vector into DF-1 cells is shown relative to transcript abundance following transfection with empty miRNA expression vector. Error bars show maximum and minimum relative quantification (RQ) values as calculated by 7500 Fast software (Applied Biosystems) from Ct values, normalised to *RPL7* levels.

3.3 Discussion

3.3.1 Viral miRNA *mdv2-miR-M21* is targeting *DNMT3B*

Using the TargetScan custom miRNA target prediction program and dual-luciferase assay this study was unable to definitively demonstrate novel targeting of *mdv2-miR-M21* to the 3'UTR of the host *DNMT3B* gene. When the predicted target site within the 3'UTR of the *DNMT3B* gene was cloned downstream of the renilla luciferase gene in the psiCHECK-2 vector, the levels of renilla luciferase expression were significantly down-regulated when co-transfected with the *mdv2-miR-M21* miRNA expression vector. The down-regulation of renilla luciferase gene expression could be rescued by mutating just three residues within the predicted 'seed region' target site in the *DNMT3B* 3'UTR. However this same knock-down of luciferase expression between the wild-type and mutant reporter constructs was demonstrated when they were co-transfected with an empty miRNA expression vector. It has now been demonstrated within another lab that the host miRNA *gga-miR-29b* is targeting the *DNMT3B* gene (Rengaraj et al. 2011), therefore it seems reasonable to assume that this knock-down of luciferase expression from the wild-type vector when co-transfected with an empty miRNA expression vector could be a result of endogenous *gga-miR-29b* targeting the reporter construct. The data does go some way to support this suggestion as there is slightly increased knock-down when a miRNA expression vector is co-transfected (although not statistically significant, P-value >0.05). Endogenous levels of *gga-miR-29b* could therefore be targeting the wild-type reporter construct, obscuring the targeting of reporter constructs by the over-expressed miRNAs. This effect could have been confirmed by silencing the expression of endogenous *gga-miR-29b*, through the use of an Antagomir or RNA sponge, and remains a strategy that could be pursued in the future.

By using a TaqMan gene expression assay, the ability of both the host and viral miRNA to decrease the levels of *DNMT3B* transcript when over-expressed in cells, has been demonstrated. Initially concerns in analysing changes in gene transcript levels brought about by miRNAs were highlighted. However there is now a great deal of research that supports the idea that miRNAs direct their targets to the mRNA decay pathway, where upon removal of the poly-A tail the transcript is decapped and digested 5'-to-3'

via endonucleases (discussed further in the introduction section 1.4.2). In fact it has been identified that as many as 84% of protein level changes induced by miRNA regulation are down to changes in mRNA expression (H. L. Guo et al. 2010). This research suggests that if a miRNA is indeed targeting a gene then an observable decrease in the poly-adenylated transcript mRNA would be expected.

The limitations of analysing the gene expression levels of a miRNA-target of interest in this manner must be considered. It must be accepted that a change in mRNA levels will not always translate to a change in protein levels, this study only looked at relative levels of *DNMT3B* gene expression, and therefore the exact copy number of transcripts has not been calculated. Although in both the case of *gga-miR-29b* and *mdv2-miR-M21* there is approximately a 50% reduction in mRNA levels, the transcript levels could still be high enough to ensure strong levels of DNMT3B protein. Additionally the higher physiological levels of both miRNAs induced following transfection could be forcing unnatural targeting of the miRNA to the mRNA therefore demonstrating artificial changes in gene expression. Despite the drawbacks of this approach analysing gene expression levels remains a genuine method of validating miRNA targets (Y. Zhao et al. 2011).

It was originally confirmed that *miR-29* family miRNAs do target the *DNMT3B* gene in humans (Garzon et al. 2009), and has subsequently been confirmed in chickens (Rengaraj et al. 2011). Therefore using TaqMan gene expression to determine whether or not they are targeting *DNMT3B* seems appropriate, it would be reasonable to argue that the down-regulation of the *DNMT3B* mRNA transcript following over-expression of *gga-miR-29b* confirms the targeting that has previously been validated. The fact that over-expression of *mdv2-miR-M21* induces similar changes in transcript abundance, and has the same effect in luciferase assays, suggests that it too is targeting the *DNMT3B* gene.

Ideally a demonstration of decreased protein levels of DNMT3B, following transfection of the *mdv2-miR-M21* and *gga-miR-29b* miRNA expression vectors, would have provided the best indication of a genuine effect of viral miRNA targeting on *DNMT3B*

Information gained from the *DNMT3B* dual-luciferase experiments from the first part of this chapter was utilised in other areas of this research project. Since the target site of the miRNAs was towards the end of the 3'UTR of the *DNMT3B* gene it could be mutated using with a single primer, and still amplify the entire 3'UTR. Additionally only a short region surrounding the predicted miRNA target site was amplified to create a mutant construct. This was done to determine whether the entire 3'UTR was needed for miRNA targeting, or if just the miRNA response element (MRE), along with some flanking sequence, was sufficient. Since the same pattern of down-regulation of luciferase expression was seen with both the full-length and short 3'UTR, this suggests that the miRNA doesn't require the setting of the entire 3'UTR to target the MRE. This was a useful finding as it meant long oligos could be annealed together to create the MRE and short flanking region, which could then be cloned into psiCHECK-2 vectors, making target site mutations and reporter construct generations a more efficient process enabling it to be utilised in other areas of this project.

3.3.2 Identification of viral miRNA targets

mdv2-miR-M21 is the only MDV-2 miRNA that that shows a homology to a host encoded miRNA, within the seed region. Additionally the HVT encoded miRNA, *hvt-miR-H14**, was identified as having an almost identical sequence to the host miRNA *gga-miR-221*. The strong sequence homology between these two miRNAs suggests that *hvt-miR-H14** is acting as an ortholog of the host miRNA, however this was not explored further during this study as this was being explored by another member of the lab.

Using the above approaches four targets of different virally encoded miRNAs have been identified, along with the exact site of miRNA-mediated targeting in the gene 3'UTR. Three of these targets showed a decrease in protein abundance when the targeting miRNA expression vector was transfected into the cells. No decrease in protein abundance for the fourth target, *RALA*, could be observed as no band was present at the expected size during western blot analysis. No decrease in transcript abundance was observed by TaqMan gene expression for any of the four targets.

3.3.2.1 TargetScan custom

The reasons for choosing this prediction algorithm are simple; it was the only publically available miRNA target prediction program that would allow us to search for predicted targets of virally encoded miRNAs in host genes at the time of this study, and did not require the input of a bioinformatician to manipulate an algorithm. TargetScan custom provided an invaluable tool to begin our research into the functions of the virally encoded miRNAs. The merits of different miRNA target prediction algorithms have been discussed in the introduction (section 1.6.1) and are explored further in a review by Yue et al (Yue et al. 2009). A particular feature of the TargetScan custom algorithm is that it searches for seed matches only within the 3'UTR region of genes. While it is acknowledged that the majority of miRNA targeting occurs in the 3'UTR region of genes, targeting of miRNAs have been shown in the coding sequence (CDS) and even 5'UTR of the gene (Hausser et al. 2013). This means that by only searching for targets with gene 3'UTRs, genuine targeting of the viral miRNAs to other regions of the gene could be ignored. The advantages however of TargetScan custom (and others) lies in its ability to quickly provide a list of potential target genes of single (or group of) miRNAs, without the initial need for bench work. From this list the researcher can decide which of the predicted targets will be explored further and validated as a genuine target.

With bioinformatic approaches, a bias can be introduced into the dataset depending upon which algorithm is used or even which targets are investigated further. Each algorithm predicts targets based on different criteria, therefore a gene may be predicted to be targeted by a miRNA in one algorithm but not in another. Finding targets predicted by multiple algorithms is therefore considered the best approach and can help remove an algorithm selection bias. In the case of this project only one algorithm was readily available to search for chicken targets of viral miRNAs, so using multiple algorithms and looking for a consensus would have required outsourcing the work to a bioinformatician to manipulate other algorithms.

The performance of TargetScan custom in this project could perhaps best be analysed by the false positive rate of the predictions from our small sample of luciferase assays. The miRNA targeting of a selection of predicted target genes was validated by dual-luciferase assay, in this sample 14 predicted targets of different virally encoded miRNAs were selected for validation, and the number of predicted target sites that were genuine was determined.

Of the 14 predicted targets subjected to dual-luciferase assay, five of these targets saw a statistically significant down regulation of the luciferase gene, between the wild-type construct co-transfected with miRNA expression vectors, compared with all other co-transfections. It can therefore be concluded this down-regulation is caused by miRNA mediated targeting of the 3'UTR from the predicted target gene. Additionally due to the manner in which we performed the luciferase assay the exact target site of the miRNA, predicted by TargetScan custom, was also confirmed. Protein knockdown was also observed in the presence of miRNA expression vector for three of the targets highlighted by luciferase assay using this methodology. A disadvantage of the luciferase assay, which was observed in this study, was that any targeting of the gene of interest by host-encoded miRNAs appeared to hide targeting of the gene by the co-transfected miRNA. This was demonstrated in the luciferase assays for both DNMT3B-miR-M21 and AKT3-miR-M21, as this targeting was later validated by different methods.

Although the 14 predicted targets chosen for validation is quite a small sample size, it shows that the false positive rate of TargetScan in this study is around 65%, much higher than the predicted 30% by Yue et al (Yue et al. 2009). These false positive rates (FPR) were based only on statistical analysis, using miRNA sequence shuffling, so perhaps the higher FPR observed in this study is a result of more stringent testing of predicted targets. Nonetheless as a quick method of identifying target genes of miRNAs the TargetScan custom programme has been an extremely useful tool in this study.

3.3.2.2 PANTHER (Protein ANalysis THrough Evolutionary Relationships) Classification

The Panther Classification System (Mi et al. 2013) allowed some kind of 'biological meaning' from predicted targeting of the virally encoded miRNAs to be extracted. By grouping the predicted targets of all of the virally encoded miRNAs, for both MDV-2 and HVT, into distinct biological processes, it highlighted that the virally encoded miRNAs appear to target similar biological processes.

This classification analysis was largely performed as an alternative to simply choosing targets to analyse 'at will'. However, it soon became clear that the grouping of the different biological processes was quite broad; the statistical overrepresentation analysis provided a more accurate analysis of which specific biological processes were genuinely targeted when compared to the classification of all chicken genes. The predicted targets that were chosen for further analysis all fit into the biological processes that scored low P-values on the statistical overrepresentation test. Finally the targets which were actually chosen for luciferase analysis validation were picked from these biological processes, essentially 'at will', with the emphasis placed on predicted targets containing an '8mer' match.

This analysis, while interesting, is probably only able to provide a basic insight into the targeting of viral miRNAs. For instance within the statistical overrepresentation analysis there is a great deal of overlap of parent and daughter biological processes, and even overlap of the genes that are placed in these categories, which causes problems. Nonetheless, this analysis gave an idea of which targets might be of interest to explore further as genuine miRNA targets, as opposed to wholly choosing targets at will.

3.3.2.3 Dual-luciferase Assay validation of predicted targets

Dual-luciferase assays were chosen as the first route to validate the TargetScan custom predictions, as they provide a quick and relatively cheap way to demonstrate miRNA targeting to a specific region on a gene. The overall methodology of the luciferase assay largely followed the protocols of other members of this laboratory (Y. Zhao et al. 2009) whereby oligonucleotides were annealed together to create the predicted target site in the 3'UTR of the target gene. This is one approach to luciferase assays, other methods have been described (Le et al. 2009) in which only one reporter construct is

made containing the entire 3'UTR the miRNA of interest. This is co-transfected with the miRNA predicted to target, while a non-targeting small RNA, which should have no targeting, is used as a negative control, and the differences are compared.

The reasoning behind our methodology is simple, a 103bp long of the 3'UTR is used, as once restriction overhangs are added, this reached the 110bp limit of synthesis for oligonucleotides, that at the time of the experiment we were able to order. Within this 110bp limit however we are able to include the predicted miRNA seed target site, and also flanking region of around 45bp either side. This flanking region should ensure that the target site appears in the natural context of the 3'UTR, and in previous work using this dual-luciferase system we saw a similar pattern of miRNA targeting to the 110bp 3'UTR fragment as the full-length 3'UTR cloned downstream of the renilla luciferase gene (section 3.1.4).

The dual-luciferase methodology used in this study has some significant advantages over using a single reporter construct and co-transfecting a genuine miRNA and non-targeting small RNA. By mutating just a few bases in the seed sequence of the target gene 3'UTR the exact site of targeting by the miRNA can be determined, if genuine down-regulation of renilla luciferase is seen. Additionally using a mutated 3'UTR as opposed to just a wild-type 3'UTR reporter construct compared to empty reporter construct, eliminates background repression caused by random miRNA targeting to the 3'UTR.

Since the reporter constructs were synthesised there has been the introduction of cheap custom gene fragments up to 500bp (gBlocks® Gene Fragments, Integrated DNA technologies). This technology would have allowed for relatively simple construction of longer wild-type and mutant reporter constructs, albeit at an increased price. However the resultant knock-down of target protein levels of targets highlighted using the described dual-luciferase reporter assay methodology, suggests that it is working effectively.

3.3.2.4 Further validation of confirmed viral miRNA targets

Western blots were performed with the aim of showing miRNA-mediated down-regulation of validated target genes protein levels. This was performed on four targets of virally encoded miRNAs identified in the dual-luciferase assay.

The western blots demonstrated knock-down in protein levels of three of the four analysed proteins. Amount of knockdown was calculated with ImageJ software (http://rsb.info.nih.gov/ij/index.html) (Schneider et al. 2012) after normalising protein levels to the abundance of α-tubulin loading control. The knock-down demonstrated further validates the viral miRNA targeting that was highlighted from the luciferase assay.

It was unfortunate that there appeared to be no cross-reactivity in chicken cell lysate of the RALA antibody. This is not uncommon when working with chicken cells, as the described cross-reactivity of this antibody in the manufacturer datasheet was based on sequence homology with the human protein of which it was raised against. Dilutions of 1:500 (not shown) and 1:250 were used for the anti-RALA antibody in this study, the 1:250 dilution was in the middle of the manufacturer suggested concentrations but no lower dilution was tried. The effectiveness of the anti- α-tubulin blot, performed on the same membrane, suggests that sufficient sample was loaded, but nonetheless no band of expected size was produced. A band was visible in the blot at ~100kD, but this is a long way from the predicted size of ~22kD, so it was ignored for this analysis.

Analysis of transcript abundance was performed on four of the highlighted targets. Using TaqMan gene expression assays any transcript levels in cells, following transfection of miRNAs, could be observed and compared relative to cells transfected with empty miRNA expression construct. None of the four transcripts showed any significant (P-value <0.05) down-regulation of transcript. This is not an entirely surprising observation as it is known that miRNA targeting does not always result in a decrease in transcript levels. However Guo et al's study suggested that 84% of miRNA-mediated targeting resulted in transcript degradation (H. L. Guo et al. 2010), so it is surprising that none of our targets

showed any decrease in transcript level by TaqMan gene expression, despite showing a drop in protein abundance. Closer analysis of the TaqMan data shows that there was quite a lot of variation within the data, visible by the size of the error bars.

3.3.2.5 Identified potential targets of the viral miRNAs

Finally it is worthwhile to investigate the roles played by the human homologs of these validated viral miRNA targets and see how their expression levels might influence the virus life cycle.

3.3.2.5.1 V-akt murine thymoma viral oncogene homolog 3 (*AKT3*)

AKT3 is a serine/threonine protein kinase that regulates multiple process including cell survival, growth, proliferation and metabolism. There are two further, better studied, closely related protein kinases; *AKT1* and *AKT2*. Regulation of the processes described above is a result of phosphorylation of serine or threonine residues, and thus activation, of multiple different proteins.

AKT3 is a known modulator of several tumours including melanoma, ovarian cancer and glioma. Levels of active *AKT3* increase in line with melanoma tumour progression and the highest levels are found in advance-stage melanomas. Active *AKT3* promotes the progression of tumours via the inhibition of apoptosis, this was observed in a study where the down regulation of *AKT3* lead to a decrease in the levels of phosphorylated Bcl-2-associated death promoter (*BAD*), thus inducing apoptosis (Hers et al. 2011; Wright et al. 2008).

AKT3 has also been shown to be targeted by *miR-29* in humans, an interaction that was shown to reduce proliferation of mouse C2C12 myoblasts and facilitate myotube formation (Wei et al. 2013). This is an exciting discovery as it not only provides another example of miRNA targeting of *AKT3*, but also adds weight to the idea that *mdv2-miR-M21* is acting as an ortholog of *miR-29*.

Numerous studies have demonstrated changes in levels of *AKT* signalling pathways after viral infection of cells. Many viruses stimulate *AKT* activity after infection of cells leading to; the inhibition of apoptosis, continuation of DNA synthesis or promotion of viral attachment, all of which create a

beneficial environment for the viruses (Dunn and Connor 2012). Additionally other studies have shown that some RNA viruses down-regulate the expression of active *AKT* upon infection, which is thought to result in inhibition of immune cell proliferation, in the case of measles virus (Carsillo et al. 2010). Many of the impacts on *AKT* signalling described in the review by Dunn and Connor are a result of indirect regulation of the *AKT* pathway, similar regulation of the *AKT3* isoform following viral infection, are yet to be demonstrated in other studies.

3.3.2.5.2 *DEK* Oncogene

There are two transcript variants of the *DEK* oncogene that encode two isoforms of the DEK protein (Kappes et al. 2004). The DEK protein binds superhelical DNA, playing a role in splice site selection in mRNA processing and chromatin organisation (Hu et al. 2007). Changes in the *DEK* gene, increased expression and anti-DEK antibodies, have all been identified in a number of different disease states. An example of such is in acute non-lymphocytic leukaemia, which is a result of mutations within the chromosomal region containing the *DEK* gene (Vonlindern et al. 1992).

3.3.2.5.3 Ras-related protein 1α (*RAP1A*)

The RAP1A protein is a member of the family of RAS-related proteins sharing many structural features and around 50% sequence identity with the *RAS* oncogene. RAP proteins are known to competitively interact with activated RAS and RAF proteins, the antagonism of these proteins has implications in the MAPK kinase pathways that are normally activated by activated *RAS* (Sebzda et al. 2002).

The immunological implications of *RAP1* antagonism of *RAS* were first apparent when RAP1 protein was shown to be capable of reverting the phenotype of RAS-transformed fibroblasts (Kitayama et al. 1989), additionally high expression levels of *RAP1* are found in T-cells that are no longer capable of recognising antigen (Boussiotis et al. 1997). It has been suggested in a study, whereby *RAP1* activation was partially inhibited, that in order to generate an optimal T cell response activation of *RAP1* has to be disrupted (Carey et al. 2000).

3.3.2.5.4 V-Ral Simian Leukaemia Viral Oncogene Homolog A *(RALA)*

RalA and the closely related isoform RalB are GTPases which have been found to be involved in the control of multiple cellular functions including, cell proliferation, membrane trafficking and oncogenic transformation (Bodemann and White 2008). RalA and RalB have around 85% homology in their amino acid sequences, however only some of the functions of the two isoforms are shared. For example RalA and RalB have similar functions within cell growth but opposing roles in cancer cell migration (Oxford et al. 2005).

Of particular interest of this study is the identification of *RALA* as a target for the human miRNA *miR-181a* (Fei et al. 2012). By using similar methodology as described in this project, Fei et al have demonstrated a role for miRNA targeting of *RALA* to inhibit growth and apoptosis, both useful functions for herpesviruses maintaining latency.

3.3.2.6 Conclusion

3.3.2.6.1 Is mdv2-miR-M21 a functional ortholog of gga-*miR-29*b?

There is good evidence that the viral miRNA *mdv2-miR-M21* is targeting the host gene encoded the DNA methyltransferase, *DNMT3B* demonstrated by gene expression TaqMan in the first part of this chapter. Additionally, it was shown that the *mdv2-miR-M21* was targeting *AKT3*, another known validated target of *miR-29* (Wei et al. 2013), demonstrated by a reduction in protein levels after viral miRNA overexpression. This study was unable to clearly identify the actual site of miRNA targeting as dual-luciferase assays for both genes were unable to show significant down-regulation of luciferase expression when co-transfected with the miRNA compared to empty vector. It was an interesting observation that both genes showed comparable levels of down-regulation of luciferase expression, when the wild-type miRNA target site was present, adding weight to the idea that the knock-down was caused by the host miRNA *gga-miR-29b*, hiding the targeting of the viral miRNAs in the luciferase assays.

Previous studies that have shown a viral miRNA to be acting as a functional ortholog (Skalsky et al. 2007; Y. Zhao et al. 2009) have gone down the similar route of identifying common targets between orthologous miRNAs. In both of these examples of the *miR-155* orthologs; *kshv-miR-K12-11* and *mdv1-miR-M4*, one of the conserved targets is analysed in detail (*BACH1* and *PU.1* respectively) and shown to be targeted by both the host and viral miRNA.

To this end, validated targeting of two confirmed *miR-29* targets by *mdv2-miR-M21* would suggest that it can regulate expression levels of similar genes and that *mdv2-miR-M21* is a functional ortholog of *gga-miR-29b*. Since they do share an identical 'seed' sequence, the predicted targets (using the TargetScan custom programme) are identical between the two miRNAs. Therefore in terms of other predicted targets these miRNAs would appear to be functional orthologs. The results demonstrate that the viral miRNA is having a similar effect as the host-encoded miRNA on the *DNMT3B* and AKT3 gene, and therefore in an infected cell could be acting in a similar manner as the host miRNA.

3.3.2.6.2 Using a combination of bioinformatics and biochemical assay validation to find targets of virally encoded miRNAs

In conclusion, targets of some of the viral miRNAs have been identified with confidence using a combination of the dual-luciferase reporter system and western blot analysis. Of interest also, is that by mutating just 3 nucleotides in the 3'UTR targeted by the seed region, there is a significant reduction in miRNA targeting effects, thus highlighting the exact region targeted by the corresponding miRNA as predicted by TargetScan custom. Important to this study was the validation of the effect of miRNA targeting on protein levels of the target genes, as this provides the most valuable evidence of miRNA targeting having a tangible effect within the cells.

4 Proteomics Approach to Identify HVT miRNA Targets

4.1 Introduction

4.1.1 Global Identification of viral miRNA targets

Following on from the work described in the chapter 3, an alternative global approach for identifying targets of the virally encoded miRNAs was adopted so that miRNA mediated knockdown of protein levels could be observed. In recent years, a number of different biochemical assays have been developed that can identify large numbers of putative miRNA targets. The various different biochemical assays used to identify miRNA targets are discussed in more detail in section 1.6.2 of this thesis and reviewed by Thomas et al. 2010. In short, these biochemical approaches can be broadly divided into two groups; analysis of proteome or transcriptome changes, following over- or under-expression of the miRNAs of interest, or isolation of the miRNA induced silencing complex (miRISC) and analysis of the associated transcripts.

Over the years, slight variations of these techniques have been developed and optimised to identify targets of miRNAs (Bargaje et al. 2012; Jovanovic et al. 2010; Skalsky et al. 2012). The merits and draw-backs of these different approaches have been discussed (section 1.6.2); this chapter will describe personal experiences and conclusions of a few different biochemical approaches and an explanation as to why a proteomics based approach was decided on.

4.1.2 Ago2 Immunoprecipitation

Initially in this project, inspiration was taken from the work performed by Dölken et al and others to isolate miRNA target transcripts by Ago2 (a major constituent of the miRISC) immunoprecipitation in virally infected cells (Dölken et al. 2010b). By immunoprecipitating the miRISC, via Ago2, the targeted transcripts are also isolated, then the identity of these transcripts are analysed either by microarray or deep-sequencing. Work was performed on developing a chicken-specific Ago2 antibody, directed against the 5’ end of the chicken protein. Production of a useful antibody in-house was ultimately unsuccessful as the antibody was unable to recognise chicken-Ago2 from any of the samples we

tested. However during this work a commercial human Ago2 antibody (Abcam (ab57113)) with cross-reactivity to the chicken protein did become available.

Preliminary immunoprecipitations with this antibody in the MDV1 and MDV2 infected cell line MSB-1 were performed, and viral miRNAs were detected via qRT-PCR (data not shown). Enrichment levels of the viral miRNAs relative to the control immunoprecipitation were favourable, although they were not at the same levels as observed by other groups (Dölken et al. 2010b). Only two attempts at the Ago2 IP were performed in this study, and the controls used were not stringent enough for the data be presented in this thesis. At the same time further validation of the dual-luciferase assays of bioinformatically predicted miRNA targets was presenting problems, because although targeting of the transcript could be demonstrated, chicken-reactive commercial antibodies to the target genes were unavailable in a number of cases. If a miRISC immunoprecipitation followed by microarray analysis (RIP-Chip) approach was used.

The RIP-Chip method has been developed further in recent years in response to concerns that transcripts could be associating with the miRISC following cell lysis prior to immunoprecipitation (Mili and Steitz 2004). Possible solutions to this problem were to cross-link the target transcripts to the miRISC prior to cell lysis and immunoprecipitation (Chi et al. 2009), or additionally using a specific photoactivatable ribonucleoside (Hafner et al. 2010). These are without doubt powerful tools for miRNA target identification, however they have to date only been performed in human cells, and because of the lower number of chicken-reactive antibodies to validate highlighted miRNA targets such studies remain unsuitable for our purposes. This was enough to suggest that alternative approaches should be explored.

4.1.3 Proteomics

It soon became clear that the most appropriate biochemical method of identifying viral miRNA targets for this study was to use a proteomics approach, the key advantage being that targets are identified at the protein rather than mRNA level, and thus changes in protein levels can be observed without the need for a chicken reactive antibody. The first description of using proteomics to identify miRNA targets was by Baek and colleagues who identified targets of *miR-223* using quantitative mass spectrometry (Baek et al. 2008). Cells underwent stable isotope labelling of amino acids in cell culture (SILAC), whereby heavy and light isotopes of carbon were used to determine expression of 3,819 proteins between mouse neutrophils, where *miR-223* expression had been knocked out, and control cells.

In this study the aim was to identify targets of all of the viral (HVT) miRNAs in one experiment, as this could provide an additional insight into how the miRNAs might be acting co-operatively to target host proteins. The aim of this study was initially to study both HVT and MDV-2 encoded miRNAs; however it soon became clear that the work required to produce the reagents needed for proteomic analysis of both set of virally encoded miRNAs would not fit into the timeframe of this project. Additionally we were aware of another group using a different approach to identify the global targetome of both MDV-1 and MDV-2 encoded miRNAs, which has since been published (Parnas et al. 2014), therefore it seemed sensible to focus on the HVT encoded miRNAs.

Proteomic analysis is an extremely sophisticated and expensive methodology and was therefore performed at the Institute of Integrative Biology at the University of Liverpool. Instead of using radioactive isotope labelling, the Liverpool facility has developed a label-free quantitative proteomics methodology that uses data from mass-spectrometry runs performed side-by-side and compares the relative abundance of proteins in different runs (Wastling et al. 2012). This meant that once we had generated a system of expressing the viral miRNAs in cells, the mass spectra for both the miRNA-

expression cells, and control cells could be generated and differences between traces could be analysed.

4.2 Results

4.2.1 Generating inducible HVT miRNA expression construct

Since the effects of long-term expression of the viral miRNAs on the DF-1 cells is not known, a vector with inducible expression would allow expression of the miRNAs only when required. The pRTS vector used for the final construct (described in section 2.2) has a bi-directional inducible promoter under the control of doxycycline that used to control HVT miRNA expression. The pRTS-HVT miRNA construct, named pRTS-HVT-miR-H1-H18, was generated as described in section 2.3.17 and once confident that the correct construct had been generated (as shown in figure 23), testing of miRNA expression, following induction, began.

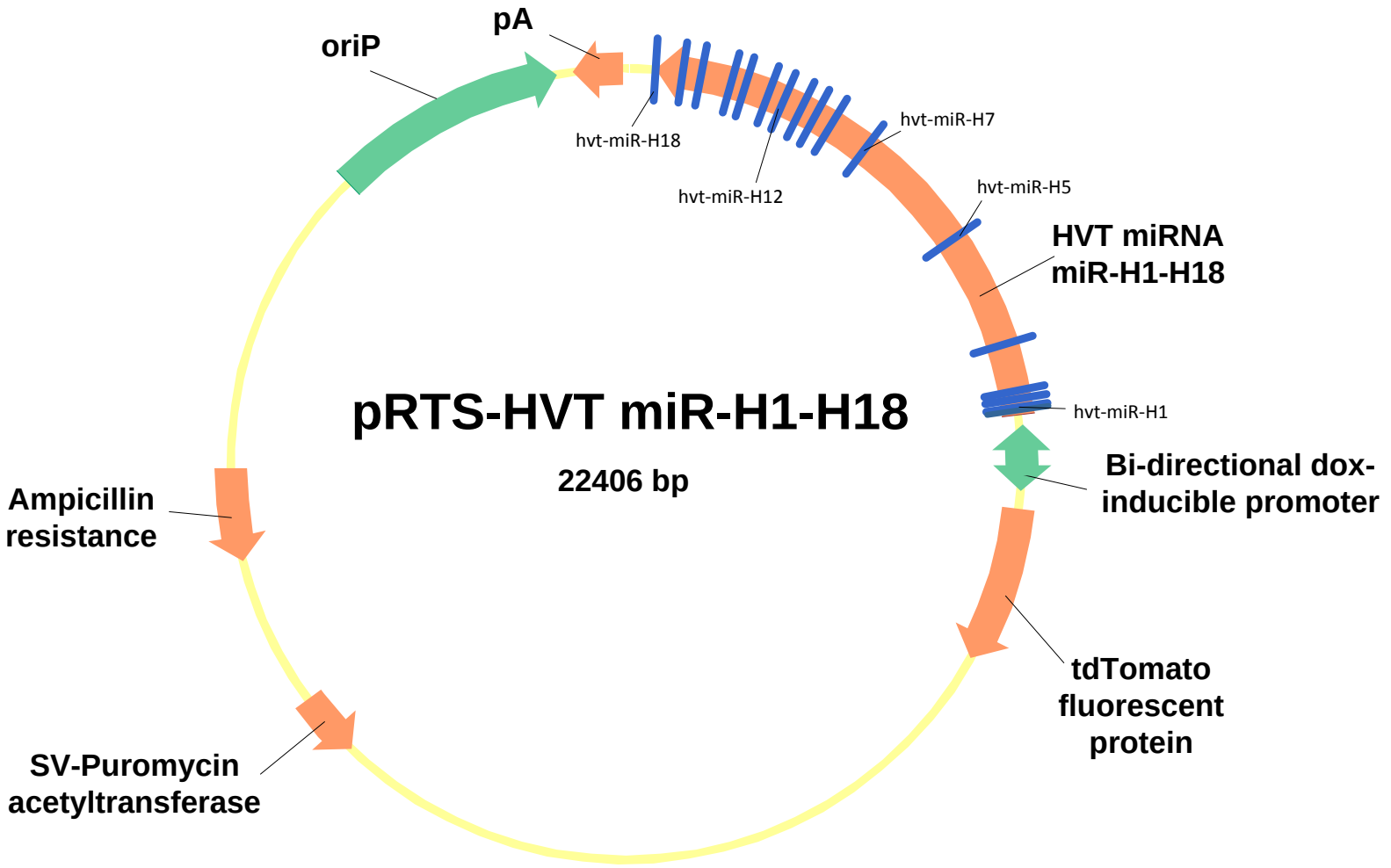


Figure 23–Simplified vector map of pRTS-HVT miRNA H1-H18 construct. Generated to scale using vector NTI software (Invitrogen). Abbreviations in figure: pA = PolyA tail (multiple adenosine monophosphates), tdTomato = Tomato fluorescent protein gene, oriP = origin of plasmid replication. Blue lines indicate the locations of each HVT miRNA as amplified from BAC DNA, with a few miRNA labelled for reference.

4.2.2 Testing miRNA expression from the pRTS construct

To test miRNA expression, pRTS-HVT miRNA constructs were stably transfected into DF-1 cells, as described in section 2.3.18. Cells were cultured and once confluent, doxycycline was added to a final concentration of 1µg/ml to the selected cells. The doxycycline induced expression from the bi-directional promoter driving expression of both the tomato fluorescent protein gene and the HVT miRNA cassette. 48-hours after doxycycline induction, fluorescent microscope images were taken of the selected, transfected DF-1 cells as shown in figure 24.

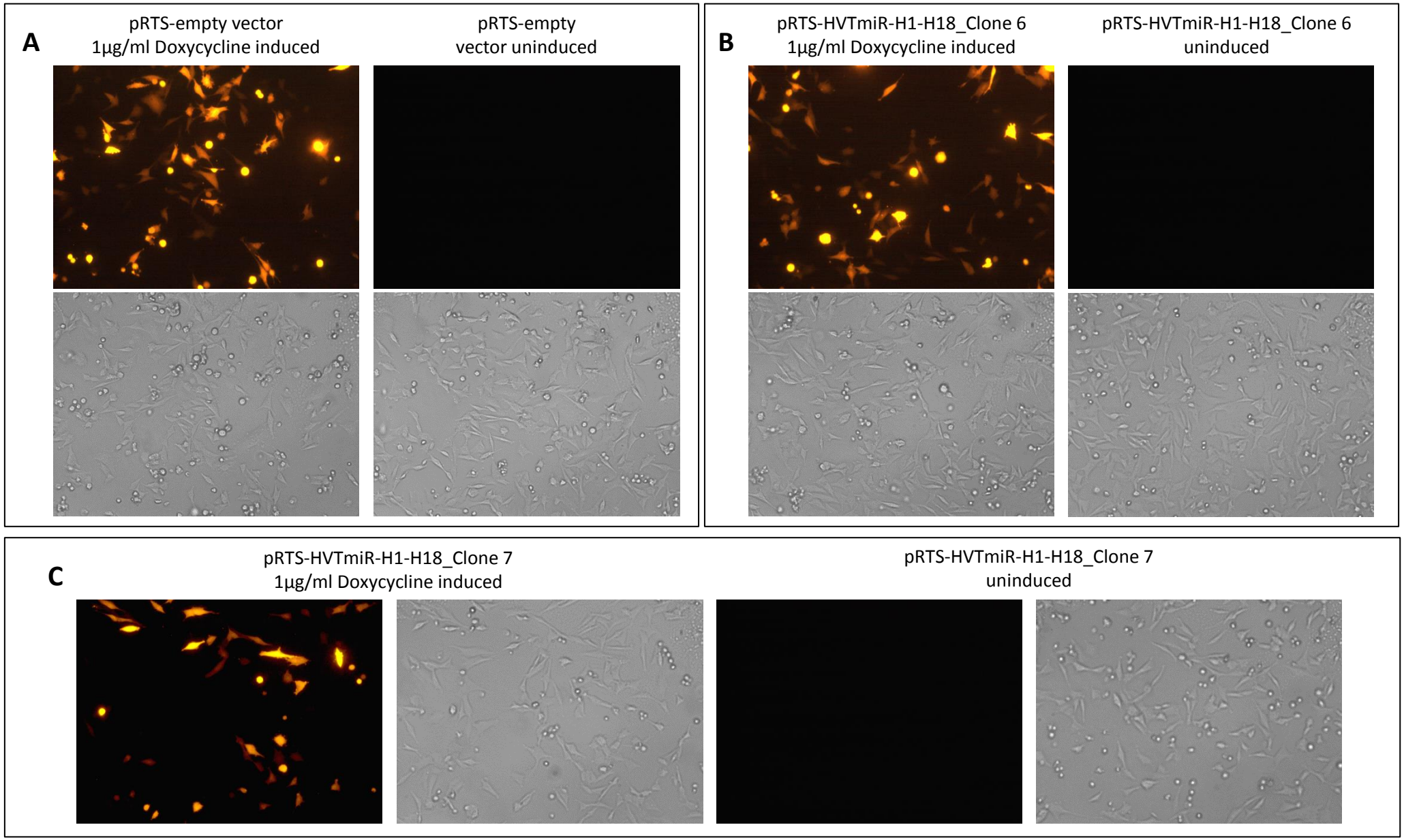


Figure 24 - Fluorescent microscope images of puromycin selected, stably transfected DF-1 cells, containing either: pRTS-empty vector (A), pRTS-HVT miRNA vector clone 6 (B) or clone 7 (C). Two pictures in each set show bright field and UV fluorescence microscopy. Title above pairs of pictures describes if expression from the pRTS bi-directional promoter has been induced by the addition of 1µg/ml doxycycline or not.

From the images in figure 24, it is clear that the addition of doxycycline induces expression from the bi-directional promoter, demonstrated by the presence of the tomato fluorescent protein in the cells. From the pictures it can also be seen that a high percentage of the DF-1 cells contain the pRTS-HVT miRNA construct. Expression from the bi-directional promoter remains appears to be under control of doxycycline, as there appears to be no tomato fluorescent protein present in the uninduced cells, compared to induced cells.

The presence of tomato fluorescent protein however, is no guarantee of miRNA expression from the same promoter, so initially a quick check for expression of the HVT miRNA cassette was performed by testing for the expression of a selected HVT miRNA (*hvt-miR-H15*) in induced cells compared to uninduced and empty vector induced and uninduced cells via miRNA qRT-PCR. RNA was harvested following induction (from the cells pictured in figure 24), using miRNeasy Mini Kit (Qiagen), following the manufacturers protocol. Detection of *hvt-miR-H15* was performed on the freshly extracted RNA as detailed in the methods (section 2.3.14) using the specific TaqMan miRNA Assay (Applied Biosystems, Cat #4440885). Expression was determined relative *to hvt-miR-H15* expression levels in pRTS-empty vector, uninduced (background) and levels of RNA normalised to levels of host miRNA, *gga-miR-let7a*. The results are shown in figure 25.

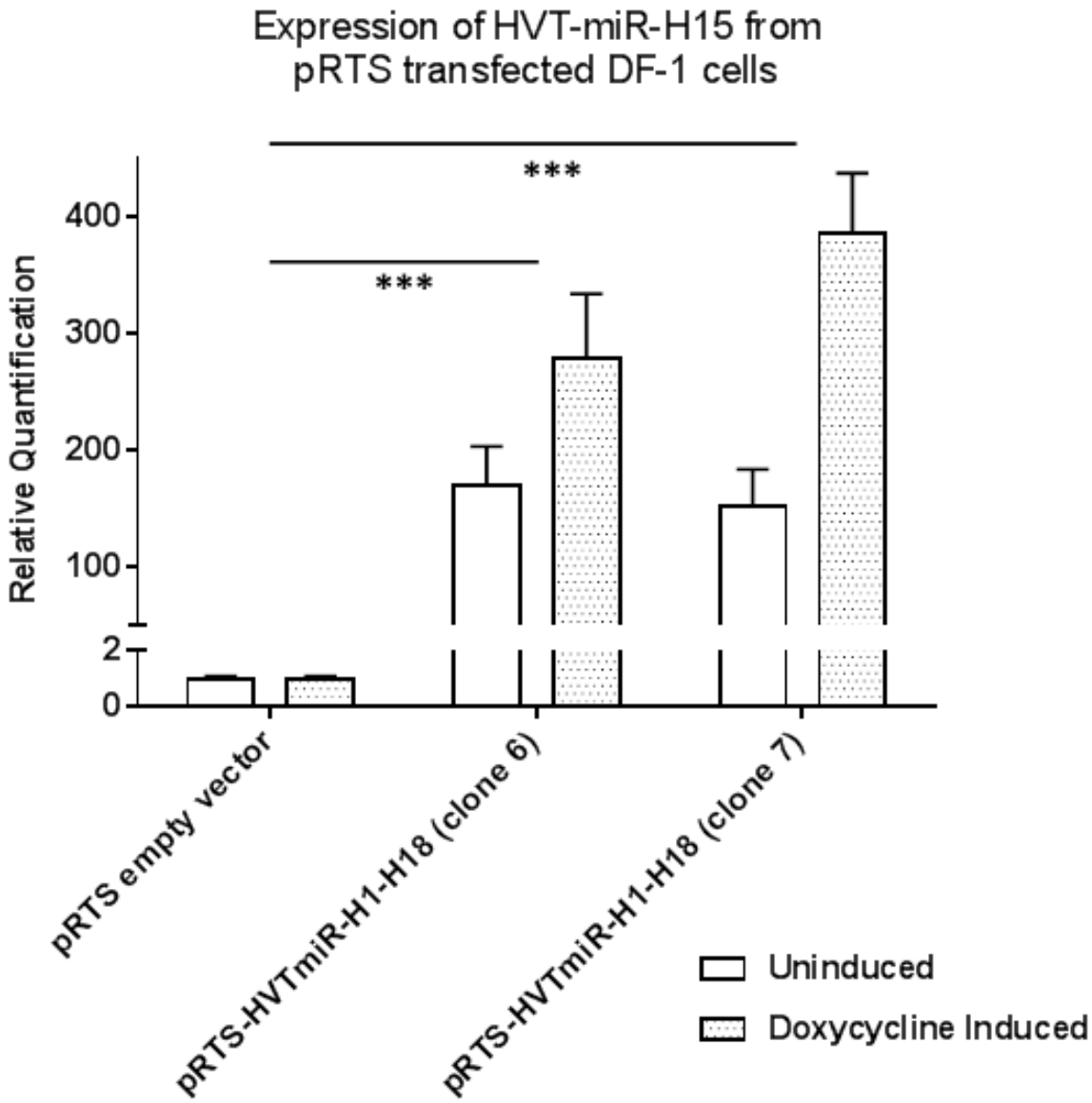


Figure 25 – Initial TaqMan analysis of *hvt-miR-H15* expression from both; doxycycline induced and uninduced DF-1 cells stably transfected with different clones of the pRTS-HVT miRNA vector compared to empty vector. Error bars show the 95% confidence intervals and *** denotes significant increase in *hvt-miR-H15* expression in samples, relative to control, as calculated by a P-value under 0.001, calculated by a paired 2-tailed T-test.

4.2.3 Initial analysis of miRNA expression from pRTS-HVT miRNA transfected DF-1 cells

Relative to empty vector there is significant expression (calculated by a paired 2-tailed T-test), of *hvt-miR-H15* in both of the pRTS-HVT miRNA construct (clones 6 and 7) transfected cells (figure 25). However the data was unexpected as it showed that there is expression of *hvt-miR-H15* in transfected, selected cells both before and after induction. The relative miRNA expression is higher in both cases following induction, however levels of *hvt-miR-H15* expression is significant in uninduced cells.

This observation initially led to questions about possible 'leakiness' of the inducible promoter and was investigated further with a PCR to test for the expression of tomato florescent protein gene. PCR amplification was performed as described in section 2.3.6 using GoTaq DNA polymerase on cDNA generated from pRTS construct transfected cells. Electrophoresis analysis of the PCR reactions are shown in figure 26, two PCR reactions were performed on each cDNA (both reverse transcription (RT) positive and negative) to amplify the tomato fluorescent protein gene and chicken *β-actin* gene (as a control), the sequence of the primers used are shown in section 2.3.33.2.

From figure 26 it becomes clear that there is some leakiness of the doxycycline-inducible promoter, as in uninduced (0hr) pRTS transfected cells there is some amplification of the tomato fluorescent protein gene. The level of amplification suggests that the level of tomato fluorescent protein is lower in uninduced cells compared to cells 24 and 48 hours after induction with dox. This approach is only semi-quantitative; therefore the only sure conclusion to draw is that the bi-directional promoter is not under complete control of doxycycline.

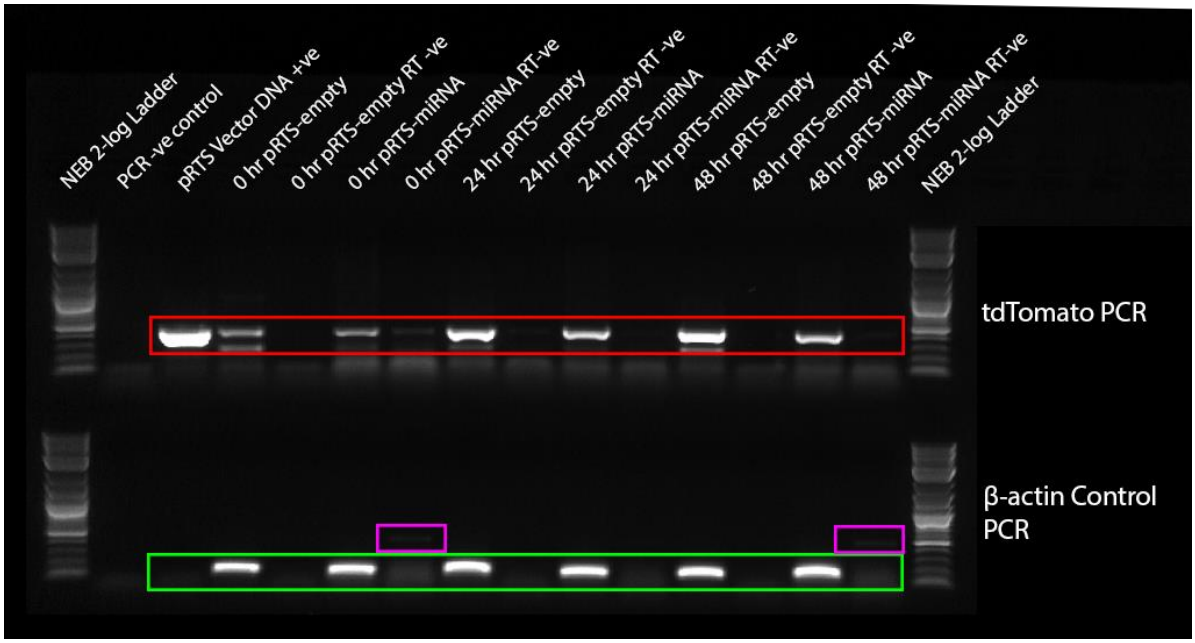


Figure 26 – PCR amplification of the tdTomato fluorescent protein gene and chicken *β-actin* from DF-1 cells stably transfected with pRTS-empty and pRTS-HVT miRNA constructs. The red box highlights the expected size PCR product generated from the *tdTomato* PCR, the green box highlights the expected size PCR product generated from the *β-actin* control PCR and the purple box highlights the larger size fragment produced by the *β-actin* PCR if genomic DNA is present (suggesting genomic DNA contamination in the RNA used for producing cDNA).

Another explanation for the high levels of *hvt-miR-H15* was considered, a test was performed to determine whether or not there was an internal promoter within the 4.6kb HVT miRNA cassette. Levels of *hvt-miR-H15* expression in DF-1 cells, which were transfected with the subcloning vector pCR-XL-TOPO-HVT miRNAs (containing no eukaryotic promoter) were analysed. Analysis from this test showed that there was indeed expression of *hvt-miR-H15* in cells transfected with the pCR-XL-TOPO promoter-less construct (appendix 2). It was therefore determined that the high levels of viral miRNA in uninduced cells was probably a combination of promoter 'leakiness' and the presence of an internal promoter that was driving expression of at least one, and probably more, of the viral miRNAs.

4.2.4 Confirming expression of all HVT miRNAs from pRTS-HVT miRNA transfected DF-1 cells

Since expression of *hvt-miR-H15* appeared to be slightly higher in pRTS-HVT miRNA clone 7 (compared to clone 6 in figure 25), this clone was carried forward and used in all further experiments. 200µg of highly purified plasmid was prepared by plasmid maxiprep kit (Qiagen) following manufacturers protocol. Transfection of DF-1 cells using lipofectamine 2000 transfection reagent (Invitrogen) was repeated using the maxiprep plasmid DNA, however this time the transfection was performed directly in a T75 tissue culture flask, cells and reagents were scaled up as per the manufacturer's protocol. 24 hours after transfection the cells were trypsinized and then transferred to a fresh T75 flask with 20ml DF-1 medium containing 1µg/ml puromycin. Transfected cells continued to be cultured and selected at 38.5°C and 5% CO_2 (DF-1 selection medium refreshed every 3 days), until the flask reached confluency. miRNA expression was induced with the addition of doxycycline at a concentration of 1µg/ml and 48 hours after induction RNA was harvested.

The most efficient way to test expression of all of the HVT miRNAs from the pRTS-HVT miRNA construct was to perform miRNA microarray on the RNA extracted from induced, transfected, selected DF-1 cells. At the time of this experiment custom TaqMan miRNA expression assay were both timely to design and costly to purchase, using a miRNA microarray provided an efficient one step process to

ensure all viral miRNAs were being expressed, in one experiment. Expression of the miRNAs would be compared alongside induced and selected DF-1 cells transfected with pRTS-empty vector construct. The miRNA microarray was performed by LC Sciences (Houston, Texas. USA), 6µg of total RNA from both empty and miRNA vector transfected cells was shipped on dry ice, and the microarray was performed with 6 replicates for each group. The microarray detected expression of all the chicken miRNAs in the samples (based on miRBase release 18.0) and 28 custom sequences, which we requested to detect all of the mature HVT miRNAs. The results of the microarray are displayed in figures 27 and 28.

	pRTS-empty vector Doxycycline Induced			pRTS-HVT miRNA Doxycycline Induced		
miRNA	**Mean**	**StDev**	**p-value**	**Mean**	**StDev**	**p-value**
hvt-miR-H14*	4,503	356	0.0E+00	4,412	402	0.0E+00
hvt-miR-H9-5p	21	13	1.1E-01	2,409	395	1.3E-08
hvt-miR-H14	2	9	8.4E-01	1,988	156	0.0E+00
hvt-miR-H17	21	11	6.8E-02	1,234	119	0.0E+00
hvt-miR-H7-5p	45	16	6.0E-03	1,087	127	0.0E+00
hvt-miR-H15	0	7	1.0E+00	970	81	0.0E+00
hvt-miR-H13	0	7	1.0E+00	941	107	0.0E+00
hvt-miR-H12-5p	5	10	6.2E-01	902	178	3.3E-16
hvt-miR-H18-5p	210	29	1.7E-13	540	61	0.0E+00
hvt-miR-H17*	8	11	4.5E-01	368	47	1.3E-14
hvt-miR-H16-5p	6	11	5.8E-01	350	72	2.1E-10
hvt-miR-H16-3p	23	13	6.9E-02	285	42	2.9E-12
hvt-miR-H18-3p	0	7	1.0E+00	128	32	3.7E-07
hvt-miR-H3-3p	51	17	3.4E-03	89	27	9.6E-04
hvt-miR-H1	34	14	1.9E-02	73	39	5.8E-02
hvt-miR-H3-5p	32	14	2.1E-02	62	27	1.9E-02
hvt-miR-H15*	0	6	1.0E+00	50	21	4.0E-04
hvt-miR-H5	12	11	3.3E-01	29	25	1.9E-01
hvt-miR-H8	8	11	5.4E-01	24	23	2.3E-01
hvt-miR-H9-3p	0	7	1.0E+00	14	21	2.3E-01
hvt-miR-H12-3p	0	8	1.0E+00	12	22	3.3E-01
hvt-miR-H4*	0	8	9.7E-01	6	22	6.0E-01
hvt-miR-H10	0	7	1.0E+00	4	19	6.5E-01
hvt-miR-H4	1	9	9.2E-01	4	19	7.0E-01
hvt-miR-H2	0	8	9.9E-01	2	18	7.9E-01
hvt-miR-H7-3p	0	7	1.0E+00	2	19	8.3E-01
hvt-miR-H11	0	7	1.0E+00	2	19	8.4E-01
hvt-miR-H5*	0	7	1.0E+00	1	19	9.2E-01

Figure 27 – Mean number of counts of all of the HVT miRNAs detected by miRNA microarray analysis performed by LC Sciences. The left-hand column shows the number of miRNA counts in doxycycline-induced, pRTS-empty vector stably transfected DF-1 cells. The right-hand column shows the number of miRNA counts in doxycycline-induced, pRTS-HVT miRNA vector stably transfected DF-1 cells. Standard deviation of different runs and p-values are also shown. The signal values are derived by background subtraction and normalisation. A transcript to be listed as detectable must meets at least two conditions: signal intensity higher than 3×(background standard deviation) and spot CV < 0.5. CV is calculated by (standard deviation)/(signal intensity).

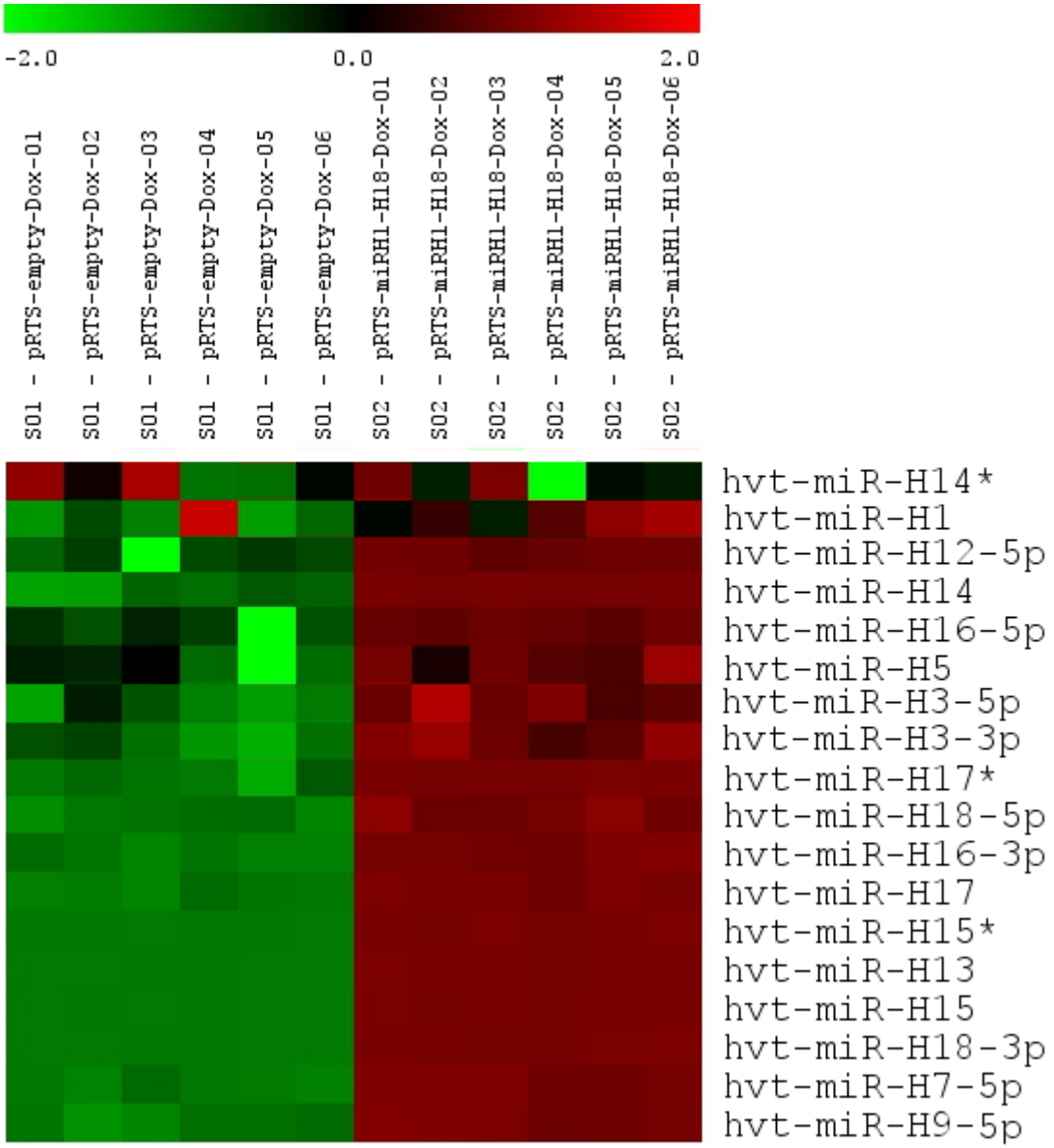


Figure 28 – Heat-map (Provided by LC Sciences) showing detection of the 18 most highly detected viral miRNAs in the pRTS-HVT miRNA transfected DF-1 cells. The detection from the six repeats for each sample are shown, where dark red demonstrates high relative levels of miRNA, bright green demonstrates low levels.

The general picture indicated from the miRNA microarray (figures 27 and 28) is that, compared to empty vector transfected cells, the HVT miRNAs are present in the induced, pRTS-HVT miRNA vector transfected DF-1 cells. What is clear however is that the level of expression of each of these miRNAs is not equal. Firstly there is an extremely high level of expression of *hvt-miR-H14** in both induced empty vector and induced HVT miRNA vector transfected cells. This observation can most likely be explained by a coincidental sequence homology (91.3% or 21/23 nucleotides) to the host miRNA *gga-miR-221*, suggesting that the host miRNA could likely have bound to our custom *hvt-miR-H14** probe and given a false positive sequence. Other than H14* the expression levels of HVT miRNAs are always higher (even if detection levels, derived by background subtraction and normalisation, are low) in the pRTS-HVT miRNA transfected cells.

Additionally to the HVT miRNAs, expression levels of all of the chicken miRNAs were detected within the microarray. There were some variations in the expression of the host encoded miRNAs between the pRTS-empty and pRTS-HVT miRNA transfected DF-1 cell samples, however the fold-change in difference of detection levels was not as dramatic between the two samples as seen for the HVT miRNAs. Of note 15 host-encoded miRNAs saw a 2 fold-change or greater, with the largest fold change being 10-fold (*gga-miR-1592*). These slight variations in signal detection of the host-encoded miRNAs were not explored further, since primarily the miRNA microarray was used as a means of confirming expression of the viral miRNAs from the pRTS construct.

4.2.5 Preparing samples for label-free proteomics

Large scale (T75 culture flask) transfections of pRTS-empty and pRTS-HVT miRNA vectors were performed once again using maxiprep-purified plasmid DNA. Transfected cells were cultured and selected by the addition of puromycin in the medium. Once the culture flasks were 95% confluent, expression was induced by the addition of doxycycline at a concentration of 1µg/ml. For both pRTS-empty and pRTS-HVT miRNA constructs, three T75 culture flasks containing selected, transfected cells

were cultured. Three flasks were set up so that the cells could be harvested at different time points following doxycycline induction: 0 hours, 24 hours and 48 hours.

For each run of the label-free proteomics, 200µg of protein was needed from each sample. Some preliminary work was performed that showed $3x10^6$ DF-1 cells, harvested as described in the protocol in the methods (section 2.3.12), provided approximately 320µg of protein. This meant that we would have some excess of sample from a T75 flask, which could be used to analyse viral miRNA expression ensuring there was viral miRNA in the actual samples that were being used for proteomic analysis (as observed in figure 29). The samples were all harvested by removal of growth medium (an appropriate time after induction), one quick wash with ice-cold PBS, and then harvested in ice-cold PBS by cell scraping, on ice. The cell suspension was then pelleted by centrifugation at 4000xg for 5mins and the supernatant completely removed. The cell pellet was resuspended in 1ml of PBS and counted, $3x10^6$ DF-1 cells were removed, pelleted and frozen at -80°C ready to be sent to Liverpool for proteomic analysis, the process is summarised in a workflow diagram in appendix 7. 700µl Qiazol was added to the remaining cell and total RNA extracted using miRNeasy Mini Kit (Qiagen) following manufacturer's protocol. Viral miRNA expression was then analysed via miRNA TaqMan comparing expression of the viral miRNAs *hvt-miR-H1*, *hvt-miR-H15* and *hvt-miR-H18* between the different samples: pRTS-empty uninduced (0 hours), pRTS-empty dox 24 hours, pRTS-empty dox 48 hours, pRTS-HVT miRNA uninduced (0 hours), pRTS-HVT miRNA dox 24 hours, pRTS-HVT miRNA dox 48 hours (figure 29).

Figure 29 demonstrates that there is strong viral miRNA expression in pRTS-HVT miRNA vector transfected cells compared to pRTS-empty vector transfected cells. Expression levels of *hvt-miR-H15* and *hvt-miR-H18* remained high, with little difference across the time points. As before there is strong expression of the viral miRNAs from the uninduced cells, suggesting leakiness of the dox-inducible promoter as described in section 4.2.3.

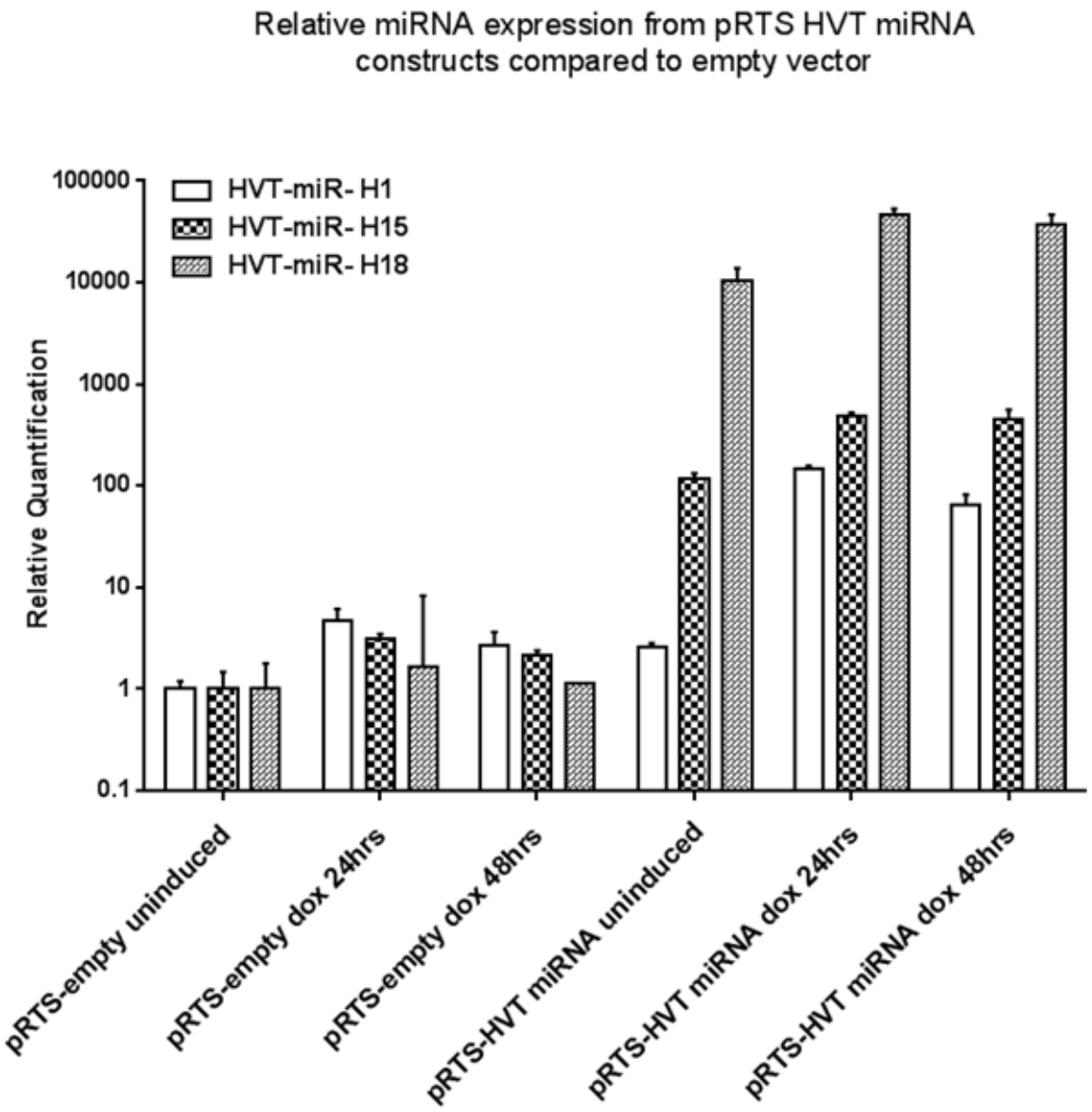


Figure 29 – Log_{10} relative expression levels of three different HVT miRNAs (H1, H15 and H18) from DF-1 cells stably transfected with either pRTS-empty vector pRTS-HVT miRNA vector, clone 7. Cells were harvested at different time points after doxycycline induction of pRTS bi-directional promoter, 0 hours (uninduced), 24 hours and 48 hours. Expression levels are relative to expression of the miRNAs detected in pRTS-empty uninduced (background). Error bars show maximum and minimum relative quantification (RQ) values as calculated by 7500 Fast software (Applied Biosystems) from Ct values, normalised to gga-miR-let7a.

4.2.6 Label-Free Quantitative Proteomics

Protein was extracted from the cell pellets, containing $3x10^6$ cells, of each sample in Liverpool. Label-free mass spectrometry analysis was performed by Dr Dong Xia in Liverpool, comparing the abundance of different peptides (which were then ordered and associated to chicken proteins) between the six different samples (each sample having two replicates). Raw files collected by mass spectrometry were searched in Mascot (Matrix Science) assuming a 1% peptide false-discovery rate (to correct for multiple comparisons) and 791 chicken proteins were identified. Raw files were also imported into Progenesis LC-MS (Nonlinear Dynamics) where global normalisation was applied to all features detected. After removing proteins with single peptide identifications (two peptides per protein is considered the standard), the normalised abundance of 362 proteins was able to be determined. Protein levels were normalised using the global normalisation method, in this method the average peptide abundance for all peptides in both the experimental and control sample is determined, this mean is then used as a fixed constant to multiply the abundance of individual peptides from each group by. The assumption of this normalisation method is that most peptide abundances do not change, therefore any peptides which show a change in abundance after normalisation should not be a result of differences in sample loading. This method of normalisation is often used because it's difficult to nominate any particular housekeeping genes because it has been found that the expression levels of housekeeping proteins are not always constant (Callister et al. 2006).

The initial data analysis of the proteomics experiment was carried out by Dr Dong Xia and provided as a Microsoft Excel spread sheet containing normalised protein abundance from each of the duplicate runs and an average. The fold change in expression for each protein between empty vector and miRNA containing vector was simply calculated by dividing average normalised protein abundance from pRTS-HVT miRNA transfected cells by average normalised protein abundance from pRTS-empty transfected cells.

The fold change of all 362 proteins is represented by the heat map shown in figure 30, generated by GENE-E software (Broad Institute) with a minimum blue-colour graduation cut-off of 0.5 times fold-change and a maximum red-colour graduation cut-off of 2 times fold-change being used to highlight subtle changes in protein abundance, this does not represent a cut-off for exclusion of any results. The aspect of adding a timescale to the experiment had largely become redundant at this point due to the unregulated expression of miRNAs in pRTS-HVT miRNA transfected cells. Therefore only the fold-change in normalised abundance of the identified proteins 48 hours after addition of doxycycline is shown, the rows are ordered by Uniprot accession code in descending order (protein accession numbers are omitted due to space constraints, full data can be seen in appendix 4). Despite the fact that a time course was initially set up for this experiment, the results from above sections highlight the fact there are only marginal increases in viral miRNA expression after the addition of doxycycline compared to uninduced. The 48 hour after doxycycline induction samples were chosen for further analysis as they produced the lowest median coefficient of variation (CV) (described in section 4.2.6.1) between runs, and previous luciferase studies were all performed 48 hours after addition on miRNA expression vector therefore keeping this continuity seemed sensible.

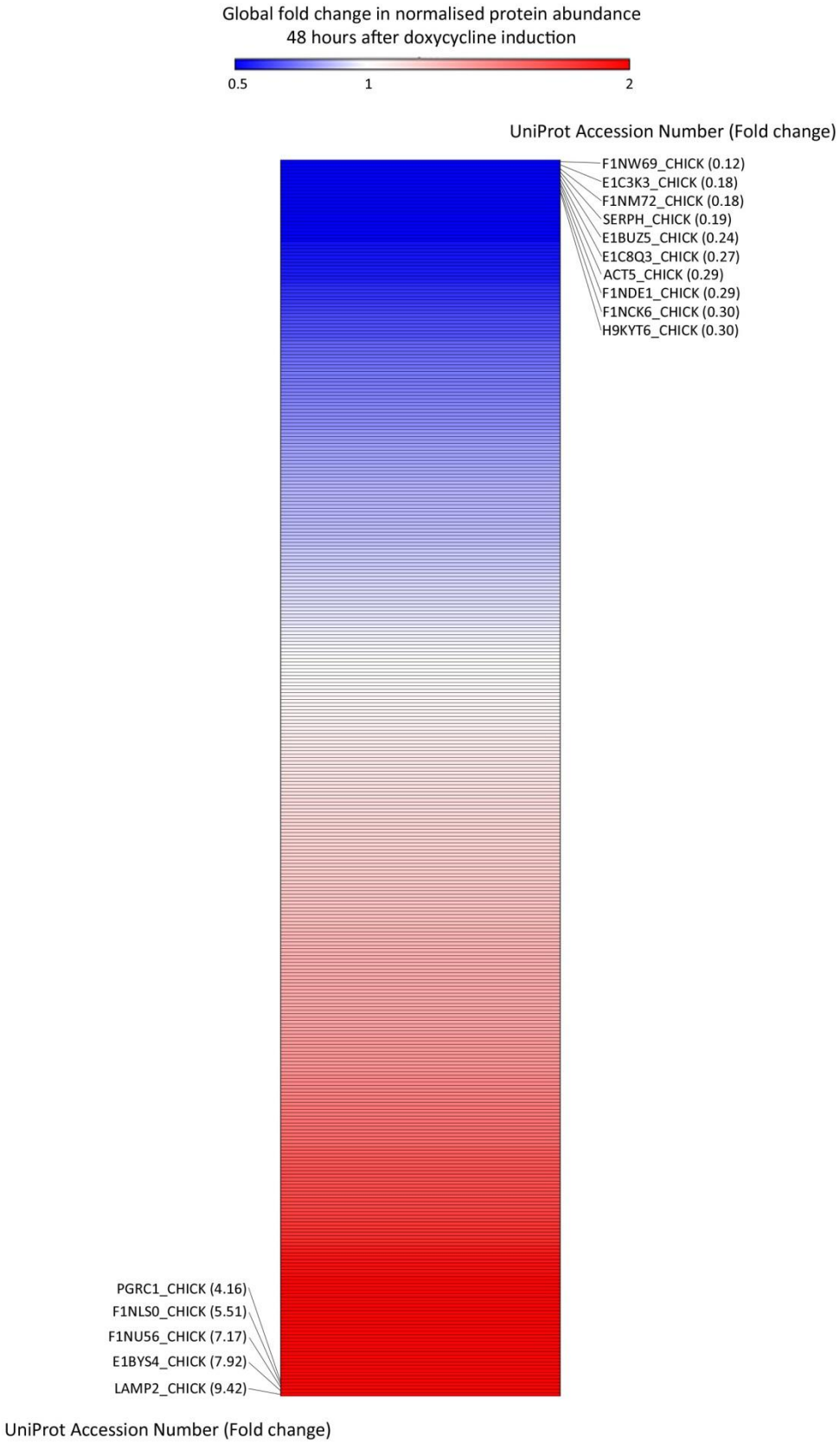


Figure 30 - Heat map generated using GENE-E software (Broad Institute), showing the fold change of 362 chicken proteins as detected by more than 2 peptides label-free proteomics experiment. Fold change was calculated by dividing average normalised protein abundance from pRTS-HVT miRNA transfected cells by average normalised protein abundance from pRTS-empty transfected cells. Uniprot accession numbers and specific fold changes are given for the 5 greatest fold increases, and 10 greatest fold decreases in protein abundance.

4.2.6.1 Statistical analysis of duplicate quantitative proteomic runs for both pRTS-HVT-miRNA and pRTS-empty transfected DF-1 cells

As mentioned briefly above, CV values were calculated comparing the duplicate runs for each sample. This was to give an idea of the reproducibility of the normalised abundance of each identified protein so that a more reliable analysis could be made about any increase or decrease of protein abundance in the presence of the viral miRNAs. Any of the 362 proteins with a CV cut-off value above 0.2 (as recommended by Dr Dong Xia) between duplicate normalised abundances were removed, leaving 108 proteins. The results following this analysis are shown in the heat map in figure 31.

As before, proteins are ordered by Uniprot accession code in descending order (starting top of left column going down, full data can be seen in appendix 4). Again a minimum cut-off of 0.5 times fold-change and a maximum cut-off of 2 times fold-change were used in the colouring of the heat map, produced using GENE-E software (Broad Institute).

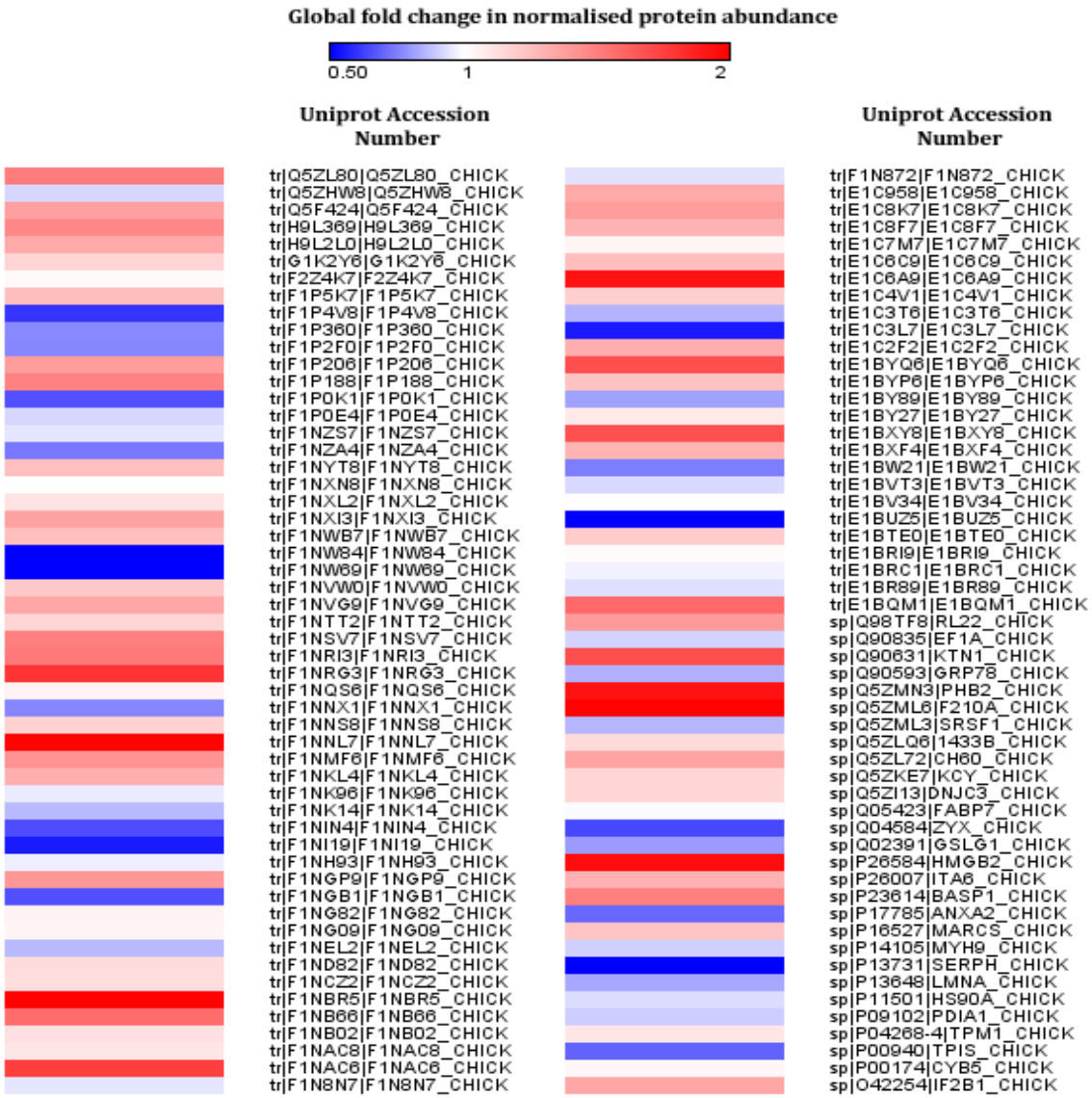


Figure 31 - Heat map generated using GENE-E software (Broad Institute), showing the fold change of 108 chicken proteins whose CV value between duplicate run was >0.2. Fold change was calculated by dividing average normalised protein abundance from pRTS-HVT miRNA transfected cells by average normalised protein abundance from pRTS-empty transfected cells. Uniprot accession numbers are displayed next to the colour representing the amount fold-change of that protein in the presence of HVT miRNAs.

Only 108 of the original 362 proteins produced a CV value of less than 0.2. This highlights the fact that there was a great deal of natural variation in protein abundance between duplicate runs. When this was presented to Dr Dong Xia he utilised the Progenesis LC-MS software (Nonlinear Dynamics) to perform power test analysis. This analysis is useful in designing future experiments as it predicts the number of replicates needed (based on your current result) to ensure 80% of the data has a power greater than 0.8 (80% confidence).

The result of this test is shown in figure 32, it highlights that currently, with duplicate runs, only 34% of the average normalised protein abundances have a power greater than 0.8. Additionally it shows that in order to have greater than 80% of the average normalised protein abundances with a power greater than 0.8, 19 replicates would need to be run using the current methodology.

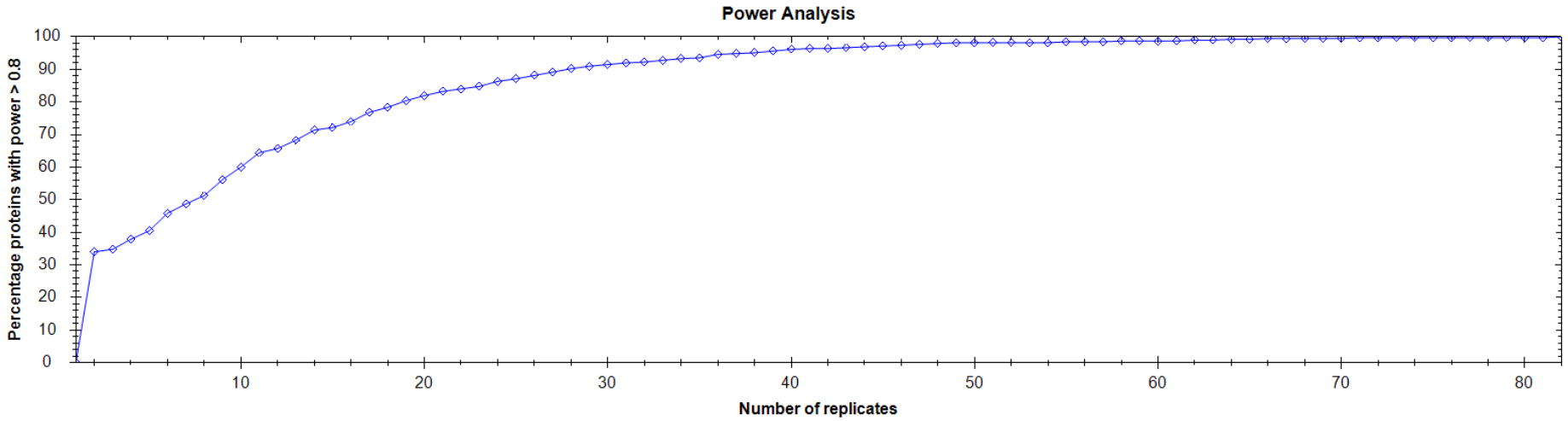


Figure 32 - Power analysis performed on the label-free proteomics experimental data, using Progenesis LC-MS software (Nonlinear Dynamics). Image provided by Dr Dong Xia.

4.2.7 Further analysis of the Proteomics Data

4.2.7.1 Using the proteomics data to validate earlier TargetScan custom predictions

Despite the potential problems with the experimental design and results of the label-free proteomics experiment, it is still informative to see if any of the targets predicted (by TargetScan Custom) to be targeted by HVT miRNAs (described in chapter 3.2) show a knock-down in protein abundance. Table 17 lists all of the proteins detected with at least 2 peptides, in the label-free proteomics experiments that were previously predicted to be targeted by HVT encoded miRNAs by TargetScan custom (section 3.2.2). The fold change in protein abundance is displayed, and immediately it is clear that not all of these predicted targets are showing a knock-down in protein level. Only 10 out of the 33 proteins show a knock-down of 10% or more, while 18 actually show an up-regulation of protein abundance of 10% or greater. Additionally only 2.74% (33/1204) of the total predicted targets of all HVT encoded miRNAs were detected with 2 or more peptides in the label-free proteomics.

Uniprot Accession Number	Gene Name	UniProt Description	Fold Change of Normalised Protein Abundance	HVT miRNAs predicted to Target Gene 3'UTR by TargetScan custom
tr|F1P4F4|F1P4F4_CHICK	SSR1	Uncharacterized protein OS=Gallus gallus GN=SSR1 PE=4 SV=1	0.545335153	H17
tr|E1C3L7|E1C3L7_CHICK	ASPH*	Uncharacterized protein OS=Gallus gallus GN=ASPH PE=4 SV=1	0.557969585	H16-3p
tr|F1NGG0|F1NGG0_CHICK	MYH10	Uncharacterized protein (Fragment) OS=Gallus gallus GN=MYH10 PE=4 SV=1	0.649395699	H17
tr|F1NSA8|F1NSA8_CHICK	RAP1A	Uncharacterized protein (Fragment) OS=Gallus gallus GN=RAP1A PE=1 SV=1	0.753467389	H7-5p
sp|Q5ZLC7|MARE1_CHICK	MAPRE1	Microtubule-associated protein RP/EB family member 1 OS=Gallus gallus GN=MAPRE1 PE=2 SV=1	0.77403397	H16-3p
tr|F1NPC3|F1NPC3_CHICK	P4HA1	Prolyl 4-hydroxylase subunit alpha-1 (Fragment) OS=Gallus gallus GN=P4HA1 PE=4 SV=1	0.811754179	H16-3p
sp|Q90593|GRP78_CHICK	HSPA5*	78 kDa glucose-regulated protein OS=Gallus gallus GN=HSPA5 PE=1 SV=1	0.850468265	H16-3p, H17
tr|F1NEV9|F1NEV9_CHICK	RAN	GTP-binding nuclear protein Ran (Fragment) OS=Gallus gallus GN=RAN PE=4 SV=1	0.854452686	H17
tr|F1NSP8|F1NSP8_CHICK	HNRNPU	Uncharacterized protein (Fragment) OS=Gallus gallus GN=HNRNPU PE=4 SV=1	0.855682104	H13
tr|Q5ZME1|Q5ZME1_CHICK	HNRNPA2B1	Uncharacterized protein OS=Gallus gallus GN=HNRNPA2B1 PE=2 SV=1	0.901738584	H5, H12-5p, H18-3p
tr|F1NG09|F1NG09_CHICK	PDCD6IP*	Uncharacterized protein OS=Gallus gallus GN=PDCD6IP PE=4 SV=1	1.04884096	H16-3p
tr|E1BZE6|E1BZE6_CHICK	HNRNPA3	Uncharacterized protein OS=Gallus gallus GN=HNRNPA3 PE=4 SV=1	1.051382495	H9-5p, H10, H14
tr|F1NW23|F1NW23_CHICK	CLTC	Uncharacterized protein (Fragment) OS=Gallus gallus GN=CLTC PE=4 SV=1	1.072961291	H7-5p, H8
sp|Q5ZMD1|1433T_CHICK	YWHAQ	14-3-3 protein theta OS=Gallus gallus GN=YWHAQ PE=1 SV=1	1.100766923	H17
sp|P12003-1|VINC_CHICK	VCL	Isoform 1 of Vinculin OS=Gallus gallus GN=VCL	1.118377571	H14
tr|H9L297|H9L297_CHICK	PURB	Uncharacterized protein OS=Gallus gallus GN=PURB PE=4 SV=1	1.171217544	H14
tr|F1N927|F1N927_CHICK	HMGB1	High mobility group protein B1 OS=Gallus gallus GN=HMGB1 PE=4 SV=1	1.201867937	H14, H17
sp|Q5ZIQ3|HNRPK_CHICK	HNRNPK	Heterogeneous nuclear ribonucleoprotein K OS=Gallus gallus GN=HNRNPK PE=2 SV=1	1.21623206	H17
sp|P16527|MARCS_CHICK	MARCKS*	Myristoylated alanine-rich C-kinase substrate OS=Gallus gallus GN=MARCKS PE=1 SV=2	1.236509972	H7-5p, H10, H15, H16-5p, H17, H18-3p
tr|F1NLM4|F1NLM4_CHICK	RHOA	Uncharacterized protein (Fragment) OS=Gallus gallus GN=RHOA PE=3 SV=1	1.32700178	H17
tr|F1NXI3|F1NXI3_CHICK	DDX5*	Uncharacterized protein OS=Gallus gallus GN=DDX5 PE=3 SV=1	1.371671238	H16-3p
tr|E1C1Q2|E1C1Q2_CHICK	MAP1B	Uncharacterized protein OS=Gallus gallus GN=MAP1B PE=4 SV=1	1.378065143	H14
tr|E1C8K7|E1C8K7_CHICK	EIF5B*	Uncharacterized protein OS=Gallus gallus GN=EIF5B PE=4 SV=1	1.396596548	H7-5p, H9-5p, H17, H18-5p
tr|F1N8C2|F1N8C2_CHICK	CNBP	Cellular nucleic acid-binding protein OS=Gallus gallus GN=CNBP PE=4 SV=1	1.446261481	H7-5p
tr|F1NHE0|F1NHE0_CHICK	STAU1	Uncharacterized protein (Fragment) OS=Gallus gallus GN=STAU1 PE=4 SV=1	1.450206022	H5
tr|F1NSV7|F1NSV7_CHICK	GLS*	Uncharacterized protein OS=Gallus gallus GN=GLS PE=3 SV=1	1.509664517	H16-3p
sp|P23614|BASP1_CHICK	BASP1*	Brain acid soluble protein 1 homolog OS=Gallus gallus GN=BASP1 PE=2 SV=4	1.509918339	H17
tr|F1NKN0|F1NKN0_CHICK	CCT5	Uncharacterized protein (Fragment) OS=Gallus gallus GN=CCT5 PE=3 SV=1	1.546560544	H16-3p
sp|P21566|COF2_CHICK	CFL2	Cofilin-2 OS=Gallus gallus GN=CFL2 PE=1 SV=2	1.713874113	H16-3p
sp|Q5ZKC9|1433Z_CHICK	YWHAZ	14-3-3 protein zeta OS=Gallus gallus GN=YWHAZ PE=2 SV=1	1.736474699	H10, H11
tr|F1P0H9|F1P0H9_CHICK	COL1A2	Collagen alpha-2(I) chain OS=Gallus gallus GN=COL1A2 PE=4 SV=1	1.896448214	H10
tr|F1NBR5|F1NBR5_CHICK	CTGF*	Uncharacterized protein (Fragment) OS=Gallus gallus GN=CTGF PE=4 SV=1	2.600130415	H18-5p
sp|Q90WD0|ARP3_CHICK	ACTR3	Actin-related protein 3 OS=Gallus gallus GN=ACTR3 PE=2 SV=1	2.732100066	H7-5p

Table 17 - List of all proteins that were both; predicted to be targeted by HVT miRNAs by TargetScan custom (chapter 3) and identified by at least 2 peptides in the label-free proteomics experiment (chapter 4). The fold change in normalised protein abundance in cells transfected with pRTS-HVT miRNA construct compared with pRTS-empty construct is shown. Also shown are the HVT miRNAs that were predicted to be targeting the specific protein genes. * represents the proteins that has a CV value <0.2 between duplicate runs (see section 4.2.6.1).

4.2.7.2 Comparison of gene ontology of proteomic highlighted targets of HVT miRNAs and TargetScan custom predicted targets

Panther Classification System (http://www.pantherdb.org/) (Mi et al. 2013) was used as described in section 3.2.2.1, to highlight which biological processes the proteins that showed at least a 10% knock-down are involved in. Figures 33 and 34 represent the data from this gene ontology analysis. The pie chart in figure 33 displays the 'top' headings for each of the biological process terms, which as described previously have further sub-headings (listed in table 19, section 8.5), and the distribution of involvement in these processes by the knocked-down proteins. Figure 34 shows the P-values generated for specific biological process terms following the statistical overrepresentation test in Pantherdb, this compares the number of proteins involved in biological processes from your sample (as a percentage) to the involvement of all chicken proteins in these biological processes.

The pie chart generated by the proteins knocked-down in the proteomics experiment is slightly different to the pie chart of biological processes predicted to be targeted by HVT miRNAs in figure 14 (section 3.2.2.1). There are two fewer biological processes highlighted in figure 33, however "metabolic process" and "cellular process" remain the most targeted biological processes, as they were in the predicted targets by TargetScan custom.

The statistical over representation analysis, of the biological process gene ontology on proteins knocked-down in the proteomic experiment (figure 34) was quite different from the same analysis on TargetScan custom predicted targets (figure 15, section 3.2.2.1). The most striking difference is the number of biological processes that created a P-value<0.05, analysis of the associated biological processes of the knocked-down proteins produced only 9 biological processes. The highest of these being 'translation' which produced a P-value of 7.26E-06, suggesting that proteins involved in translation were preferentially knocked-down in the presence of the HVT miRNAs, in this experiment. Of the 9 biological processes producing a P-value<0.05 in the proteomics study, only three produced a P-value<0.05 from the list of predicted miRNA targets from TargetScan custom (figure 15).

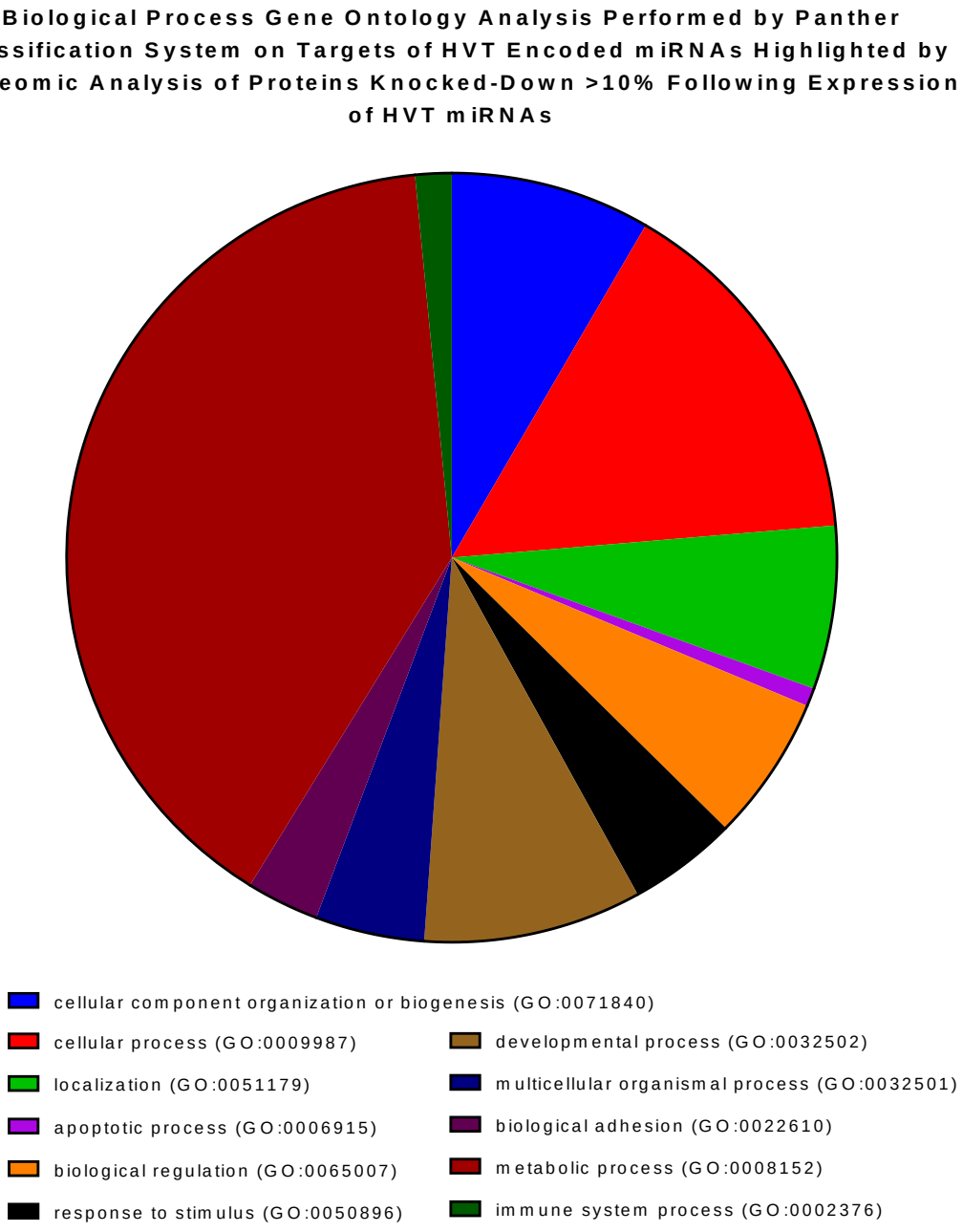


Figure 33 - Biological process gene ontology analysis of proteins with a greater than 10% knock-down in the proteomic analysis following overexpression of HVT encoded miRNAs. Analysis was performed by Panther Classification System (www.pantherdb.org).

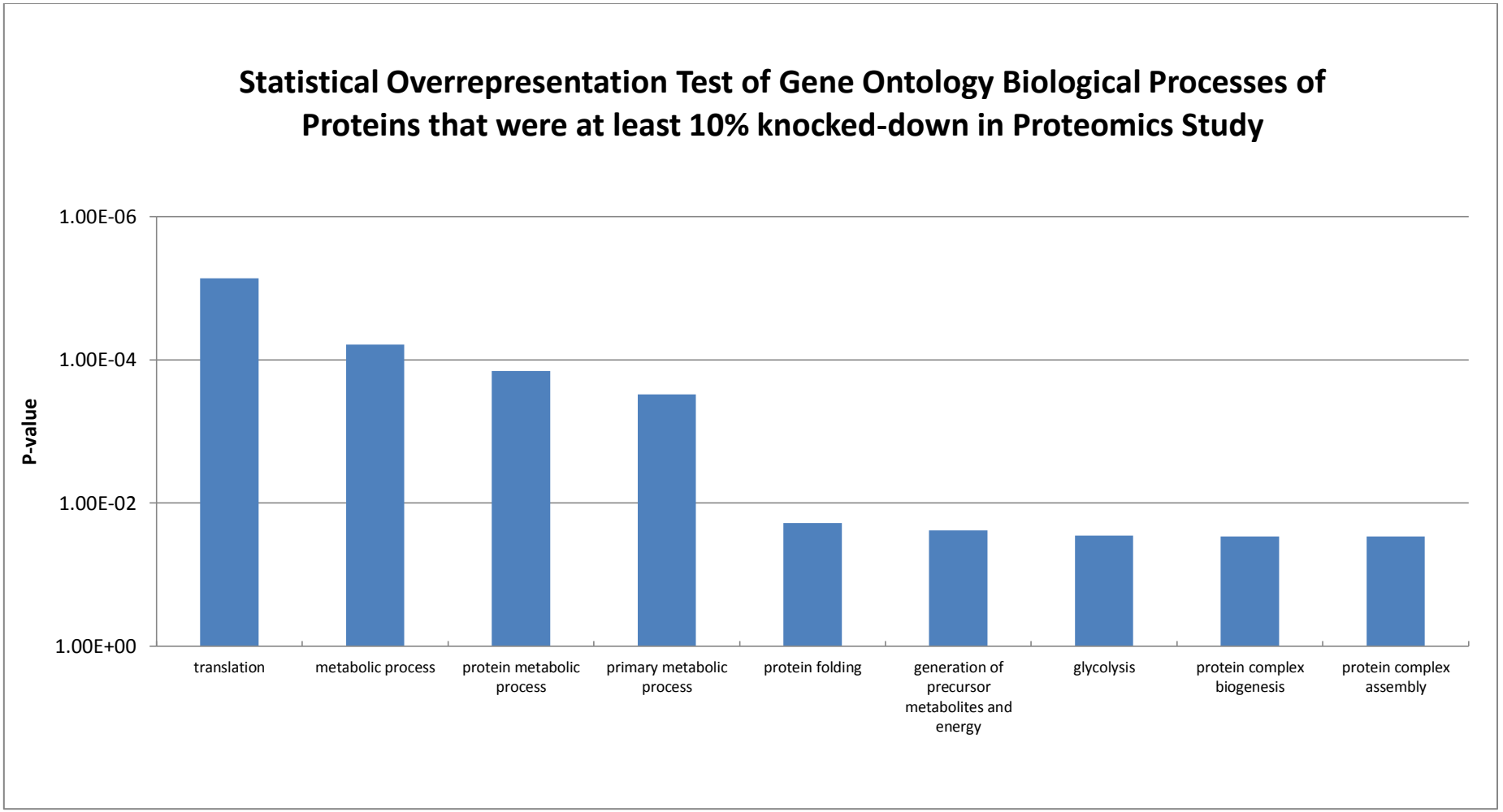


Figure 34– Bar chart to show the results of the statistical overrepresentation analysis performed by Pantherdb on biological processes of HVT miRNA targets from proteomic analysis, to determine if the frequency of predicted targets involved in certain biological processes, is significantly above background levels.

4.3 Discussion

4.3.1 Creating cell line to examine proteome changes induced by viral miRNA expression

Before changes in host proteins induced by viral miRNAs could be explored, a method of reliable viral miRNA expression in cells had to be established. Originally this project aimed to look for changes between chick embryo fibroblasts (CEF) infected with pHVT3 BAC virus and CEF infected with pHVT3 BAC-double miRNA copy knockout virus. However this was decided against, as viral infection of cells causes a great deal of stress, which could result in large changes in protein expression that might not be repeatable between the regular BAC and the miRNA knockout BAC. Therefore creation of an expression construct in which the expression of the viral miRNAs could be kept under control, and transfected cells selected for using antibiotics until a high percentage of cells contained the miRNA expression construct, was opted for.

The system used involved the pRTS-SVP-Tom vector which contains a doxycycline inducible bi-directional promoter that drives expression of the tomato fluorescent protein and also any product inserted in the adjacent cloning site. By inserting the HVT miRNAs into this site it was hoped that this would create a tightly controlled system of viral miRNA expression, which would additionally give a visual indicator of expression. The two-step cloning of the pRTS-HVT miRNA construct, via the pCR-XL TOPO sub-cloning vector proved to be relatively simple, and upon sequencing no mutations were found within the pre-miRNA sequences of the miRNAs. Viral miRNA expression was examined from two clones (6 and 7) of the pRTS-HVT miRNA construct by looking at the expression levels of *hvt-miR-H15* relative to DF-1 cells transfected with pRTS-empty vector. *hvt-miR-H15* was chosen as the miRNA to test expression of the cassette as the probe and primer set were immediately available, it also seemed to be an appropriate miRNA to test expression of the cassette as it was towards the end of the cluster of miRNAs.

Expression of *hvt-miR-H15* was confirmed in doxycycline induced, pRTS-HVT miRNA construct transfected DF-1 cells. Surprisingly however, there was expression of *hvt-miR-H15* in the uninduced pRTS-HVT miRNA vector transfected DF-1 cells. Further analysis suggested this expression was a result of a combination of 'leakiness' of the inducible promoter and the presence of an internal promoter within the 4.6kb fragment containing the HVT. This meant that for the proteomic analyses it was unsuitable to compare induced and uninduced, instead empty vector induced was compared to pRTS-HVT miRNA induced. This did have the benefits however, as that any changes in protein abundance brought about by either the addition of doxycycline or expression of the tomato fluorescence protein to the cells was cancelled out, however it was no longer possible to perform a time course analysis of the changes in protein abundance.

Expression of all HVT miRNAs was confirmed using miRNA microarray from RNA extracted from pRTS-HVT miRNA stably transfected cells. There were differences in the expression levels of different viral miRNAs, which could be down to a number of factors, for example strength of hybridisation of miRNA with the probe or stability of the miRNA following expression, but there didn't appear to be any particular section of the HVT miRNA cassette that was not being expressed. Based on these observations it was clear that the viral miRNAs were being expressed at a suitably differential level between empty vector and HVT miRNA vector that this system could be used to determine the effects of the viral miRNAs at the protein level, using proteomics.

No comparison was performed to compare the levels of viral miRNAs in the induced, pRTS-transfected DF-1 cells and miRNA levels in cells infected with virus, via microarray. This would have been useful, to determine if the viral miRNA levels were representative of levels in infected cells. The problem faced is that HVT virus is cultured within chicken embryo fibroblasts (CEF) cells which, from experience, show much lower levels of transfection (and require a different method) compared to DF-1 cells. This meant that a meaningful comparison of viral miRNA levels following transfection and infection within the same cell type is extremely difficult, if not impossible. The issue of whether or not the expression

levels are representative of genuine infection is not resolved here, however this is a pitfall for many miRNA target studies. Had the proteomic work proved more fruitful it would have been vital to validate the targets further in infected cells (with physiologically relevant levels of viral miRNAs), using other biochemical methods.

4.3.2 Changes in host-cell proteome as a result of viral miRNA targeting

Upon validation of viral miRNA expression, cell line samples were sent for proteomic analysis. Large amounts of sample were produced from both empty vector and miRNA vector transfected cells, which then were safely despatched to Liverpool. Prior to dispatch RNA taken from excess sample was used to confirm HVT miRNA expression from this exact batch of samples.

There were no concerns about viral miRNA expression in the samples and by allowing the samples to be prepared in Liverpool from the cell pellet this would remove the likelihood of unexperienced operator errors during sample preparation. All of the mass spectrometry work and analysis was performed at the Institute of Integrative Biology at the University of Liverpool, as this central facility has the equipment and expertise required to perform such an analysis. The proteomic analyses were performed in duplicate on each sample.

As described in section 4.2.6 proteomic analysis had initially intended to have been performed over a time course. The expression of viral miRNAs in uninduced cells, made this analysis impossible as it was clear that at least some viral miRNAs were being constitutively expressed. The initial analysis of changes in protein abundance, between pRTS-empty and pRTS-HVT miRNA transfected DF-1, performed by Progenesis LC-MS (Nonlinear Dynamics) software (not shown) based the global normalisation of protein abundance on expression levels of all peptides. This normalisation produced an unrealistic picture that nearly all proteins were down regulated (many to levels great than 95%). An update of the Progenesis LC-MS software allowed the normalisation of protein abundance to be performed against a selection of identified peptides, after mass spectrometry runs were aligned. This provided quite a different picture of changes in protein abundance, one that showed a range of both

up- and down-regulation in the abundance of proteins and none showing a greater than 90% reduction (figure 31).

The result from the proteomics work was subjected to further analysis, including CV and power analysis. The CV analysis is a measure of the variability of the two replicates from the proteomics analysis, and ideally replicates should score a CV value <0.2. Analysis of the sample replicates in this experiment revealed that the lowest median CV score was 0.149 (between replicates of 48 hour pRTS-empty transfections). Since this was only the median score it highlights the problem that nearly half of the proteins are showing too much variability between replicates, making it hard to deduce any meaningful changes in protein abundance. Problems with the experimental design were also highlighted from the power analysis performed by Progenesis LC-MS software, which suggested that with the level of variability seen in these samples, 19 replicates would needed before 80% of the average normalised protein abundances would have a power greater than 0.8, which is considered necessary to draw relevant conclusions from the data.

4.3.3 Examining proteomics data for correlation with luciferase validation data of TargetScan custom data

Despite the apparent problems with the lack of reproducibility between replicates in the proteomics data, it did seem worthwhile to compare the results from the proteomics experiment with the TargetScan custom miRNA target predictions. RAP1A, which was validated as a target for *hvt-miR-H7* by both luciferase assay and western blot following prediction of an interaction by TargetScan custom, was also down-regulated in the proteomic study. However this down-regulation was to a greater extent than observed in the western-blot analysis and the variability between the two pRTS-empty DF-1 cells replicates produced a CV score greater than 0.2 (0.373 compared to a CV value between pRTS-HVT miRNA replicates of 0.00379), both reasons to be cautious of this result.

4.3.4 Analysis of comparative gene ontology study

Comparing the biological processes gene ontology of the proteins found down-regulated in the proteomics study and comparing it to the gene ontology of TargetScan custom predicted targets of the HVT miRNAs highlighted both similarities and differences. The most obvious difference is the number of genes/proteins submitted for analysis, only 76 of the 155 proteins showing at least 10% knock-down found a match in the PANTHER classification system compare to 883 from the TargetScan predicted targets. This difference in the number of IDs submitted to PANTHER for classification can probably explain the differences in the statistical overrepresentation analysis. What is of interest is the targeting of biological processes by viral miRNAs in both the predicted targets and proteins knocked down in the proteomics experiment, especially the biological process 'translation'. Any evidence of regulation of translation by the viral miRNA supports the widely regarded idea that viruses are using miRNAs to manipulate the environment within the host to suit their needs (Sarnow et al. 2006).

4.4 Conclusion

The main purpose of using this approach in this project was to provide an opportunity to demonstrate viral miRNA targeting of genes that resulted in knock-down of protein abundance. Using alternative approaches some targets of viral miRNAs were identified, with the targeting of the viral miRNAs creating a decrease in protein abundance, however to demonstrate this decrease in protein abundance in this manner requires the availability of chicken-reactive antibodies, something which cannot be taken for granted. Using proteomics to first demonstrate a change in the protein level, then 'working-back' to figure out which viral miRNA is responsible for the change this problem can be circumvented.

At the time of writing, this was the first example using label-free quantitative proteomic to identify targets of viral encoded miRNAs. Other studies have used the similar technique of pulsed stable labelling with amino acids in cell culture (pSILAC) to identify targets of KSHV miRNAs in conjunction with microarray analysis to observe changes in mRNA levels as well (Gallaher et al. 2013).

The observations discussed in this section suggests there is some merit in a proteomics based approach to highlight targets of virally encoded miRNAs, but also emphasises the importance of producing repeatable results before making solid conclusions.

5 What effect does the deletion of miRNAs have on HVT and MDV-2?

5.1 Introduction

So far this study has focussed on identifying the mRNA targets of the virally encoded miRNAs of HVT and MDV-2. This 'bottom-up' approach has provided an insight into the roles played by these viral miRNAs; however this work has required the over-expression of miRNAs in cell-lines that are different from the natural target of infection of these viruses. Similar approaches have been used in the identification of targets of other virally encoded miRNAs; however there is evidence that any targets identified in this manner might not be genuine, as overexpression of miRNAs, more than physiological levels could be saturating the RISC complexes and inhibiting endogenous miRNAs (Thomson et al. 2011).

This part of the project describes a broader look at the role played by the virally encoded miRNAs, by observing the effects of removal of the miRNAs on virus infection and replication.

5.1.1 BAC mutagenesis

In order to carry out this study, miRNA-deleted viruses were generated and then compared with parental intact BAC-derived virus containing miRNAs. As mentioned previously bacterial artificial chromosome (BAC) clones of both the MDV-2 SB-1 strain virus, named pSB-1 BAC 3 (Petherbridge et al. 2009) and HVT FC126 strain virus, named pHVT-3 (Baigent et al. 2006) have been generated. BACs are fertility (mini-F) factor-based plasmids that are capable of stable replication at low copy number in *E. coli*. Furthermore the use of BAC technology has allowed the manipulation and analysis of various herpesvirus genes, advancing our understanding of herpesviruses (Feederle et al. 2010). BAC clones allow for efficient manipulation of the viral genome in bacterial culture via BAC mutagenesis and this was used to delete the viral miRNAs. The structure of both the HVT and MDV-2 genomes are similar, in that they contain internal and terminal repeat long and short regions and also unique short and unique long regions. In both HVT and MDV-2 the viral miRNAs are found in these repeat regions of the virus genome, this meant that the deletion of the miRNAs required a two-step deletion approach to ensure

that there was no miRNA expression. Deletion in both steps was via homologous recombination; this required inserting an antibiotic resistance cassette in place of the miRNAs in the viral genome. Clones in which the miRNAs were replaced by the antibiotic resistance cassette became apparent under positive selection with the appropriate antibiotic pressures. The strategy used in this study is outlined in figure 35, and the locations of the miRNAs within the HVT genome can be seen in figure 1.

5.1.2 The effect of miRNA deletion on virus infection and replication

Besides differences in oncogenicity between MDV-1, MDV-2 and HVT (described briefly in section 1.1.2), other studies have described individual phenotypic features of both the HVT and MDV-2 viruses. Specific features of HVT include the ability to produce cell-free virus in cell culture and its ability to infect chicken embryos, both of which are beneficial to its role as a vaccine allowing the production of freeze dried cell-free vaccine or vaccination of chicks in ovo, respectively (Baigent et al. 2006). MDV-2 also has specific features compared to MDV-1 including enhancement of lymphoid leukosis (Bacon et al. 1989), persistence in transformed B cells (Fynan et al. 1992) and reticuloendotheliosis (Aly et al. 1996). These different phenotypes of the vaccine viruses have yet to be mapped to MDV-2 or HVT specific genes, which prompted Yao et al to suggest the differential expression of miRNAs from these viruses could, in part, be behind these features (Yao et al. 2007).

Other investigations have been performed to determine the importance of viral miRNAs in different viruses; in both MDV-1 (Y. Zhao et al. 2011) and EBV (Feederle et al. 2011) the loss of certain clusters of miRNAs has been shown not to be terminal to virus replication, but does remove or potentiate the transforming ability of the viruses. These studies provided a basis for the observations in this study, it was therefore predicted that the miRNA-deletion viruses would still replicate in cell culture, however the kinetics of viral infection in birds might differ, which could in turn be attributed to roles played by miRNAs.

Both of these previous studies have been performed using oncogenic viruses, therefore it was not clear what the deleted phenotype could be in this study. As both HVT and MDV-2 are vaccine viruses, if

there was a drop in the protection, against the oncogenic MDV-1, it could suggest that the miRNAs are responsible for ensuring a favourable environment for vaccine virus replication, needed to provide protection when birds are infected with the oncogenic MDV-1. Analyses on the levels of MDV-1 and vaccine virus at the end of the trial provide an additional insight to effects of miRNA deletion on virus growth and replication.

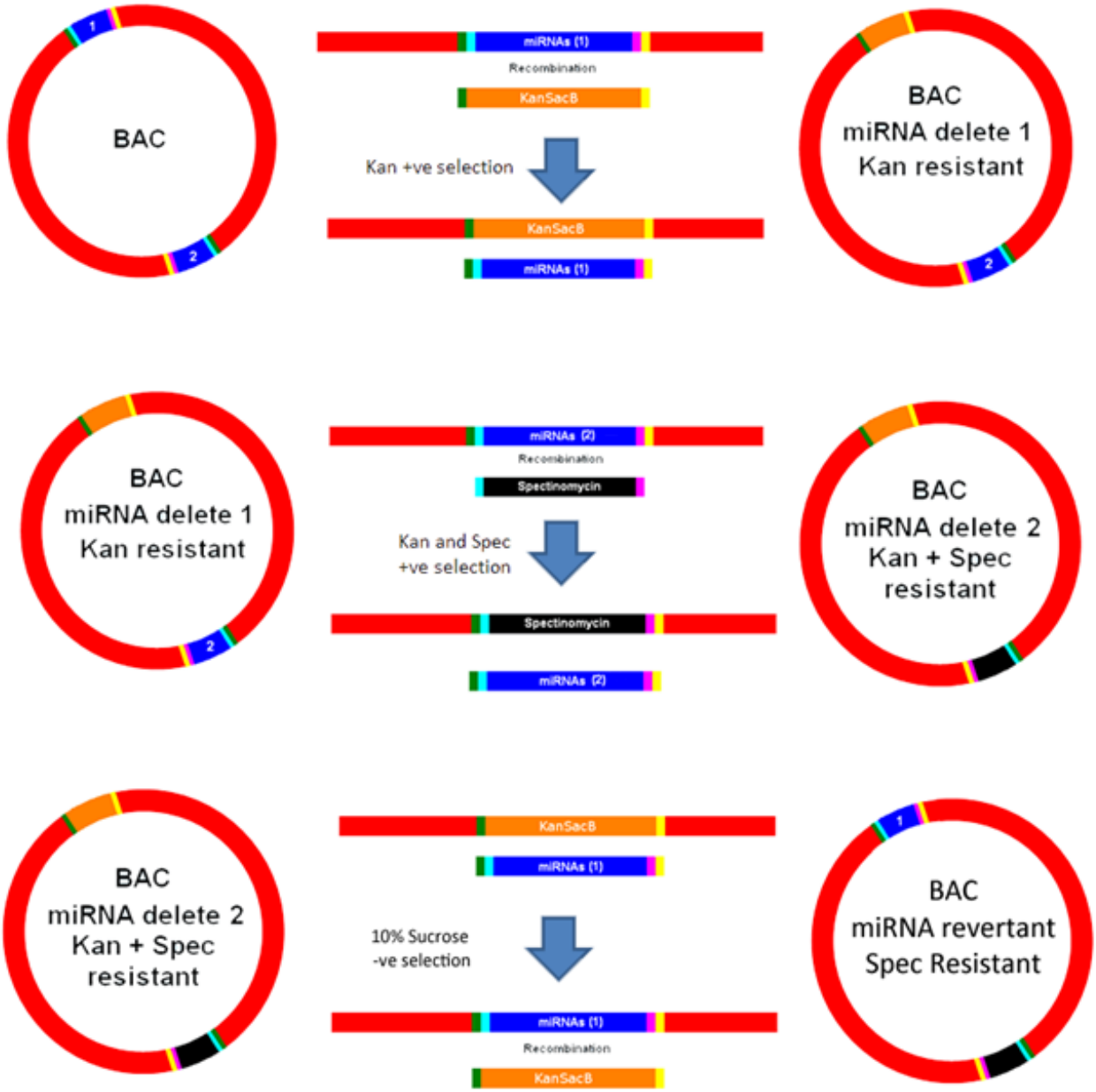


Figure 35 - Overview of the BAC mutagenesis strategy. Note the different colours representing the different regions of homology utilised for each homologous recombination event.

5.2 Results

5.2.1 Creating miRNA deletion HVT and MDV-2 BAC clones

5.2.1.1 First miRNA copy deletion

As discussed in section 5.1.1 the viral miRNAs sit within a repeat region of the viral genome, therefore in order to remove miRNA expression both copies were deleted. For the first deletion the KanSacB cassette was inserted in the BAC DNA clones of the viruses, in place of the miRNAs. This cassette consists of the kanamycin resistance gene coupled with the *sacB* gene from the *H. pylori flagellin* promoter, resulting in positive clones sensitive to sucrose and resistant to kanamycin.

Section 2.3.34.1 describes the methodology used to create the single-copy miRNA knockout of both the HVT and MDV-2 BAC viruses. The DNA from the 6 clones was analysed by restriction digest, using *EcoR*I for pSB-1 BAC3 and *BamH*I for pHVT3, to check that the purified DNA showed a similar restriction pattern to the wild-type BAC. Figure 36 shows that the digestion patterns of both the pHVT3 (*BamH*I digestion) and pSB-1 BAC3 (*EcoR*I digestion) clones are extremely similar to those of their respective parental BAC DNA in the adjacent lanes. This observation indicates that there has been no major rearrangement of the BAC DNA during recombination.

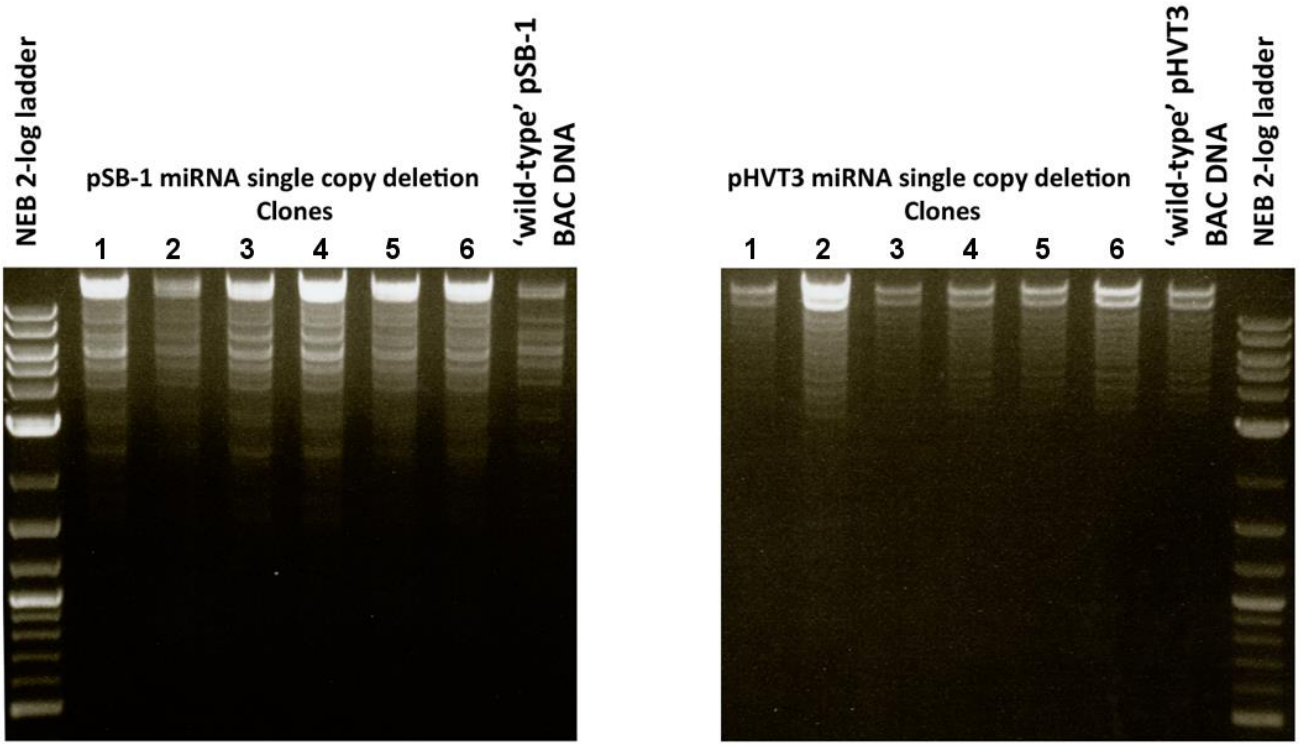


Figure 36 - Restriction digests of both pSB-1 BAC3 (*EcoRI*) *and* pHVT3 (*BamHI*) single-copy miRNA deletion BAC DNA extracted from bacterial clones (1-6).

5.2.1.1.1 Testing sucrose sensitivity of clones

After restriction digest analysis of clones, to confirm that they firstly contained BAC DNA and also that the BAC DNA had no major rearrangements, it was important to ensure that the *SacB* portion of the KanSacB cassette was functional. The *SacB* gene makes the EL250 cells sensitive to sucrose, and therefore acts as a negative selection tool to create a single copy revertant later. Functionality of the *SacB* gene was tested as described in section 2.3.34.1.5 and table 18 shows that for 2/6 pHVT3 miRNA single-copy deletion clones the *SacB* gene was not functioning, this was true for only 1/6 of the pSB-1 BAC3 miRNA single-copy deletion clones. On the remaining plates there was a definite sensitivity to the sucrose, and the clone from both pHVT3 and pSB-1BAC3 miRNA single-copy deletions that produced the fewest number of colonies was chosen to be used for the downstream recombination steps.

	Number of colonies present on 10% sucrose LB agar plate	
Clone Number	**pSB-1 ΔmiR-1**	**pHVT3 ΔmiR-1**
1	4	10
2	6	lawn
3	6	3
4	lawn	8
5	1	20
6	12	lawn

Table 18 - Table showing the number of colonies present on each plate following overnight incubation of pHVT miRNA single-copy deletion (pHVT3 ΔmiR-1) and pSB-1 BAC3 miRNA single-copy deletion (pSB-1 BAC3 ΔmiR-1) clones. Lawn indicates that colonies were greater than 500 and too close together to accurately count.

5.2.1.2 Second miRNA copy deletion

The second-copy of the miRNAs was deleted from the BAC viral genome by the insertion of a spectinomycin resistance cassette via homologous recombination. Section 2.3.34.2 describes the methodology used to create the double-copy miRNA knockout of both the HVT and MDV-2 BAC viruses from the previously generated single-copy knockouts. Glycerol stocks and BAC STET minipreps were performed as before and clones analysed briefly by restriction digest, as before, shown in figure 37.

Clones 2 and 3 from pSB-1 BAC3 and clone 3 from pHVT3 digest in a similar manner to the parental BAC DNA, and were therefore taken forward in this study.

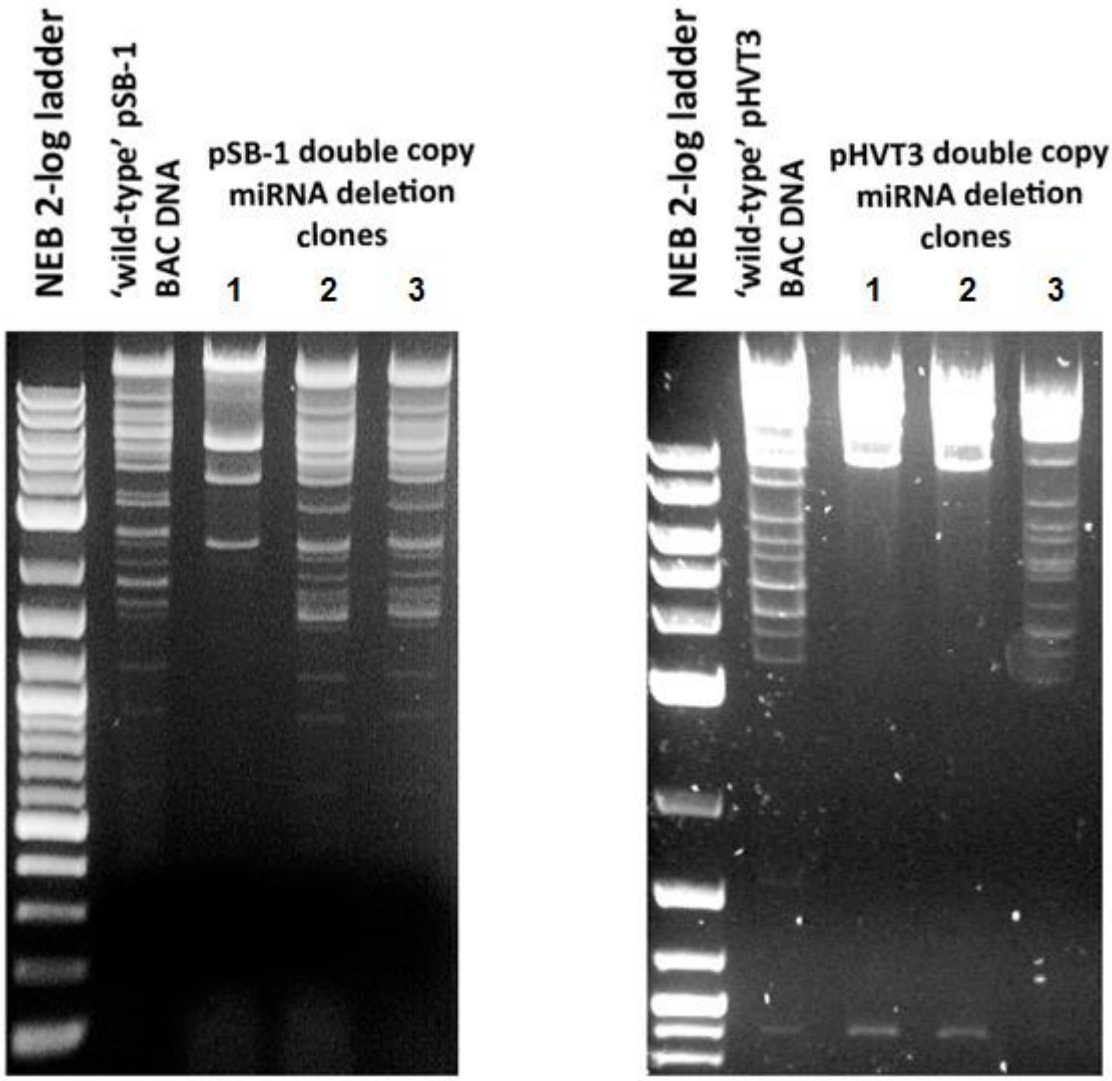


Figure 37 -Restriction digests of both pSB-1 BAC3 (*EcoRI*) and pHVT3 (*BamHI*) double-copy miRNA deletion BAC DNA extracted from clones (1-3) analysed alongside parental (described a 'wild-type') BAC DNA.

5.2.2 Further analysis of miRNA-single and –double copy miRNA deletion BAC clones

The restriction digests of the miRNA deletion BAC viral genomes only provided the information that there had been no major rearrangements in the BAC clones. Having reached the point where both the single and double copy-miRNA deletions had been generated for both pHVT3 and pSB-1 BAC3, it was decided the clones should be analysed further.

5.2.2.1 Fluorescent imaging of CEF transfected with BAC-miRNA deletion clones

In order to determine if the miRNA deletion BAC DNA clones were still capable of infecting cells *in vitro* the clones were transfected using lipofectamine transfection reagent in duplicate wells of CEF, as described in the methods (section 2.3.28). Following transfection the cells were cultured at 38.5°C, 5% CO_2 for four to five days, after incubation the cells were fixed in the culture plate using acetone: methanol prior to immunofluorescent staining, as described in the methods (section 2.3.29). Staining of the pHVT3 BAC clone transfected CEF was performed using HVT polyclonal serum (primary) and anti-chicken IgG heavy and light chains Alexa Fluor® 488 (secondary) (Life Technologies) both at dilutions shown in table 12 section 2.3.35. Staining of the pSB-1 BAC3 clone transfected CEF was performed using Y5.9 MDV2-specific monoclonal (primary) (L. F. Lee et al. 1983) and anti-mouse IgG heavy and light chains Alexa Fluor® 488 (Life Technologies) (secondary) dilutions shown in table 12, section 2.3.35.

Figure 38 shows that plaques formed in both the single- and double-copy miRNA deletions of the BAC viral genomes, compared with the wild-type BACs, for both pHVT3 and pSB-1 BAC3. Figure 38 only demonstrates a small region of the plate, but in all cases fluorescent staining was visible throughout the well, indicating that the deletion of the miRNAs from the BAC clones had not removed the ability to infect CEF *in vitro.*

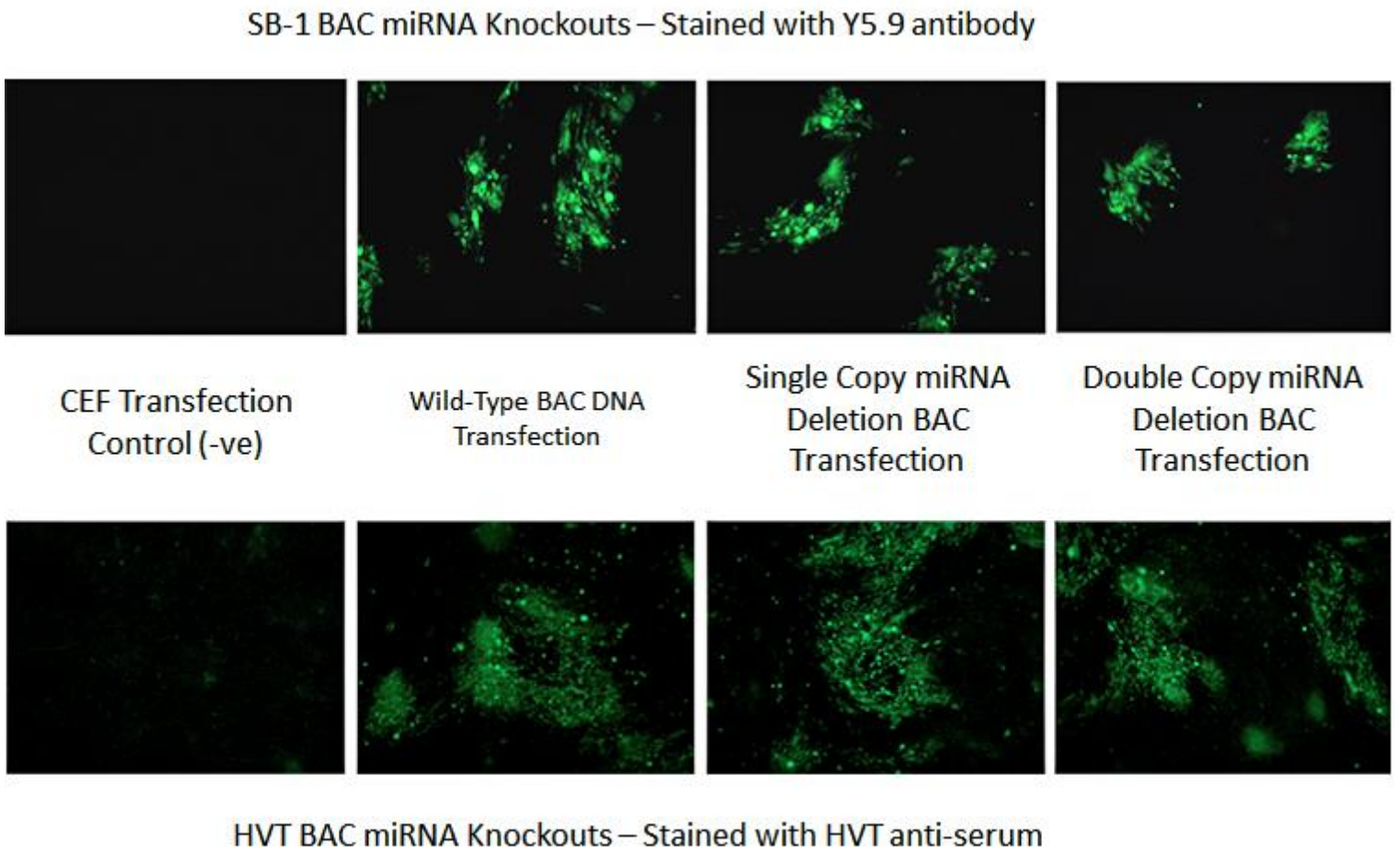


Figure 38–Fluorescent images of CEF transfected with DNA of different miRNA deletion BAC clones after fixing with ice-cold acetone:methanol and staining with either serum from HVT vaccinated birds (HVT BAC transfected CEF) or anti-MDV-2 Y5.9 monoclonal antibody (SB-1 BAC transfected CEF) followed by an Alexa Fluor® 488 secondary antibody.

5.2.3 Generation of single-copy miRNA revertant BAC clones

As an additional control virus, prior to beginning any animal studies to observe the effect of miRNA deletion on the BAC viral genomes, a revertant BAC clone was generated containing a single copy of the miRNAs. A single copy revertant was created as the reinsertion of the miRNAs that were removed using the KanSacB cassette could be readily detected due to the negative selection pressure of sucrose on the *SacB* gene. However there was no negative selection pressure on the spectinomycin cassette, therefore finding a clone in which the viral miRNAs had been swapped back (trying to create a double-copy revertant) would be nearly impossible.

The methods used to generate multiple colonies of possible pHVT3 and pSB-1 single-copy miRNA revertants are described in section 2.3.34.3. For pSB-1 BAC3 single-copy revertant colonies 26/48 colonies appeared to have lost kanamycin and therefore 8 colonies were inoculated were grown overnight for BAC STET miniprep purification and restriction digest analysis. For the pHVT3 single-copy revertant colonies 0/48 of the picked clones had lost kanamycin resistance therefore 96 more colonies were screened for loss of kanamycin resistance. Only 1/96 of these colonies had lost kanamycin resistance but nonetheless this colony was inoculated and incubated as above for analysis.

5.2.3.1 Further analysis of positive colonies that had lost kanamycin resistance

DNA from the 8 colonies from the pSB-1 BAC3 single-copy miRNA revertant and the single colony from pHVT3 single-copy miRNA revertant was purified from the overnight cultures, following the preparation of a glycerol stock, by BAC STET miniprep as described in the methods (section 2.3.4). Restriction digest analysis was performed as before on the different clone STET minipreps (*EcoR*I digestion pSB-1, *BamH*I digestion pHVT3). All 8 of the pSB-1 BAC3 single-copy miRNA revertants and the single pHVT3 single-copy miRNA revertant produced a similar digestion pattern to the parental corresponding BAC viral genome (not shown).

Two colonies were selected from the pSB-1 BAc3 single-copy miRNA revertant clones and, along with the single pHVT3 single-copy miRNA revertant clone, transfected into duplicate wells of a six-well plate

seeded 24 hours previously with CEF, using lipofectamine transfection reagent (Invitrogen) as described in methods (section 2.3.28). Following transfection the cells were cultured at 38.5°C, 5% CO_2 for four to five days before either being fixed for immunofluorescent staining or harvested for RNA extraction and miRNA TaqMan gene expression analysis, in the manner described in section 5.2.2.1.

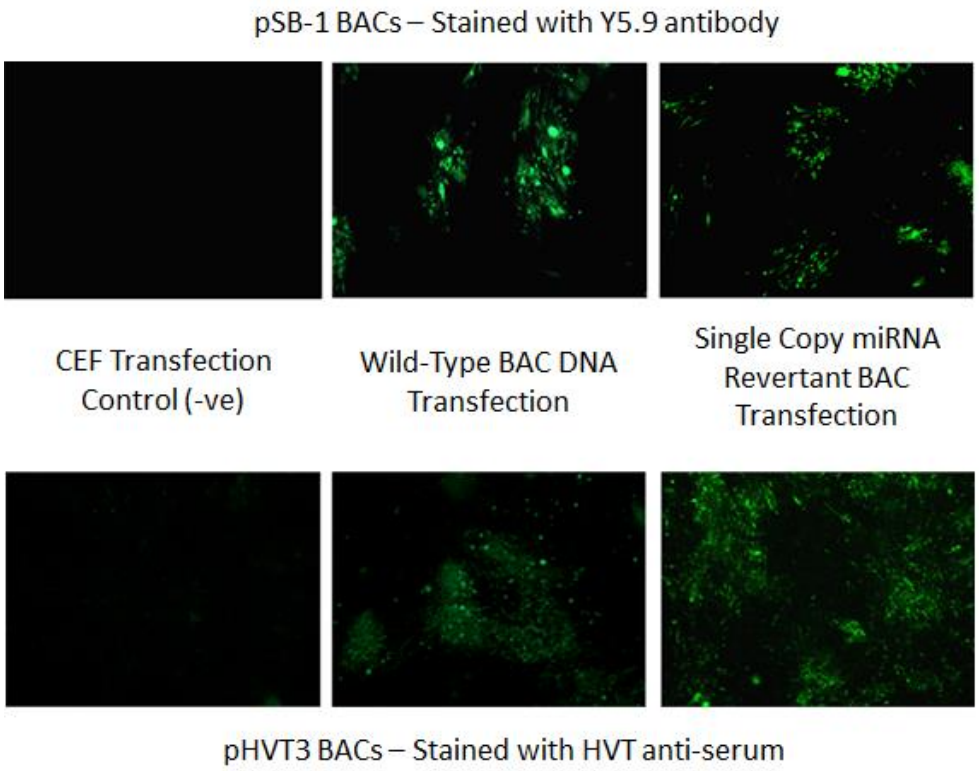


Figure 39– Fluorescent microscope images of CEF transfected with either parental or single-copy miRNA revertant pHVT3 or SB-1 BAC3 clones after fixing with ice-cold acetone:methanol and staining with either serum from HVT vaccinated birds (HVT BAC transfected CEF) or anti-MDV-2 Y5.9 monoclonal antibody (SB-1 BAC transfected CEF) followed by an Alexa Fluor® 488 secondary antibody.. Negative control image of mock transfected CEF is visible in the left-hand panes.

The fluorescent cell images in figure 39 demonstrate that both the pHVT3 and pSB-1 BAC3 single-copy miRNA revertant clones are capable of producing virus that is stained by the respective virus specific antibody. This confirmed that the recombination event that has occurred, the replacement of the KanSacB cassette with the miRNA encoding sequence, did not dramatically alter the BAC viral genome, preventing infection of CEF.

5.2.3.2 TaqMan analysis of miRNA expression from miRNA-deletion BAC clones

To ensure that the regions containing the miRNAs had been removed from the BAC viral genomes, when the antibiotic resistance cassettes had been inserted during homologous recombination, miRNA TaqMan analysis was performed to confirm that viral miRNA expression could not be detected in CEF transfected with the double-copy miRNA deletion BAC clones.

Cells were harvested from cells transfected with BAC DNA 4 days previously and RNA extraction was performed using miRNeasy mini kit (Qiagen) following manufacturer's protocol. RNA was finally eluted in 50µl RNase-free water and stored immediately at -80°C. miRNA TaqMan was performed as described in the methods (section 2.3.14), using *hvt-miR-H15* and *mdv2-miR-M17* probe and primer sets to determine expression of pHVT3 and pSB-1 miRNAs, respectively, in the transfected CEF. Triplicate runs were performed for each sample, from two separate transfections per construct (totalling 6 runs per construct) and miRNA expression levels were calculated relative to the miRNA levels from the 'wild-type' BAC virus. Relative expression levels were normalised to levels of endogenous *gga-miR-let 7a* and calculated by 7500 Fast Software (Applied Biosystems) using relative quantification study analysis.

Figure 40 shows the relative expression levels of *mdv2-miR-M17* (40A) and *hvt-miR-H15* (40B) from CEF transfected with the corresponding BAC viral genome (wild-type, single-copy deletion, double-copy deletion and single-copy miRNA revertant). The important observation from this experiment was that in the pHVT3 and pSB-1 double-copy miRNA deletion transfected CEF, the miRNA expression levels were virtually undetectable compared to the 'wild-type' BAC clone transfected CEF. While

miRNA expression levels in the single-copy miRNA deletion and single-copy revertants clones remained somewhere between the two.

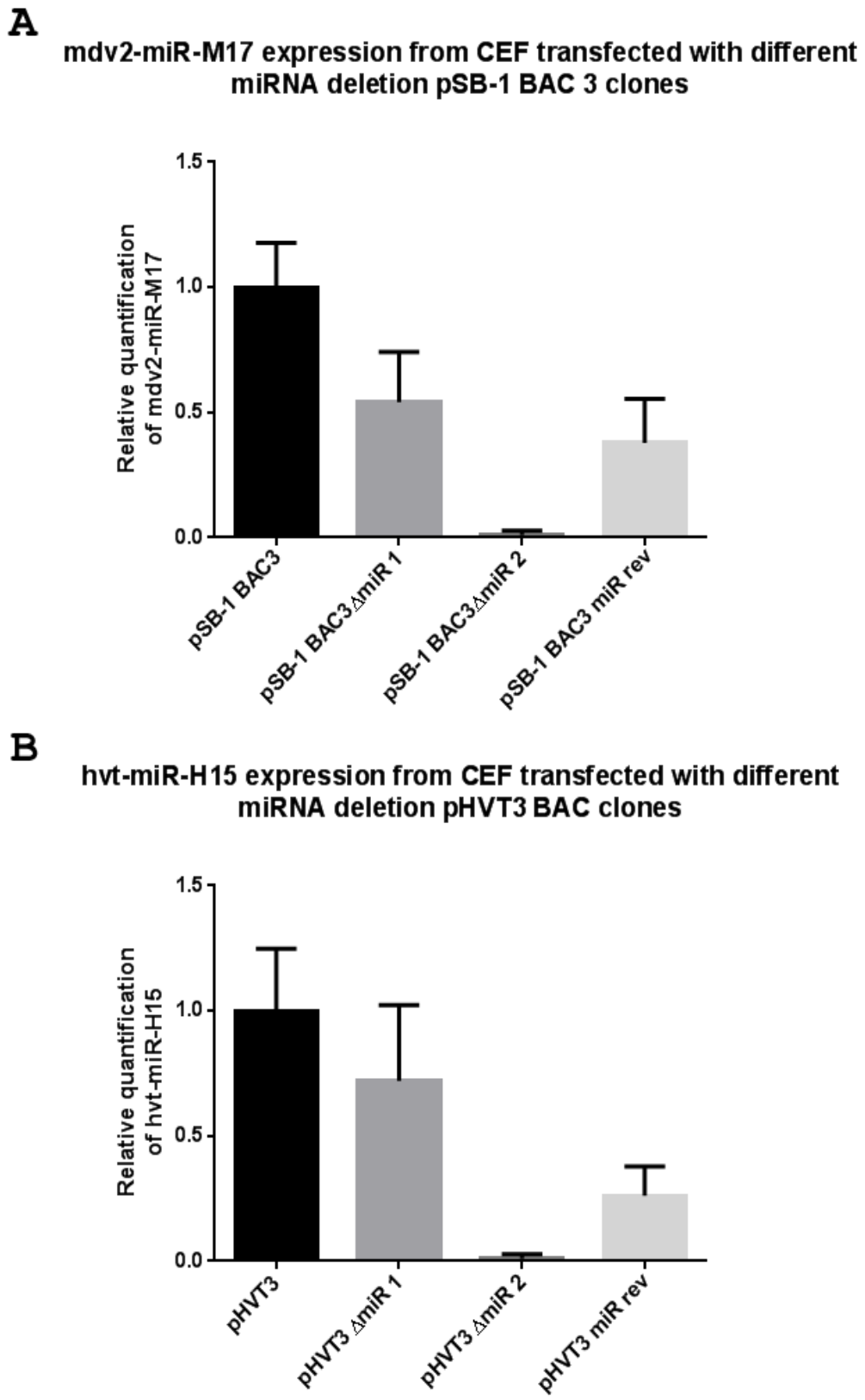


Figure 40 – TaqMan analysis of miRNA expression from CEF transfected with different miRNA deletion clones of either pSB-1 BAC3 (A) or pHVT3 (B). All expression levels are relative to CEF transfection control and normalised to the host endogenous miRNA *gga-miR-let7a*. Error bars show maximum and minimum relative quantification (RQ) values as calculated by 7500 Fast software (Applied Biosystems) from Ct values, normalised to gga-miR-let7a.

5.2.3.3 PCR analysis of all pHVT3 and pSB-1 BAC DNA clones

A final analysis of the BAC DNA was performed before viral stocks were generated. PCR amplification of the miRNA-containing regions of each of the pSB-1 and pHVT3 BAC constructs was performed as described in section 2.3.6, using Platinum Pfx DNA polymerase, with primers 'HVT miR PCR F/R' and 'MDV2 miR PCR F/R' (listed in section 2.3.33.3) for pHVT3 and pSB-1 BAC respectively. The PCR reactions were analysed by electrophoresis, shown in figure 41.

The pattern of the PCR products from each of the different BAC constructs is different, this highlights the different DNA sequences within the miRNA containing region of the BAC constructs. In the 'wild-type' (WT) constructs there is a band present at around 4.5-5 kb (highlighted by a blue box) that represents the amplification of the viral miRNAs. In the single-copy knockout constructs (Δ1) a new band is present at around 3.5-4 kb (highlighted by a green box) representing the KanSacB cassette, the other copy of the viral miRNAs does not appear to have been amplified. In the double-copy knockout constructs (Δ2) two clear bands are visible one at around 3.5-4 kb (highlighted by a green box) representing the KanSacB cassette, and another band at around 2-2.5kb (highlighted by a red box) representing the spectinomycin cassette. Finally in the single-copy revertant constructs (miR Rev) two bands are visible representing the viral miRNAs (blue box) and the spectinomycin cassette (red box).

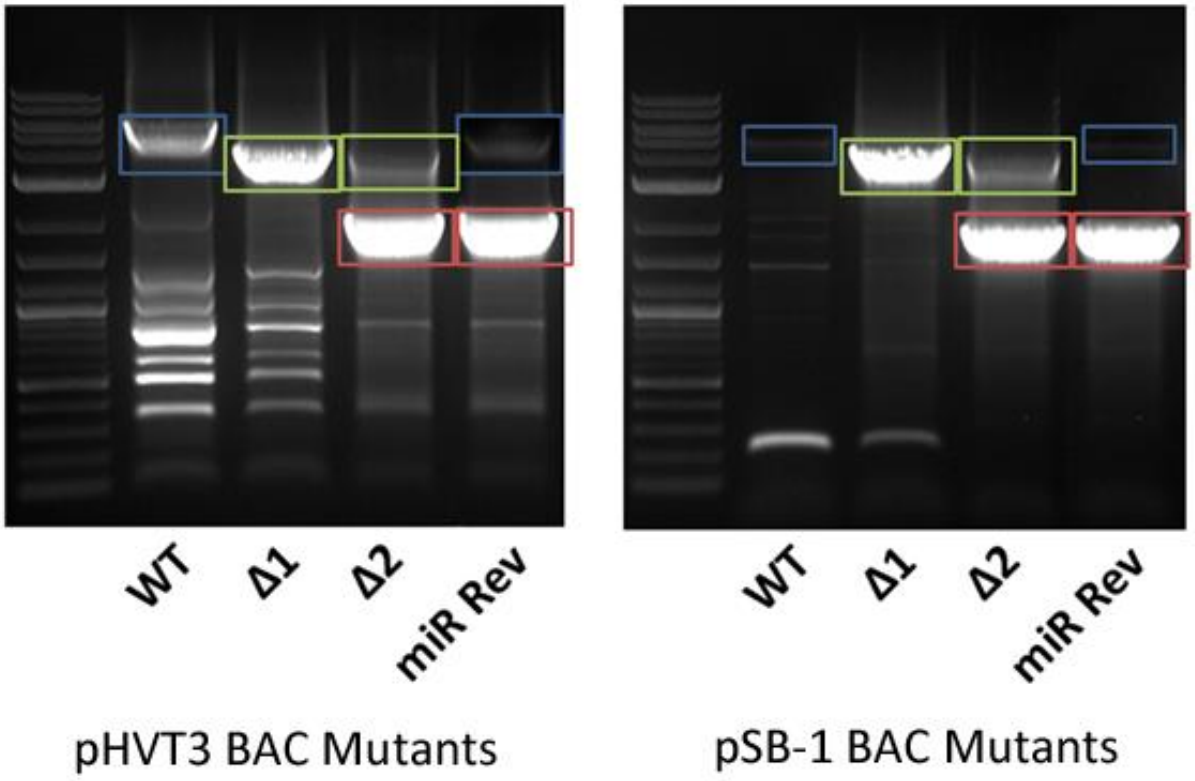


Figure 41 – PCR analysis on BAC DNA of the pHVT3 and pSB-1 miRNA manipulation constructs. DNA was analysed by gel electrophoresis on a 1% agarose gel with NEB 2-log ladder run in the left hand lane for reference. Blue boxes highlight the band of expected size for viral miRNA clusters, green boxes highlight the band of expected size for KanSacB cassette and red boxes highlight the band of expected size for spectinomycin resistance cassette.

5.2.4 Creating viral stocks of miRNA-deletion BAC viral genomes

Viral stocks were all generated and titres calculated in the same manner, as described in the methods (section 2.3.30). Stocks were made for the following BACs to be used in the animal experiment: pHVT3, pHVT3–double copy miRNA deletion, pHVT3-single copy miRNA revertant, pSB-1 BAC3, pSB-1 BAC3–double copy miRNA deletion and pSB-1 BAC3-single copy miRNA revertant. Single-copy deletion was not included as to do so would require the use of an additional animal experiment room per virus, increasing the number of birds and cost. Additionally the single-copy knockout was primarily only generated due to the two-step deletion strategy require to remove both copies of the miRNAs. The inclusion of the single-copy revertant, which contains one copy of the viral miRNAs, albeit with a different antibiotic resistance cassette, should provide enough evidence on the effect of removing a single-copy of the miRNAs.

5.2.5 Analysis of viral miRNA levels from CEF cells infected with virus stock

Triplicate wells of CEF were infected with 100pfu of both pSB-1 BAC3 and pHVT3 wild-type, ΔmiR-1, ΔmiR-2 and miR Rev virus. Four days after infection RNA was harvested and miRNA TaqMan was performed as described in section 2.3.14. The relative quantification of two viral miRNAs was determined from both pHVT3 and pSB-1 BAC3 derived viruses (*hvt-miR-H15, hvt-miR-H18, mdv2-miR-M16* and *mdv2-miR-M21* respectively). The levels of miRNA quantification were normalised to amount of a viral gene; *SORF1* in pHVT3 and DNA polymerase in pSB-1 BAC3, to give the best representation of viral miRNA levels relative to the levels of infection. The results are shown in figure 42.

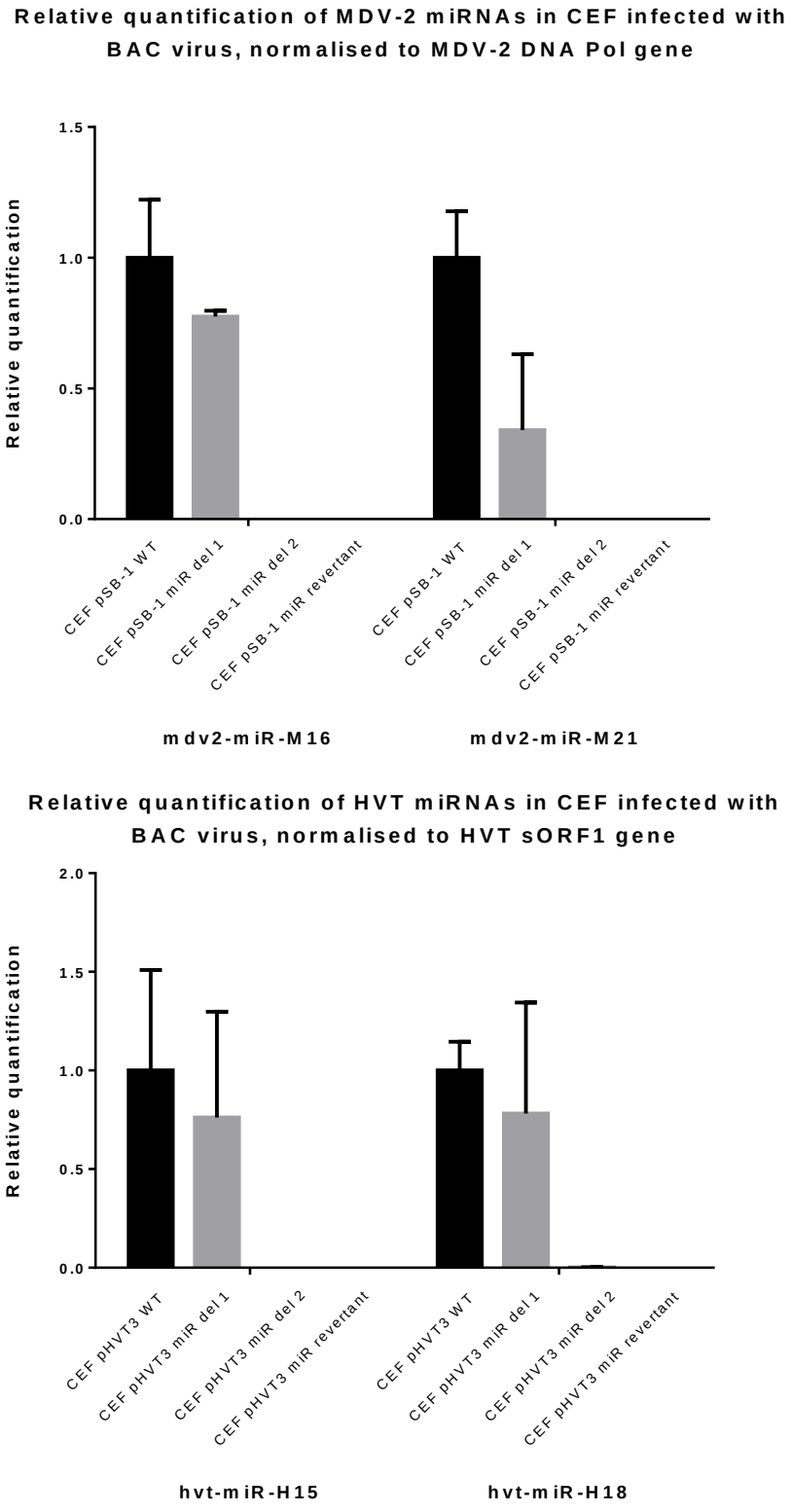


Figure 42 – Relative levels of viral miRNAs detected in infected CEF cells four days after infection with the BAC derived virus. miRNA expression levels are normalised to the viral genes described in each graph title. Error bars show the upper limits of relative quantification, calculated to 95% confidence by 7500 FAST software (Applied Biosystems).

The results from this analysis are a cause for concern; most striking is the observation that there is no expression of either miRNA for both pSB-1 BAC3 and pHVT3 revertant virus infected cells, also there appears to be no difference in miRNA expression between the wild-type BAC virus and single-copy miRNA knockout BAC virus.

This analysis was only performed after the start of the animal experiment, which in retrospect was a mistake. This analysis suggests that the only true comparison can be between the wild-type BAC viruses and the double-copy miRNA knockout viruses (ΔmiR 2) as both of these are behaving as expected and the data shows that there is no expression of viral miRNAs from the ΔmiR2 BAC derived viruses.

5.2.6 Animal experiment to observe *in vivo* effects of miRNA deletion from viral genomes

5.2.6.1 Sampling schedule

The animal experiment was performed 'in-house' at The Pirbright Institute, Compton within the experimental animal house (EAH) under licence from the UK Home Office. The goal of this experiment was to measure the replication of the miRNA-deletion BAC viruses *in vivo* via TaqMan, while also observing any effects on the protective abilities of pSB-1 BAC3 and pHVT3 against clinical signs and mortality caused by MDV-1.

Fifty-six wing-banded specific pathogen free (SPF), maternal antibody negative, closed flock Rhode Island Red (RIR) birds entered the EAH at day old and were allocated between two rooms (one for pHVT3 BACs, one for pSB-1 BACs, 28 per room) in three floor pens. There were seven groups of birds (the 6 different BAC clones and one unvaccinated), with groups 1-6 (eight birds per group) distributed into six pens; group seven (unvaccinated) was split between the six pens, such that there were nine birds in four pens, and ten birds in the remaining two. Bird numbers of eight per group were chosen following power calculations by Sue Baigent (unpublished, methodology described in appendix 1), which determined eight birds was a sufficient number from which to draw statistical conclusions from, while adhering to the 3R principles of animal research.

At two-days old the chicks in groups 1-6 were vaccinated with 1,000 plaque forming units (pfu) in 100µl via the subcutaneous route as follows:

Room 1	**Room 2**
Group 1 pHVT3	Group 4 pSB-1 BAC 3
Group 2 pHVT3 ΔmiR double-copy deletion	Group 5 pSB-1 BAC3 ΔmiR double-copy deletion
Group 3 pHVT3 miR revertant	Group 6 pSB-1 BAC3 miR revertant

Group 7 remained unvaccinated and were distributed among the six pens in the two different rooms as a control group (summarised in figure 43). Aliquots were taken from the same diluted samples of BAC viral stocks that were used for vaccination above, for titration on CEF as described in the methods (section 2.3.31), to check that dilutions of the virus had been performed correctly and that the viral titres did not differ from the previously calculated values following recovery from liquid nitrogen. Each bird in groups 1-6 received 1,000pfu of the appropriate vaccine virus. As discussed in section 5.2.5 the vaccinations for the animal experiment were performed prior to the realisation that there was no viral miRNA expression from the miR revertant BAC derived viruses, this is why a miR revertant virus group was included for both pHVT3 and pSB-1 BAC3.

An initial blood sample was taken from the chicks four-days after vaccination (-3 days post challenge (dpc)), a 50µl blood sample was taken from each bird by wing vein pin-prick and collected by pipette. Blood samples were mixed immediately with an equal volume of 3% Sodium citrate and Peripheral blood lymphocytes (PBLs) were isolated from the samples by centrifugation over Histopaque and stored at -20°C.

At nine days of age all birds (groups 1-7) were challenged with 1,000 pfu of the MDV-1 strain, RB-1B in a volume of 100 µl via the intraperitoneal route and once again virus levels were titrated onto CEF to check the actual dose of virus administered to each bird . Prior to challenging the birds, on the same day (0 dpc) 150µl blood samples were taken and PBLs were harvested in the same manner as described above. Further 150µl blood samples were taken and PBLs harvested and stored in the same manner on the following days post-infection: 3, 6, 13, 20, 27, 41, and 55. Any deaths (or birds killed upon reaching humane end point) within the different groups were recorded and the trial was terminated 60 dpc.

From other RB-1B challenge studies, it is known that around 50% non-vaccinated birds died from neural symptoms during severe early cytolytic infection at around 8-10 dpc and the remaining 50% went on to develop tumours and die between 28-41 dpc (Singh et al. 2010). Since the aim of this study

was to explore the effects on both viral replication and protection following deletion of miRNAs from pHVT3 and pSB-1, continuing the experiment out to 60 dpc, gives the opportunity to assess whether the mutated vaccines remain significantly protective, rather than merely delaying mortality by a few days.

During the trial all blood samples were taken from the birds, once rounded up, by named Home Office Licence holders (Lorraine Smith and Lydia Kgosana). Once blood was taken from the birds, all subsequent processing and analysis was performed by James Popplestone.

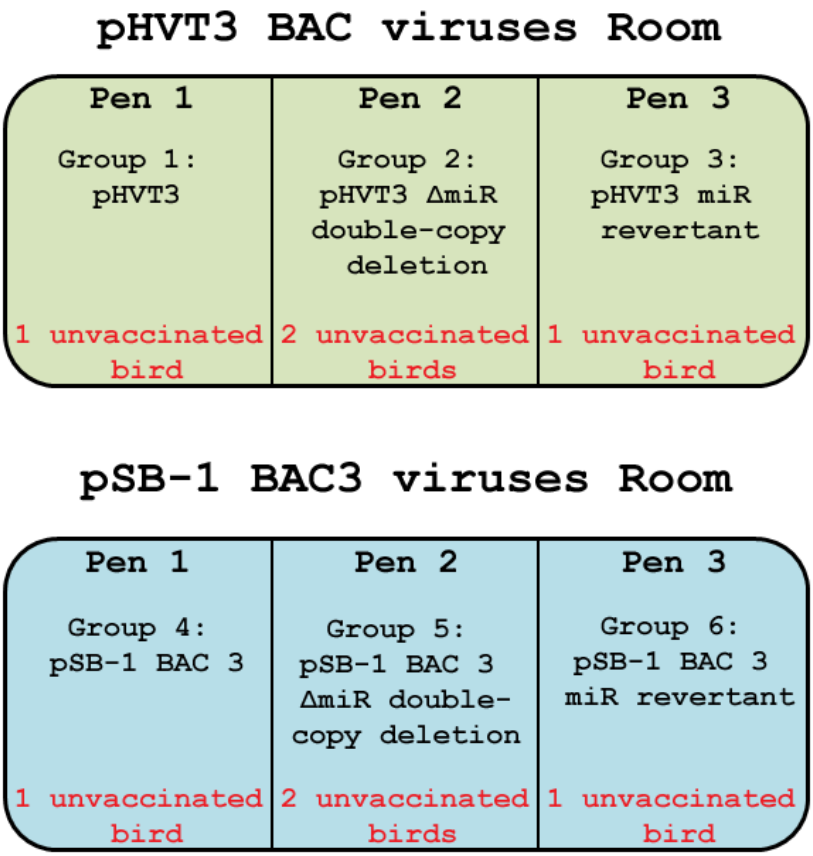


Figure 43 - Distribution of birds for KV86 trial. Location of each group is shown by its number and name. The birds in group 7 (unvaccinated) are shown in red and their distribution amongst vaccinated birds can be seen.

5.2.6.2 Analysis of animal experiments

As described above deaths of any birds in the different groups were recorded throughout the trial, while blood samples were taken to harvest PBLs at specific time points. PBLs were harvested to extract DNA from so that viral genome copies could be calculated (as a number of viral genome copies per 10,000 cells) and used as an indication of viral replication through the study. DNA was extracted from the PBLs using DNeasy 96 Blood & Tissue Kit (Qiagen) as described in the methods, section 2.3.10.

The levels (genome copy number) of both the RB-1B and BAC viral genome (pHVT3 or pSB-1 BAC3 various miRNA manipulations) were calculated within the PBLs extracted throughout the study using specific probe and primer sets designed by Sue Baigent. Virus copy numbers were accurately calculated against a standard curve and were normalised against the host reference gene *Ovotransferrin* (details of TaqMan analysis are described in section 2.3.31, the sequence of primers and probes used in this analysis are shown in table 13, section 2.3.36). All TaqMan runs were performed on 7500 Fast Real-Time PCR System with Ct-values determined using 7500 Fast Software (Applied Biosystems) before being transferred to previously generated Microsoft Excel analysis template performing analysis as described by Baigent et al (Baigent et al. 2005).

5.2.6.3 Results of animal trial

5.2.6.3.1 Bird Survival

Figure 44 displays the percentage survival of the vaccinated birds in different groups (and different rooms) over the length of the trial. Figure 44A shows the survival of birds that were vaccinated with either: pHVT3, pHVT3 ΔmiRNA or pHVT3 miRNA revertant (groups 1, 2 and 3 respectively) and unvaccinated birds (group 7). Vaccination was performed seven days prior to infection (challenge) with 1,000pfu of RB-1B strain of MDV1. Once again survival in all groups of vaccinated birds was significantly higher than in the unvaccinated group (P-value <0.001 calculated by Log-rank (Mantel-Cox) test), additionally there were a small number of mortalities within the three vaccinated groups however there were no statistically significant (calculated by Log-rank (Mantel-Cox) test) differences in percentage survivals between groups 1,2 and 3.

Part B of figure 44 shows the survival of birds that were vaccinated with either: pSB-1 BAC3, pSB-1 BAC3 ΔmiRNA or pSB-1 BAC3 miRNA revertant (groups 4, 5 and 6 respectively) and unvaccinated birds (group 7). Vaccination was performed seven days prior to infection (challenge) with 1,000pfu of RB-1B strain of MDV1. Within figure 44B the first noticeable observation is that survival in all groups of vaccinated birds was greater than the survival of unvaccinated birds, all of which had died or reached 'humane end point' by 26 dpc. Additionally there were mortalities within the three vaccinated groups, and there was a lower percentage survival in groups 5 and 6 compared with group 4. A statistical significance was observed in the differences in mortalities between unvaccinated birds and the different vaccinated groups (P-value <0.001 calculated by Log-rank (Mantel-Cox) test) however there was no statistical significance in the variations in mortality between the parental pSB-1 BAC3 and miRNA deletion and revertant pSB-1 BAC3 vaccinated birds.

Two birds were excluded from all analysis; one bird from pHVT3 vaccinated and one bird from the unvaccinated group. The bird excluded from the pHVT3 vaccinated group (group 1) died three days after vaccination (four days post-hatch) before the introduction of the challenge virus, this was a result

of an inability to feed. The bird excluded from the unvaccinated group analysis survived the entire trial and during the post-mortem showed no signs of any tumour formation, based on this observation it was decided that this bird had very likely accidently not received a dose of the challenge virus, strongly supported by only background levels of challenge virus being detected by TaqMan in the bird (number 352) throughout the duration of the trial.

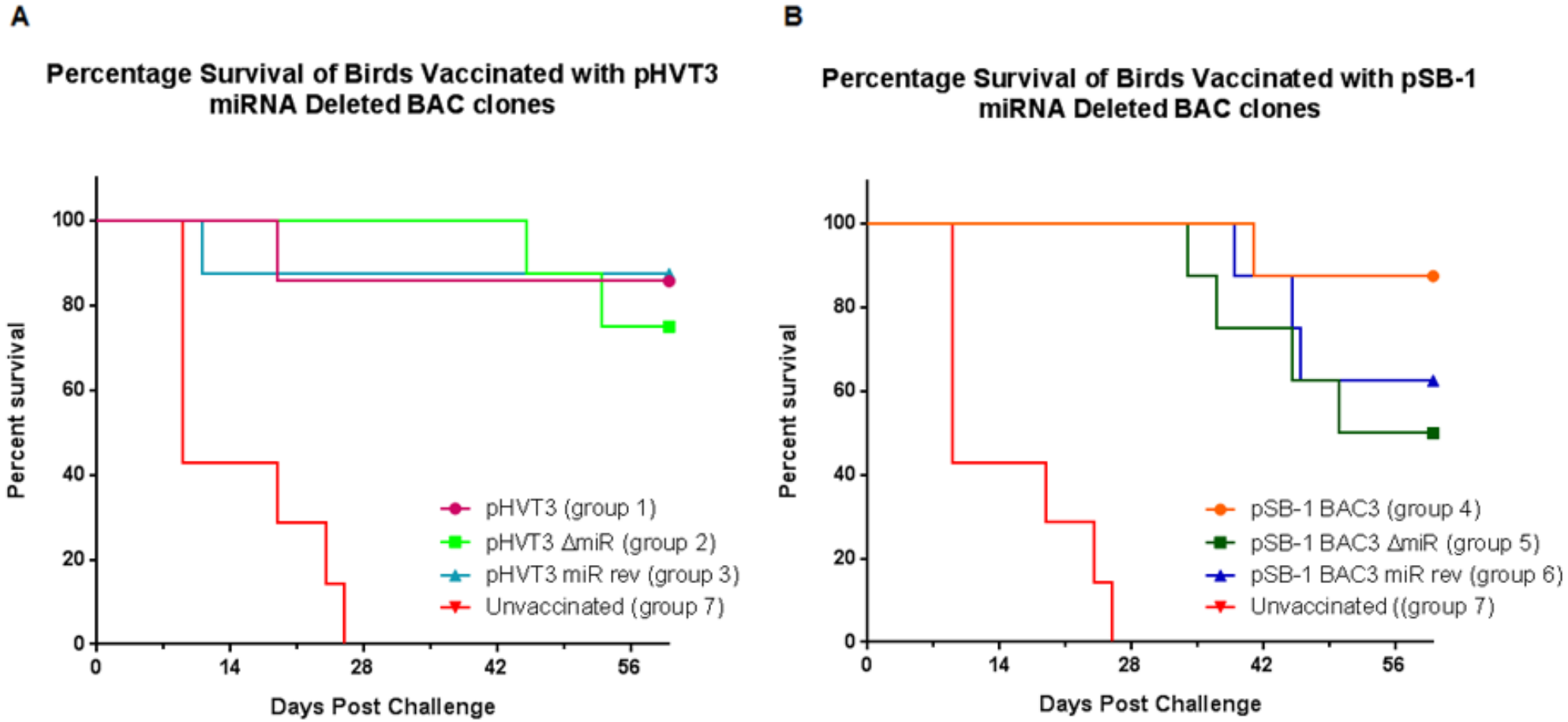


Figure 44–Survival graphs of Birds in KV86 experiment. (A) Shows groups 1, 2, and 3 that were vaccinated with different miRNA deletion clones of the pHVT3 BAC and group 7 – unvaccinated. (B) Shows groups 4, 5, and 6 that were vaccinated with different miRNA deletion clones of the pSB-1 BAC and group 7 – unvaccinated. The percentage survival of the birds is displayed relative to the days post challenge (dpc) with 1,000pfu of RB-1B challenge virus.

5.2.6.3.2 Replication of challenge (RB-1B) virus

Figures 45 and 46 show the mean rate of replication of challenge virus RB-1B (as calculated by the mean number of RB-1B genomes per 10^4 Peripheral Blood Lymphocytes (PBLs)) in birds within the different groups (1-7). Figure 45 shows RB-1B levels in birds vaccinated with different miRNA manipulations of pHVT3 BAC virus (groups 1, 2 and 3) as well as unvaccinated birds (group 7). RB-1B levels are significantly higher (calculated using Minitab 16 statistical software ANOVA general linear model, Tukey method 95% confidence) in unvaccinated birds compared with all three groups of vaccinated birds whereas RB-1B levels remain fairly consistent between groups 1, 2 and 3. The rate of replication (gradient of the line) appears fairly consistent throughout the four groups, however at 4 days post challenge there is a big increase in the levels of RB-1B virus within the unvaccinated birds, compared with the other groups, and from that point on RB-1B levels remains consistently higher.

Figure 46, displaying RB-1B virus levels within pSB-1 BAC3 virus manipulations (groups 4, 5 and 6) and unvaccinated birds, shows a very similar pattern to that of figure 45. Once again RB-1B levels are significantly (calculated using Minitab 16 statistical software ANOVA general linear model, Tukey method) higher in unvaccinated birds compared to all three groups of vaccinated birds where RB-1B levels remain fairly consistent between the vaccinated groups. The rate of replication (gradient of the line) appears fairly consistent again throughout the four groups. The increase in RB-1B levels 4 days post challenge in unvaccinated birds is also visible.

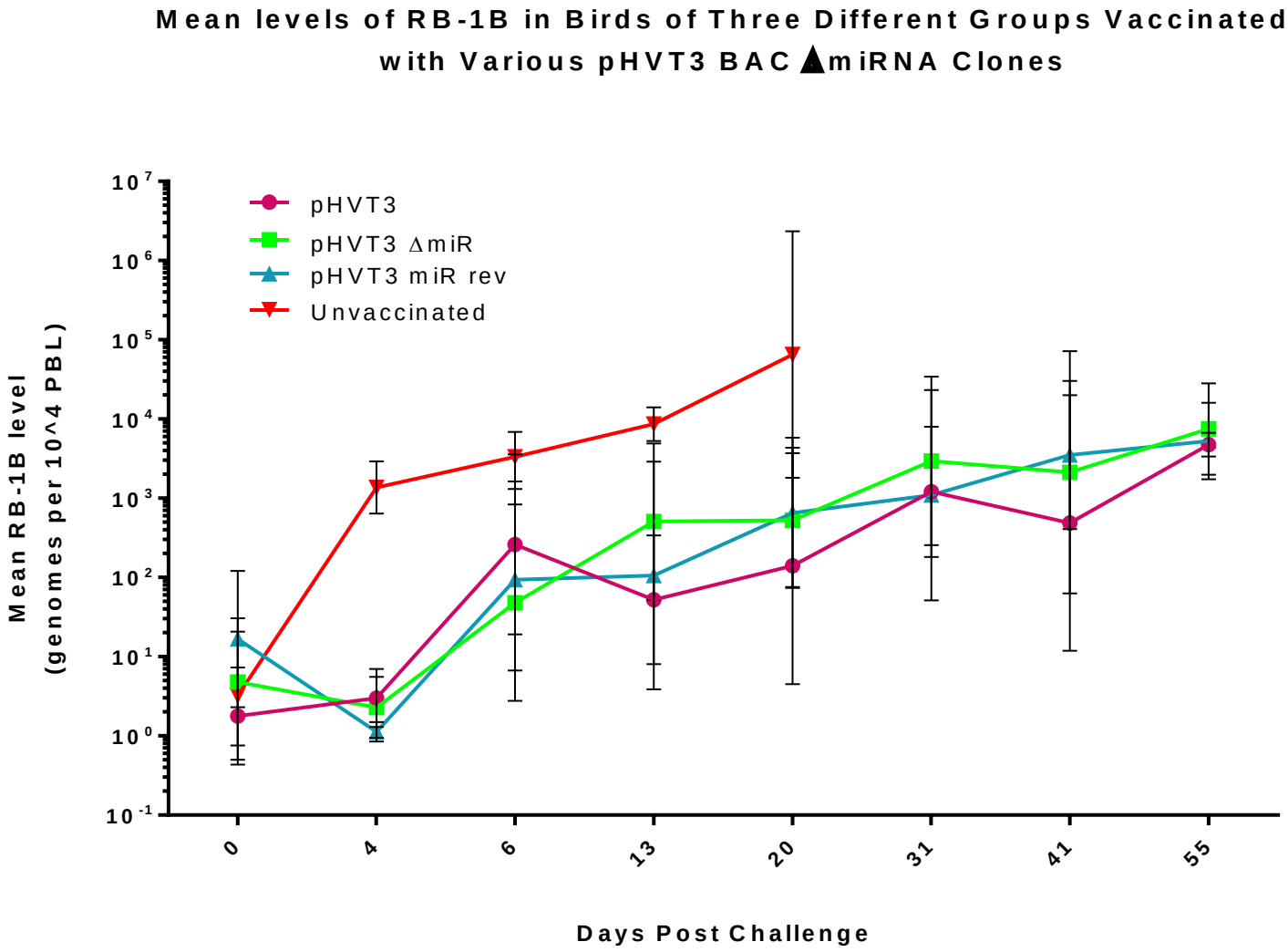


Figure 45–Mean RB-1B levels in the different groups that were vaccinated with the different pHVT3 BAC clones throughout the KV86 animal trial, as calculated by the mean number of RB-1B genomes per 10^4 Peripheral Blood Lymphocytes (PBLs) extracted from each bird. Error bars display upper and lower limits of the 95% confidence intervals.

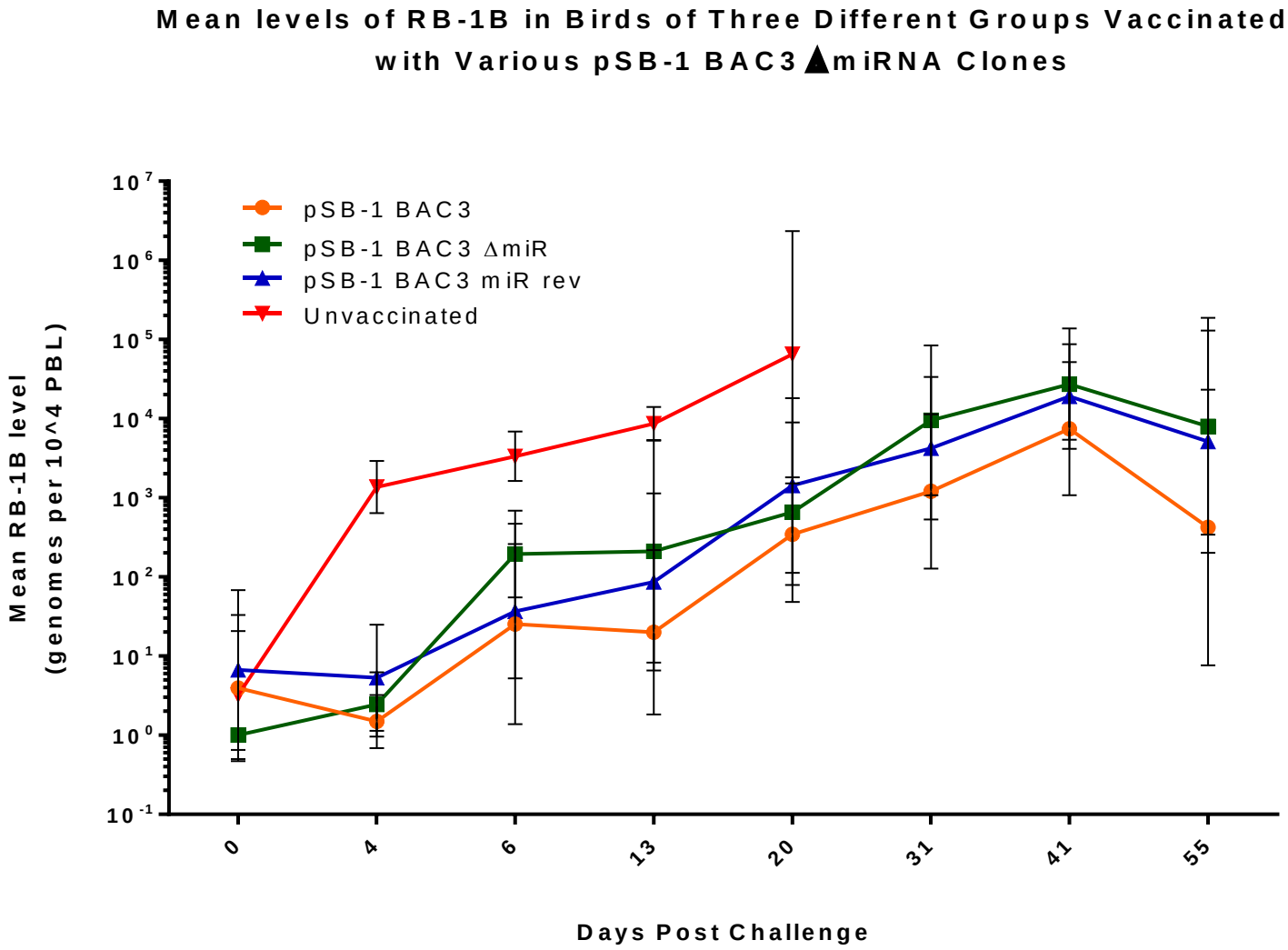


Figure 46 - Mean RB-1B levels in the different groups that were vaccinated with the different pSB-1 BAC3 clones throughout the KV86 animal trial, as calculated by the mean number of RB-1B genomes per 10^4 Peripheral Blood Lymphocytes (PBLs) extracted from each bird. Error bars display upper and lower limits of the 95% confidence intervals.

5.2.6.3.3 Replication of vaccine (pHVT3 or pSB-1 BAC3) virus

Figure 47 shows the mean levels of the different pHVT3 BAC vaccines in birds in groups 1, 2, 3 and 7 (unvaccinated). The general trend between the different groups is that vaccine virus levels remain steady to begin with, and then increase followed by a plateau. This is only a broad description of the different groups, and it is clear to see that in the beginning of the trial there are fluctuations in the vaccine virus levels. The detection of BAC virus in the unvaccinated birds, which remains present until all of the unvaccinated birds have died, was a worrying observation. Over the length of the study (up to 27 dpv for unvaccinated) there was no significant difference in the detectable levels of BAC virus between all the groups (calculated using Minitab 16 statistical software ANOVA general linear model, Tukey method 95% confidence). There is a significant difference (calculated using Minitab 16 statistical software ANOVA general linear model, Tukey method 95% confidence) between groups 3 (pHVT3 miR Rev) and 7 (unvaccinated) and groups 1 (pHVT3) and 2 (pHVT3 ΔmiR), at 13 and 20 days post vaccination (dpv). Groups 3 and 7 showed an increase in vaccine virus levels between 13 and 20 days post vaccination (dpv), whereas groups 1 and 2 showed this increase between 20 and 27 dpv.

Figure 48 shows the mean levels of the different pSB-1 BAC3 vaccines in birds in groups 4, 5, 6 and 7. Again, vaccine virus levels remained steady to begin with then increased and plateaued. The biggest increase in vaccine virus levels for all groups was between 13 and 20 days post vaccination, at which point the vaccine virus levels remained largely constant until the end of the trial. Once again BAC virus is detectable in unvaccinated birds (because this is the same control group for pHVT3 group) and there is no significant difference in detectable BAC virus between all groups throughout the trial (calculated using Minitab 16 statistical software ANOVA general linear model, Tukey method 95% confidence).

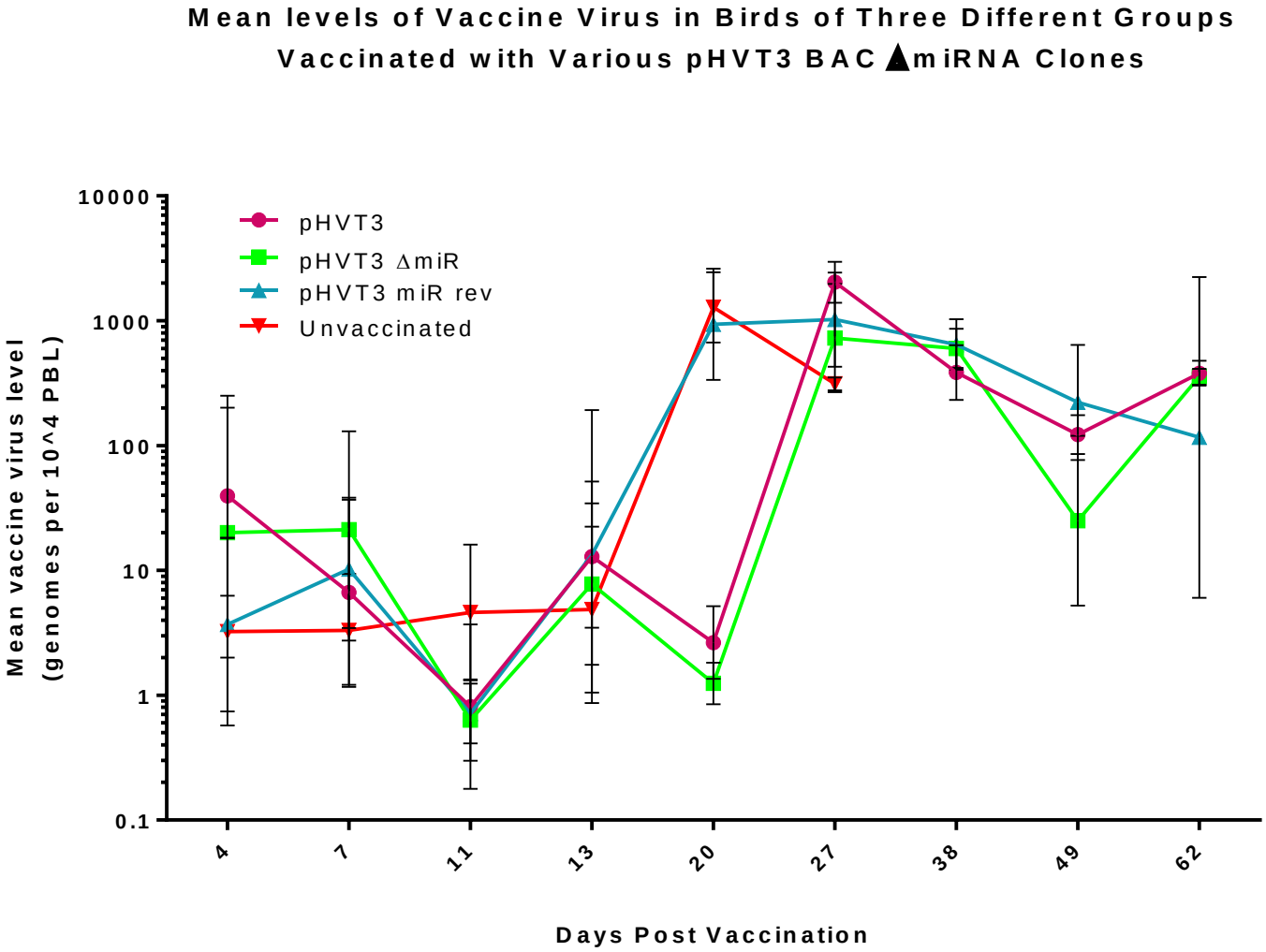


Figure 47 - Mean pHVT3 BAC vaccine virus levels in the different groups that were vaccinated with the different pHVT3 BAC clones throughout the KV86 animal trial, as calculated by the mean number of BAC genomes per 10^4 Peripheral Blood Lymphocytes (PBLs) extracted from each bird. Error bars display upper and lower limits of the 95% confidence intervals.

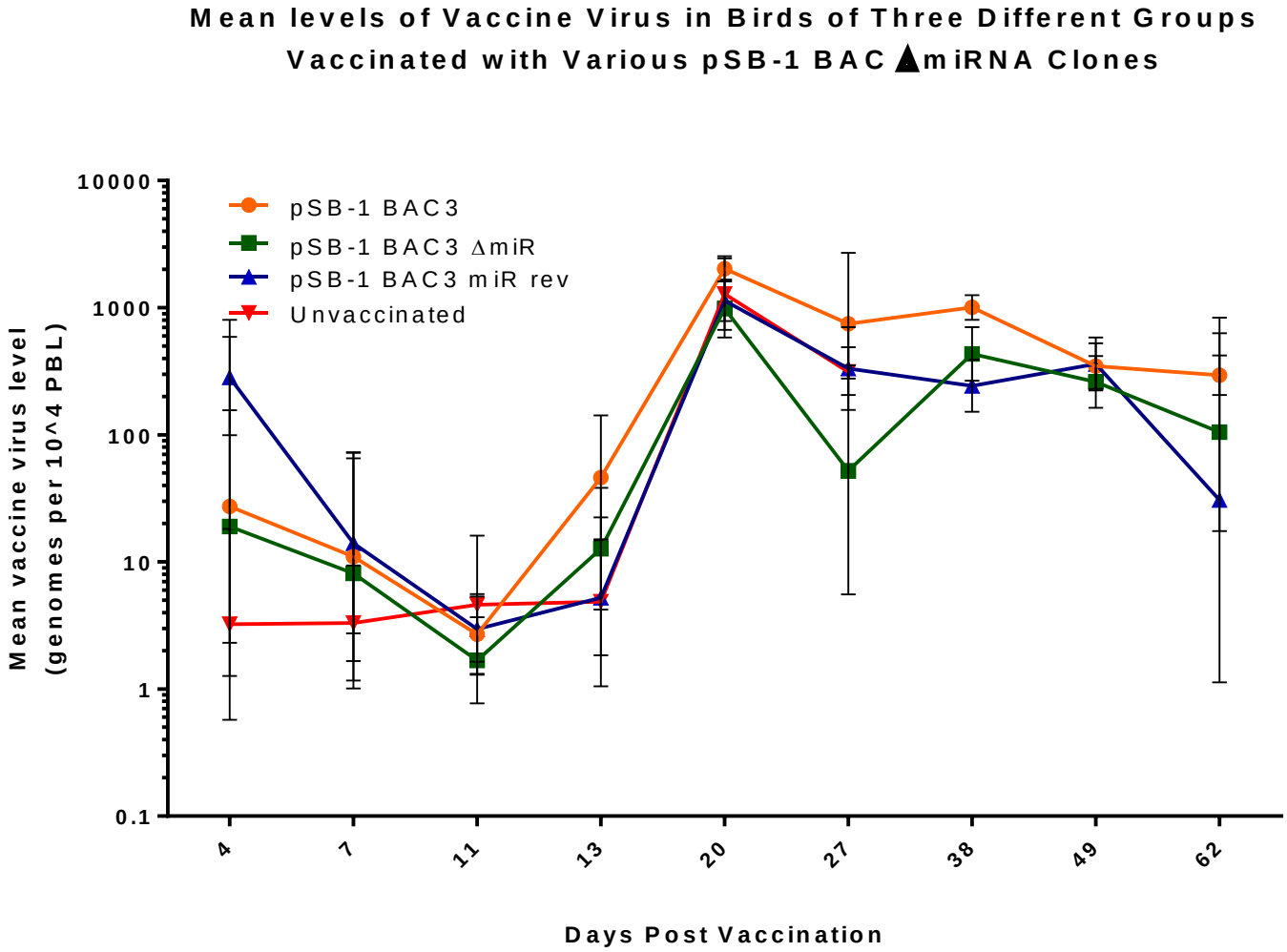


Figure 48 - Mean pSB-1 BAC3 vaccine virus levels in the different groups that were vaccinated with the different pSB-1 BAC3 clones throughout the KV86 animal trial, as calculated by the mean number of BAC genomes per 10^4 Peripheral Blood Lymphocytes (PBLs) extracted from each bird. Error bars display upper and lower limits of the 95% confidence intervals.

5.3 Discussion

5.3.1 Creation of the miRNA deletion BACs

The generation of the BAC DNA clones of both the pHVT3 and pSB-1 miRNA single- and double- copy knockouts proved to be relatively straight forward. The BAC mutagenesis protocol used has previously been developed and well optimised (Zhao et al. 2008). The positive selection pressure for the incorporation of the antibiotic resistance cassette proved to be a strong driver for recombination, making positive colonies easy to distinguish. The generation of single-copy miRNA revertant clones however was more challenging, and a higher number of colonies were screened before a positive clone was identified, especially in the case of pHVT3 BAC.

Only around 50% of the colonies present on the pSB-1 miRNA single copy revertant plate, and <1% on the pHVT3 miRNA single copy revertant plate had lost kanamycin resistance, an indicator that the miRNAs had been 'flipped' back into the BAC (single-copy revertant). The ability of the colonies to survive on the kanamycin and spectinomycin LB agar plates demonstrates that the spectinomycin resistance and KanSacB cassette remained within the BAC clone. Therefore the *SacB* part of the KanSacB cassette (inferring a toxic sensitivity to sucrose) was not performing as expected. The reasons for this are not entirely clear, it seemed to be more of an issue in the pHVT3 BAC revertant than the pSB-1 BAC3, it could have been a result of a random mutation occurring during PCR amplification that was not corrected by the proof-reading polymerase.

These issues could have been avoided if the screening of sucrose sensitivity had been better. In section 5.2.1.1.1 colonies were analysed, following the insertion of the KanSacB cassette, for their sensitivity to sucrose, this was done using a 10^{-2} dilution of bacteria and the number of colonies present following overnight incubation was counted. In retrospect, a lower dilution of culture should have been used and clones screened until a clone produced zero colonies on the 10% sucrose LB agar plates. This would have demonstrated strong sensitivity to sucrose, and would have saved time in the generation of a revertant clone.

5.3.2 Testing of viral stocks generated from BAC clones

As discussed briefly in the results section the analysis of miRNA expression from virus generated from cells transfected with BAC DNA was only tested after the animal experiment had begun. The analysis of expression levels of two viral miRNAs from both pSB-1 BAC3 and pHVT3 derived viruses showed no significant differences between 'wild-type' and single-copy knockout clones, and no detectable miRNA expression in the single-copy revertant virally infected cells.

miRNA expression levels were normalised to expression levels of other viral genes, so these unexpected results were not due to differing levels of infection in the different cells. It was suggested following personal communication with Lawrence Petherbridge (the person who generated both the pSB-1 BAC3 and pHVT3 BAC clones) that during the creation of the viral stocks the virus had simply copied across the opposite repeat region; i.e. miRNA cluster in the single-copy knockout or spectinomycin cassette in the single-copy revertant. Figure 42 and sequencing data certainly suggests that the DNA of the different BAC clones was as expected when it was transfected into CEF to create the viral stocks, but for whatever reason expression of viral miRNAs was not quite as expected when cells were infected with 100 pfu of the viral stocks. As discussed before, had this been detected before the start of the animal trial it would have meant that changes could have been made to the animal trial.

Ultimately time constraints have meant that only a comparison between 'wild-type' and double-copy miRNA knockout BAC clones can be made. Had there been any large changes in protection or rate of replication, then the presence of a genuine revertant would have been crucial to show the changes were not the result of a massive rearrangement of the viral genome.

5.3.3 Outcome of animal trial

5.3.3.1 Impact of miRNA deletion from vaccine viruses on bird survival

As described in the results (section 5.2.6.3.1) there doesn't appear to be a significant impact on the survival rate of birds vaccinated with the parental pHVT3 BAC and the miRNA deletion BAC. In the pSB-1 BAC miRNA deletion vaccinated birds there did appear to have a lower survival rate compared to the parental pSB-1 BAC vaccinated birds however the P-value of 0.127 generated by the Log-rank (Mantel-Cox) test suggests this is not statistically significant.

While in previous studies removal of the miRNAs from a virus have shown to alter the phenotype of the virus, for example increased lytic activity in KSHV (C. C. Lu et al. 2010) or decrease in lymphoma induction in MDV1 (Y. Zhao et al. 2011), however these are disease causing strains of virus, not vaccines. It is therefore likely then that the HVT and MDV-2 miRNAs, while still being important to the virus, are not crucial players in creating immunity to the oncogenic MDV-1 virus.

5.3.3.2 Impact of miRNA deletion from vaccine viruses on growth of the challenge virus RB-1B

Once again no significant difference was seen in the growth of RB-1B virus in birds vaccinated with either: parental, miRNA double-copy deletion or miRNA single-copy revertant pHVT3 or pSB1-BAC3. There remained a statistically significant difference in RB-1B virus levels between unvaccinated and all vaccinated groups, which again links with the observation in section 5.2.6.3.1 that the deletion of the miRNAs has no effect on the ability of pHVT3 and pSB-1 BAC3 to provide immunity against the MDV-1 strain RB-1B

5.3.3.3 Impact of miRNA deletion on growth of vaccine viruses

The initial observation of this part of the study is that overall there is no significant difference in the growth rates between the parental, miRNA double-copy deletion and miRNA single-copy revertant pHVT3 and pSB1-BAC3 clones, in vaccinated birds. This demonstrates that the deletion of the miRNAs has not caused any catastrophic changes to the viruses and suggests that the miRNAs have no

observable effect on the replication rate of the virus. This is in line with the observation in MDV-1 that the miRNAs are not essential for MDV replication (Y. Zhao et al. 2011).

However there is a concerning observation that within the unvaccinated birds there is highly detectable levels of vaccine virus as determined by TaqMan. A number of possible avenues that might explain this detection were explored; initially this observation was thought to be a result of a minor detection of background levels that became amplified through multiplication in the TaqMan analysis template, but on closer inspection of the raw data in became evident that this detection was genuine. DNA from unvaccinated birds was then reanalysed from 20 dpv samples via TaqMan using MDV2 or HVT specific probes and primers (as opposed to general BAC specific probes and primers) which again showed genuine levels of vaccine (data not shown). The possibility that there could have been cross contamination of the DNA samples when performing mass DNA extractions from the PBLs, or that the high levels of RB1B in the unvaccinated birds may have led to a degree of false positive detection cannot be ruled out. The fact that the unvaccinated group was due to serve as a negative control for the analysis of the other groups, means that any interpretation of the data on the replication of the different pSB-1 BAC3 and pHVT3 should be treated with extreme caution.

There is an outside possibility that the removal of the miRNAs from the BAC viruses could be promoting spread of the vaccine between birds leading to the detection of vaccine virus via TaqMan. The unvaccinated bird group (containing 7 birds) was used as the same control for analysis of vaccine levels for both pHVT3 and pSB-1 BAC3. As described in section 5.2.6.1 unvaccinated birds were spread throughout all pens, but only three birds were remaining by 20 days post vaccination, two in a pen with birds vaccinated with pHVT3 ΔmiR and one in a pen with pSB-1 BAC3 miR Rev. The fact that no vaccine virus was detected in unvaccinated birds penned with the parental pHVT3 and pSB-1 BAC3 vaccinated birds does add some weight to this theory. However, the birds with detectable levels of vaccine virus received no overall protection against MDV-1 challenge virus as the birds died, or reached humane end point, before the end of the trial. Additionally if there was effective transfer of

vaccine virus it did nothing to lower levels of RB-1B virus, this could be because the RB-1B infection was too high by the time the BAC viruses spread and therefore couldn't provide sufficient protection.

Further analysis on the vaccine and challenge virus level of the individual birds within the 'unvaccinated' group (appendices 8 and 9), points strongly to the possibility of contamination of samples during DNA extraction. The levels of the challenge virus (RB-1B) in the remaining 'unvaccinated' birds at both 13 and 20 days post challenge, are approximately 100-fold greater than those detected in any of the vaccinated groups, while the apparent vaccine virus levels appear similar. If it had been a case of the birds accidently receiving vaccine virus, the levels of challenge virus in these birds would resemble the levels of other vaccinated birds.

6 Summary of results, general discussion, further work, and conclusions

In the last decade the understanding of the roles played by miRNAs has improved greatly. A great deal is now known about their expression states in numerous diseases and multiple targets of miRNAs have been identified in various species, which are now recorded in ever expanding databases. Research into viral miRNAs has come a long way in this time as well, work performed by numerous laboratories, including ours, has identified miRNAs encoded by many different viruses. Further research has elucidated some of the functions of the viral miRNAs in maintaining disease states within the host. Less studied however are the functions of miRNAs in the vaccine viruses, MDV-2 and HVT, and it was the purpose of this study to characterise the functions of these miRNAs following their detection.

The importance of the viral miRNAs *in vivo* has been previously explored through the analysis of MDV-1 encoded miRNAs. Much of this work has focused on one miRNA in particular, *mdv1-miR-M4,* and the cluster that it sits in. This miRNA has been identified as an ortholog of the host miRNA, *gga-miR-155* (Y. Zhao et al. 2009), a miRNA whose overexpression has been implicated in a number of cancers and is itself described as an 'oncomiR' (Jiang et al. 2010). The research performed on the MDV-1 miRNAs paved the way for the work in this study on the miRNAs encoded by the vaccine viruses MDV-2 and HVT. Many similar techniques have been used either in validating targets or removing the miRNAs from the viral genome and observing the effects.

The initial work in this study focused solely on identifying potential targets of the viral miRNAs. The start of chapter three focussed on a single MDV-2 encoded miRNA, *mdv2-miR-M21*, and the observation that it contained an identical 'seed' sequence to the host encoded miRNA, *gga-miR-29b*. In line with work performed by other groups, it was hypothesised that the viral miRNA might be acting as an ortholog of the host miRNA. It was demonstrated that the viral miRNA was indeed able to target a well-defined *miR-29b* target, *DNMT3B*. The chapter discusses the implications of the viral miRNA targeting this important epigenetic factor. Work later in chapter three also highlighted another target

of *mdv2-miR-M21*, *AKT3*, which was also validated as a target of *miR-29*(Wei et al. 2013) (albeit only in humans) which adds further support to the idea that the virally encoded miRNA is acting as an ortholog to the host miRNA with an identical 'seed sequence'.

Throughout the time-frame of this project various new techniques were being developed to identify targets and as described in the relevant sections a number of these different approaches were explored. This study briefly describes trials with different techniques before settling on the proteomics based approach. The bioinformatic approach described in chapter 3.2, is the most simplistic approach that would be accessible to any researcher in search of targets of their chosen miRNA. This approach ultimately did prove to be quite fruitful providing a long list of potential targets for both HVT and MDV-2 encoded miRNAs. From this list a picture of the different biological processes, predicted to be targeted by the viral miRNAs, was constructed using Panther Classification System (http://www.pantherdb.org/) (Mi et al. 2013). Although targets of some of the virally encoded miRNAs were confirmed using biochemical assays, there were some issues. This ultimately led us to explore different approaches that would be capable of identifying a large number of viral miRNA targets at a time.

Multiple biochemical assays exist now to identify targets of miRNAs, and the merits and drawbacks of different approaches were considered. The use of label-free proteomics to identify targets of multiple virally encoded miRNAs was appropriate in this study as it allowed the identification of changes in protein level, following the expression of viral miRNAs, something that had proved difficult in other approaches due to a lack of chicken reactive antibodies for a number of genes. It is fair to say that there are criticisms of this approach (as discussed in chapter 4), many of which could be said for other techniques.

The proteomics analysis performed during this study proved to be largely unsuccessful. Problems were highlighted with the initial inducible expression vector that meant a time course analysis could no longer be performed. There were also larger concerns about the degree of variation between the two

replicates for both empty vector and HVT miRNA vector transfected cells. Later analysis showed that many more replicates would be needed with the current methodology before strong conclusion could be drawn from this data alone. Other groups have used proteomic screening to identify targets of viral miRNAs (Gallaher et al. 2013), however the proteomic methods used in this particular study utilised the more traditional radiation-based labelling, which may have created more reproducible results. A brief gene ontology analysis of the targets of the HVT miRNAs, highlighted through the proteomics work, did show some similarities with the biological processes predicted to be targeted earlier. This was an interesting observation but the issues of reproducibility in the proteomic study make drawing any firm conclusions impossible.

While the initial part of this study focussed on identifying targets of the virally encoded miRNAs, in order to highlight the pathways in the host affected by viral miRNA expression, the second part of this study (chapter five) focused on the role of the miRNAs specific to the HVT and MDV-2 viruses as vaccines. The regions of the BAC genomes containing the viral miRNAs, in both pHVT3 BAC (HVT) and pSB-1 BAC3 (MDV-2), were deleted via BAC mutagenesis. These miRNA deficient BAC clones of the HVT and MDV-2 viruses were then used to vaccinate birds against the RB-1B strain of MDV-1 in an animal experiment.

This part of the study determined that the viral miRNAs were not essential for providing protection against MDV-1, and to some degree showed there was no effect on viral replication, an observation that was in line with other research. However vaccine virus levels were detected in unvaccinated birds, making the analysis of virus replication between wild-type and miRNA-deletion BAC viruses impossible. Further analysis of vaccine virus levels in unvaccinated birds was unable to provide any clear reason as to why it was detected, meaning there is a possibility that deletion of the miRNAs could have induced spread of the BAC derived vaccine viruses. Wild type HVT and SB-1 vaccine strains can be easily transmitted from bird to bird via the respiratory route, and despite the fact that BAC-derived viruses have been demonstrated to share most of the biological properties of their wild type counterparts,

they do not appear to spread from bird-to-bird in this manner. This phenomenon has been demonstrated in MDV-1 where the US2 and UL13 regions (which are absent in the BAC) have been implicated (Jarosinski et al. 2007). This is a tentative observation and the fact that the unvaccinated birds, in which vaccine viruses was detected, still died from the challenge virus most likely points to some degree of probe cross-reactivity or sample contamination.

6.1 Future work

6.1.1 Chapter 3

To give more support to the functional ortholog role by *mdv2-miR-M21* it would have been interesting to imitate the work of Y. Zhao et al on *mdv1-miR-M4* (Y. Zhao et al. 2011), and replace *mdv2-miR-M21* in the viral genome with the host miRNA, *gga-miR-29b* to examine the phenotype of the virus. If no changes were seen in viral phenotype then we could likely determine that the host miRNA is acting as a functional ortholog.

With regards to the broader scale analysis of viral miRNA targets using bioinformatic and biochemical approaches, further work could have been performed using the same methodology. To perform this analysis for all predicted targets would be extremely labour intensive and require a huge number of resources to determine any effects of miRNA targeting at the protein level. Instead a different approach was used; initially looking for global changes in protein levels following expression of an entire viral miRNA collection, then working back to explore specific miRNA:mRNA interactions responsible for the changes.

6.1.2 Chapter 4

Changes are obviously needed in the methodology used to create the samples needed for proteomic analysis, so that a higher level of reproducibility is achieved between replicates. There are still clear merits of using a proteomics based approach to identify targets of miRNAs, as ultimately it is decreases in protein level that will have an effect on the cell in which miRNAs are expressed. If better reproducibility can be achieved it would then be interesting to compare proteome changes following miRNA expression with the bioinformatic predictions to get a clearer picture at the effectiveness of the algorithm at predicting genuine targets.

6.1.3 Chapter 5

The focus of this part of the study was largely to determine if there was any effect on the replication and subsequent protection of the pSB-1 BAC3 and pHVT3 BAC derived viruses, following removal of

the miRNAs. To that end, it would appear that removal of the miRNAs did not result in a significant drop in protection when challenged with the MDV-1 strain RB1B. Any changes in the replication of the vaccine viruses, *in vivo,* could not conclusively be determined due to anomalous detection of vaccine virus in the negative control unvaccinated birds. Ideally the replication of the vaccine viruses following removal of the miRNAs should be measured again, and the TaqMan analysis of virus could be performed in parallel with plaque counting to get a more accurate idea of the levels of vaccine virus in birds.

Most MDV vaccines are now given by *in ovo* vaccination, in this study birds were vaccinated post hatch. It would therefore be interesting to explore whether or not the virally encoded miRNAs have a specific role during the embryonic stages of infection. Additionally it could be interesting to explore if the removal of the miRNAs has any effect on the protective synergism seen when vaccinating with a combination of MDV-2 and HVT viruses (Witter and Lee 1984), as the precise cause of this phenomenon remains unclear.

Finally the faint possibility that removal of miRNAs from the BAC clones could be promoting spread of the vaccine viruses. If proven to be genuine, it would be interesting to explore the pathways that are involved in the spread of vaccine virus and see if any viral miRNAs are targeting the pathways preventing this spread. Increasing the spread of recombinant vaccines between birds would be extremely useful for new recombinant vaccines that are being developed against MDV-1 and other viruses.

6.2 Concluding remarks

During the time of this project the field of miRNA research has come a long way, with new techniques being developed to identify targets of miRNAs and characterise their role. miRNAs are now widely identified as key players in the modulation of gene expression, and have been implicated in numerous disease states. This project has gone some way in characterising the miRNAs encoded by both the HVT and MDV-2 viruses; however more work must be done to determine their precise role. By using a number of different techniques, often in combination, targets of specific viral miRNAs have been identified. This targeting could have knock-on effects that may be important to the virus in maintaining optimal conditions for virus survival. It is clear however from the *in vivo* study that the bigger picture must be kept in mind when identifying targets of miRNAs. That is to say, that just because miRNA-mediated changes in protein abundance can be demonstrated this might not necessarily translate to a function change in phenotype of the virus.

7 References

Afonso, C. L., et al. (2001), 'The genome of turkey herpesvirus', *J Virol,* 75 (2), 971-8.

Aldridge, S. and Hadfield, J. (2012), 'Introduction to miRNA profiling technologies and cross-platform comparison', *Methods Mol Biol,* 822, 19-31.

Altuvia, Y., et al. (2005), 'Clustering and conservation patterns of human microRNAs', *Nucleic Acids Res,* 33 (8), 2697-706.

Aly, M. M., Witter, R. L., and Fadly, A. M. (1996), 'Enhancement of reticuloendotheliosis virus-induced bursal lymphomas by serotype 2 Marek's disease virus', *Avian Pathol,* 25 (1), 81-94.

Ambros, V. (2001), 'microRNAs: tiny regulators with great potential', *Cell,* 107 (7), 823-6.

Ambros, V. (2004), 'The functions of animal microRNAs', *Nature,* 431 (7006), 350-55.

Ambros, V., et al. (2003), 'A uniform system for microRNA annotation', *Rna-a Publication of the Rna Society,* 9 (3), 277-79.

Aravin, A. and Tuschl, T. (2005), 'Identification and characterization of small RNAs involved in RNA silencing', *FEBS Lett,* 579 (26), 5830-40.

Atkins, G. B. and Jain, M. K. (2007), 'Role of Kruppel-like transcription factors in endothelial biology', *Circulation Research,* 100 (12), 1686-95.

Bacon, L. D., Witter, R. L., and Fadly, A. M. (1989), 'Augmentation of retrovirus-induced lymphoid leukosis by Marek's disease herpesviruses in White Leghorn chickens', *J Virol,* 63 (2), 504-12.

Baek, D., et al. (2008), 'The impact of microRNAs on protein output', *Nature,* 455 (7209), 64-71.

Baigent, S. J., et al. (2005), 'Absolute quantitation of Marek's disease virus genome copy number in chicken feather and lymphocyte samples using real-time PCR', *J Virol Methods,* 123 (1), 53-64.

Baigent, S. J., et al. (2006), 'Herpesvirus of turkey reconstituted from bacterial artificial chromosome clones induces protection against Marek's disease', *J Gen Virol,* 87 (Pt 4), 769-76.

Baigent, S. J., et al. (2011), 'Differential quantification of cloned CVI988 vaccine strain and virulent RB-1B strain of Marek's disease viruses in chicken tissues, using real-time PCR', Research in Veterinary Science, 91 (1), 167-74.

Baigent, S. J., et al. (2013), 'Relationship between levels of very virulent MDV in poultry dust and in feather tips from vaccinated chickens', *Avian Dis,* 57 (2 Suppl), 440-7.

Bargaje, R., et al. (2012), 'Identification of Novel Targets for *miR-29*a Using miRNA Proteomics', *Plos One,* 7 (8).

Barnes, D., et al. (2008), 'Harnessing endogenous miRNAs to control virus tissue tropism as a strategy for developing attenuated virus vaccines', *Cell Host Microbe,* 4 (3), 239-48.

Beitzinger, M., et al. (2007), 'Identification of human microRNA targets from isolated argonaute protein complexes', *RNA Biol,* 4 (2), 76-84.

Bellare, P. and Ganem, D. (2009), 'Regulation of KSHV lytic switch protein expression by a virus-encoded microRNA: an evolutionary adaptation that fine-tunes lytic reactivation', *Cell Host Microbe,* 6 (6), 570-5.

Berezikov, E., Cuppen, E., and Plasterk, R. H. A. (2006), 'Approaches to microRNA discovery', *Nature Genetics,* 38, S2-S7.

Bianchi, M. E. and Agresti, A. (2005), 'HMG proteins: dynamic players in gene regulation and differentiation', *Current Opinion in Genetics & Development,* 15 (5), 496-506.

Bird, A. (2007), 'Perceptions of epigenetics', *Nature,* 447 (7143), 396-98.

Bodemann, B. O. and White, M. A. (2008), 'Ral GTPases and cancer: linchpin support of the tumorigenic platform', *Nat Rev Cancer,* 8 (2), 133-40.

Bogerd, H. P., et al. (2010), 'A Mammalian Herpesvirus Uses Noncanonical Expression and Processing Mechanisms to Generate Viral MicroRNAs', *Molecular Cell,* 37 (1), 135-42.

Boussiotis, V. A., et al. (1997), 'Maintenance of human T cell anergy: Blocking of IL-2 gene transcription by activated Rap1', *Science,* 278 (5335), 124-28.

Brennecke, J., et al. (2005), 'Principles of MicroRNA-target recognition', *Plos Biology,* 3 (3), 404-18.

Brodersen, P. and Voinnet, O. (2009), 'Revisiting the principles of microRNA target recognition and mode of action', *Nature Reviews Molecular Cell Biology,* 10 (2), 141-48.

Brousse, C., et al. (2014), 'A non-canonical plant microRNA target site', *Nucleic Acids Research,* 42 (8), 5270-9.

Bulow, V., Biggs, P. M., and Frazier, J. A. (1975), 'Characterisation of a new serotype of Marek's disease herpesvirus', in M. A. Epstein and H. Z. Hausen (eds.), *Oncogenesis and herpesvirus II* (Lyon: International Agency for Research in Cancer), 329-36.

Burnside, J., et al. (2006), 'Marek's disease virus encodes microRNAs that map to meq and the latency-associated transcript', *J Virol,* 80 (17), 8778-86.

Cai, X., et al. (2006), 'Epstein-Barr virus microRNAs are evolutionarily conserved and differentially expressed', *PLoS Pathog,* 2 (3), e23.

Cai, X., Hagedorn, C. H., and Cullen, B. R. (2004), 'Human microRNAs are processed from capped, polyadenylated transcripts that can also function as mRNAs', *Rna-a Publication of the Rna Society,* 10 (12), 1957-66.

Calin, G. A., et al. (2002), 'Frequent deletions and down-regulation of micro-RNA genes miR15 and miR16 at 13q14 in chronic lymphocytic leukemia', *Proc Natl Acad Sci U S A,* 99 (24), 15524-29.

Callister, S. J., et al. (2006), 'Normalization approaches for removing systematic biases associated with mass spectrometry and label-free proteomics', *J Proteome Res,* 5 (2), 277-86.

Calnek, B. W., et al. (1983), 'Field trials with a bivalent vaccine (HVT and SB-1) against Marek's disease', *Avian Dis,* 27 (3), 844-9.

Carey, K. D., et al. (2000), 'CD28 and the tyrosine kinase Lck stimulate mitogen-activated protein kinase activity in T cells via inhibition of the small G protein Rap1', *Molecular and Cellular Biology,* 20 (22), 8409-19.

Carsillo, M., Kim, D., and Niewiesk, S. (2010), 'Role of AKT kinase in measles virus replication', J Virol, 84 (4), 2180-3.

Chekulaeva, M. and Filipowicz, W. (2009), 'Mechanisms of miRNA-mediated post-transcriptional regulation in animal cells', *Current Opinion in Cell Biology,* 21 (3), 452-60.

Chendrimada, T. P., et al. (2005), 'TRBP recruits the Dicer complex to Ago2 for microRNA processing and gene silencing', *Nature,* 436 (7051), 740-4.

Chi, S. W., et al. (2009), 'Argonaute HITS-CLIP decodes microRNA-mRNA interaction maps', *Nature,* 460 (7254), 479-86.

Choy, E. Y., et al. (2008), 'An Epstein-Barr virus-encoded microRNA targets PUMA to promote host cell survival', *J Exp Med,* 205 (11), 2551-60.

Churchill, A. E. and Biggs, P. M. (1967), 'Agent of Marek's disease in tissue culture', *Nature,* 215 (100), 528-30.

Churchill, A. E., Payne, L. N., and Chubb, R. C. (1969), 'Immunization against Mareks Disease Using a Live Attenuated Virus', *Nature,* 221 (5182), 744-&.

Costinean, S., et al. (2006), 'Pre-B cell proliferation and lymphoblastic leukemia/high-grade lymphoma in E(mu)-miR155 transgenic mice', Proc Natl Acad Sci U S A, 103 (18), 7024-9.

Croce, C. M. (2009), 'Causes and consequences of microRNA dysregulation in cancer', *Nature Reviews Genetics,* 10 (10), 704-14.

Cullen, B. R. (2011), 'Viruses and microRNAs: RISCy interactions with serious consequences', *Genes Dev,* 25 (18), 1881-94.

Davis, B. N. and Hata, A. (2009), 'Regulation of MicroRNA Biogenesis: A miRiad of mechanisms', *Cell Commun Signal,* 7, 18.

Didiano, D. and Hobert, O. (2006), 'Perfect seed pairing is not a generally reliable predictor for miRNA-target interactions', *Nat Struct Mol Biol,* 13 (9), 849-51.

Doench, J. G. and Sharp, P. A. (2004), 'Specificity of microRNA target selection in translational repression', *Genes & Development,* 18 (5), 504-11.

Dölken, L., et al. (2010a), 'Cytomegalovirus microRNAs facilitate persistent virus infection in salivary glands', *PLoS Pathog,* 6 (10), e1001150.

Dölken, L., et al. (2010b), 'Systematic analysis of viral and cellular microRNA targets in cells latently infected with human gamma-herpesviruses by RISC immunoprecipitation assay', *Cell Host Microbe,* 7 (4), 324-34.

Du, T. T. and Zamore, P. D. (2005), 'microPrimer: The biogenesis and function of microRNA', *Development,* 132 (21), 4645-52.

Dunn, E. F. and Connor, J. H. (2012), 'HijAkt: The PI3K/Akt pathway in virus replication and pathogenesis', Prog Mol Biol Transl Sci, 106, 223-50.

Ebert, M. S., Neilson, J. R., and Sharp, P. A. (2007), 'MicroRNA sponges: competitive inhibitors of small RNAs in mammalian cells', *Nat Methods,* 4 (9), 721-6.

Elbashir, S. M., Lendeckel, W., and Tuschl, T. (2001), 'RNA interference is mediated by 21-and 22-nucleotide RNAs', *Genes & Development,* 15 (2), 188-200.

Elmen, J., et al. (2008), 'LNA-mediated microRNA silencing in non-human primates', *Nature,* 452 (7189), 896-9.

Eulalio, A., et al. (2009), 'Deadenylation is a widespread effect of miRNA regulation', *Rna-a Publication of the Rna Society,* 15 (1), 21-32.

Eulalio, A., Huntzinger, E., and Izaurralde, E. (2008), 'Getting to the root of miRNA-Mediated gene silencing', *Cell,* 132 (1), 9-14.

Fabbri, M., et al. (2007), 'MicroRNA-29 family reverts aberrant methylation in lung cancer by targeting DNA methyltransferases 3A and 3B', *Proc Natl Acad Sci U S A,* 104 (40), 15805-10.

Feederle, R., Bartlett, E. J., and Delecluse, H. J. (2010), 'Epstein-Barr virus genetics: talking about the BAC generation', *Herpesviridae,* 1 (1), 6.

Feederle, R., et al. (2011), 'A viral microRNA cluster strongly potentiates the transforming properties of a human herpesvirus', *PLoS Pathog,* 7 (2), e1001294.

Fei, J., et al. (2012), 'miR-181a post-transcriptionally downregulates oncogenic RalA and contributes to growth inhibition and apoptosis in chronic myelogenous leukemia (CML)', *Plos One,* 7 (3), e32834.

Felli, N., et al. (2005), 'MicroRNAs 221 and 222 inhibit normal erythropoiesis and erythroleukemic cell growth via kit receptor down-modulation', Proc Natl Acad Sci U S A, 102 (50), 18081-6.

Filipowicz, W., Bhattacharyya, S. N., and Sonenberg, N. (2008), 'Mechanisms of post-transcriptional regulation by microRNAs: are the answers in sight?', *Nature Reviews Genetics,* 9 (2), 102-14.

Forman, J. J., Legesse-Miller, A., and Coller, H. A. (2008), 'A search for conserved sequences in coding regions reveals that the let-7 microRNA targets Dicer within its coding sequence', *Proceedings of the National Academy of Sciences of the United States of America,* 105 (39), 14879-84.

Friedman, R. C., et al. (2009), 'Most mammalian mRNAs are conserved targets of microRNAs', *Genome Research,* 19 (1), 92-105.

Fynan, E., et al. (1992), 'Persistence of Marek's disease virus in a subpopulation of B cells that is transformed by avian leukosis virus, but not in normal bursal B cells', *J Virol,* 66 (10), 5860-6.

Gallaher, A. M., et al. (2013), 'Proteomic screening of human targets of viral microRNAs reveals functions associated with immune evasion and angiogenesis', *PLoS Pathog,* 9 (9), e1003584.

Gao, H. B., et al. (2011), 'Expression of HA of HPAI H5N1 Virus at US2 Gene Insertion Site of Turkey Herpesvirus Induced Better Protection than That at US10 Gene Insertion Site', *Plos One,* 6 (7).

Garofalo, M., et al. (2009), 'miR-221&222 regulate TRAIL resistance and enhance tumorigenicity through PTEN and TIMP3 downregulation', Cancer Cell, 16 (6), 498-509.

Garzon, R., et al. (2009), 'MicroRNA-29b induces global DNA hypomethylation and tumor suppressor gene reexpression in acute myeloid leukemia by targeting directly DNMT3A and 3B and indirectly DNMT1', *Blood,* 113 (25), 6411-8.

Gebeshuber, C. A., Zatloukal, K., and Martinez, J. (2009), '*miR-29*a suppresses tristetraprolin, which is a regulator of epithelial polarity and metastasis', *Embo Reports,* 10 (4), 400-05.

Giraldez, A. J., et al. (2006), 'Zebrafish MiR-430 promotes deadenylation and clearance of maternal mRNAs', *Science,* 312 (5770), 75-79.

Gnanasekar, M., Thirugnanam, S., and Ramaswamy, K. (2009), 'Short hairpin RNA (shRNA) constructs targeting high mobility group box-1 (HMGB1) expression leads to inhibition of prostate cancer cell survival and apoptosis', *Int J Oncol,* 34 (2), 425-31.

Goher, M., Hicks, J. A., and Liu, H. C. (2013), 'The interplay between MDV and HVT affects viral miRNa expression', *Avian Dis,* 57 (2 Suppl), 372-9.

Gottwein, E. and Cullen, B. R. (2008), 'Viral and cellular MicroRNAs as determinants of viral pathogenesis and immunity', *Cell Host Microbe,* 3 (6), 375-87.

Gregory, R. I., et al. (2005), 'Human RISC couples microRNA biogenesis and posttranscriptional gene silencing', *Cell,* 123 (4), 631-40.

Grey, F., et al. (2005), 'Identification and characterization of human cytomegalovirus-encoded microRNAs', *J Virol,* 79 (18), 12095-9.

Griffiths-Jones, S. (2004), 'The microRNA Registry', *Nucleic Acids Res,* 32 (Database issue), D109-11.

Griffiths-Jones, S., et al. (2006), 'miRBase: microRNA sequences, targets and gene nomenclature', *Nucleic Acids Res,* 34 (Database issue), D140-4.

Griffiths-Jones, S., et al. (2008), 'miRBase: tools for microRNA genomics', *Nucleic Acids Res,* 36 (Database issue), D154-8.

Grishok, A., et al. (2001), 'Genes and mechanisms related to RNA interference regulate expression of the small temporal RNAs that control C. elegans developmental timing', *Cell,* 106 (1), 23-34.

Grundhoff, A. and Sullivan, C. S. (2011), 'Virus-encoded microRNAs', *Virology,* 411 (2), 325-43.

Guo, H. L., et al. (2010), 'Mammalian microRNAs predominantly act to decrease target mRNA levels', *Nature,* 466 (7308), 835-U66.

Guo, L. and Lu, Z. (2010), 'The fate of miRNA* strand through evolutionary analysis: implication for degradation as merely carrier strand or potential regulatory molecule?', *Plos One,* 5 (6), e11387.

Guo, Z. S., et al. (2013), 'Life after death: targeting high mobility group box 1 in emergent cancer therapies', *Am J Cancer Res,* 3 (1), 1-20.

Hafner, M., et al. (2010), 'Transcriptome-wide Identification of RNA-Binding Protein and MicroRNA Target Sites by PAR-CLIP', *Cell,* 141 (1), 129-41.

Han, Y. C., et al. (2010), 'microRNA-29a induces aberrant self-renewal capacity in hematopoietic progenitors, biased myeloid development, and acute myeloid leukemia', *Journal of Experimental Medicine,* 207 (3), 475-89.

Hatfield, S. D., et al. (2005), 'Stem cell division is regulated by the microRNA pathway', *Nature,* 435 (7044), 974-8.

Hausser, J., et al. (2013), 'Analysis of CDS-located miRNA target sites suggests that they can effectively inhibit translation', *Genome Research,* 23 (4), 604-15.

He, L. and Hannon, G. J. (2004), 'MicroRNAs: small RNAs with a big role in gene regulation', *Nature Reviews Genetics,* 5 (7), 522-31.

Helwak, A., et al. (2013), 'Mapping the human miRNA interactome by CLASH reveals frequent noncanonical binding', Cell, 153 (3), 654-65.

Hendrickson, D. G., et al. (2008), 'Systematic identification of mRNAs recruited to argonaute 2 by specific microRNAs and corresponding changes in transcript abundance', *Plos One,* 3 (5), e2126.

Hers, I., Vincent, E. E., and Tavare, J. M. (2011), 'Akt signalling in health and disease', *Cellular Signalling,* 23 (10), 1515-27.

Hsu, S. D., et al. (2011), 'miRTarBase: a database curates experimentally validated microRNA-target interactions', *Nucleic Acids Res,* 39 (Database issue), D163-9.

Hu, H. G., et al. (2007), 'The distribution of the DEK protein in mammalian chromatin', *Biochem Biophys Res Commun,* 358 (4), 1008-14.

Hunter, S. E., et al. (2013), 'Functional Genomic Analysis of the let-7 Regulatory Network in Caenorhabditis elegans', *PLoS Genet,* 9 (3), e1003353.

Huntzinger, E. and Izaurralde, E. (2011), 'Gene silencing by microRNAs: contributions of translational repression and mRNA decay', *Nature Reviews Genetics,* 12 (2), 99-110.
Imamura, T., et al. (2001), 'Interaction with p53 enhances binding of cisplatin-modified DNA by high mobility group 1 protein', *Journal of Biological Chemistry,* 276 (10), 7534-40.
Islam, A. and Walkden-Brown, S. W. (2007), 'Quantitative profiling of the shedding rate of the three Marek's disease virus (MDV) serotypes reveals that challenge with virulent MDV markedly increases shedding of vaccinal viruses', *J Gen Virol,* 88 (Pt 8), 2121-8.
Islam, A., et al. (2004), 'Differential amplification and quantitation of Marek's disease viruses using real-time polymerase chain reaction', J Virol Methods, 119 (2), 103-13.
Jarosinski, K. W., et al. (2007), 'Horizontal transmission of Marek's disease virus requires US2, the UL13 protein kinase, and gC', *J Virol,* 81 (19), 10575-87.
Jha, A. and Shankar, R. (2013), 'miReader: Discovering Novel miRNAs in Species without Sequenced Genome', *Plos One,* 8 (6), e66857.
Jiang, S. A., et al. (2010), 'MicroRNA-155 Functions as an OncomiR in Breast Cancer by Targeting the Suppressor of Cytokine Signaling 1 Gene', *Cancer Res,* 70 (8), 3119-27.
Jiang, S., et al. (2010), 'MicroRNA-155 functions as an OncomiR in breast cancer by targeting the suppressor of cytokine signaling 1 gene', *Cancer Res,* 70 (8), 3119-27.
Jones, D., et al. (1992), 'Marek Disease Virus Encodes a Basic-Leucine Zipper Gene Resembling the Fos/Jun Oncogenes That Is Highly Expressed in Lymphoblastoid Tumors', *Proc Natl Acad Sci U S A,* 89 (9), 4042-46.
Jovanovic, M., et al. (2010), 'A quantitative targeted proteomics approach to validate predicted microRNA targets in C. elegans', *Nat Methods,* 7 (10), 837-42.
Jurak, I., et al. (2010), 'Numerous conserved and divergent microRNAs expressed by herpes simplex viruses 1 and 2', *J Virol,* 84 (9), 4659-72.
Kappes, F., et al. (2004), 'Phosphorylation by protein kinase CK2 changes the DNA binding properties of the human chromatin protein DEK', *Molecular and Cellular Biology,* 24 (13), 6011-20.
Kelly, E. J., et al. (2008), 'Engineering microRNA responsiveness to decrease virus pathogenicity', *Nat Med,* 14 (11), 1278-83.
Kertesz, M., et al. (2007), 'The role of site accessibility in microRNA target recognition', *Nature Genetics,* 39 (10), 1278-84.
Khvorova, A., Reynolds, A., and Jayasena, S. D. (2003), 'Functional siRNAs and miRNAs exhibit strand bias (vol 115, pg 209, 2003)', *Cell,* 115 (4), 505-05.
Kim, V. N. (2005), 'MicroRNA biogenesis: coordinated cropping and dicing', *Nat Rev Mol Cell Biol,* 6 (5), 376-85.
Kincaid, R. P. and Sullivan, C. S. (2012), 'Virus-encoded microRNAs: an overview and a look to the future', *PLoS Pathog,* 8 (12), e1003018.
Kincaid, R. P., Burke, J. M., and Sullivan, C. S. (2012), 'RNA virus microRNA that mimics a B-cell oncomiR', *Proc Natl Acad Sci U S A,* 109 (8), 3077-82.
Kitayama, H., et al. (1989), 'A Ras-Related Gene with Transformation Suppressor Activity', *Cell,* 56 (1), 77-84.
Klase, Z. A., Sampey, G. C., and Kashanchi, F. (2013), 'Retrovirus infected cells contain viral microRNAs', *Retrovirology,* 10.
Klune, J. R., et al. (2008), 'HMGB1: Endogenous danger signaling', *Molecular Medicine,* 14 (7-8), 476-84.
Knight, S. W. and Bass, B. L. (2001), 'A role for the RNase III enzyme DCR-1 in RNA interference and germ line development in Caenorhabditis elegans', *Science,* 293 (5538), 2269-71.
Kozomara, A. and Griffiths-Jones, S. (2011), 'miRBase: integrating microRNA annotation and deep-sequencing data', *Nucleic Acids Res,* 39 (Database issue), D152-7.
Kriegel, A. J., et al. (2012), 'The *miR-29* family: genomics, cell biology, and relevance to renal and cardiovascular injury', *Physiol Genomics,* 44 (4), 237-44.
Krutzfeldt, J., et al. (2005), 'Silencing of microRNAs in vivo with 'antagomirs'', *Nature,* 438 (7068), 685-89.

Lai, E. C. (2002), 'Micro RNAs are complementary to 3 ' UTR sequence motifs that mediate negative post-transcriptional regulation', *Nature Genetics,* 30 (4), 363-64.
Landthaler, M., et al. (2008), 'Molecular characterization of human Argonaute-containing ribonucleoprotein complexes and their bound target mRNAs', *Rna-a Publication of the Rna Society,* 14 (12), 2580-96.
Le, M. T. N., et al. (2009), 'MicroRNA-125b is a novel negative regulator of p53', *Genes Dev,* 23 (7), 862-76.
Lee, L. F., et al. (2008), 'Recombinant Marek's disease virus (MDV) lacking the Meq oncogene confers protection against challenge with a very virulent plus strain of MDV', *Vaccine,* 26 (15), 1887-92.
Lee, L. F., Liu, X., and Witter, R. L. (1983), 'Monoclonal antibodies with specificity for three different serotypes of Marek's disease viruses in chickens', *Journal of Immunology,* 130 (2), 1003-6.
Lee, R. C., Feinbaum, R. L., and Ambros, V. (1993), 'The C. elegans heterochronic gene lin-4 encodes small RNAs with antisense complementarity to lin-14', *Cell,* 75 (5), 843-54.
Lee, S. H., et al. (2012), 'BclAF1 restriction factor is neutralized by proteasomal degradation and microRNA repression during human cytomegalovirus infection', *Proc Natl Acad Sci U S A,* 109 (24), 9575-80.
Lee, Y. S., et al. (2004b), 'Distinct roles for Drosophila Dicer-1 and Dicer-2 in the siRNA/miRNA silencing pathways', *Cell,* 117 (1), 69-81.
Lee, Y., et al. (2003), 'The nuclear RNase III Drosha initiates microRNA processing', *Nature,* 425 (6956), 415-9.
Lee, Y., et al. (2004a), 'MicroRNA genes are transcribed by RNA polymerase II', *Embo J,* 23 (20), 4051-60.
Lewis, B. P., Burge, C. B., and Bartel, D. P. (2005), 'Conserved seed pairing, often flanked by adenosines, indicates that thousands of human genes are microRNA targets', *Cell,* 120 (1), 15-20.
Lim, L. P., et al. (2003), 'Vertebrate microRNA genes', *Science,* 299 (5612), 1540.
Lim, L. P., et al. (2005), 'Microarray analysis shows that some microRNAs downregulate large numbers of target mRNAs', *Nature,* 433 (7027), 769-73.
Lin, X., et al. (2011), 'miR-K12-7-5p encoded by Kaposi's sarcoma-associated herpesvirus stabilizes the latent state by targeting viral ORF50/RTA', *Plos One,* 6 (1), e16224.
Lu, C. C., et al. (2010), 'MicroRNAs encoded by Kaposi's sarcoma-associated herpesvirus regulate viral life cycle', *Embo Reports,* 11 (10), 784-90.
Lu, S. H. and Cullen, B. R. (2004), 'Adenovirus VA1 noncoding RNA can inhibit small interfering RNA and microRNA biogenesis', *J Virol,* 78 (23), 12868-76.
Lubbert, M. (2000), 'DNA methylation inhibitors in the treatment of leukemias, myelodysplastic syndromes and hemoglobinopathies: Clinical results and possible mechanisms of action', *DNA Methylation and Cancer,* 249, 135-64.
Lund, E., et al. (2004), 'Nuclear export of microRNA precursors', *Science,* 303 (5654), 95-8.
Lupiani, B., et al. (2004), 'Marek's disease virus-encoded Meq gene is involved in transformation of lymphocytes but is dispensable for replication', *Proc Natl Acad Sci U S A,* 101 (32), 11815-20.
Ma, F., et al. (2011), 'The microRNA miR-29 controls innate and adaptive immune responses to intracellular bacterial infection by targeting interferon-gamma', Nature Immunology, 12 (9), 861-9.
Marek, J. (1907), 'Multiple Nervenentzundung (polyneuritis) bei Huhnern. Dtsch Tie'.
Marquitz, A. R., et al. (2011), 'The Epstein-Barr Virus BART microRNAs target the pro-apoptotic protein Bim', *Virology,* 412 (2), 392-400.
Mathonnet, G., et al. (2007), 'MicroRNA inhibition of translation initiation in vitro by targeting the cap-binding complex eIF4F', *Science,* 317 (5845), 1764-67.
Meijer, H. A., et al. (2013), 'Translational repression and eIF4A2 activity are critical for microRNA-mediated gene regulation', *Science,* 340 (6128), 82-5.

Mi, H., Muruganujan, A., and Thomas, P. D. (2013), 'PANTHER in 2013: modeling the evolution of gene function, and other gene attributes, in the context of phylogenetic trees', *Nucleic Acids Research,* 41 (Database issue), D377-86.

Mili, S. and Steitz, J. A. (2004), 'Evidence for reassociation of RNA-binding proteins after cell lysis: Implications for the interpretation of immunoprecipitation analyses', *Rna-a Publication of the Rna Society,* 10 (11), 1692-94.

Moore, P. S. and Chang, Y. (2010), 'Why do viruses cause cancer? Highlights of the first century of human tumour virology', *Nat Rev Cancer,* 10 (12), 878-89.

Morgan, R. W. and Burnside, J. (2011), 'Roles of avian herpesvirus microRNAs in infection, latency, and oncogenesis', Biochim Biophys Acta, 1809 (11-12), 654-9.

Mott, J. L., et al. (2007), '*miR-29* regulates Mcl-1 protein expression and apoptosis', *Oncogene,* 26 (42), 6133-40.

Nachmani, D., et al. (2009), 'Diverse herpesvirus microRNAs target the stress-induced immune ligand MICB to escape recognition by natural killer cells', *Cell Host Microbe,* 5 (4), 376-85.

Noonan, E. J., et al. (2009), 'miR-449a targets HDAC-1 and induces growth arrest in prostate cancer', *Oncogene,* 28 (14), 1714-24.

Okano, M., et al. (1999), 'DNA methyltransferases Dnmt3a and Dnmt3b are essential for de novo methylation and mammalian development', *Cell,* 99 (3), 247-57.

Olsen, P. H. and Ambros, V. (1999), 'The lin-4 regulatory RNA controls developmental timing in Caenorhabditis elegans by blocking LIN-14 protein synthesis after the initiation of translation', *Developmental Biology,* 216 (2), 671-80.

Ossowski, S., Schwab, R., and Weigel, D. (2008), 'Gene silencing in plants using artificial microRNAs and other small RNAs', *Plant Journal,* 53 (4), 674-90.

Oxford, G., et al. (2005), 'RalA and RalB: antagonistic relatives in cancer cell migration', *Cancer Res,* 65 (16), 7111-20.

Parnas, O., Corcoran, D. L., and Cullen, B. R. (2014), 'Analysis of the mRNA Targetome of MicroRNAs Expressed by Marek's Disease Virus', *MBio,* 5 (1).

Pasquinelli, A. E. (2012), 'MicroRNAs and their targets: recognition, regulation and an emerging reciprocal relationship', *Nature Reviews Genetics,* 13 (4), 271-82.

Pasquinelli, A. E., et al. (2000), 'Conservation of the sequence and temporal expression of let-7 heterochronic regulatory RNA', *Nature,* 408 (6808), 86-9.

Pekarsky, Y. and Croce, C. M. (2010), 'Is *miR-29* an Oncogene or Tumor Suppressor in CLL?', *Oncotarget,* 1 (3), 224-27.

Petersen, C. P., et al. (2006), 'Short RNAs repress translation after initiation in mammalian cells', *Molecular Cell,* 21 (4), 533-42.

Petherbridge, L., et al. (2009), 'Cloning of Gallid herpesvirus 3 (Marek's disease virus serotype-2) genome as infectious bacterial artificial chromosomes for analysis of viral gene functions', *J Virol Methods,* 158 (1-2), 11-7.

Piao, X. H., et al. (2010), 'CCR4-NOT Deadenylates mRNA Associated with RNA-Induced Silencing Complexes in Human Cells', *Molecular and Cellular Biology,* 30 (6), 1486-94.

Pratt, Z. L., et al. (2009), 'The microRNAs of Epstein-Barr Virus are expressed at dramatically differing levels among cell lines', *Virology,* 386 (2), 387-97.

Ramalingam, D., Kieffer-Kwon, P., and Ziegelbauer, J. M. (2012), 'Emerging themes from EBV and KSHV microRNA targets', *Viruses,* 4 (9), 1687-710.

Rehmsmeier, M., et al. (2004), 'Fast and effective prediction of microRNA/target duplexes', *Rna-a Publication of the Rna Society,* 10 (10), 1507-17.

Reinhart, B. J., et al. (2000), 'The 21-nucleotide let-7 RNA regulates developmental timing in Caenorhabditis elegans', *Nature,* 403 (6772), 901-6.

Rengaraj, D., et al. (2011), 'Expression patterns and miRNA regulation of DNA methyltransferases in chicken primordial germ cells', *Plos One,* 6 (5), e19524.

Riley, K. J., et al. (2012), 'EBV and human microRNAs co-target oncogenic and apoptotic viral and human genes during latency', *EMBO J,* 31 (9), 2207-21.

Rispens, B. H., et al. (1972), 'Control of Marek's disease in the Netherlands. I. Isolation of an avirulent Marek's disease virus (strain CVI 988) and its use in laboratory vaccination trials', *Avian Dis,* 16 (1), 108-25.

Sarnow, P., et al. (2006), 'MicroRNAs: expression, avoidance and subversion by vertebrate viruses', *Nat Rev Microbiol,* 4 (9), 651-9.

Sato, F., et al. (2011), 'MicroRNAs and epigenetics', *Febs Journal,* 278 (10), 1598-609.

Schat, K. A. and Calnek, B. W. (1978), 'Protection against Marek's disease-derived tumor transplants by the nononcogenic SB-1 strain of Marek's disease virus', *Infect Immun,* 22 (1), 225-32.

Schmitt, M. J., et al. (2012), 'miRNA-29: A microRNA Family with Tumor-Suppressing and Immune-Modulating Properties', *Curr Mol Med*.

Schmitter, D., et al. (2006), 'Effects of Dicer and Argonaute down-regulation on mRNA levels in human HEK293 cells', *Nucleic Acids Research,* 34 (17), 4801-15.

Schneider, C. A., Rasband, W. S., and Eliceiri, K. W. (2012), 'NIH Image to ImageJ: 25 years of image analysis', *Nat Methods,* 9 (7), 671-5.

Sebzda, E., et al. (2002), 'Rap1A positively regulates T cells via integrin activation rather than inhibiting lymphocyte signaling', *Nature Immunology,* 3 (3), 251-58.

Seggerson, K., Tang, L. J., and Moss, E. G. (2002), 'Two genetic circuits repress the Caenorhabditis elegans heterochronic gene lin-28 after translation initiation', *Developmental Biology,* 243 (2), 215-25.

Selbach, M., et al. (2008), 'Widespread changes in protein synthesis induced by microRNAs', *Nature,* 455 (7209), 58-63.

Shirdel, E. A., et al. (2011), 'NAViGaTing the micronome--using multiple microRNA prediction databases to identify signalling pathway-associated microRNAs', *Plos One,* 6 (2), e17429.

Singh, S. M., et al. (2010), 'Comparative efficacy of BAC-derived recombinant SB-1 vaccine and the parent wild type strain in preventing replication, shedding and disease induced by virulent Marek's disease virus', *Research in Veterinary Science,* 89 (1), 140-5.

Skalsky, R. L. and Cullen, B. R. (2010), 'Viruses, microRNAs, and host interactions', *Annu Rev Microbiol,* 64, 123-41.

Skalsky, R. L., et al. (2007), 'Kaposi's sarcoma-associated herpesvirus encodes an ortholog of miR-155', *J Virol,* 81 (23), 12836-45.

Skalsky, R. L., et al. (2012), 'The Viral and Cellular MicroRNA Targetome in Lymphoblastoid Cell Lines', *PLoS Pathog,* 8 (1).

Sullivan, C. S. (2008), 'New roles for large and small viral RNAs in evading host defences', *Nature Reviews Genetics,* 9 (7), 503-7.

Sullivan, C. S., et al. (2005), 'SV40-encoded microRNAs regulate viral gene expression and reduce susceptibility to cytotoxic T cells', *Nature,* 435 (7042), 682-6.

Taby, R. and Issa, J. P. J. (2010), 'Cancer Epigenetics', *Ca-a Cancer Journal for Clinicians,* 60 (6), 376-92.

Thermann, R. and Hentze, M. W. (2007), 'Drosophila miR2 induces pseudo-polysomes and inhibits translation initiation', *Nature,* 447 (7146), 875-78.

Thomas, M., Lieberman, J., and Lal, A. (2010), 'Desperately seeking microRNA targets', *Nat Struct Mol Biol,* 17 (10), 1169-74.

Thomson, D. W., Bracken, C. P., and Goodall, G. J. (2011), 'Experimental strategies for microRNA target identification', *Nucleic Acids Research,* 39 (16), 6845-53.

Umbach, J. L., et al. (2009), 'Analysis of Human Alphaherpesvirus MicroRNA Expression in Latently Infected Human Trigeminal Ganglia', *J Virol,* 83 (20), 10677-83.

van Rooij, E., et al. (2006), 'A signature pattern of stress-responsive microRNAs that can evoke cardiac hypertrophy and heart failure', *Proc Natl Acad Sci U S A,* 103 (48), 18255-60.

Vonlindern, M., et al. (1992), 'The Translocation (6-9), Associated with a Specific Subtype of Acute Myeloid-Leukemia, Results in the Fusion of 2 Genes, Dek and Can, and the Expression of a

Chimeric, Leukemia-Specific Dek-Can Messenger-Rna', *Molecular and Cellular Biology,* 12 (4), 1687-97.

Voortman, J., et al. (2010), 'MicroRNA expression and clinical outcomes in patients treated with adjuvant chemotherapy after complete resection of non-small cell lung carcinoma', *Cancer Res,* 70 (21), 8288-98.

Waidner, L. A., et al. (2009), 'MicroRNAs of Gallid and Meleagrid herpesviruses show generally conserved genomic locations and are virus-specific', *Virology,* 388 (1), 128-36.

Wastling, J. M., et al. (2012), 'Parasites, proteomes and systems: has Descartes' clock run out of time?', *Parasitology,* 139 (9), 1103-18.

Wei, W., et al. (2013), '*miR-29* targets Akt3 to reduce proliferation and facilitate differentiation of myoblasts in skeletal muscle development', *Cell Death Dis,* 4, e668.

Witter, R. L. (1997), 'Increased virulence of Marek's disease virus field isolates', *Avian Dis,* 41 (1), 149-63.

Witter, R. L. (2001), 'Protective efficacy of Marek's disease vaccines', *Curr Top Microbiol Immunol,* 255, 57-90.

Witter, R. L. and Lee, L. F. (1984), 'Polyvalent Marek's disease vaccines: safety, efficacy and protective synergism in chickens with maternal antibodies', *Avian Pathol,* 13 (1), 75-92.

Witter, R. L., et al. (1970), 'Isolation from turkeys of a cell-associated herpesvirus antigenically related to Marek's disease virus', *Am J Vet Res,* 31 (3), 525-38.

Wright, G. L., et al. (2008), 'VEGF stimulation of mitochondrial biogenesis: requirement of AKT3 kinase', *Faseb Journal,* 22 (9), 3264-75.

Xiao, F. F., et al. (2009), 'miRecords: an integrated resource for microRNA-target interactions', *Nucleic Acids Research,* 37, D105-D10.

Xu, S., et al. (2011), 'Marek's disease virus type 1 microRNA miR-M3 suppresses cisplatin-induced apoptosis by targeting Smad2 of the transforming growth factor beta signal pathway', *J Virol,* 85 (1), 276-85.

Yao, Y. X., et al. (2007), 'Marek's disease virus type 2 (MDV-2)-encoded microRNAs show no sequence conservation with those encoded by MDV-1', *J Virol,* 81 (13), 7164-70.

Yao, Y. X., et al. (2008), 'MicroRNA profile of Marek's disease virus-transformed T-cell line MSB-1: Predominance of virus-encoded microRNAs', *J Virol,* 82 (8), 4007-15.

Yao, Y. X., et al. (2009), 'Novel MicroRNAs (miRNAs) Encoded by Herpesvirus of Turkeys: Evidence of miRNA Evolution by Duplication', *J Virol,* 83 (13), 6969-73.

Yee, J., et al. (2011), 'Latent Epstein-Barr virus can inhibit apoptosis in B cells by blocking the induction of NOXA expression', *Plos One,* 6 (12), e28506.

Yekta, S., Shih, I. H., and Bartel, D. P. (2004), 'MicroRNA-directed cleavage of HOXB8 mRNA', *Science,* 304 (5670), 594-96.

Yeom, K. H., et al. (2006), 'Characterization of DGCR8/Pasha, the essential cofactor for Drosha in primary miRNA processing', *Nucleic Acids Res,* 34 (16), 4622-9.

Yi, R., et al. (2003), 'Exportin-5 mediates the nuclear export of pre-microRNAs and short hairpin RNAs', *Genes Dev,* 17 (24), 3011-6.

Yu, Z. H., et al. (2014), 'Virus-encoded miR-155 ortholog is an important potential regulator but not essential for the development of lymphomas induced by very virulent Marek's disease virus', *Virology,* 448, 55-64.

Yue, D., Liu, H., and Huang, Y. F. (2009), 'Survey of Computational Algorithms for MicroRNA Target Prediction', *Current Genomics,* 10 (7), 478-92.

Zhang, Y. and Verbeek, F. J. (2010), 'Comparison and integration of target prediction algorithms for microRNA studies', *J Integr Bioinform,* 7 (3).

Zhao, J. J., et al. (2010), 'microRNA expression profile and identification of *miR-29* as a prognostic marker and pathogenetic factor by targeting CDK6 in mantle cell lymphoma', *Blood,* 115 (13), 2630-39.

Zhao, Y., et al. (2008), 'Self-excision of the BAC sequences from the recombinant Marek's disease virus genome increases replication and pathogenicity', *Virol J,* 5, 19.
Zhao, Y., et al. (2009), 'A functional MicroRNA-155 ortholog encoded by the oncogenic Marek's disease virus', *J Virol,* 83 (1), 489-92.
Zhao, Y., et al. (2011), 'Critical role of the virus-encoded microRNA-155 ortholog in the induction of Marek's disease lymphomas', *PLoS Pathog,* 7 (2), e1001305.
Zhou, X., et al. (2009), 'Abundant conserved microRNA target sites in the 5'-untranslated region and coding sequence', *Genetica,* 137 (2), 159-64.
Zhu, H., et al. (2011), 'The Lin28/let-7 Axis Regulates Glucose Metabolism', *Cell,* 147 (1), 81-94.
Ziegelbauer, J. M., et al. (2009), 'Tandem array-based expression screens identify host mRNA targets of virus-encoded microRNAs', *Nature Genetics,* 41 (1), 130-4.

8 Appendices

8.1 Appendix 1 – Methodology of power calculations to determine chicken group sizes, provided by Sue Baigent

We are ethically bound to follow the '3R' principles, particularly in reducing the numbers of animals used for experiments, where possible, but without compromising the validity of the research findings.

The number of birds in each group was determined using 'power of experiment' calculations based on q-PCR data (means & standard deviations) from previous experiments, using the same breed of chicken (Rhode Island Red), and the same strain of challenge virus (RB-1B), in order to demonstrate a statistically significant difference at a "p" value of 0.05 and a power of 80%.

Using data obtained from previous pilot experiments the following equation was used to determine sample size to achieve the parameters described above:

$$\mathbf{(((Group\ 1\ SD)^2 + (Group\ 2\ SD)^2) \times 7.8) \div (\bar{x}\ Group\ 1 - \bar{x}\ Group\ 2)^2}$$

Group 1 and 2 = 2 groups of chickens in previously performed pilot study (by Sue Baigent) comparing protection provided to RB-1B challenge virus by pHVT3 vaccine

SD = Standard deviation

$\bar{x}$ = Sample mean

7.8 = A result of $(z(\alpha/2) + z(\beta))^2$ – a calculation taking the desired P value 0.05 – $\alpha/2$ and Power 80% - β

For this particular study:

$(((0.523)^2 + (0.463)^2) \times 7.8) \div (2 - 2.68)^2 = 8.23$ – *Rounded to a sample size of 8*

A simplified Excel spreadsheet that performs the above calculation can be downloaded from:

http://tinyurl.com/animal-sample-size-calculator

8.2 Appendix 2 – Evidence for the presence of internal promoter in 4.6kb HVT miRNA 'cassette', following detection of *hvt-miR-H15* in cells transfected with the HVT-miR-H1-H18 cassette in a promoter-less vector – (page 151)

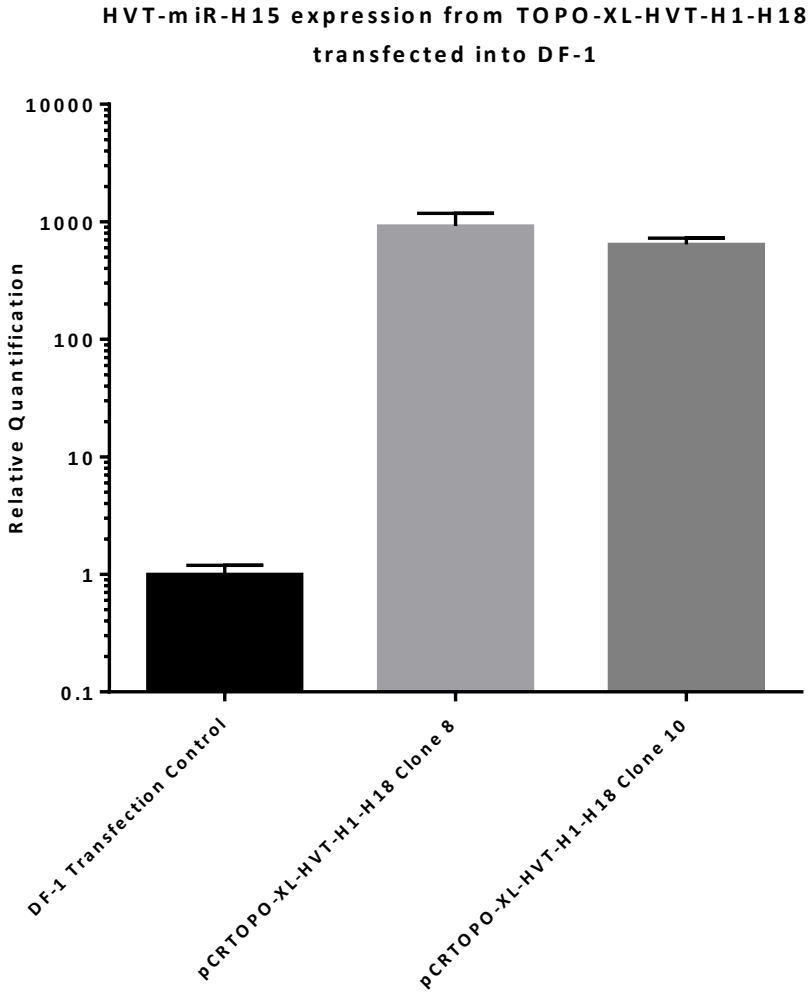


Figure 49 - TaqMan analysis of *hvt-miR-H15* expression from DF-1 cells transfected with different clones of the promoter-less TOPO-XL-HVT-H1-H18 vector. Quantification levels are relative to *hvt-miR-H15* expression from DF-1 cells transfected with empty TOPO-XL vector. Error bars show maximum and minimum relative quantification (RQ) values as calculated by 7500 Fast software (Applied Biosystems) from Ct values, normalised to gga-miR-let7a.

8.3 Appendix 3 – Full dataset of TargetScan predicted targets of MDV-2 and HVT encoded miRNAs

A full dataset of the transcripts predicted, by the TargetScan custom program, to be targeted by the MDV-2 and HVT encoded miRNAs can be downloaded in an excel spreadsheet from the links below:

MDV-2 predicted targets:

https://drive.google.com/file/d/0B6tx56cTGYTVTG93VWp4VlIwNTQ/view?usp=sharing

HVT predicted targets:

https://drive.google.com/file/d/0B6tx56cTGYTVa0Yxd2JQcm53QWc/view?usp=sharing

8.4 Appendix 4 - Full dataset from proteomic analysis of DF-1 cells following stable transfection with either pRTS-HVT-miR-H1-H18 or pRTS-empty

Full proteomic data set containing the relative abundance of all 362 proteins with statistical analysis between replicate runs can be downloaded from the link below:

https://drive.google.com/file/d/0B6tx56cTGYTVd0xyNnpfekR3MkE/edit?usp=sharing

8.5 Appendix 5 – Statistical Analysis of dual-luciferase assay analysis of predicted viral miRNA targeting of host genes

Tukey's multiple comparisons test	Mean Diff.	95% CI of diff.	Significant?	Summary
CTBP1 hvt-miR-H7				
pEF6-miR Wild-Type 3'UTR vs. pEF6-miR Mutant 3'UTR	-19.8	-32.00 to -7.609	Yes	***
pEF6-miR Wild-Type 3'UTR vs. pEF6-empty Wild-Type 3'UTR	-13.88	-26.07 to -1.685	Yes	*
pEF6-miR Wild-Type 3'UTR vs. pEF6-empty Mutant 3'UTR	-19.8	-32.00 to -7.609	Yes	***
pEF6-miR Mutant 3'UTR vs. pEF6-empty Wild-Type 3'UTR	5.924	-6.270 to 18.12	No	ns
pEF6-miR Mutant 3'UTR vs. pEF6-empty Mutant 3'UTR	0	-12.19 to 12.19	No	ns
pEF6-empty Wild-Type 3'UTR vs. pEF6-empty Mutant 3'UTR	-5.924	-18.12 to 6.270	No	ns
JUN hvt-miR-H12				
pEF6-miR Wild-Type 3'UTR vs. pEF6-miR Mutant 3'UTR	-7.498	-20.67 to 5.672	No	ns
pEF6-miR Wild-Type 3'UTR vs. pEF6-empty Wild-Type 3'UTR	9.282	-2.911 to 21.48	No	ns
pEF6-miR Wild-Type 3'UTR vs. pEF6-empty Mutant 3'UTR	-7.498	-20.67 to 5.672	No	ns
pEF6-miR Mutant 3'UTR vs. pEF6-empty Wild-Type 3'UTR	16.78	3.610 to 29.95	Yes	**
pEF6-miR Mutant 3'UTR vs. pEF6-empty Mutant 3'UTR	0	-14.08 to 14.08	No	ns
pEF6-empty Wild-Type 3'UTR vs. pEF6-empty Mutant 3'UTR	-16.78	-29.95 to -3.610	Yes	**
AKT3 mdv2-miR-M21				
pEF6-miR Wild-Type 3'UTR vs. pEF6-miR Mutant 3'UTR	-59.14	-72.31 to -45.97	Yes	****
pEF6-miR Wild-Type 3'UTR vs. pEF6-empty Wild-Type 3'UTR	-12.02	-24.22 to 0.1714	No	ns
pEF6-miR Wild-Type 3'UTR vs. pEF6-empty Mutant 3'UTR	-59.14	-72.31 to -45.97	Yes	****
pEF6-miR Mutant 3'UTR vs. pEF6-empty Wild-Type 3'UTR	47.12	33.95 to 60.29	Yes	****
pEF6-miR Mutant 3'UTR vs. pEF6-empty Mutant 3'UTR	0	-14.08 to 14.08	No	ns
pEF6-empty Wild-Type 3'UTR vs. pEF6-empty Mutant 3'UTR	-47.12	-60.29 to -33.95	Yes	****
RALA mdv2-miR-M22				
pEF6-miR Wild-Type 3'UTR vs. pEF6-miR Mutant 3'UTR	-49.19	-62.36 to -36.02	Yes	****
pEF6-miR Wild-Type 3'UTR vs. pEF6-empty Wild-Type 3'UTR	-49.19	-61.38 to -37.00	Yes	****
pEF6-miR Wild-Type 3'UTR vs. pEF6-empty Mutant 3'UTR	-49.19	-62.36 to -36.02	Yes	****
pEF6-miR Mutant 3'UTR vs. pEF6-empty Wild-Type 3'UTR	0.001053	-13.17 to 13.17	No	ns
pEF6-miR Mutant 3'UTR vs. pEF6-empty Mutant 3'UTR	0	-14.08 to 14.08	No	ns
pEF6-empty Wild-Type 3'UTR vs. pEF6-empty Mutant 3'UTR	-0.001053	-13.17 to 13.17	No	ns
RAP1A hvt-miR-H7				
pEF6-miR Wild-Type 3'UTR vs. pEF6-miR Mutant 3'UTR	-39.65	-52.82 to -26.48	Yes	****
pEF6-miR Wild-Type 3'UTR vs. pEF6-empty Wild-Type 3'UTR	-46.25	-58.44 to -34.06	Yes	****
pEF6-miR Wild-Type 3'UTR vs. pEF6-empty Mutant 3'UTR	-39.65	-52.82 to -26.48	Yes	****
pEF6-miR Mutant 3'UTR vs. pEF6-empty Wild-Type 3'UTR	-6.601	-19.77 to 6.570	No	ns
pEF6-miR Mutant 3'UTR vs. pEF6-empty Mutant 3'UTR	0	-14.08 to 14.08	No	ns
pEF6-empty Wild-Type 3'UTR vs. pEF6-empty Mutant 3'UTR	6.601	-6.570 to 19.77	No	ns
TIAM1 mdv2-miR-M30				
pEF6-miR Wild-Type 3'UTR vs. pEF6-miR Mutant 3'UTR	-4.1	-16.29 to 8.094	No	ns
pEF6-miR Wild-Type 3'UTR vs. pEF6-empty Wild-Type 3'UTR	-17.72	-29.91 to -5.522	Yes	**
pEF6-miR Wild-Type 3'UTR vs. pEF6-empty Mutant 3'UTR	-4.1	-16.29 to 8.094	No	ns
pEF6-miR Mutant 3'UTR vs. pEF6-empty Wild-Type 3'UTR	-13.62	-25.81 to -1.423	Yes	*
pEF6-miR Mutant 3'UTR vs. pEF6-empty Mutant 3'UTR	0	-12.19 to 12.19	No	ns
pEF6-empty Wild-Type 3'UTR vs. pEF6-empty Mutant 3'UTR	13.62	1.423 to 25.81	Yes	*
DEK mdv2-miR-M30				
pEF6-miR Wild-Type 3'UTR vs. pEF6-miR Mutant 3'UTR	-42.59	-54.79 to -30.40	Yes	****
pEF6-miR Wild-Type 3'UTR vs. pEF6-empty Wild-Type 3'UTR	-40.94	-53.13 to -28.74	Yes	****
pEF6-miR Wild-Type 3'UTR vs. pEF6-empty Mutant 3'UTR	-42.59	-54.79 to -30.40	Yes	****
pEF6-miR Mutant 3'UTR vs. pEF6-empty Wild-Type 3'UTR	1.655	-10.54 to 13.85	No	ns
pEF6-miR Mutant 3'UTR vs. pEF6-empty Mutant 3'UTR	0	-12.19 to 12.19	No	ns
pEF6-empty Wild-Type 3'UTR vs. pEF6-empty Mutant 3'UTR	-1.655	-13.85 to 10.54	No	ns

Tukey's multiple comparisons test	Mean Diff.	95% CI of diff.	Significant?	Summary
MYBL1 mdv2-miR-M30				
pEF6-miR Wild-Type 3'UTR vs. pEF6-miR Mutant 3'UTR	-25.27	-37.46 to -13.07	Yes	****
pEF6-miR Wild-Type 3'UTR vs. pEF6-empty Wild-Type 3'UTR	-10.61	-22.80 to 1.587	No	ns
pEF6-miR Wild-Type 3'UTR vs. pEF6-empty Mutant 3'UTR	-25.27	-37.46 to -13.07	Yes	****
pEF6-miR Mutant 3'UTR vs. pEF6-empty Wild-Type 3'UTR	14.66	2.468 to 26.86	Yes	*
pEF6-miR Mutant 3'UTR vs. pEF6-empty Mutant 3'UTR	0	-12.19 to 12.19	No	ns
pEF6-empty Wild-Type 3'UTR vs. pEF6-empty Mutant 3'UTR	-14.66	-26.86 to -2.468	Yes	*
ERBB4 hvt-miR-H14				
pEF6-miR Wild-Type 3'UTR vs. pEF6-miR Mutant 3'UTR	-12	-24.20 to 0.1895	No	ns
pEF6-miR Wild-Type 3'UTR vs. pEF6-empty Wild-Type 3'UTR	5.087	-7.106 to 17.28	No	ns
pEF6-miR Wild-Type 3'UTR vs. pEF6-empty Mutant 3'UTR	-12	-24.20 to 0.1895	No	ns
pEF6-miR Mutant 3'UTR vs. pEF6-empty Wild-Type 3'UTR	17.09	4.898 to 29.28	Yes	**
pEF6-miR Mutant 3'UTR vs. pEF6-empty Mutant 3'UTR	0	-12.19 to 12.19	No	ns
pEF6-empty Wild-Type 3'UTR vs. pEF6-empty Mutant 3'UTR	-17.09	-29.28 to -4.898	Yes	**
RAN hvt-miR-H17				
pEF6-miR Wild-Type 3'UTR vs. pEF6-miR Mutant 3'UTR	9.594	-2.600 to 21.79	No	ns
pEF6-miR Wild-Type 3'UTR vs. pEF6-empty Wild-Type 3'UTR	16.16	3.971 to 28.36	Yes	**
pEF6-miR Wild-Type 3'UTR vs. pEF6-empty Mutant 3'UTR	9.594	-2.600 to 21.79	No	ns
pEF6-miR Mutant 3'UTR vs. pEF6-empty Wild-Type 3'UTR	6.57	-5.623 to 18.76	No	ns
pEF6-miR Mutant 3'UTR vs. pEF6-empty Mutant 3'UTR	0	-12.19 to 12.19	No	ns
pEF6-empty Wild-Type 3'UTR vs. pEF6-empty Mutant 3'UTR	-6.57	-18.76 to 5.623	No	ns
BCL11A hvt-miR-H17				
pEF6-miR Wild-Type 3'UTR vs. pEF6-miR Mutant 3'UTR	-6.651	-18.84 to 5.543	No	ns
pEF6-miR Wild-Type 3'UTR vs. pEF6-empty Wild-Type 3'UTR	-18.19	-30.39 to -6.000	Yes	***
pEF6-miR Wild-Type 3'UTR vs. pEF6-empty Mutant 3'UTR	-6.651	-18.84 to 5.543	No	ns
pEF6-miR Mutant 3'UTR vs. pEF6-empty Wild-Type 3'UTR	-11.54	-23.74 to 0.6506	No	ns
pEF6-miR Mutant 3'UTR vs. pEF6-empty Mutant 3'UTR	0	-12.19 to 12.19	No	ns
pEF6-empty Wild-Type 3'UTR vs. pEF6-empty Mutant 3'UTR	11.54	-0.6506 to 23.74	No	ns
ERBB4 mdv2-miR-M16				
pEF6-miR Wild-Type 3'UTR vs. pEF6-miR Mutant 3'UTR	-7.43	-19.62 to 4.764	No	ns
pEF6-miR Wild-Type 3'UTR vs. pEF6-empty Wild-Type 3'UTR	-14.98	-27.18 to -2.791	Yes	**
pEF6-miR Wild-Type 3'UTR vs. pEF6-empty Mutant 3'UTR	-7.43	-19.62 to 4.764	No	ns
pEF6-miR Mutant 3'UTR vs. pEF6-empty Wild-Type 3'UTR	-7.554	-19.75 to 4.639	No	ns
pEF6-miR Mutant 3'UTR vs. pEF6-empty Mutant 3'UTR	0	-12.19 to 12.19	No	ns
pEF6-empty Wild-Type 3'UTR vs. pEF6-empty Mutant 3'UTR	7.554	-4.639 to 19.75	No	ns
TIAM1 mdv2-miRM16				
pEF6-miR Wild-Type 3'UTR vs. pEF6-miR Mutant 3'UTR	-20.45	-32.64 to -8.256	Yes	***
pEF6-miR Wild-Type 3'UTR vs. pEF6-empty Wild-Type 3'UTR	-9.741	-21.93 to 2.452	No	ns
pEF6-miR Wild-Type 3'UTR vs. pEF6-empty Mutant 3'UTR	-20.45	-32.64 to -8.256	Yes	***
pEF6-miR Mutant 3'UTR vs. pEF6-empty Wild-Type 3'UTR	10.71	-1.485 to 22.90	No	ns
pEF6-miR Mutant 3'UTR vs. pEF6-empty Mutant 3'UTR	0	-12.19 to 12.19	No	ns
pEF6-empty Wild-Type 3'UTR vs. pEF6-empty Mutant 3'UTR	-10.71	-22.90 to 1.485	No	ns
DNMT3B hvt-miR-H16				
pEF6-miR Wild-Type 3'UTR vs. pEF6-miR Mutant 3'UTR	-55.76	-67.95 to -43.56	Yes	****
pEF6-miR Wild-Type 3'UTR vs. pEF6-empty Wild-Type 3'UTR	3.03	-9.163 to 15.22	No	ns
pEF6-miR Wild-Type 3'UTR vs. pEF6-empty Mutant 3'UTR	-55.76	-67.95 to -43.56	Yes	****
pEF6-miR Mutant 3'UTR vs. pEF6-empty Wild-Type 3'UTR	58.79	46.59 to 70.98	Yes	****
pEF6-miR Mutant 3'UTR vs. pEF6-empty Mutant 3'UTR	0	-12.19 to 12.19	No	ns
pEF6-empty Wild-Type 3'UTR vs. pEF6-empty Mutant 3'UTR	-58.79	-70.98 to -46.59	Yes	****

8.6 Appendix 6 – List of the different subheadings found under main headings identified in the PantherDB pie chart figures

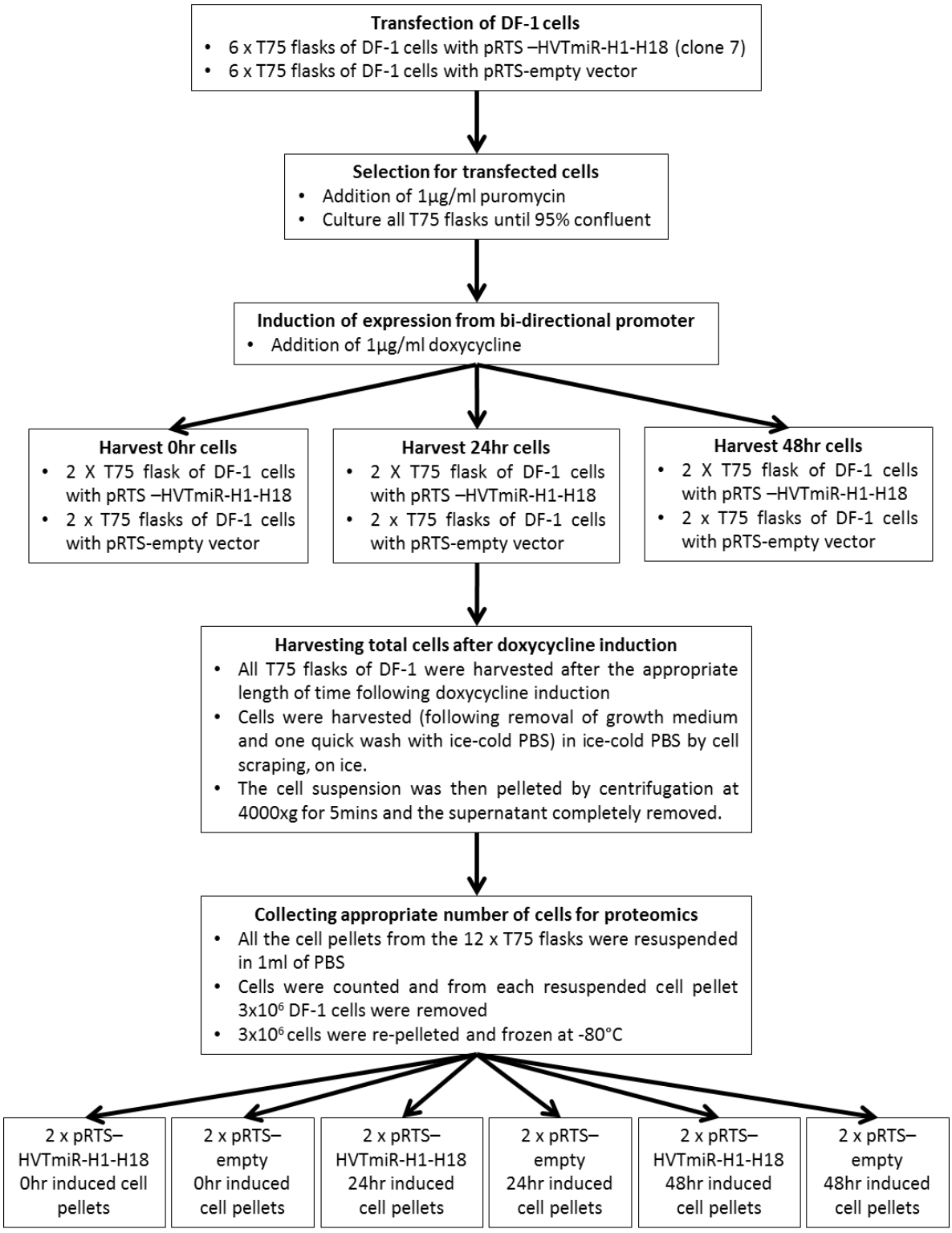
Cellular component organization or biogenesis (GO: 0071840)
Cellular component biogenesis (GO: 0044085)
Cellular component organization (GO: 0016043)
Cellular process (GO: 0009987)
Cell communication (GO: 0007154)
Cell cycle (GO: 0007049)
Cell growth (GO: 0016049)
Cell proliferation (GO: 0008283)
Cellular component movement (GO: 0006928)
Chromosome segregation (GO: 0007059)
Cytokinesis (GO: 0000910)
Localization (GO: 0051179)
RNA localization (GO: 0006403)
Protein localization (GO: 0008104)
Transport (GO: 0006810)
Apoptotic process (GO: 0006915)
Induction of apoptosis (GO: 0006917)
Negative regulation of apoptotic process (GO: 0043066)
Reproduction (GO: 0000003)
Fertilization (GO: 0009566)
Gamete generation (GO: 0007276)
Biological regulation (GO: 0065007)
Homeostatic process (GO: 0042592)
Regulation of biological process (GO: 0050789)
Regulation of molecular function (GO: 0065009)
Response to stimulus (GO: 0050896)
Cellular defines response (GO: 0006968)
Defines response to bacterium (GO: 0042742)
Immune response (GO: 0006955)
Response to endogenous stimulus (GO: 0009719)
Response to external stimulus (GO: 0009605)
Response to stress (GO: 0006950)

Developmental process (GO: 0032502)
Anatomical structure morphogenesis (GO: 0009653)
Cell differentiation (GO: 0030154)
Death (GO: 0016265)
Ectoderm development (GO: 0007398)
Embryo development (GO: 0009790)
Endoderm development (GO: 0007492)
Mesoderm development (GO: 0007498)
Pattern specification process (GO: 0007389)
Sex determination (GO: 0007530)
System development (GO: 0048731)
Multicellular organismal process (GO: 0032501)
Single-multicellular organism process (GO: 0044707)
Locomotion (GO: 0040011)
Biological adhesion (GO: 0022610)
Cell adhesion (GO: 0007155)
Metabolic process (GO: 0008152)
Biosynthetic process (GO: 0009058)
Catabolic process (GO: 0009056)
Coenzyme metabolic process (GO: 0006732)
Generation of precursor metabolites and energy (GO: 0006091)
Nitrogen compound metabolic process (GO: 0006807)
Phosphate-containing compound metabolic process (GO: 0006796)
Primary metabolic process (GO: 0044238)
Sulphur compound metabolic process (GO: 0006790)
Growth (GO: 0040007)
Cell growth (GO: 0016049)
Immune system process (GO: 0002376)
Antigen processing and presentation (GO: 0019882)
Immune response (GO: 0006955)
Macrophage activation (GO: 0042116)

Table 19 - List of sub-headings found under the initial 'biological processes' in Panther Gene Classification

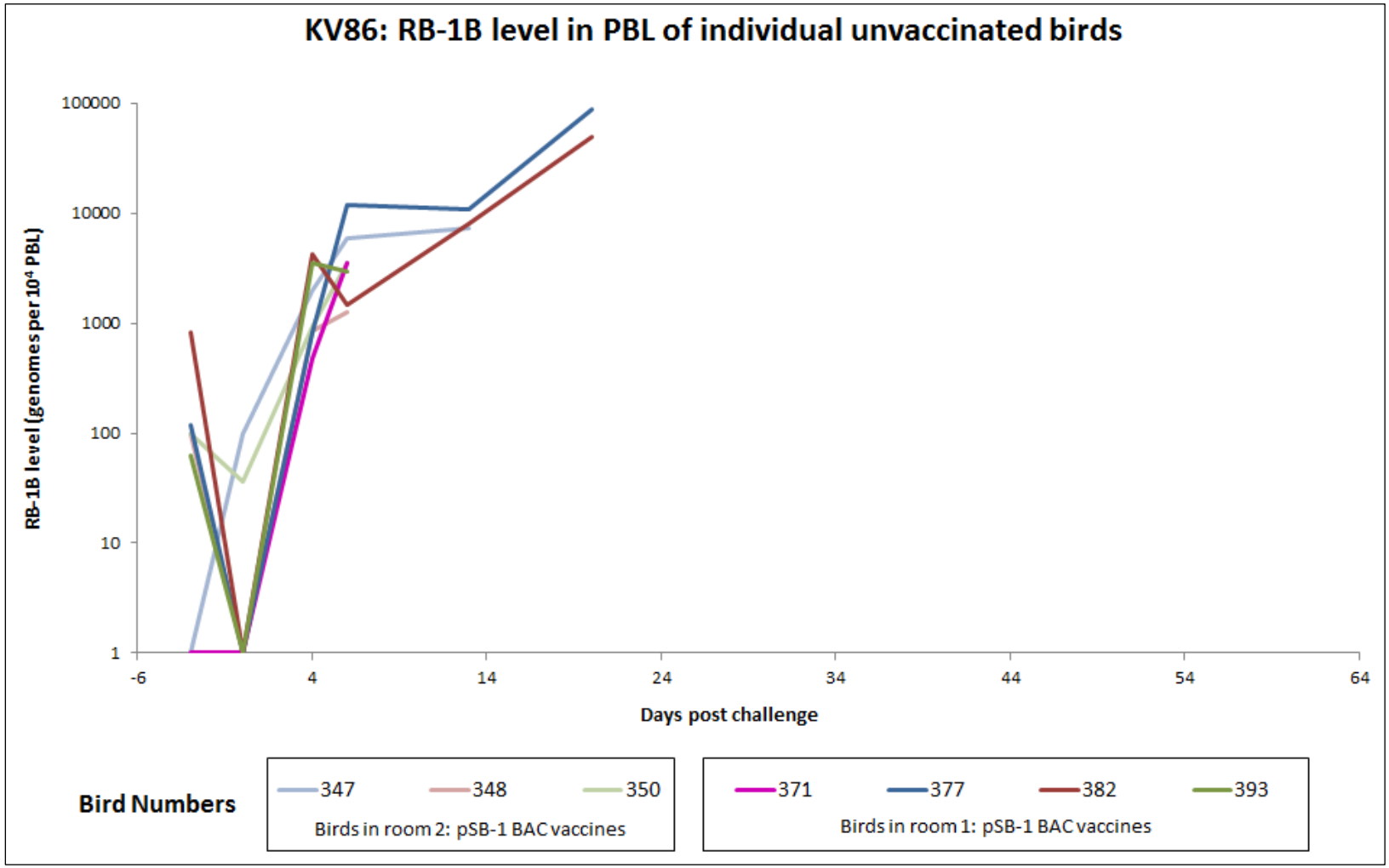
8.7 Appendix 7 – Workflow diagram to describe how stably transfected DF-1 cells were prepared for proteomics work in chapter

The workflow diagram below describes how duplicate samples were prepared, prior to dispatch to Liverpool, for pRTS-HVT miRNA transfected DF-1 cells and pRTS-empty transfected DF-1 cells (0hr, 24hr and 48hr post doxycycline induction) following separate transfections in T75 flasks of DF-1



8.8 Appendix 8 – Analysis of challenge virus levels in individual unvaccinated birds from KV86 trail

The graph below shows the levels of RB-1B MDV-1 challenge virus detected in each individual bird within the unvaccinated control group. The legend at the bottom shows the bird numbers which correspond to each individual line, and the experimental rooms that the individual birds were distributed throughout.



8.9 Appendix 9 – Analysis of vaccine virus levels in individual unvaccinated birds from KV86 trail

The graph below shows the levels of vaccine virus (pSB-1 and pHVT3) detected in each individual bird within the unvaccinated control group. The legend at the bottom shows the bird numbers which correspond to each individual line, and the experimental rooms that the individual birds were distributed throughout.

